Optimization of small-scale low-cost anaerobic digestion system: Model based analysis

Raymond Ogundu Owhondah

Submitted in accordance with the requirements for the degree of
Doctor of Philosophy

Under the supervision of

Prof. William Gale

Dr Lin Ma

Prof Bill Nimmo

Prof Derek Ingham

Prof Mohamed Pourkashanian

Dr Mark Walker

The University of Leeds
School of Chemical and Process Engineering

July 2019

Declaration

The candidate confirms that the work submitted is his/her own, except where work which has formed part of a jointly authored publication has been included. The contribution of the candidate and the other authors to this work has been explicitly indicated below. The candidate confirms that appropriate credit has been given within the thesis where reference has been made to the work of others.

The work which appears in the jointly authored publication (with Raymond Ogundu Owhondah as the lead author) appears in chapter 4, and the details of the publication is as follow:

Raymond O. Owhondah., Mark Walker., Lin Ma., Bill Nimmo., Derek B. Ingham., Davide Poggio., Mohamed Pourkashanian.

“Assessment and parameter identification of simplified models to describe the kinetics of semi-continuous biomethane production from anaerobic digestion of green waste and food waste” Bioprocess & Biosystem Engineering

The work in the case was directly attributed to the lead author with the co-author performing supervisory role.

Acknowledgements

I would first like to thank my supervisor prof William Gale, prof Mohamed Pourkashanian, Dr Lin Ma, Dr Bill Nimmo, and Prof Derek Ingham for their support, encouragement and critical comments during the research and the writing up of the thesis.

To my beloved elder brother, Sir Collyns Owhondah for his tireless effort, encouragement and the opportunity given to me to study at this level in one of the most prestigious University in the United Kingdom.

Also, from the depth of my heart I acknowledged the almighty God for the grace he has given me to complete this thesis report and for good health.

I also appreciate the support of Dr Mark Walker and Dr Davide Poggio for their insight and thought concerning certain issues aspects of the research.

Finally, I would like to thank my friends Stanley Omosigho, Oyinade Akinbohum, Chioma Kirsteen Nwaubani, and Dr Ijeoma Maxs.

Publication

Raymond O. Owhondah., Mark Walker., Lin Ma., Bill Nimmo., Derek B. Ingham., Davide Poggio., Mohamed Pourkashanian. “Assessment and parameter identification of simplified models to describe the kinetics of semi-continuous biomethane production from anaerobic digestion of green waste and food waste” Bioprocess & Biosystem Engineering.

Abstract

In this research thesis, the modelling of biogas production through the anaerobic digestion (AD) process is investigated, with key focus on the modelling of low cost small -scale plastic bag types digester, which has a potential application in the rural communities of the developing countries. The present work investigated the thermal modelling of the plastic bag digester and its integration with simplified anaerobic digestion models to assess feasibility and to develop operating protocols.

In order to develop the AD process model, a parameter estimation method was developed, and this was used to describe the methane production of from food waste, green waste and pig manure, using data obtained from batch and semi-continuous experiments. It was found that in the case of semi-continuous process, the model structure, rather than kinetic parameter values or kinetic equation used, determines the ability of the models to describe the degradation of food waste and green waste. For food waste, inhibition also played an important role in the model's ability to reproduce methane production data obtained experimentally. Further, it was found the kinetic parameter values obtained from the batch and semi-continuous processes are different.

The kinetic parameter values or the best kinetic equation obtained from the parameter estimation method were used as input in the biochemical model, which is combined with a thermal model to simulate the performance of different designs of the plastic bag digester in Port Harcourt In Nigeria and Cuzco in Peru. Three designs of the digester were model; CASE 1 simple plastic bag digester without greenhouse cover, CASE 2 plastic bag digester with a greenhouse cover, and CASE 3 plastic bag digester with greenhouse cover and solar heating system. It was found that the addition of external heating sources such as greenhouse and solar heating system in CASE 2 and CASE 3 in Port Harcourt in Nigeria and Cuzco in Peru, has a positive impact on the performance of the digester (improved slurry temperature) compared with CASE 1. However, CASE 3 is not suitable in Port Harcourt, in Nigeria, since the difference in the slurry temperature in CASE 3 and

CASE 2 is 1.48 ^{o}C, while the model predicts the suitability of CASE 3 in Cuzco, in Peru.

The combined thermal model (CASE 2) and the biochemical model (3R) was used to model the operational protocol for small scale digester in different climate of developing countries. The protocol was developed for mono and co-digestion processes. It was found that minimum HRT (Hydraulic retention time) and maximum OLR (Organic loading rate) of a specific feedstock is different given the difference in. For the co-digestion process, the substrate characteristics and the substrate mix ratio have a strong influence on minimum HRT and maximum OLR.

Table of Contents

List of Tables

List of Figures

Nomenclature

Symbols

C	Concentration of inorganic carbon
D	dilution rate
I_N	Ammonia inhibition rate factor
I_{vfa}	VFA inhibition rate factor
k_n	Reaction stoichiometric coefficient n
k_x	Contois half saturation constant
k_s	Half saturation constant
k_i	Haldane inhibition constant for VFA
k_{ivfa}	General inhibition constant for VFA
$k_{i,N}$	General inhibition constant for ammonia
n	Number of experimental data points
N	Concentration of ammonia
p_{opt}	Best fitting parameter set
q_m	Modelled methane flowrate
$q_{m,exp}$	Experimental methane flowrate
S_1	Concentration of organic substrate
S_{1a}	Carbohydrate and fats concentration in substrate
S_{1b}	Protein concentration in substrate
S_2	Concentration of VFA in the two-reaction model
$X_{1,1a,1b}$	Concentration of hydrolysis biomass
X_2	Concentration of methanogenic biomass
Z	Total alkalinity
ζ	Vector of state variables
μ_n	Specific growth of microorganism n
$\mu_{n,max}$	Maximum growth rate of microorganism n
$\sigma_{qm,exp}$	Mean Experimental methane flow rate

β_1	Carbohydrate and fats content of organic matter
β_2	Protein content of organic matter

Acronyms/abbreviations

ABC-K	Association of biogas contractors of Kenya
AD	Anaerobic digestion
ADM1	Anaerobic digestion model 1
AFPRO	Action for food production
AEPC	Alternative Energy Promotion Centre, Nepal
BCE	Biogas Construction Enterprise
BCSIR	Bangladesh Council of scientific and industrial research, Bangladesh
BPO	Biogas project office
BRAC	Building Resources Across Communities
BRP	Banque Populaire du Rwanda, Rwanda
BSP	Biogas Support Program, Nepal
BSU	Biogas Solution Uganda
BTAL	Biogas Technology Africa Ltd, Ghana
CAMARTEC	Centre for agricultural mechanization and rural technology, Tanzania
CEDAC	Cambodian Centre for Study and Development in Agriculture, Cambodia
CIECD	Cambodia India Entrepreneurship Development Centre, Cambodia
COD	Chemical oxygen demand
COD_{th}	Theoretical chemical oxygen demand
DANIA	Danish International Development Agency, Bangledash.
DARD	Department of Agriculture and Rural Development, Vietnam
DBPO	District Biogas Programme Office
DFID	Department of International Development
DFO	Dairy Farmer of Ontario, Canada

DGIS	Directorate General for International Cooperation, Nepal, Rwanda etc.
GHG	GreenHouse Gas
EPCD	Environment Pollution Control Development
ELCT	Evangelical Lutheran Church in Tanzania,
FMO	Netherlands Development bank
FIDE	Friends in Development Trust Fund
GGC	Gobar Gas company, Nepal
PID	Proportional-Integral-derivative
GTZ	Organization for Technical Cooperation (-Germany)
HIVOS	Humanist Institute for Cooperation with Developing Countries, African and Asia
HRT	hydraulic retention time
IDCOL	Infrastructural Development Company limited, Bangladesh.
IFAD	International Fund for Agriculture and Development, Cambodia
IRDI	Integrated Rural Development Initiatives
KFW	Kreditanstalt fuer Wiederaufbau
KENBIC	Kenya National Biogas Committee
KENFAP	Kenya national federation of agricultural producers
LGED	Local Government Engineering Department, Bangladesh.
MARD	Ministry of Agriculture and Rural Development, Vietnam
MoEST	Ministry of Environment, Science, and Technology
NBMMP	National Biogas and Manure Management Programme
NBPA	Nepal Biogas Promotion Association
NBP	National biogas programme
NBPO	National Biogas programme office
NBSC	National Biogas Steering Committee
NDBP	National Domestic Biogas Programme

NGO	Non-Governmental Organization
NOGAMU	National organic agricultural movement of Uganda
OECD	Organization for Economic Cooperation and Development
OMAFRA	Ontario Ministry of Agriculture, Food and Rural Affairs, Canada.
PBPO	Provincial Biogas Programme Office
PVC	Polyvinyl Chloride
SACCO	Saving and Credit Cooperative Society, Tanzania
SCCULT	Saving and Credit Cooperative Union of Tanzania
SNV	Netherland Development Organisation, Nepal, Rwanda etc.
TS	Total solid
TPC	Thaneakea Phum Cambodia
UMN	United mission of Nepal
VEDCO	Volunteer efforts for development Concerns
VFA	Volatile fatty acid
VS	Volatile solid
Ode15s	Ordinary differential equation solver

Chapter 1 Introduction

1.1 General Background

Globally, there are two issues that require attention; the first is the increase in emission of air pollutants and global climate change. The second issue is the increasing energy consumption and security of energy supplies [1-4]. This occurs simultaneously with the environmental problems linked to the disruption of the balance of the ecosystem [5]. Man's activities threaten the sustainability of environmental and socio-economical systems. Realizing this challenge and its direction, the international communities are coerced to take steps aimed at reducing greenhouse gas emission and addressing climate changes. Renewable energy sources provide an alternative to the use of fossil fuels [6], and energy efficiency policies are used to bridge the gap between sustainable development and renewable energy sources [7].

Energy policy includes climate change and energy security, energy reliability, energy affordability and market competitiveness for businesses, industries and household [4, 7] Energy security is the uninterrupted access to a source of energy, and it is very important [4, 7]. If the supply is discontinued or severely affected due to price volatility, natural disasters, political instability and war, The financial functioning and social welfare of countries will be disturbed. The growth of Chinese economy implies that it relies heavily on the importation of crude oil to cover the shortage in the demand for electricity. In most cases, the oil imports are likely to be interrupted as the delivery routes are choked and vulnerable to maritime blockage [7, 8]. This disruption in the supply of energy is the key reason why EU aimed to strengthen energy security by setting an ambitious goal of increasing the share of renewable energy sources in the energy mix by 2020 [4, 9].

The second aspect of the energy efficiency policy is the impact of climate change as most developed and developing countries are under pressure to

reduce greenhouse gas emission as it has a huge consequence on a domestic scale. United Nation Framework Convention on Climate Change was enacted in 1992 with the view to developing policies to address greenhouse gas emission. The objective of the UNFCCC is to achieve the stabilization of greenhouse gas concentration in the atmosphere at a level that would prevent dangerous anthropogenic interference with the climate system in a timely manner enough to allow natural adaptation of the ecosystem to climate change. To ensure there is no adverse effect on the food security and economic development of a country. Various international agreements have been developed under the United Nation Framework Climate Change Convention. Example, the Kyoto Protocol which was developed by the industrialized nations with a commitment to reducing the level of greenhouse gas emission. A key aspect of the protocol includes the allocation of emission target to participating countries and the development of a mechanism that allows trading of underutilized emission targets. The Paris Agreement is another international agreement, which provides a framework for the international climate change scheme. Paris Agreement aims to consolidate the global response to the dangers of climate change, in the context of sustainable development and attempts to eliminate poverty. This can be achieved by maintaining the increase in global average temperature below 2 ^{o}C above pre-industrial level and to pursue efforts to limit the temperature increase below 1.5 ^{o}C above pre-industrial levels, recognizing that it would significantly reduce the risk associated with climate change. The Paris Agreement also ensures that there is no threat to food security, by increasing the ability to adapt to the adverse impacts of climate change and fostering climate resilience, and low greenhouse gas emission development. The Provision of finance is a key aspect of the Paris Agreement. Finance is required to ensure consistency in the pathway towards low greenhouse gas emissions and climate-resilience developed. The implementation of the agreement allows for different countries that are a party to the convention contribute to the global response to climate changes based on their different national circumstances.

The third concern is the impact of pollution associated with the combustion of fossils fuels. This affects air, water, and soil quality, and has a severe implication on health, food, and water security. Finally, the fourth is the impact on the deployment of renewable energy technology, since most rural communities still rely heavily on the burning of traditional biomass to meet their energy need. Renewable technology such as photovoltaic and solar water has the capacity to improve the livelihood of people in such rural communities [7]. Also, energy efficiency policy involves the need for a strategic and legislative framework where personnel elected are responsible for the management of energy as well as organize awareness campaign. Other energy efficiency policy includes the improvement of the standards for commercial building codes and the standardization of contracts for companies providing energy services in public building.

1.1.1 Renewable energy technology

Renewable energy technology can be used to meet the need for sustainable and clean energy production, reducing dependence on the use of fossil fuels and lowering carbon emission. They are known to be more competitive than the traditional energy source, an example is solar and winds energy. It is used for large scale or small-scale energy generation either as stand-alone or an integrated system of the various energy systems.

Renewable energy technologies have been studied based on a number of key indicators, such as the impact on the society, energy conversion efficiency, land requirement, water consumption, atmospheric gas emission, price of electricity generated, and the availability of the energy sources [10]. Other studies, considers the saving from the demands of energy, improvement in energy production and the extent to which renewable energy technology is replacing traditional energy sources [11]. The economic and environmental impacts of renewable energy technology have been considered [12-14]. Renewables energies are the fastest-growing source of energy for electricity generation, with annual increases averaging 2.9% from 2012 to 2040. In particular, non-hydropower

renewable resources are the fastest-growing energy sources for new generation capacity in both the OECD and non-OECD regions [15]. The comparison of the contribution from the various renewable energy mix shows that hydropower leads, followed by wind energy, biomass, and waste with solar energy contributing the least.

Hydropower energy is the energy derived from the movement of water. It is classified as hydroelectricity which is the energy generated via the gravitational motion of water and ocean energy. In other words, it is generated from the ocean waves or tides [12]. It can be implemented as a large-scale centralized unit and involves the building of huge dams. Large artificial lakes can be created by placing massive barriers of concrete, rock, and earth across river valleys [16, 17]. They produce a reliable power supply, provide irrigation and flood control benefits. However, in most cases, the dams spill over to fertile land destroying crops and displacing the local people leading to serious environmental problems [16, 17]. It has the advantage of a much longer operational life span of about 50 - 100 years. It is cheaper to operate and maintained and can be easily adapted to new technologies [18, 19]. Small-scale or low-head hydropower system represents “Run-of-Rivers” projects which generally store little or no water and purely serves the function of regulating water to the hydro-plant. It is a promising source of producing sustainable, cheap energy in rural or developing countries. The magnitude or scale of the small-scale hydropower (SSH) plant differs in a different country and it is between the scale of 2.5 MW to 25 MW [20]. There is a different scale of SSH such as Mini-hydro, Micro-hydro, and Pico-hydro, which has a production capacity of less than 2 MW [20, 21].

Wind energy technology involves the conversion of rotational energy due to the motion of the wind into electrical or mechanical power through the aerodynamics of the wind turbine blade. The use of wind energy dates to 200 BC and 1300-1875 AD with the installation of a simple wind turbine. The technology reaches approaches maturity in the 19th Century with the installation of over 6 million wind devices in the USA, the design of airplane

propellers and monoplane in some parts of Europe and US [22]. A substantial aspect of the history of wind energy is a result of the two-oil crisis in the US. The first is the oil crisis in the 1970s which was a result of the cut in production of crude oil by the Arab member of OPEC leading to an increase in the price of crude oil. The cut in the production of crude oil was in response to the fall in the value of US dollar and the rising US inflation which eroded the Tehran/Tripoli agreement between the oil companies and government of oil-producing countries. Another key reason for the high price of oil is the political conflict in the Middle East around the same period. The second oil crisis occurred in the 1980s, and it is due to the increase in the prices of American WTI crude from $ 36 to $ 38 in January 1981 [23]. These events led to the development of commercial wind turbine for domestic, agricultural and utility purpose. In order to effectively generate electricity using a wind turbine, an accurate estimation of the wind speed distribution, selection of the site to install the wind farm and the management of the energy conversion processes is crucial. However, wind energy is severely influenced by weather condition and its technical viability is based on the distribution of the wind in some locations [12].

The history of solar energy technology is long, and it has been used to generate steam, run engines and irrigation pumps, by capturing the sun's heat, between the 1840 and First World War [24, 25]. In the 1950s, solar photovoltaic (PV) cells were developed in the United States, and they have been used to generate electricity in space satellites [25, 26]. The interest in solar energy started in the 1970s after the oil-shock with the development and commercialization of the solar energy technology. However, as the price of global crude oil drops, there was a lack of policy to sustain the development of solar technology [25, 27]. Early 21st Century saw an increase in the market for solar energy technologies and by the end of 2010, the total capacity of electricity generated from solar energy was 40 GW [25, 28]. Solar energy is considered one of the potential sources of energy for electricity generation globally [12]. The increase in the use of solar energy technologies plays a key role in the reduction of greenhouse

gas and could assist in preventing the release of 100Gt of CO_2 during the period 2008 - 2050 [29]. The benefits of using solar energy technology are that it can be installed easily in remote areas, it requires no land allocation and reduces the cost of grid connection. Solar radiation can be converted to electricity using solar photovoltaic cells and heat using the solar thermal collector. Nonetheless, some deficiencies of solar energy technology include poor capture of energy using the PV panels and unavailability of enough solar radiation during winter.

Bioenergy is energy that is derived from biomass. Biomass is a material made from living organism (Plants and animals). It can be burned directly to produce electricity or heating for industries and home use or can be converted into various types of biofuels (Biogas, Bioethanol, and biodiesel) via different processes that are grouped into physical, thermochemical and biochemical. The benefits of biomass as an energy source includes; the ability installed at low cost, bioenergy assists in the reduction of CO_2 emission into the atmosphere, it has the potential to replace fossil fuels and it is abundant in nature.

Biogas is produced from the decomposition of organic matter in the absence of oxygen. It consists about 40 – 70 % methane with the remaining consisting of carbon dioxide and other trace gases. Biogas production was first noticed by a Roman scholar Pilney in 50 BC, and it was believed that biogas was the source of energy use in the heating bath in Assyria around 10 BC [30]. The decay of organic material into biogas was first recorded by Van Helmont in the 17th century, while Volta concluded that there is a link between the biogas produced and the amount of organic matter used. The combustible gas produced from organic matter was called methane after the completion of independent work by John Dalton and Humphrey Davy between 1804 -1808 [30]. Also, there were reports of the decomposition of the organic matter by microorganism in the 18th century, while hydrogen, acetic acid, and butyric acid were produced as intermediates when some microbes are isolated during fermentation [31]. Methane is produced via

decarboxylation as well as via the interaction between hydrogen and carbon dioxide [30].

1.2 Anaerobic Digestion Technology

Anaerobic digestion is the decomposition of organic matter via a series of interconnected biological reactions in the oxygen-free environment [32]. The technology has been applied over the years to wastewater sludge generated from the industrial and municipal wastewater treatment plant. The anaerobic digester utilizes this sludge to produce biogas, and the biogas is used to generate heat and electricity to offset the cost of electricity generation in the wastewater treatment plant site [33]. The anaerobic digestion process produces less amount of sludge and does not require large amount of energy compared to the energy-intensive aerobic treatment process. This makes it more economical than the aerobic process and it is characterized by the low yield of micro-organisms. The anaerobic digestion processes requires an extended period of time is for the micro-organism to prevent the wash-out of the cells in the reactor [34]. Over the years, anaerobic digestion technology has been applied for the treatment of municipal solid waste especially in Europe and the USA owing to strict regulation on landfilling waste [35]. The landfill site has been modified such that the methane produced naturally from the degradation of OFMSW is collected by means of wells and convey to a boiler or turbine via pipes to produce heat and electricity [35].

Biogas offers farmers the opportunity of growing crops in arable land whilst retain the full value-added benefits from the anaerobic digestion process on-site. Generally, the anaerobic digestion process has been applied in the agricultural farm, and this is mainly driven by the utilization of the biogas produced in the AD plant to generate electricity. In the US, in addition to the generation of electricity in agricultural farms, the anaerobic digester plants are installed to mitigate pollution and reduced odour generated in farm and to prevent groundwater pollution with phosphate as this the main concern by the Environmental protection Agency (EPA). Also, anaerobic digestion plant installation in agricultural farms in the US is encouraging

due to the technical support received by farms from the Agstar program as well as capital grants and interest-free loans. The increase in the use of digestate as animal bedding material is in practice in most agricultural farms in the US after the digestate is made to pass through a solid separator. This helps the farmer reduced expenditure on farm input, as most farms import foods and bedding materials. The digestate produced from agricultural farms are used as domestic compost thereby generating income for the farmer. In the EU, the main drivers for on-farm AD operation and production of renewable energy are government incentives and operational profit [36]. The government incentives come in the form of financial benefits and grant support. Also, remuneration is paid to renewable energy producers per kWh of electricity and heat they produce. In the UK, the incentive is the Renewable Obligation Certificate and the Feed-in-Tariff. The Renewable Obligation certificate is applicable to large-scale renewable electricity projects. While, the Feed-in-Tariff was developed to support small-scale electricity generation and this is further divided into generation tariff, which is paid by the electricity supplier to a household that generates the electricity and the export Tariff paid by the electricity suppliers pays to a household that export electricity back to the electricity grid. The amount per kWh electricity generated from renewable under the renewable obligation certificate 7.8 p. In Germany, the main drivers of the on-farm AD plant are co-digestion of different feedstock, and the need to move away from Nuclear energy development and dependence on Russia for gas supply. The use of anaerobic digestion in the Germany farms increase when the renewable energy ACT and its amended was implemented in Germany. The biogas plant was installed on the farm for the purpose of generating electricity and supplied to the local electricity grids. Unlike the UK, the feed-in-Tariff implemented is a function of the plant size and cost, and the substrates.

Another application of the anaerobic digestion processes involves the conversion of gas to liquid fuels for transportation purpose. The biogas produced is pump from the gas holder to a gas-upgrading facility to remove CO_2 so that the methane content increase to 97 %. The resulting bio-

methane is transported to the filling station or used for heat production in a gas boiler onsite [37]. The application of AD in the transport sector is encouraged by government incentive such as the Renewable Transport Fuel Obligation tariff. In Sweden, the incentive by the government of Sweden and effective policy has encouraged the development of biogas for transport fuel. The biogas is mainly produced from the sewage treatment plant, landfill plant, and co-digestion plant. Currently, there is 38 upgrading plant for the processing of raw biogas for vehicle fuel.

Anaerobic digestion process has record increasing use in the disposal of organic waste in the UK, and this is driven by policy and legislation on the use of landfill for disposal of food waste to the recovery of energy. It is estimated that 8.3 million tonnes of food waste will be potentially available [38, 39]. This food waste is mostly generated from businesses involved in food processing and manufacturing, transportation, distribution, storage and sales, and from commercial and local government kitchens. In many parts of the world, the anaerobic digestion plant has been installed to process the food waste generated. Example, the installation of an AD plant in Perth in Western Australia. This plant has the capacity to process 35,000 tonnes of food waste collected from markets, supermarket, abattoirs, agricultural companies, and food processing companies to produce biogas which is consumed in the CHP plant to generate electricity and supply to grid [40, 41]. AD application in food waste degradation is to prevent the spread of animal disease resulting from direct consumption of food waste by a domestic or wild animal. This has been a major concern in parts of Europe and North America. Hence stringent regulations are implemented to ensure food waste is treated [39].

Anaerobic digestion process can either be operated as a wet process with a total solid content of 1 - 15 % or as a dry process with a total solid content of about 20 – 40 %. Recently, the process has been widely deployed in rural area as an environmentally sustainable means of providing energy for cooking [42].

1.2.1 Small Scale Anaerobic digestion process

The deployment of small scale anaerobic digester as part of a sustainable approach mitigates the use of traditional fuels; reduce the health risk associated with pollution, while at the same time provides effective means for cooking [42, 43]. Small scale or low-cost digesters have been significant in countries like India and China. In China, the first biogas digester fed with household waste was installed in the Guangdong province, while at the same time a digester utilizing agricultural waste was installed in Germany. In India, the Grama Laxmi digester was installed by the Indian Agricultural Research Institute using manure as the substrate. This digester design is used as the model for the development of floating drum digester [42-44]. The installation of small scale (low-cost) biogas plants have increased over the years due to support by various national governments and collaboration with non-governmental agencies. The number of installed household digester in developing countries is more than 30 million, with an installed capacity of around 2 -10 m^3 [42].

The increase in the number of anaerobic digesters installed in a developing countries are attributed to the various national biogas extension programs initiated by the national government in partnership with various private organisations. In China, the Chinese Guorui Biogas company started building and selling biogas plant in 1920 [45], for the purpose of utilizing the biogas effluent as fertilizer and for cooking. The biogas programme started in 1958 and was encouraged by the support of the National Chairman of the “Biogas for Every Household”. In 1978, 7 million plants have been built under the programme [45, 46].

The lack of proper materials of construction has led to a decrease in the number of anaerobic digester plant installed [47]. The programme focussed more on quantity than quality since it is driven by political activists that encouraged individuals to build the system themselves [45, 48]. The establishment of training centres [45], the standardization of the biogas design and other biogas appliance [49] , and the involvement of the Chinese Government ensured the continuation of the programme. Biogas

technicians were trained on the design of biogas plant, and cash subsidy was offered to cover the cost of construction of the biogas plant. As the programme becomes more organised at the centre. The number of digesters constructed increased slowly and steadily. Most of the non-functional digester or defect digester were replaced and the number of digesters increases to 8 million [45]. The average life-span of a biogas plant installed in China is 4 and a half years.

The increasing effort from the government of China combined with local advocacy ensure the increase in the number of biogas plant constructed. The government developed a 10-year biogas plan which involves increase investment in biogas [49]. Funds were obtained from treasury bonds and the sum of 1 billion Yuan was invested in the national biogas programme. In 2008, the investment in the biogas sector was about 6 billion Yuan [47]. Also, the number of digesters installed increase due to the participation of women in the dissimilation of the biogas technology in their locality [50].

The biogas programme in China resulted in the development of integrated systems [51]. These includes the three-in-one system consisting of the pig farm, toilet, and biogas plant; four-in-one system consisting of the pig farm, toilet, biogas plant and greenhouse [45]. There is a five-in-one system which includes a fish pond in addition to a pig farm, toilet, biogas plant, and greenhouse. These systems are used to produce fuels (biogas) for cooking and compost for agricultural practice. The anaerobic digester are covered with a greenhouse to ensure minimal fluctuation in slurry temperature during the cold season [47]. Over time, the interest in China's biogas programme has shifted towards the disposal of waste generated from food and agricultural processing industry. Biogas plants were installed in large and medium scale farms [47, 52]. This is encouraged by public and private sector participation and by 2011, the biogas sector has employed over 40,000 people in over 13,000 promotional institutions at the provincial, state and local levels [47]. 2000 biogas companies are involved in the construction of biogas plants with over 30,000 employees and the total output value of 8 Billion Yuan has been achieved [47, 53].

In India, the first digester use to generate biogas from human waste is built in Bombay in 1897 [54, 55]. In 1900, there was an attempt to build biogas for manure utilisation in Bombay, and this was unsuccessful. In 1937, the Indian Technology Research Institute built the first successful biogas plant to utilise manure. This design of digester was not accessible to India farmers because it is very expensive [45, 55, 56]. In 1950, several designs of the anaerobic digesters were developed due to rigorous research in anaerobic digestion technology. Notable of the design of digester is the Gramalaxmi design of biogas plant develop by J.J Patel [45, 55, 57]. This design was later adopted by the Khadi and Villages Industries Commission (KVIC) as the prototype for her biogas programme [55, 58]. The other designs of the biogas plant include; the Janata biogas plant which is a version of the Chinese biogas design developed by Gobar Gas Research Centre established by the government of Uttar Pradesh [55, 59]. The "Famers friend" design of the biogas plant was developed by Action for Food production (AFRO). This version of the Chinese design does not require casing during construction.

After the increase in price of crude oil in the 1970s, the government of India in partnership with various organisations and NGO became actively involved in the biogas technology. The KVIC became the leading organisation responsible for developing training courses and coordinating the extension programme. Other organisations invited to participate in the training of technicians in the construction of biogas plant include Action for Food Production (AFPRO) and Planning, Research and Action Division (PRAD).

National Project on Biogas Development was launched in the 1980s under the Ministry of New and Renewable Energy (MNRE) to provide subsidies for the biogas plant. The Ministry of New and Renewable Energy pays the subsidy directly to the extension agencies to reduce the cost of construction of biogas plant. Additional subsidies were paid to extension workers by the state government, and loans were provided to farmers to cover the cost of biogas plant by some rural financial institution e.g. Germeen bank. MNRE

allocates the number of biogas plants that each extension agency will install per year. Promotion of the biogas plant was done by the National Dairy Development Board. The installation of biogas plants occurred mainly at the state or local levels by extension agencies and NGO involved in the biogas technology [45].

National Biogas and Manure management programme (NBMMP) estimated that about 4 million biogas plants have been installed. Although there is a variability in the number of biogas installed and maintained. Most successful biogas projects were done by an NGO (SKG Sangha), and a key component of the biogas project is high-quality control and follow-up procedures [60]. A total of 125,000 biogas plants were installed at the end of 2013. Recently small and large-scale digesters were built in India for the purpose of processing food waste into cooking gas [61, 62]. These digesters were installed in household, institution, and markets. Some of the large-scale digesters are used for processing municipal solid waste and by the end of 2009, there are about 15 large scale digesters utilising municipal solid waste to produce electricity.

SNV has been involved in the development and implementation of national biogas programme in various parts of Asia and Africa in the last 20 years. Specifically, the programmes in Nepal and Vietnam have been ongoing for a long time and have received international acknowledgement [63]. The national biogas programmes were implemented through five interrelated approaches adopted by SNV. The first approach is that the biogas programme should be specific to the country situation. This requires preparatory feasibility study in collaboration with relevant stakeholders such as government, civil society and private sector to determine the market potential of domestic biogas, choosing a specific technique design, institutional set-up, and the modalities of implementing the programme. Also, the assessment of the environmental, socio-cultural, economic and institutional aspects is performed in detail. The potential demand for the biogas plants and the challenge facing the current and future service

provides are examined in detail. The inclusion of women and disadvantaged groups are analysed. This provides detailed results on the commercial scope of the programme, highlighting a potential area within the country and providing the first sketch of the programme and its environment, as well as identifying potential key stakeholders. A formal proposal for the national programme is drawn up detailing output target, estimated expenditure, and the budget. The institution that will be responsible for coordinating the programme is set up and the financial requirement is agreed up on before the commencement of the programme.

In the second approach, SNV's long term objective is the development of a commercially viable biogas sector that is sustained by a capable stakeholder and financed without the need for external donor support. This involves direct marketing of the biogas plants to the household by biogas companies on a competitive basis. Providing access to credit facilities to the customer to finance biogas project. A key component is the development of the carbon finance scheme to reduce the financial burden on national and regional governments. The third approach involve the relationship between access to biogas plant by household, and strengthen the organisations and institutions involved in the biogas extension programme. Hence, the development of the capacity of the biogas companies in the technical skill for construction of the biogas plant, quality control, establishment of various training centres, business training for biogas companies, after-sale service, etc. Promotion of the biogas technology involves the implementation of the quality standard. The quality standard is applied in every aspect of the biogas project like the design of the digester, materials of construction, training of technicians, after-sale service, as well as the quality of information made available to potential customers. This is important because a dissatisfied customer or a low-quality biogas plant implies that new potential customer may put on hold or refuse to participate in the biogas project. SNV ensures that the supply side is accountable to the customer and interact with them in order to meet the user-satisfaction while increasing their business. This process involves an

agreement in writing between the programme office and the biogas companies. Quality control checks on all installed biogas plant by an official of the biogas programme office to ensure the plant is properly functioning. The adoption of a multi-stakeholder approach to the execution of the activities is very crucial. Hence, different agencies and organisation are giving one or more activities to perform, except for the operation and maintenance that is performed by the customer. SNV builds on the existing organisation and institutions in a country to promote biogas technology [63].

1.2.1.1 Background of the present study

The application of anaerobic digestion technology in Nigeria is very limited. This is despite the potential of generating 25.53 billion m^3 of biogas, and 88.10 million tons of bio-fertilizer from 542.5 million tons of organic waste generated in Nigeria [64, 65]. Nigeria, the most populous country with the largest economy in Africa is faced with indiscriminate disposal of waste specifically municipal solid waste (MSW) and it is as a result of poverty, poor governance, population growth, urbanisation, etc.[66, 67]. In Nigeria, the current practices in the disposal of solid waste are by burning in designated dumpsite across major cities. In Lagos, there are few recycle plants that recycling paper, plastic, and the other wastes are composted [67, 68]. While, the solid waste management strategy is lacking in Rivers State [67], especially in Port Harcourt, the state capital where solid waste management practices have failed due to poor implementation, enforcement and lack of awareness of the waste management policy [69]. Salami et al [67] reported that 117,825 tonnes of waste is generated in Rivers State per month, and MSW makes up 44.2 percent of the total waste. This quantity of waste is based on the population of Rivers in the 2006 census. Ogunjuyigbe et al [70] projecting the amount of MSW generated in Port Harcourt found that 284,446, and 293,548 tonnes per year was generated in 2017 and 2018 respectively, and it is projected that in 2019, 302,942 tonnes per year of waste will be generated. This figure is based on the population of Port Harcourt obtained from the national

population commission at a 3.2 % growth rate and 0.86 kg/capita/day of waste generated.

Ogunjuyigbe et al [70], found that among the various technology assessed (landfill gas to energy, incineration, and anaerobic digestion). Anaerobic digestion offers a cost-effective means of generating electricity from MSW in Port Harcourt. Therefore, giving the enormous challenge of solid waste disposal in Port Harcourt, the lack of solid waste disposal in the rural area in Rivers State. This thesis is aimed at the application of anaerobic digestion as a waste treatment solution in Rivers State. Anaerobic digestion processes have been adopted in developing countries for the disposal of household and farm waste. Various designs of household or farm digester have been developed such as the fixed dome, floating drum and the plastic bag digester [45]. These digesters are operated at ambient temperature and are affected by the changes in the daily air temperature [71]. A comparison of the price of the digester reveals that the plastic bag digester is cheaper than fixed dome digester and floating drum digester, but it has less durability. Like other digesters, plastic bag digester is buried underground [72], some designs of the plastic bag digester include a greenhouse cover [73]. Other designs of household digester have included a solar collector usually mounted on the cover of the digester [74-77]. However, with plastic bag digester, no study has explored the integration of solar collector and plastic bag digester. Hence, as a first step in the application of AD in Port Harcourt, this Ph.D. thesis will investigate the performance of various design of plastic bag digester. The plastic bag digester is adopted in the present study because it will be easy to install for demonstration purpose in Port Harcourt.

Generally, the household digester is fed daily with the appropriate amount of slurry. The feed is mixed properly, and the inlet pipe of the digester is locked during this process. The feed is mixed with either water or urine and allow to settle for a few minutes before it is charged into the digester. Generally, the feed slurry is mixed in the ratio of 1:1 (one litre of organic

matter to one litre of water). There are different types of feedstock suitable for biogas production, and during feedstock requirement, the amount of water required to mix with the feedstock differs. In the assessment of feedstock for anaerobic digestion process given 2 m^3 of biogas produced per day, estimated that the amount of dung slurry fed into the digester is 50 litres (50 kg). For Jatropha press cake, 1 kg requires 7 litres of water, if the same amount (50 kg) of Jatropha press cake is used, the amount of slurry fed into the digester will be 175 litres. This difference in the quantity of slurry is due to the amount of water added. Hence, suggesting that different types of feedstock require different amounts of water for dilution. The anaerobic digestion process is heavily influenced by the operating temperature. At low operating temperature, more water is required for dilution of the feedstock, increasing the hydraulic retention time of the anaerobic digestion process [78]. The hydraulic retention time of a typical plastic bag digester reported in the literature is within the ranges of 20 - 90 days. However, some reported suggested that the real HRT time for the plastic bag digester is different from the value estimated in the design phase. For example, Marti et al [79] reported a real hydraulic retention time of 80 days compared with 50 days estimated in the design phase, and Marti et al [80] reported an average hydraulic retention time of 120 days. This difference in the real hydraulic retention times is due to the organic loading rate, and the composition of the animal manure. Further, the operating conditions of most plastic bag digesters reported in the literature are based on the use of animal excreta as the main substrate. There are limited data on the performance of plastic bag digester using different substrates such as food waste etc. Therefore, in the present thesis, the performance of the plastic bag digester using food waste and green waste will be investigated in two different locations namely; Port Harcourt and Cuzco. The operating condition such as HRT and OLR with respect to the feedstock will be investigated as well as the impact of weather condition since Port Harcourt and Cuzco represent different extreme temperatures.

1.3 Research Motivation

This research study is motivated by the need to improve the performance of a small-scale anaerobic digestion process. This could be achieved by an improvement in the operating conditions of the biogas digester for which the temperature has the largest influence. The implementation of technology in rural areas has alleviated some of the challenges facing rural communities, such as the need for cooking in an efficient and effective manner, while reducing health risks, etc. The weather condition in Nigeria is not as severe as it is in some parts of the world and it benefits from a very high solar intensity. Hence the study will explore the benefits of implementation of low-cost anaerobic digestion process in Nigeria and particularly in Port Harcourt.

1.4 Research Aim and Objectives

The research thesis is aimed at the application of anaerobic digestion technology specifically rural anaerobic digester as a waste treatment solution in various cities in Rivers state. This is because of the lack of an effective solid waste management strategy in River State, and also as the first step in the development of the biogas programme in the Rivers State. The research objective is as follows:

i. To investigate the performance of different designs of plastic bag digester in Port Harcourt, Nigeria, and Cuzco, Peru.
ii. The performance of the plastic bag digester using food waste, green waste, and pig manure, and the investigation of operating parameters with respect to the food waste and green waste in Port Harcourt and Cuzco.

1.5 Research Methodology

The research methodology involves the use of mathematical models for the simulation of the thermal performance of the digester and the experimental method [81] for the calibration of biochemical models. The mathematical model consists of a thermal model which is coupled with a biochemical model. The thermal of the plastic bag digester is adopted from Perrigault, Weatherford [73] because it is a complete model and allows for the integration of the various heating terms, such as solar, preheated input slurry, etc. The thermal model of the solar collector is adopted from [82].

The ADM1 model [83] is widely used to simulate the biochemical reactions which take place in anaerobic digestion processes. However, the model is too complex in that it requires the estimation of many parameters in order to fully describe the process. There are various simplifications of the model in the literature which includes two or three microbial populations [84, 85]. These models include specific parameters such as VFA concentration, pH, alkalinity and ammonia that influences the process.

1.6 Scope of the Research

The temperature is the most critical factor in anaerobic digestion processes. Hence, maintaining the desired temperature will enhance the performance of the process. The research work is limited to the modelling of small-scale anaerobic digestion processes. A zero-dimensional heat model for investigating the influence of environmental conditions on the anaerobic process (small-scale). The modelling of the effects of different heating technologies such as greenhouse and solar collector. Finally, the thesis will conclude by investigating the effects of the organic loading rate and hydraulic retention time on thermal performance.

1.7 Structure of the thesis

The thesis is organised into eight chapters and a brief description of the chapters is given below.

Chapter 1 starts with an outline of the current need for alternative energy sources to meet the global demand and supply. The key drivers of the implementation of renewable energy such as improvement of energy security and the policies and agreement reached by various organisations and governments in order to ensure a speedy deployment of renewable technology. A brief overview of the application of anaerobic digestion and the small-scale anaerobic digestion technology is presented. The problem statement was developed from where the objectives of the thesis are highlighted. The Chapter ends with a discussion of the motivation and scope of the research, and the structure of the thesis.

Chapter 2 presents a historical review of the global statistics of the world energy from crude oil, gas, coal, nuclear and renewable source. Then, a detailed review of the various forms of bioenergy was presented. A detailed review of anaerobic digestion processes was discussed. An overview of small-scale anaerobic digestion technology was presented. A critical review of biogas extension programme in various parts of Africa and Asia was discussed. The literature review highlighted the influence of temperature on anaerobic digestion process and thermal modelling of the small-scale anaerobic digestion process. A critical review of the anaerobic digestion model was discussed.

Chapter 3 gives the methodology used in this research with a detailed discussion of the modelling and experimental techniques used in the thesis. The thermal modelling of different designs of the plastic bag digester is presented in detail. The experimental and analytical methods were discussed in detail. The Chapter also include the parameter estimation methods and sensitivity analysis method employed in the thesis. Finally,

the general description of the model implemented in Matlab and the procedure for the simulation of the model are presented.

Chapter 4: This chapter is titled “Assessment and parameter identification of simplified models to describe the kinetics of semi-continuous biomethane production from anaerobic digestion of green and food waste”. The aim of the chapter is to investigate the impact of the choice of the reaction rate equation, complexity of the model structure as well as the inclusion of inhibition plays on the ability of the anaerobic digestion model to describe the methane production from batch and semi-continuous anaerobic digestion of green waste (GW) and food waste (FW).

Chapter 5: presents the mathematical modelling of different designs of the plastic bag digester. The chapter is aimed at determining the most suitable design for digester installed in a different location. The thermal modelling of the design of digester was implemented in Matlab to determine the slurry temperature. The slurry temperature is fed into the biochemical model to determine the biogas production rate. The first design is a plastic bag digester without a greenhouse (CASE 1). The second design consists of a plastic bag digester inside a greenhouse (CASE 2), and third design is a plastic bag digester inside a greenhouse with a solar collector mounted on the inlet of the digester (CASE 3).

Chapter 5: This chapter is titled Operational Strategy for anaerobic digestion system in a rural community. The aim of the chapter is to develop the optimal feeding protocol for the plastic bag digester to ensure stability giving the fluctuation in the external temperature. The methodology employed will consist of mathematical model and experiment. The mathematical model employed consists of a thermal model, temperature dependent kinetic model, and the biochemical model.

Chapter 7 presents a general discussion chapter where the results of the thesis are discussed in detail, and compared to results obtained in the literature.

Chapter 8 presents a summary of conclusion and future work**.**

Chapter 2 Literature Review

2.1 Introduction

In 2013, the consumption and production increase for all types of fuels. The increase in the consumption and production reached a record level for crude oil, natural gas, coal, hydropower, and renewables except for nuclear power. Further, the consumption of fossil fuels increased more rapidly than production. This suggests a rapid increase in the global CO_2 emission from energy use. Although the amount of CO_2 emitted remains below the targeted limit. The increase in global energy use was influenced by the emerging economies, but the increase was less than the 10-year historical average value for the emerging countries and above average in the OECD countries. This increase in energy use globally is highest in China, followed by the US. While, the consumption of energy in the EU and Japan fall to the lowest level since 1995 and 1993 respectively [86].

Global consumption and production of the crude increased above historical values by 1.4 % and 0.6 %, respectively, in 2013 compared with 2012. The increase in the consumption and production of natural gas globally rose by 1.4 % and 1.1 %, respectively. However, this value is below the 10-year average of 2.6 % and 2.5 % for the consumption and production of natural gas, respectively. The production and utilisation of coal increased by 0.8 % and 3.0 %. India and China recorded the highest amount of coal utilised, while Indonesia and Australia lead the global production of coal. The generation of energy from nuclear sources increased by 0.9 %. This is due to the increase in the energy output from nuclear energy sources in the US, China and Canada that cancelled the decline in the production of energy from the nuclear energy sources in South Korea, Spain, Russia, and Ukraine. The global production and consumption of energy are driven by increase in industrialization and electrification of emerging economies and non-OECD countries, notably China and India. Further, by sector, the growth in the primary energy consumption still dominated by the industry, signified by the direct and indirect use of energy in the form of electricity.

The industry accounts for more than half of the global consumption of energy according to EIA energy outlook 2040 [87]. The next largest consumer of energy in the form of electricity include residential, service, and agriculture sectors, while the transportation sector contributes a small percentage to the primary energy consumption. However, it is forecasted that the net primary energy consumption by the transport sector will continue to grow steadily at 55 % in 2040; the residential and commercial building will consume 21 % of the primary energy in 2040. The share of world energy consumed by the industry will decline from 69 % in 2015 to 68 % in 2040. While the share of energy consumed by service and agriculture will increase from 18 % to 19 % in 2040.

Energy from renewable sources continues to improve with growth in consumption at about 2.7 %, and the contribution of renewable energy used in the generation of electricity grew by 16.3 % in 2013. Amongst which wind energy contributes about half of the total globally generated energy from renewable sources, followed by solar energy and biofuels [86]. The use of renewable energy will increase in the share of the energy mix as it replaces the primary energy source, for example, coal. The increase in the production of renewable energy sources will increase more than the total energy consumption and will accounts for about 18% and 4.3 % in both OECD and non-OECD countries. Renewable energy will be used to replace the decrease in power generation from nuclear energy sources and the low growth of hydropower generation. Furthermore, the increase in renewable energy for power generation is influenced by effective policy implementation in a different part of EU. Biofuel contributes the lowest to the global energy mix. However, its production increased in 2013, and this is driven by the increase in the production of biofuels in the US and Brazil [86].

Primary energy sources emit carbon dioxide, and the increase in global emission of carbon dioxide between 2012 and 2035 will be 29 % [88]. The non-OECD countries contribute more to the emission of carbon dioxide globally (1.9 %). In OECD countries, carbon dioxide emission is reduced. However, once a country’s Gross Domestic Product increases and it

becomes more advanced; the fuel mix branches out to a more sustainable energy source. The extent of the change in the fuel mix depends on technology, resource endowments, tradability and the economic structure of the country. This results in higher energy consumption and fewer emissions of carbon dioxide as the energy mix push towards the removal of carbon. Biofuels offer the advantages of decarbonisation as a cleaner source of energy produced from several feedstocks of biological origin using several different processes. It is used for heating, electricity, transportation and classified as solid, liquid and gaseous fuels. The solid biofuels include firewood, woodchips, charcoal and wood gas, used for cooking and heating. The application of solid biofuels (traditional biomass) has improved gradually from 27.7EJ in 2005 to about 28.4EJ in 2016. Although, its share in the total global energy consumption has declined from 9.2 % in 2005 to 7.8 % in 2016. Liquid biofuel mainly includes bioethanol, biodiesel. This fuel can be classified base on the types of feedstock used as first, second and third generation liquid biofuels.

United States, Brazil, and EU account for 80 % of the biofuels (Bioethanol and Biodiesel) produced and utilised globally. The production of biofuel increased by 2.5 %, to 143 billion litres in 2017 compared to the year 2016. The largest producers are the United States, Brazil, Germany, Argentina, China, and Indonesia. The biofuel produced in these countries includes ethanol, biodiesel and HVO/HEFA. 65 % of the estimated biofuel produced is ethanol, biodiesel account for 29 %, while HVO/HEFA account for 6 %. The global production of ethanol increased by 3.8 % from 101 billion litres to 105.5 billion litres in 2017. The United States and Brazil account for 84 % of the total volume of biofuel produced in 2017, China, Canada and Thailand contributed the remaining 26 %. The production of ethanol in the US increased by 2.8 % to 60 billion litres following the corn harvest in 2017, and 90 % of the volume produced is utilised in the US while the remainder is exported. In Brazil, the ethanol production was maintained at 28.5 billion litres in 2017, notwithstanding the high price of sugar which favoured the production of sugar. The production of ethanol in China, Canada, and

Thailand in 2017 was 3.3 billion litres, 1.7 billion litres, and 1.5 billion litres, respectively.

The global production of biodiesel spread among different countries in contrast to the production of ethanol. In 2017, 36.6 billion litres of biodiesel were produced signifying 1 % increase in the production of biodiesel compared to 2016. The US account 16%, Brazil 11 %, Germany and Argentina 9 %, and Indonesia 7 %. At the regional level, the highest producers of biodiesel in 2017 is the European Union (EU). The production in the US and Brazil increased to 6 billion litres and 4.3 billion litres, respectively. Furthermore, Germany produced 3.5 billion litres of biodiesel in 2017, Argentina and Indonesia, accounted for 8 % and 10 % of the global biodiesel produced. The volumes of biofuel produced in these countries are 3.3 billion litres and 2.5 billion litres respectively. The global production of HVO/HEFA increased to 6.5 Billion litres in 2017 compared to 2016 production, and its production is mainly concentrated in countries such as Netherlands, Finland, Singapore, and the United States.

Renewable energy contributes 3.1 % of the total global energy consumed in the transport sector. Ethanol and biodiesel provide 2.8 % of the world energy consumed in the transport sector. Liquid biofuels are used in the transport sector as fuel in the conventional engine of cars, trucks, etc. globally. It is blended with fossil fuel or used as 100 % liquid fuel. In 2017, several countries sanctioned liquid biofuel mandate aimed at increasing the amount of liquid biofuel used in transportation. Argentine increased the percentage of ethanol blend in transport fuels to E12, Romania increased the ethanol percentage in the transport fuel from E4.5 to E8. In Zimbabwe, the ethanol percentage in the transport fuel was returned to E10 after temporary reduction to E5. Mexico reduced the amount of ethanol content of its fuel to E10 from E5.8 in most of its cities.

Also, the biodiesel directive was reviewed in 2017, Brazil increases the percentage of biodiesel use in its fuel from B8 to B10. In Colombia, the amount of biodiesel in the transport fuel increases from B8 to B9. In New Zealand, the maximum amount of methanol in fuel increases from 1 % - 3

% and 5 % - 7 % for biodiesel. In the US, the amount of biofuel used in the transport sector varies from state to state. The biodiesel directive for Minnesota will be increased to B20 and will come effect from May 2018.

Further, various government organisations have organised debates on the continuous use of biofuel in the transport sector. Some advocate that it is a solution to the problem relating to climate change and global energy security, while the opposition argues that it is a threat to food supply and could lead to hunger and famine. The contribution of biofuel to the reduction of greenhouse gas emission has been questioned. The controversy surrounding biofuel has reduced the interest in the production of biofuels. Many countries have reviewed the policies regarding food crop for the production of liquid biofuel. For example, the Government of China stopped producing biofuels from corn; Brazil introduced a regulation that allocated land for cultivating sugarcane and palm oil. India shifts her policies towards the production of biofuels from molasses and Jatropha

Liquid biofuel is produced from thermochemical and biochemical processes. The thermochemical process involves the decomposition of biomass at high temperature in the absence of oxygen to produce bio-oil, charcoal and wood gas. Thermochemical processes include pyrolysis, hydrothermal process, etc. pyrolysis is the thermal degradation of organic matter in the absence of oxygen. It is cheap and the most energy efficient processes to produce liquid fuels from biomass [89]. Fast pyrolysis occurs at intermediate temperatures (450-550 ^{o}C), high heating rates (103-104 cs^{-1}) and low residence time of 1s. This is to allow rapid cooling of the volatiles and to achieve a bio-oil yield of 60 - 75 %. The process proceeds in three consecutive stages, the first stage being the removal of free moisture, thereafter the primary decomposition and secondary reaction takes place. In the primary decomposition, various components of the biomass (cellulose. Hemicellulose, lignin, and extractives) under decomposition at a temperature of 200 ^{o}C and 400 ^{o}C to produce volatiles (liquid and gas) and solid.

Collard [90] reported the various processes that occur during primary decomposition of biomass. The biomass is converted to a solid with aromatic polycyclic structure resulting in char formation, the release of monomer structure from the polymers through depolymerisation processes and, the formation of the gaseous compound and several organic compounds from the monomers. The secondary reaction stages of the fast pyrolysis involve the production of liquid and gas product from the unstable volatiles production from the primary decomposition process at temperature 400 ^{o}C. The product of the pyrolysis varies depending on the type of biomass, the pyrolysis reactor design, heating rate, operating temperature, residence time and catalyst. Further, the composition of the pyrolysis product is determined by the structure of the biomass. The decomposition temperature is vital as it affects the quantity of the product and it differs for the different component of the biomass. For instance, the decomposition temperature of lignin is approximately 200 - 500 ^{o}C, hemicellulose decomposes at 220 ^{o}C, and cellulose decomposes at 280 ^{o}C.

Hydrothermal processes involve the conversion of biomass into valuable product or biofuel in the presence of water. The process occurs at the temperature of 250 - 374 ^{o}C and pressure of 4 - 22 MPa. Also, hydrothermal processes take place under self-generated pressure, and it does not require pre-drying of the biomass. Hydrothermal processes occur under two condition; subcritical and supercritical water condition. This condition is a function of the critical point of water. Under the supercritical condition biomass component such as cellulose and lignin becomes soluble, leading to the release of the gaseous product. However, at subcritical condition, cellulose and lignin decompose to form bio-oil. Three stages of decomposition of biomass component occur during hydrothermal processes. Some soluble components of the biomass dissolve in water when the temperature is 100 ^{o}C, and the hydrolysis process takes place at 150 ^{o}C. Biomass component such as cellulose and hemicellulose disintegrate into monomers. Increasing the operating temperature and pressure to 200 ^{o}C and 1 MPa, the biomass decomposes into a slurry.

When the temperature increases to 300 ^{o}C and 10 MPa, the biomass decomposes into an oily product. The hydrothermal process consists of the following processes; hydrothermal liquefaction, hydrothermal gasification, and hydrothermal carbonization.

Gaseous biofuel, consisting of biomethane and biohydrogen, is produced from anaerobic digestion processes. The United State is the largest market for biomethane, and the production of biomethane started in 2015 after it was introduced in the category of advanced cellulose biofuels in the EPA's RFS. The global consumption of biomethane increased six-fold between 2014 and 2016, and by another 15 % in 2017 to 17.4 PJ. In Europe, the consumption of biomethane in the transport sector increased by 12 % between 2015 and 2016 to 6.1 PJ. Germany is the leading producer of biogas in the EU (311 PJ), followed by Italy and the United Kingdom. The biogas produced in Europe mainly comes from landfill 18%, sewage sludge 9 % and 72 % comes from other feedstock such as farm-based waste and industrial organic waste.

A wide range of feedstocks is suitable to produce biogas using AD technology. In Europe, the common substrate used in the production of biogas includes animal manure and slurry, sewage sludge, municipal solid waste, and food waste. Lignocellulose component of biomass collected from agricultural and municipal waste are feedstocks for biogas production. Co-digesting the lignocellulose feedstock with a substrate of higher organic content, produces biogas of higher yield. Other methods employed in the digestion of lignocellulose biomass include feedstock pre-treatment to enhance the degradation of the substrate and the process efficiency. Various treatment processes such as mechanical, chemical, thermal or enzymatic are used to improve the decomposition process.

2.2 The development of anaerobic digestion technology

Anaerobic digestion technology started 100 years ago, and it is applied in waste treatment plants for the stabilisation of the sludge produced after the wastewater the treatment process. It produces methane, carbon dioxide and biomass from the complex organic and inorganic matter in the wastewater [83, 91].

The process requires less energy input and produces less sludge when compared to the aerobic processes, making it more economically attractive. It is characterised by a low yield of micro-organisms, and a longer residence is required for the micro-organisms to avoid wash-out of the micro-organisms in the digester [34]. Two main groups of microbial organisms are involved in the process, Bacteria, and Archaea. Bacteria are predominately in the first three stages of hydrolysis, acidogenesis, and acetogenesis. The archaea are mostly found in the final stage of the anaerobic process. The rate-limiting step of the anaerobic digestion process could be decided by either the hydrolysis or methanogenic step. Hydrolysis is rate limiting when the feedstock used contains more particulate matter. Methanogenesis becomes the rate limiting step when the readily degradable matter is used, leading to an increase in the volatile fatty acids in the digester and in the effluent [34]. Anaerobic digestion processes can be operated as either a dry or wet process; the wet process consists of an influent with a total solid concentration of 1 - 10 %, while dry anaerobic digestion process as an influent concentration of 20 - 40 % total solid.

Proper functioning and stability of the anaerobic digestion process require the understanding of the microbial dynamics; which includes its interaction with changes in the external environment or process disruption. This provides a means to develop process indicators that are used as standard for distinguishing a process that is performing better from a poorly performing process [92]. A better performance of the anaerobic digestion process requires a balance of the microbial population in the system [93], because various species of bacteria are influenced by different types of feedstock and the methanogenic archaea’s are mainly influenced by the

concentration of volatile fatty acids and ammonium ions [92]. Anaerobic digestion processes consist of two distinct but coupled reactions, i.e. biochemical and physicochemical reactions, see figure 2.1.

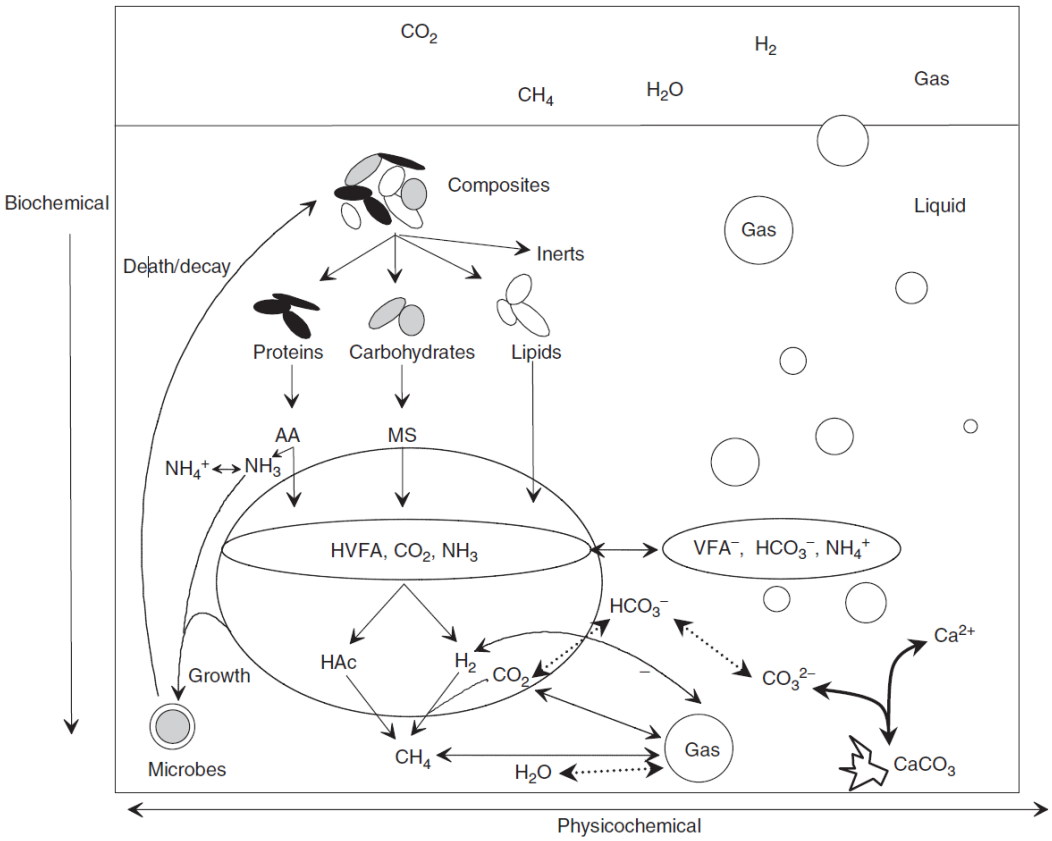

Figure 2.1 Shows the scheme of the biochemical and physicochemical reaction in AD [34].

2.2.1 Biochemical Processes

2.2.1.1 Hydrolysis

Particulate organic matter or complex organic matter undergo depolymerisation and solubilisation and are broken down into the simpler easily utilized substrate. The organic matter is generally considered to consist of particulate carbohydrate, protein, and lipid or as a single homogenous composite compound such as waste-activated sludge [34,

94]. It is an extracellular process consisting of different reactions/or processes which are not fully understood. Hydrolysis of organic matter could be either by releasing enzyme into the body of the liquid or the enzymes are attached to the microorganism [34, 94, 95]. The mechanism of the extracellular hydrolysis process is shown in figure 2.2.

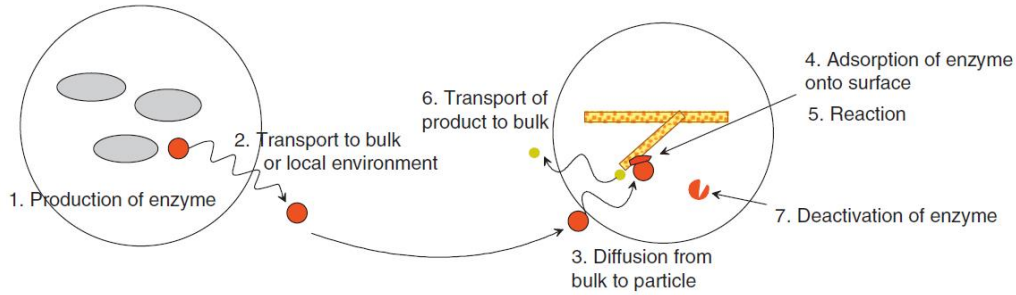

Figure 2.2 shows the mechanism of extracellular hydrolysis process adapted from [34].

The limiting rate of hydrolysis can also be a function of the digester used. When the feed material is pumped into the digester at a high loading rate, without retaining the solid for a continuous stirred tank reactor. Hydrolysis becomes limiting as the microbial cells don't have enough time to solubilise the solids. In the case of a batch and plug flow, it could be due to the reduction in the time and reacting volume of the digesters, respectively [34]. For some primary feedstock, such as; waste-activated sludge, which consist of microbial material, decay products and inert matter which are hard to degrade, hydrolysis thus becomes the rate-limiting stage of the anaerobic processes. The degradability of waste-activated sludge is a function of the age of the sludge [94, 96].

Carbohydrate mainly consists of cellulose, hemicellulose, and lignin, with a trace of tannins, soluble sugar, and ash. Hence, its degradability is mainly dependent on the structure and composition of the constituent of carbohydrate. Feed material, Containing high amount of cellulose or hemicellulose, are easily degraded than feed with a high content of lignin

which are found to be recalcitrant [94]. Generally, for feedstock derived from plants, hydrolysis is the rate-limiting step [97]. Protein is made of various groups of amino acid linked together by an amide bond but differs in function by the type of (methyl) R-group it contains. The degradation of protein is a function of its structural component, which is classified as either fibrous or globular protein. Fibrous proteins are not easily degradable because their structure is protective and connective while globular proteins are readily hydrolysable [94].

Lipids are mostly triglycerides formed by bonding with either long chain fatty acids, alcohol or ester. Hydrolysis of lipids is mediated by hydrolases, known as lipases, very active when they meet insoluble lipids. It degrades the material through the process of adsorption and chemical reaction at the acid-specific lipases and the type of bonds linking the lipids; 1, 3-specific lipases [34].

The first-order hydrolysis rate of degradation of organic matter is often applied in degradation processes since most of the phenomena occurring during hydrolysis are still unclear. This is because the hydrolysis rate is dependent on other factors such as the shape of the particulate organic matter and its bioavailability as well as the origin and acclamation of the inoculum. Nonetheless, it has been demonstrated that a high hydrolysis rate is achievable by considering the inoculum to feed ratio, which proves the dependence of the hydrolysis rate on the biomass concentration [98]. This has led to the development of various kinetic models for the description of hydrolysis of particulate organic matter. Examples include the Contois kinetics which uses a single parameter to represent the substrate and biomass concentration in the kinetic expression and surface-related kinetic expression which is a function of particles sizes, shape etc. [98-102].

2.2.1.2 Acidogenesis

This process is sometimes referred to as fermentation, and it is the further degradation of the products of hydrolysis to simpler alcohols and organic

acids. The organic compounds have dual duties; In one instance, they act as electron acceptors and in another instance, they donate election during the reaction process. The degradation of soluble monosaccharides and amino acids takes places in the absence of an external electron acceptor except for oxidation reaction of long-chain fatty acid which in the presence of an external electron acceptor. Sugar fermentation has been extensively used in the bio-industry to produce foods, drugs, chemicals, and renewable fuels. The process commonly uses pure or specialized microbial cultures in a controlled environment. However, different microbial group is responsible for the fermentation of sugar in anaerobic digestion processes, and the characteristics of the microbial group involved, and the composition of the fermentation product is a function of the process environment [103]. Amino acids undergo fermentation to produce volatile organic acids, such as butyric acid, propionic acid, acetic acid, hydrogen, and carbon dioxide. The degradation pathway for sugar fermentation follows the Embden-Meyer-Parnas pathway [104], while amino acid fermentation occurs either as direct oxidation or coupled oxidation. However, in a normal mixed protein system, the assumption is that the direct oxidation reaction is mostly favoured since it is faster than the coupled oxidation. Only a small percentage of amino acids degrades via the coupled oxidation route, and this is because of the shortage of external electron acceptor during the production of hydrogen and formate. The product mixes from the acidogenesis stage is influenced by the operating conditions, hydrogen concentration, temperature and retention time of the biomass [34]. The oxidation reaction is favoured at low hydrogen and formate concentration as well as under thermophilic conditions.

2.2.1.3 Acetogenesis

This process involved the use of hydrogen or formate in the production of acetate from organic acids and alcohol via oxidation reaction. It requires the maintenance of low concentration of the electron acceptor (hydrogen or formate) for the reaction to be thermodynamically favourable. Hence, the

stage of the anaerobic digestion process relies on a syntrophic relationship with the methanogens for it to proceed. This syntrophic relationship allows for mutual benefits of the microbial group involved, and the process takes place in a narrow concentration of hydrogen. This form of relationship between hydrogen-producers and hydrogen-consumers are commonly found in biofilm digesters, provides easy transfer of election between species, thereby increasing the global process rates.

Apart from the methanogenesis, there exits alternatives route for sinking election produces from the acetogens, and they include electron acceptors such as nitrate, sulphate, iron, and homoacetogenesis. Homoacetogenesis is favoured by a high concentration of hydrogen and the oxidation process is thermodynamically favourable at low temperature.

2.2.1.4 Methanogenesis

This microbial group belongs to the archaea domain, and they are distinctly different with respect to the cell structure, which could be regular or irregular shape of the cell to the short rod and long filaments. Methanogenesis is the final stage of the anaerobic digestion process leading to the production of methane and carbon dioxide from acetate, hydrogen and carbon dioxide. Two class of methanogens in the archaea have been identified, Methanosaetaceae from the group methanosaeta which are strict acetate consumers. Methanosarcinaceae belonging to the group methanosarcina and are involves in the production of methane by consumer hydrogen, carbon dioxide, and methylated compounds.

These two group of methanogenesis have different condition that favours their activity. The methanosaeta perform better when the concentration of acetate is below 10^{-3} M and they are very sensitive to pH and ammonia. Methanosarcina prefers a higher concentration of acetate and they are less sensitive to pH and Ammonia.

2.2.2 Physicochemical processes

This process is a spontaneous non-biological reaction that occurs in water systems. It involves the association and dissociation of weak organic acids, ammonia and carbon dioxide in water, mass-transfer of gases between the two phases (liquid and gaseous), and the precipitation of metallic ions in the solution. Because of the spontaneous nature of the physiochemical reaction (reversible), an equilibrium calculation is used to evaluate it. The states are generally expressed by the pH or the negative logarithm of the hydrogen ion concentration. The physicochemical reaction is used to describe the summation of the balance of strong and weak acids present in the reacting system and not the individual concentration of the reacting substance.

The products of the biochemical reaction provide the link between biochemical reaction and the physicochemical reaction. This is because, at very high concentrations, the free form of the weak acids and base, as well as their individual concentration are used to determine the pH of the reaction system. At low pH, there is a break in the metabolic equilibrium of the microorganism and modification of the enzymes. Further, the physicochemical reaction determines the buffer capacity of the anaerobic digestion process as the weak acid or base can be resisted when their acidity coefficient is about the same system value as the pH.

The temperature is another key factor in the understanding of the anaerobic digestion process. It exerts the most influence on the performance of the anaerobic digestion system as different microorganisms respond differently to changes in temperature (i.e. some are psychrophilic, mesophilic and thermophilic) with the optimal digester performance at the mesophilic temperature [83]. Recently, there has been an increase in research into the effect of the ambient temperature on anaerobic digestion for the purpose of providing energy for cooking in rural communities [72].

2.3 Small scale anaerobic digestion processes

Biogas technology has been Implementation in most developing and under developing countries as an alternative solution to the use of cattle dung, crop residue, firewood and coal as fuel for cooking. The burning of these materials has a negative influence on the health of the household. The World Health organisation reported that solid fuels are the cause of 1.5 million premature deaths annually, and this link to the indoor air pollution associated with the use of solid fuels [42]. In rural areas, most households prepare their meals using firewood and dung cake. The use of these traditional fuels produces obnoxious smoke and particulate that pollute the environment, causing several respiratory diseases. Most households are in direct physical health risk due to indoor air pollution and the incomplete combustion of biomass increases the risk of respiratory diseases such as acute lower respiratory infection. It also increases the risk of bronchitis, asthma, lung cancer, ear infection, etc. [105, 106]. Firewood burning, which is common in rural communities, is the principal cause of indoor air pollution. Biogas provides clean and smokes free energy, unlike firewood. Thus installation of biogas helps to reduce indoor air pollution and hence reduces the incidence of respiratory diseases [106, 107]. This is due to the introduction of more efficient biogas cooking stove that reduces the amount of particulate and smoke emitted. An improved sanitation level is another health benefit. Installation of biogas plant motivates households to construct toilets which reduce the risk of several diseases such as worms, bacterial diseases and viral infections [44, 106]. The linking of the latrine to the biogas plant offers an effective treatment of human excreta, reducing diseases such as gastrointestinal associated with night soil. Biogas digester ensures meals are properly cooked and drinking water boiled to reduced water-borne disease [108].

The high cost of fossil fuels and chemical fertiliser when these products get to the rural communities is another reason for the development of biogas technology in developing countries [109]. The dissemination of the biogas technology has resulted in less use of firewood thereby saving the forest

from deforestation. This is because one cum meter of cattle manure produces 22.5 m^3 of biogas, and one cum meter of biogas is equivalent to 5.5 kg of firewood [108]. The use of biogas plant also saves around 2,00 kg of wood per year, and the installation of 1,000 biogas plant resulted in the saving of 33.8 ha of the forest free from harvesting of wood [45].

Biogas technology improves the agricultural practices in the rural communities because it provides bio-slurry rich in the concentration of Nitrogen, Phosphorus and Potassium. The bio-slurry improves soil condition as the microbial organism already present in the slurry are added to the soil. This increases the breakdown of biomass material in the soil and increase in the nutritional value of the soil. While reducing the presence of the pathogen or any harmful chemical in the soil. The bio-slurry contains more lignin component of the organic matter and when added to the soil increases the soil ability to retain moisture and nutrient [45]. In US, the bio-slurry is separated into the liquid and solid component. The solid component is then used as bedding material in animal farms [110], and liquid component is applied in fish farming to grow algae that serve as fish feed [111].

2.3.1 Social aspects of the biogas technology

The way domestic duty is performed, and how it is done is first considered. Cooking in rural area is usually done using firewood or dung. Dung is used mostly to provide energy for cooking, it is important to analysis the number of households that own animals and the number of animals owned [43]. If the domestic animal is owned by nomadic, it will be difficult to deploy biogas technology. The other factors that contribute to the acceptance of biogas technology is the age of the household, household size, level of education, and traditional fuel. The more the household increase in the level of education and age, the adverse effect it has on the biogas technology. As educated people earn more income, they tend to look for an alternative source of energy that is suitable to their social class. The availability of land for the construction of biogas plant needs to be considered, as biogas once

installed can be operated for a number of years. Hence, it means that formal approval for the title of the land is necessary. The type of farming practice is another key issue that may affect biogas adoption. For community practicing graze farm, it means that the cattle are allowed to wander, and this makes it difficult for the collection of dung to feed the biogas plant.

Local perception of biogas technology has an adverse effect on its uptake. This is the case in Nepal where it was perceived that biogas plants installed were the cause of the spread of mosquitoes. Religious or cultural beliefs are also a factor that may limit the social acceptance of biogas technology. An example is the refusal to use pig manure in the biogas plant because of the religious belief of Jewish and Muslims [108, 109]. In India and Nepal, the use of cow dung is acceptable for feeding the biogas plant, because the cow is considered as a holy animal. However, they frown at the use of pig manure or human faeces for feeding the biogas plant. Also, people find it hard to connect their latrine to the biogas plant, although this has been overcome. In Vietnam, the bio-slurry obtained from the biogas plant can be applied to fish farming [109, 110]. While in Ethiopia, this is impossible due to social or cultural belief [109, 110].

2.3.2 Technical aspects of biogas technology

In order to establish a national biogas programme, the technical potential of the location needs to be examined. Technically, a location or community is suitable for biogas deployment if there is an abundance of feed material and water, locally available materials of construction, and availability of land. Also, the location should be free from natural disasters like floods and earthquakes.

Temperature is a factor that affects the biochemical process and it is important that the location has an average ambient temperature that will ensure stable operation of the digester. A feasibility report of the biogas programme of Ethiopia found the temperature in the range of 15 - 20 ^{o}C

[112], while in Tanzania there is a variation in the ambient temperature from 3 ^{o}C in Mbeya to 35 ^{o}C in Kilimanjaro [113]. The availability of dung for feeding the biogas plant is a function of the number of livestock owned by the household in rural areas. It plays a key role in assessing the technical potential of biogas technology. In Bangladesh, there are 22.29 million cattle/Buffalo and about 116,000 poultry farms. Furthermore, it is reported that each household must own a minimum of 3 - 5 cattle enough to produce dung essential to produce 3 m^3 day^{-1} of biogas. In Tanzania, the technical potential of biogas based on livestock shows that 1.3 million household keep over 17 million cattle, and 350,000 farm household keep over 1.1 million pigs [113]. In the Amhara district of Ethiopia, the biogas potential of 716,000 installation capacity was estimated from the survey of the number of livestock owned by the household in this region [112].

Water is used to mix the dung before feeding the digester, it is an important parameter for the deployment of biogas technology in rural areas. At minimal feeding, the average quantity of water require is 25 litres per day for small installation and over 100 litres per day for a large installation. To ensure the proper functioning of the biogas plant, the source of water must not be more than 20 minutes walking distance from the biogas installation. Although, there is a district that is far away from the source of water, and these were key concern in Ethiopia as the country sometimes has severe drought [112]. The use of urine from the animal stable has been explored in a region where there is drought. CAMARTEC ensured a proper design of the stable for the collection of the urine produces from the livestock's; while MIGESADO included a water harvesting system into the biogas project to ensure the biogas plant lack no water during the period of drought [113]. Other means of providing water to maintain hydraulic of the system include; connecting the toilet to the biogas and the use of low-quality water obtained from the washing of animal or cleaning vegetables.

Feasibility study performed found that there is ample space enough for the installation of a biogas plant. Likewise, the construction material is readily available in the villages except for the plumbing material that is sometimes

obtained from the city [112]. The decrease in the construction of biogas plant by Centre for Agricultural Mechanisation and Rural Technology, Tanzania (CAMARTEC) led to a reduction in the number of skilled masons required for the construction of the biogas plant. Hence, for the biogas plant to be adequate for the local area, training of mason is essential.

2.3.3 Environmental impact of biogas technology

The dissemination of biogas technology offers some environmental benefits including the provision of a sustainable energy resource and the improvement of soil using the liquid by-product. It is a waste management solution to treat waste and recover valuable organic material, thereby reducing the impact of the greenhouse gas emission and land use for the disposal of organic matter [114]. However, the methane component of the biogas has a greater global warming potential than carbon dioxide [43, 115]. The anaerobic digestion process also contributes to the emissions of greenhouse gases through the leakage of methane from the digester inlet and outlet pipes, and the gasholder, etc. Also, from other sources such as bio-slurry when it is applied to arable land and the solid residue that is applied to the soil. Greenhouse gas is emitted from the tools and labour used during the biogas plant installation processes. There is leakage of slurry from the slurry pit if not lined properly causing groundwater pollution. Although this might not be possible, it is important that a minimum distance away from the water source should be allowed for the installation of the biogas plant [113].

In developing countries, the environmental sustainability of the anaerobic digestion process is focused on the recovery of renewable energy, but not on the labour, material, etc. that is used in the production of the biogas plant. It has been reported that there is a limited study on the life cycle analysis of the material used in the construction of domestic biogas plant and its impact on the carbon emission [45]. This reveals the absence of considerable environmental best practices in the deployment of the biogas

plants in rural areas. Since the digesters are operated with fewer technique, it requires an all-inclusive regulatory model that covers every aspect of the anaerobic digestion process. The aspects of anaerobic digestion that requires regulation include; pre-digestion, and efficient handling of the liquid component of the digestate and post-digestion of the solid component of the effluent [116].

Recently, emergy analysis have been applied to investigate the environmental sustainability of the anaerobic digestion processes [117-119]. Emergy is the total amount of energy from renewable and non-renewable sources that are required to produce a product or service. Emergy analysis is a measure of all renewable, non-renewable and purchased inputs to a system on the common basis of solar energy equivalents.

Ciotola, Lansing [117] reported the emergy analysis of a small-scale digester operating at ambient temperature in order to access the environmental sustainability of the digester when it is used for either biogas production or biogas production and electricity generation. The emergy input was classified as renewable resources such as solar, water, wind, and manure, non-renewable and purchased resources. While, the output of the system includes biogas, nitrogen, and phosphorus. It was found that both cases (gas production alone and biogas production and electricity generation), the use of the digester is sustainable. However, the environmental sustainability index for the biogas production system is much lower than for biogas production and electricity generation. In a similar study, the emergy analysis was performed to investigate the environmental sustainability and economic performance of an integrated eco-agricultural system with more than one product [118]. Evaluating the emergy-based index and ratio, a joint transformity and weighted average of the transformity and new emergy-based indices were applied. It was found that the integrated system is environmentally sustainable as the environmental loading ratio is low compared with the independent production system. This same result was achieved by Wu, Wu [119] for an integrated system

consisting of the plant (walnut and grains), animal (pig and poultry) and biogas digester. Emergy-based indices evaluated include the recycle benefit ratio factor which determines the ability of the system to replace external input material. Having explored the environmental benefits and constraints of anaerobic digestion processes, its economic benefits and associated cost of investment of biogas plant is important.

2.3.4 Economics aspect of the biogas technology

The economic impact of rural biogas plant is focussed on the cost savings derived from the installation of biogas as opposed to the use of traditional energy sources such as kerosene, firewood, cattle dung, etc. This is attributed to the return on the investment derived from the installation of the biogas plants in most developing countries [42]. Another key impact of biogas plant is the engagement of both skilled and unskilled labour. This opens employment opportunities for masons, plumbers, civil engineers, and agronomists. Further, the construction and installation of appliances that utilize biogas and control equipment specific to the operation of a biogas plant are other key areas of employment opportunities [114].

The use of the liquid fraction of the digestate that is rich in organic fertiliser can replace chemical fertiliser used on the farmlands. This reduces the importation of chemical fertiliser and cost saving [114]. Hence, the main reason for the installation of biogas plants on agricultural farms [119]. For biogas plants to gain economic sustainability, there is a need to provide the farmers or household with complete information about the cost of the installation of the biogas plant, materials for construction as well as the cost relating to the maintenance [120]. This is important as it influences the adoption and development of the biogas digester, and determine the size of the digester that will guarantee a positive return in the investment for the user [121].

Subsidizing the cost of the biogas digester construction is another key success in the widespread implementation of biogas digesters in a rural area. An example is an increase in the installation of biogas plants in Nepal,

due to policy that encourage the importance of subsidy in the national biogas program. The subsidy structure allowed for access to funds for the installation of smaller biogas plants. Further, the subsidy policy encourages the entry of commercial entities to provide soft loan programs for the people interested in the construction of biogas plants. Farmers, as well as householders, were encouraged to make financial commitments towards the initial investment cost of the plant [122]. Elsewhere in China, the government as part of its strategy to boost the installation of small biogas plants have made commitments to pay for two-thirds of the cost of the digester while the user pays the balance [43]. There are three key issues to consider in the evaluation of the economic viability of biogas digester and these include; (i) the precise amount of feedstock that is of potential use, (ii) the percentage of the useful resource recovered and (iii) the market value of the products recovered [121, 123].

The type and size of household or farm scale digesters influence the cost of the digester, and it is a function of the geographical location. For instance, the cost of a 6 m^3 Chinese type digester in Nepal varies between 340 - 400 USD [50]. In Thailand, the cost of a 1.2 m^3 digester is 180 USD. For a 0.225 m^3 digesters the cost varies by location, for example in Peru, the cost of the digester is 250 USD [124]. in Costa Rica the same size of digester is worth 300 USD [72] and in India, the cost of a 1-6 m^3 digesters range from 200 - 400 USD [43, 125]. Singh, [126] performed an economic assessment of different types of family digesters (KVIC, Janta and deenbandhu) with different sizes. The study was performed in Punjab, India, under the National biogas programme sponsored by the Ministry of Non-conventional Energy Sources (MNES). The assessments included the cost of construction and installation, the cost associated with operating the digester and the revenue realised from the sale of biogas and the liquid slurry. The annual profit and the payback period are criteria used for the economic assessment. It found that amongst the digesters, the deenbandhu type is most economical. An increase in the size of the digester has an inverse relationship with the payback period as larger digesters have a less payback period than smaller digesters. Axaopoulos

and Panagakis [127] Examined the economic viability of the solar assisting biogas plant to meet the heating requirement. The economic index used is the initial investment cost, operating and maintenance cost, interest rate and income from the use of the biogas. Evaluating the economics of the digester based on the amount of biogas produced, the profitability index and utilisation factor are used. It was found that at a discount rate of 10 %, and a utilisation factor of 25 %, the digester is economical when the cost of replacing fuel is 4.3 cent Kwh. The profitability index revealed that an investment cost of less than $ 9000 for the digester system is economical. The investment cost consists of the cost of installing a 76 m^3 biogas plant, solar heating system, compressors, heat exchanger and labour.

Adeoti, Ilori [128] Performed an economic assessment of the benefit of a biogas plant in Nigeria. The cost estimation includes construction, facilities, and installation cost, labour and land cost, the cost associated with purchasing feedstock, treatment of the biogas and household labour cost, operational and maintenance cost. The present net value, internal rate of return, benefit-cost ratio and the payback period are criteria used to evaluate the economic benefit. It was found that for a 6m^3 digester the payback period is 6.6 years which implies that the net risk associated with the investment in the biogas plant is low.

Rejendran et al [129] reported the economics of a house digester made from textile material in Sweden. This study was sponsored by Sparbank Foundation, and Boras energy and environment. In the assessment, the biogas is used to replace LPG and kerosene, the most commonly used source of energy in developing countries. The capital cost of the digester (1.5, 2.0, 3.0 and 4.0 m^3) was calculated, with the operating costs being 8 % of the capital cost for the case of subsidy and non-subsidy of the fossil fuels and the installation of the digester. The net present value, payback period and internal rate of return are the bases for the assessment. It was found that the replacement of fossil fuel by biogas is economical under condition of subsidy and without subsidy, respectively. Furthermore, it was also found that changes in the operating cost, cost of kerosene and LPG

and the discount rate have a positive impact on the economics of the textile digester. Using linear programming, [130] performed an economic analysis of the profitability of a small-scale farm in Ontario, Canada, based on the national feed-in traffic. The study was funded by the Natural Sciences and Engineering Research Council of Canada. Statistical analyses were performed to determine the number of animals, and the size of the dairy and beef farm, respectively. Then the amount of biogas production per livestock and the energy potential for each farm as well as energy potential for all the farms considered was estimated. The measure of the profitability was based on the return on the investment and the payback period. The results show that for the dairy farm, the profitability requires less than 40 cattle while the profitability for the beef farm requires more than 70 cattle. The sensitivity analysis shows that the biogas production rate, electrical efficiency and the use of activated carbon all affects the profitability while the additional benefit from the sale of fertilizer has no effect.

Amigun and Blottnitz [131] performed an analysis to investigate the relationship between the investment cost of the small-medium digesters and the size of the digester in various countries in Africa. The study received support from AGAMA energy, South Africa, Kigali Institute of Science and Technology, Rwanda, and the Ministry of Energy, Ghana. The capital investment cost of digesters and capacity was collected from over 21 installed digesters. Using the least square method and the cost estimation model, an exponential plot of the investment cost against the digester size was performed. The cost-capacity factor was determined, and its quality was measured using a t-test. The strength of the relationship between the plant capacity and the investment cost was determined as well as the standard error between the measured and observed value. It was found that for small-to-medium scale digesters, an increase in the plant size or capacity increases the investment cost at the cost-capacity factor n=1.20.

Amigun and von Blottnitz [122] presented the impact of biogas plant capacity and its location on the cost of a biogas digester. Various data on

the cost of a biogas plant and its associated capacity and location were collated for the analysis. Using the least squares method, the digester size against its cost was plotted and it was found that for small size digesters less than 20 m^3, there is a proportional relationship between the digester size and the capital cost of the digester and this is due mostly to the slow deployment of the biogas technology in Africa. However, in the case of a digester size greater than 20 m^3, an inverse relationship exists between the plant size and its cost. It was further observed that the location of the plant has no control over its cost.

Klavon, Lansing [110] performed a feasibility study to assess the economics of small-scale dairy farm in the US. The study was funded by the Maryland Water Resource Research Centre and the USDA Beltsville Agricultural Research Centre. 16 dairy farm systems were considered, comprising of 9 existing dairy farms digester and 7 theoretical digesters. Some digester systems include a solid separation system, while others are without solid separation system. Also, some digesters have generators, while others are without a generator. The annual cost of the digester system was estimated from the initial investment cost of the owner and interest from loan or grant from the government, etc. The operating and maintenance cost are considered to be 3 % of the annual cost for the system with boiler installed and 5 % for digester system used to generate electricity. The annual revenue comprises of earnings from the electricity generation, sale of digestate, and carbon credit, tipping fees and the offset of the cost of natural gas resulting from the use of biogas. At a discount rate of 4 % and 8 %, giving a useful life of 20 years. It was found that there is a negative return on investment for all the digester system investigated. A positive return on investment is possible for the farm with 250 dairy animals when the annual cost is subsidised. Further, for a farm with less than 250 dairy cows, the installation of an anaerobic digester is economical with the addition of a tipping fee.

Anderson et al [132] developed a decision-making tool to assess the financial feasibility of farm anaerobic digesters in Ontario Canada. The

study was funded by the Ontario Ministry of Agriculture, Food and Rural Affairs (OMAFRA) and the Dairy Farmer of Ontario (DFO). The study found a positive return on investment for large scale dairy farm, running biogas or biogas and diesel. The study also evaluated the economics of the farm-AD system when external organic matter co-digested with the cow manure and found a positive return on investment when solid grease and vegetable waste is used.

Walekhwe et al [121] assessed the economic viability of various sizes of anaerobic digester plants in Uganda. This study is supported by the Swedish International Development Cooperation, South African Renewable energy Council, and the UK Department of International Development (DFID). The payback period, net present value and internal rate of return are use as the criteria. It was found that giving a discount rate of 12 % and 24 %, all three sizes of the digester (8 m^3, 12 $m^{3,}$ and 16 m^3) evaluated gave a positive net return on investment. The result further showed that a lending rate below 36 %, 37 % and 39 % for digester sizes 8m^3, 12 m^3 and 16 m^3 is economical for the household.

The development of biogas technology rural area is a result of a commitment by the various government of the developing countries to the millennium development goal of access to clean energy. And, it has been possible through the collaboration with various international organisation such as the SNV, HIVOS, and DCIS in setting up regional and national biogas programmes in various parts of Africa and Asia. This will be discussed in the following sections.

2.3.5 National Domestic biogas programme

The national domestic biogas program have been implemented in various part of Africa and Asia, with the aim to develop biogas technology so that millions of families will benefit from it. The key feature of the program is the development of a viable biogas sector that is self-financed. The national program required the inclusion of various stakeholders to perform functions necessary for the programme to succeed see figure 2.3.

The start of the biogas programme generally requires the assessment of the factors for effective implementation and management of the programme. This includes the experts who have used the technology and can provide training for others. It is very useful to examine if biogas technology is appropriate for the intending community or district. The availability of the local resource for its implementation such as construction material, and individual to train in the construction of the biogas plant .

Generally, a feasibility study is performed to obtain the information required to start the programme. The external expert visits to meet with key stakeholders in the community or district. This includes government organisations, NGO, and a local group that are already involved in biogas technology or are essential for the implementation of the programme. This is usually done on the request of the local organisation such as government department/ NGO to the external organisation such as SNV/HIVOS. Questionnaires are used to collect general information needed to assess the potential for the successful implementation of the biogas programme in the district. The assessment survey also takes into consideration key issue such as social, technical, environmental that is essential for the development of the technology in the intending community or district.

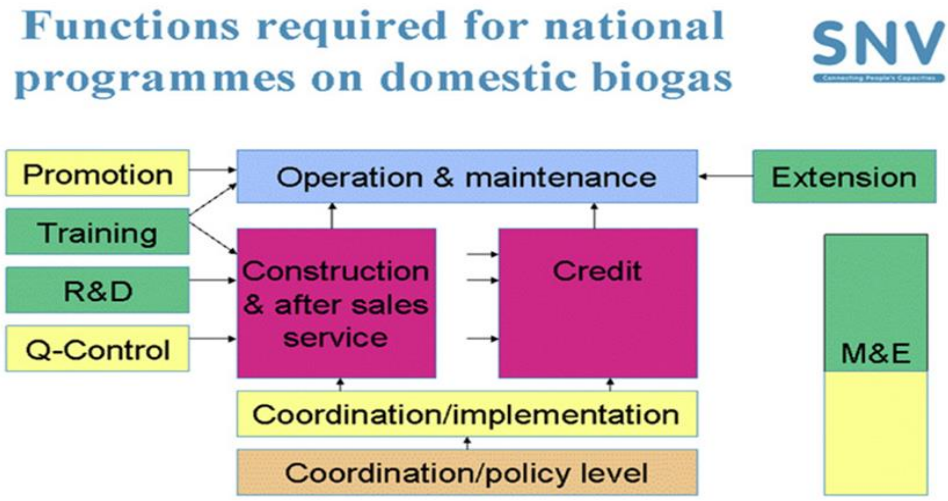

Figure 2.3 Shows the SNV programme functions [133].

2.3.5.1 Functions of the National Domestic Biogas Programme

2.3.5.1.1 Promotion and Marketing

The introduction of the biogas technology usually starts with the dissemination of information about its benefits. This is done through various means such as radio and newspapers. In Vietnam, the promotion of the biogas technology was done using public speaker fitted at different point in the village . In all provinces in Vietnam, video clips are made to display the development and achievement of the biogas technology. [134]. Biogas plants fitted on the back of a small truck is used for the promotion of the technology in schools and rural agricultural events. The printing of poster, leaflets and biogas newspaper were distributed by the extension works to individuals at the promotional workshops and public area. The posters consist of information about the benefit of biogas technology in relation to the health and the use of bio-slurry in agricultural practices. The leaflets contain information on the safe operation of the biogas plant, and the newsletter containing information on the progress of the biogas projects and innovation [134].

The word of mouth is the more effective method for spreading the benefits of biogas technology. As the satisfied user of the biogas technology is eager to tell his/ her neighbour about the benefits of the technology. Also, a site visit to a biogas plant in operation is another strategy for disseminating the biogas technology. The promotion and marketing activities of the domestic biogas programme are generally managed by the National biogas programme office in collaboration with the local Biogas office, the Biogas Construction Enterprise, etc.[135, 136].

2.3.5.1.2 Training

The quality of the biogas plant installed in the national biogas programme depends on the quality of training provided to the mason. The training includes technical training, training for programme partners, training of potential users and the training of trainer. And the strategy is to outsource

the training to various vocational training institutes and liaising with them to set up biogas training courses. In the various programme, the training programme differs in the number of days required for training of mason and supervisor. In Bangladesh, an average mason requires eight weeks consisting of one-week theory and seven weeks practical, and the training of supervisor has a duration of four days [137]. The mason training has a duration of eleven days spilled into one-day theory and ten days practical, and supervisor training has a duration of five days in Kenya [138]. The mason training in Ethiopia has a duration of twenty to thirty days, it consist of ten days in the technical vocational education and training centre, and ten to twenty days training in the building of the biogas plant at the field level [139].

The mason is usually trained in the construction, operation, and maintenance of the biogas plant, and preference is given to mason that is experienced in the construction of the biogas plant. Also, it is important for individual participating in the training to have 1-year experience in building. Training is provided in the aspect of promotion and marketing of the biogas plant. Financial institutions (both local and national), non-governmental organisation, and other key stakeholder are trained in relation to their role in the national biogas programmes. The training involves the basics of the biogas technology, quality standard, promotion, and extension services [136-139]. The managers of the biogas field office and construction enterprise are trained on various aspects of the national biogas programme covering business and programme management, marketing and promotion, and quality management [136-139]. A training programme is conducted for those responsible for training the mason and supervisors. The regional office also organises training at the district and community level for local extension worker in the promotional activities and the bio-slurry utilisation [139]. A key strategy of the training programme is the promotion of gender integration as more women can participate in the user training and training of trainers. The women receive training in decision making, application of loan and repayment of the loan, and biogas related income generation activities, health, and sanitation improvement. The

biogas user training is done during the construction and operation stages of the biogas plant and in the application of the bio-slurry [136-139].

2.3.5.1.3 Quality Control and After-sale Service

Ensuring the loans borrowed by the customer is repay to the banks, and that construction companies receive payment for their services. The biogas plant constructed must meet the standard in terms of quality of construction that is set by the biogas programme [45]. The main duty of the domestic biogas programme in Asia and Africa is to guarantee the delivery of high-quality biogas plant by the construction companies and mason. Mason working with the construction enterprise were given proper training as they work together with experience mason. And the quality of the materials used during construction must be checked by the supervisor from the biogas office [45].

The increase in the number of plants installed especially in Nepal is traced to the quality of constructed biogas plant [45, 46]. The high-quality standard of the biogas plant raises the confidence of the user. In cases where the biogas plant is faulty, the mason team are always available to fix these faults. As part of the quality management, regular plant inspection is performed on the plant constructed. The biogas support programme uses 66 parameters during plant inspection, under three heading according to the severity of the error found on the plant [45]. The quality control is focused on proper reporting, information gathering, application and quality control procedure. The quality control report is used to develop curriculum for the training of staffs or mason and to provide a remedy. It is also used to provide feedback to construction enterprise, and for grading and dismissal of construction enterprise that performs below the standard [138].

As part of the quality measure, various biogas programmes adopt and develop a design of the biogas plant that is suitable for the location. In Nepal, the original design used in the biogas programme was the GGC fixed dome and the Deenbandhu design. Nevertheless, they were modified into the simpler design in 1992 and 1995 respectively. The lack of quality

standard lowered the confidence of the biogas technology, and for the different biogas programmes, it took years to overcome this challenge. The adoption of a quality standard by the Chinese biogas programme and its enforcement by the biogas companies improved the perception of the biogas technology [45, 140]. Tomar [141] reported that out of the 24,501 digesters plant installed in the biogas programme in India, 53 % of them are functional, and 48 % had technical defects. This is because of the faults in the digester foundation, inlet-outlet chamber, and digester wall. While operational and incomplete digester installation is responsible for the defect in about 13 % and 12 % of the installed digester. According to [45, 142], a survey of 615 plants that was supposedly built, shows that 81 % is still under construction. 61 % percent of the complete biogas plant is functioning properly. In Bangladeshi, a survey carried out on 66 plant shows that a very small percentage of the digester installed are working and in good condition. Majority of the 66 digesters are either working but have defects or are not working and in a very bad condition [143]. The lack of the preliminary study of the soil before the construction of the digester is another cause of digester failure [144]. In most cases, the user lacks the ability to identify the reason for the failure and take appropriate steps to eliminate it. The inability to meet the expectation of the biogas technology, the lack of basic knowledge by the biogas plant owner, and post-installation also contributes to the limitation of the biogas technology. Since most of the masons cannot be accessed after the digesters have been installed [144].

Some organisation such as SKG Sangha in India have demonstrated that an effective quality-control process can lead to a high success rate of biogas technology. This is because they employ construction workers living within the district or community, and this makes it easy for the client to contact them when there are faults in the biogas plant. Also, priority is given to quality control and after sale service. Kigali Institute of Science, Technology, and Management were successful in the installation of biogas in the prisoner by placing emphasis on quality and reliability of the design.

They also train the prison inmate in the construction of the biogas plant [145].

2.3.5.1.4 Finance

The introduction of biogas technology implies an investment in new capital as per economics. This investment is expected to generate a financial return for the investor (Household) in terms of an increase in income or saving on expenditures. Generally, it has been reported that the cost of investment in biogas plant in a rural area is very high, and low-income household cannot afford the biogas plant.

The investment cost of the biogas plant varies for different location or country, and it is a function of the size of the biogas plant. The average size of the biogas plant constructed range from 2 - 12 m^3. For instance, the cost of a 6 m^3 Chinese type digester in Nepal varies between 440-560 USD [42], and in Tanzania, the biogas plant could be constructed at the cost of $ 928. In Thailand, the cost of a 1.2 m^3 digester is 180 USD. For 0.225 m^3 digesters the cost varies by location, for example in Peru, the digester costs 250 USD [124], while in Costa Rica the same size of the digester is worth 300 USD [72]. In India, the cost of 1-6 m^3 digesters ranges from USD 200-400 [43, 125].

To ensure the household/farmer can afford the upfront cost of the biogas plant, the cost of the biogas plant is subsidised by the national government. Generally, a flat rate subsidy is applied irrespective of the digester size. The digester sizes between 2 - 8 m^3 are approved for the subsidy. The provision of the subsidy has been in collaboration with different financial institutions. In Nepal, the Agricultural Development Bank is involved in the administration of loan and subsidy through their various local offices [146]. In Bangladesh, the various biogas projects received a subsidy from both government and other organisation involved in the project. BCSIR provided subsidy to motivate potential plant owners to install biogas plant during the first (BDT 5,000) and second (BDT 7,500) phases of the biogas

programme. LGED also reduced the cost of installation by providing a subsidy of BDT 5,000 as a motivational incentive to encourage plant owners to install biogas [147]. In Cambodia biogas programme, the subsidy was provided by SNV. However, as SNV withdraws from the biogas programme, other organisations such as Energizing Development (EnDev) and People in Need (PIN) stepped in to continue providing subsidy for the biogas programme [148].

Despite the provision of subsidy, the investment cost of the biogas plant remains high. Therefore, in addition to the subsidy, credit is giving to the rural household to complete the initial investment cost of the biogas plant. This has been provided by the various local cooperative organisations and financial institution [149]. Recognizing the challenges faced by the rural household in Rwanda, SNV/National domestic biogas programme partnered with Banque Populaire du Rwanda (BPR) to provide credit facilities to the rural household. A 6.5 years finance grant was provided by the Dutch financial institution to BRP to provide a 3 years loan scheme for biogas installation [150]. In Cambodia, loan for biogas plant installation was provided by the Improved Group Revolving Funds with the support of the International Fund for Agriculture and Development and the Asia Development Bank. The Improved Group Revolving fund is the local initiative aim to assist more family have access to the biogas plant. The loan was provided to the farmer/household at 2 % interest and does not require collateral [148].

Recently, Carbon Finance has been used to fund most domestic biogas programmes. Carbon financing of the biogas programme has been successfully carried out by Biogas support programme of Nepal in 2005, despite changes in the policy used to obtain the fund. The success of the biogas support programme has encouraged other countries in Asia [45] and Africa to apply for carbon finance in the voluntary emission reduction market [151]. Furthermore, the fund from Carbon finance is not only used for subsidizing the cost of the biogas plant; it is also used for other programme activities such as after sale service, quality control and

management, staff capacity building and the training of household on the operation and maintenance of the biogas plant [151]. The criteria for the application of the carbon finance in various biogas programme lies in the reduction of greenhouse gas emission as biogas is used to replace the conventional cooking system (firewood) and the modification of the existing manure management practices.

2.3.5.1.5 Research and Development

Most successive biogas extension programme have relied on research and development. The involvement of a different group of researcher like Luo Guoruri [152], The work of J.J. Patel and Ram Bux Singh [57] have resulted in the development of the various design of the biogas digester. This digester designs are the foundation of the various designs of digester used in the biogas extension programme in Nepal, Vietnam, and Rwanda, etc.

In the past, research and development activities are usually ignored once an effective digester design has been developed. An example is the development of a biogas plant to utilise manure from animal and food waste generated from household or institutions. The development of biogas burner in Nepal in the early 1970s. Once the design is effective working and standardised, the biogas programme makes no further improvement of the design of the burners and the digesters. The consequences are that most programmes fail to respond to new opportunities in the development of biogas programmes [45].

Research and development have played a major role in the improvement of the biogas extension programme, as various digester designs have been developed. Through research and development, the Appropriate Rural Technology Institute designed a cheaper digester that is made from a plastic material. The digester is adopted for urban household and it is used for the disposal of food waste. In India, Biotech Ltd. has developed a smokeless oven and stove, biogas engine that runs on 100% biogas, fibreglass digester and modular biogas plant [50]. Biotech Ltd and Bhanda Atomic Research Centre develop a digester design for treating food waste.

These digesters are based on the KVIC-design of floating drum digester [45].

2.3.5.1.6 Extension

The extension work includes the sale of the biogas digester plant, its installation and training of the user on the utilisation of the biogas effluent. This task is generally performed by an extension agent. More often, the extension service includes the purchasing of material needed for the construction of the biogas plant [45]. To ensure effective use of the biogas product, extension service is offered to the household via the use of project leaflets, demonstration sites and the provision of user training manuals [153]. A key aspect of the extension service is the use of the bio-slurry, whose values depends on the nutrients losses that occur during the process of storage, handling and/or application. In most biogas programmes in Asia and African considerable research were done to assess the value of the slurry as fertilizer and soil conditional. The bio-slurry extension is important as it enables the household or farmer to improve the agricultural yield by making optimal use of the bio-slurry compost as organic fertilizer. Various regional and national biogas programmes in Asia and Africa employs and train extension workers, who in collaboration with several institutions provides extension services to the district. There are number of ways the extension service is provided; the farmer is trained directly by the extension workers, by a visit to neighbours (promoter and model farmers), through various vocational training institutes, through local development NGOs, training and presentation [45, 140]. The biogas construction enterprise is encouraged to provide extension service to the customer by providing compost pit during the biogas plant installation. In Nepal biogas programme, it was reported that the provision of compost pit during installation serves a dual purpose; to protect the bio-slurry from overflow and to enhance the process of organic decomposition. The availability of space and the size of the biogas plant determine the number and size of the pit to be installed [45, 154].

2.3.5.1.7 Institutional Arrangement

A high-level organisation or body is generally required to coordinate the biogas programme on behalf of the national government. The organisation will ensure the implementation of government renewable energy policies in the biogas sector in addition to other objectives. It will ensure proper coordination between government ministries, line agencies and other stakeholder that make up the biogas sector. The apex organisation will have the responsibilities of coordinating with donor organisation, national government about the renewable energy programme, formulate policy to support the biogas programme, give instruction or advise on behalf of the government and submit a progress report to government ministries.

The apex organisation can be government owned, private limited company or NGO. In Nepal, the Ministry of Environment, Science, and Technology (MoEST) through the Alternative Energy Promotion Centre (APEC) was responsible for the coordination of the biogas programme. MoEST approves all policies relating to biogas programme and APEC formulate and promotion policies to support the biogas programme, liaise with government and donor agencies, monitor the progress of the biogas programme, and disburse subsidy and credit facilities. The government of Nepal provided tax exemption for biogas appliances. In Rwanda, Vietnam, and Bangladesh, the apex organisation for the coordination of the biogas technology is the Ministry of infrastructure, the Ministry of Agricultural and Rural Development, and the Infrastructural development company limited.

The National Biogas steering committee (NBSC) is set up at the start of the National domestic biogas programme. It is to coordinate and guide the development of the biogas sector. Implement policy and programme activities of the biogas programme. It comprises members drawn from governmental agencies, international donor organisations, Non-governmental organisation, financial institution, and local groups. The NBSC is responsible for the approval of yearly plan and report of the biogas

programme. It gives approval to the partner organisation, sets and implement quality standard and guidelines, coordinates biogas related research and development, analyses policy issue regarding subsidy, price of the biogas plant, tax, research, and development, and advises the central government. It also liaises with donor organisation to prepare programme fund, monitors and evaluates the progress of the national domestic biogas programme.

At the provincial and district level, the monitoring of the biogas activities is carried out by a similar committee like the NBSC. The district biogas steering committee will examine and approve yearly plan of the biogas sector at the district level and cooperate with the relevant government agencies to ensure the transfer of fund, enforcement of quality control, Production targets, training, promotion and extension activities. In the rural area of Tanzania, biogas activity is promoted by the rural energy agency, an independent organisation set up by the rural energy act No 8 of 2005. This agency provides subsidies and grant to the innovator of the rural energy project.

The employment of people in the rural area is one benefits of the biogas programme. Most national programme in Asia and Africa focusses on capacity building in the area of the construction and maintenance of the biogas plant and its appliances [155]. The construction and maintenance of the biogas plant are carried out by biogas construction enterprises. The biogas construction companies must request to be part of the national biogas programme by making a formal application to the National domestic biogas office. The biogas construction companies are selected by checking for compliance to the guideline set by the national domestic biogas programme. The guideline includes; adherence to the approve digester design and size, the supervisor and mason must be trained and certified by the NDBP. The construction of the biogas plant is based on the detailed quality standard, presence of the biogas companies in the respectively rural communities etc. [137, 156]. The biogas companies will receive constant technical support from the NDBP to increase their capacity building in

delivering quality service and in the marketing of the biogas plant. Also, in regions or district where it is impossible to identify local construction companies. The district biogas steering committee trains and manage a team of masons to construct biogas plant, and the mason team further develop into biogas construction companies [156].

Bank and microfinance institution are an important component of the biogas programme as they provide the credit facility required by various household to construct the biogas plant. It is very important at the initial stages of the programme to engage the various financial institutions (both local and National) to raise the enthusiasm of the biogas programme. One criterion for the recruitment of financial institution in the biogas programme is the local presence of the financial institution. This makes it very easy for the potential household to obtain loan [45], and for the promotion and marketing of the biogas [136]. In Tanzania, the saving and Credit Cooperative Union of Tanzania (SCCULT), and the saving and Credit Organisation (SACCOs) are part of the national biogas programme. They are involved because of their local presence in various part of rural Tanzania.

Other organisations that are curial for the successful implementation of the biogas programme includes, trade union organisation, such as the Uganda biogas Association and the Vietnam Biogas Association. This organisation is composed of various biogas companies as well as mason group, and it assists the Biogas companies with policy development, regulatory and legal issue. These organisations are also active in the promotion and marketing of the biogas plant [136]. A similar organisation (Nepal Biogas promotion Group) was set up in Nepal to assist the biogas companies to improve the quality control of the biogas system, importation, and distribution of gas values to the biogas companies, and technical publications. Four regional biogas coordinating committee was set up in Nepal with the main tasks of promoting and marketing biogas, slurry extension activities and the regulation of the biogas market in their various locality.

2.3.5.1.8 Management of the National Biogas programme

The proper management or coordination of national biogas programme requires the establishment of a coordinating committee at both the national and regional/provincial level at the start of the programme. Such committee usually consists of a senior civil servant so that political decisions are made early and easily in the case of Nepal and Vietnam, or the use of government establish cooperation as it is in the Bangladesh biogas programme [137].

The committee is very crucial as it shirks problems that may arise when individuals involved in the biogas programme seeks to obtain permission and license from the different government department for their specific function. The management of the biogas programme involves the allocation of specific functions to various participatory group or organisation. For example, In the SNV biogas programme in Asia and Africa, financial institutions are mainly involved in the provision of loan, subsidy as well as promotion and marking of the biogas programme. While the vocation training institutes are mainly involved in training, research, and development of biogas technology. The central management committee must allow for input from the local stakeholder as they are close to the household and understand exactly what the local people want. This is to avoid the installation of biogas plant that may not be appropriate for the household [45]. In Nepal, the control of the biogas programme by the Gobar Gas Company over time led to the installation of low-quality biogas plant and the reduction of the number of biogas plant installed by 90%. Further, the tight control of biogas development by the Bangladesh Council of Scientific and Industrial Research in Bangladesh made SNV to partner with the Industrial Development Company Limited for the development of the biogas programme in Bangladesh. In Nepal, the coordination between the central management committee under the Biogas Support programme and the licenced biogas companies ensures the development of the biogas programme.

The appointment of fund managers for the different aspects of the biogas programme (quality control, training, financial coordination, Manufacturing, material supply, publicity and research, and development) is very important as they provide the necessary support for the extension workers [45]. The different groups involve in the biogas programme have a major task of providing annual report to the central managing committee, detailing the plans for the progress and expansion of the biogas programme as well as the funds required for finance the programme, provision of loan and subsidy. The central management amongst its duties is responsible for the provision of material required for the programme, such as cement, steel reinforcement and gas pipes prior to it been used. The material can be supplied by external vendors or manufacture in-house (stoves and lights). For the in-house manufacturing of biogas appliance, proper training is provided to ensure a high-quality product [45].

2.3.5.2 National biogas programmes in Asia and Africa

2.3.5.2.1 Biogas support programme of Nepal

The development of biogas technology in Nepal started in 1955 and in 1968 a KVIC model of the Indian digester was introduced. The installation of the biogas plant at the household level began in 1974 when 250 biogas plants were installed by a farmer who received an interest-free loan, [45, 146]. The successful installation of the biogas plant encouraged the creation of the Gobar Gas and Agricultural Equipment Development Company (GGC) through the partnership of Asia Development Bank of Nepal, Fuel Corporation of Nepal and the United Mission of Nepal. Different designs of the biogas plant was develop and tested including the floating drum design that was found to be very expensive. In 1980, the modified fixed dome digester was developed by GCC and presented as the standard design for the Nepal biogas project [45, 157].

GGC was responsible for among other activities; to advise the government Ministries and agencies in charge of biogas development on setting national targets for the construction of the biogas plant, to develop policy for the provision subsidy of the biogas plant, collaborates with the Asia Development Bank of Nepal to raise fund from national and international donors sources, to create awareness of the biogas technology and build technical capacity by organising short training, study tours in and out of the country, seminars and workshops for the development of workers at different levels of planning, implementation, and to grant funds for pilot test.

The provision of funding from UMN encourage the growth of the biogas sector, and after the withdrawal of UMN from the biogas project, the sector continued to grow slowly with the financial support from United Nations Development Fund and United Nations Capital Development Fund. This encouraged the installation of 12,000 digester plants of the GGC design. However, the inability of GGC to effectively manage the increasing demand led to the establishment of the Biogas support programme in 1992 [45].

The biogas programme was funded by the Directorate General for International Corporation (DGIC) through the Netherland Development Organisation in Nepal (SNV/N) [45, 158]. The third phase of the Biogas support programme started in 1997 and ended in 2003. It was financed jointly by the Government of Nepal and the Kreditanstalt fuer Wiederaufbau of German, and it was implemented by the Biogas Support Program (BSP). The Fourth phase of the biogas programme in Nepal starts in 2003, and it had a duration of 6 years. The programme was implemented by Biogas sector partnership a non-governmental organisation. The financial and technical support was provided by the Alternative Energy Promotion Centre and SNV/N. In the fourth phase, funding for the subsidy was provided by the KFW, DGIS and the government of Nepal. The main objective of the programme in its fourth phase is to further develop and publicize the biogas plant as a renewable energy solution to the household in rural Nepal, and at the same time resolving issues relating to poverty, social inclusion, etc

[157]. The biogas programme is in its transition phase and will last for a duration of 4 years starting from 2010 [159].

The biogas programme involves a multi-stakeholder approach consisting of three levels of activities such as Installation, implementation and policy environment [63]. The installation level consists of marketing, installation of the biogas plant, after-sale service, supply of appliance and training manuals, and the training of the user on the operation and maintenance of the biogas system. This level of activities is usually coordinated by the biogas construction enterprise [63]. The customer is the focus of the activity at this level, and there is a contractual agreement between the biogas construction enterprises with the customer. In the level, the biogas construction enterprise receives training to improve its capacity building in areas such as management, marketing, installation, after-sale service and training of Mason [63].

The implementation activity is under the supervision of Alternative Energy Promotion Centre (AEPC). AEPC supervises the activities of the BSP/N and NBPA. It is responsible for the supervision and coordination of the quality control, administer and manages data relating to the disbursement of subsidy. It also outsources activities such as the biogas user survey and reports to the Government of Nepal about the progress of the biogas programme. BSP/N and SNV are responsible for coordinating the biogas programme at the initial phase. However, during the fourth phase of the programme, SNV assumed the advisory role and provided the fund for subsidy; BSP-N main task involves quality control, monitoring, and evaluation, approval of subsidy to biogas companies. Also, it is involved in the provision of training and promotional material to the participant in the biogas programme. It is responsible for research and development as well as the provision of technical support for the entire programme. The NBPA coordinated the training of mason and other staff, provision of business support as well as engaging the BSP-N, APEC and other groups. It is responsible for purchasing bulk biogas plant component and distribution to

biogas companies and is involved in promotion and extension activities [63].

The next level of activity of the biogas programme is the policy environment level which involves the formation of the Biogas Coordinating Committee. It comprises government organisation, NGOs and aid organisation. The BCC ensures a cordial relationship exists between itself and the various donor organisation for the benefit of the biogas technology. Giving the population strength of Nepal, at the end of 2014, there are more than 330,000 biogas plants installed [160, 161]. The size of the digester ranges from 4 – 10 m^3 at the household level, 15 and 20 m^3 installed at various institutions [161, 162]. Also, about 83 biogas construction companies and 18 workshops have been established and qualified, while 163 microfinance institution providing subsidies and loan through the Biogas credit fund provided by APEC [161, 163]. To encourage the development of the biogas programme, and to ensure more household have access to biogas plant, the BSP successfully register with the CDM (Clean development mechanism) set up by the Kyoto protocol under the United Nations framework convention on climate change. The CDM provided the funds required to continue the provision of subsidies, reducing dependency on SNV and other aid organisation for financial support [45].

2.3.5.2.2 National Biogas programme of Vietnam

Agriculture is the main source of livelihood for about 70% of the population in Vietnam. The animal husbandry sector has raised over 26.9 million pigs because of the increase in the demand for meat. This increase in livestock production has an impact on the health of the citizens due to the increase in smell associated manure. Also, it creates environmental pollution resulting from improper disposal of the manure generated in the pig farm.

Following the challenges in January 2003, the Vietnam government represented by the Department of Livestock in the Ministry of Agriculture and Rural Development (MARD) and SNV signed a Memorandum of

understanding for the implementation of National domestic biogas programme in provinces of Vietnam [134, 164]. The specific objective of the programme includes; the development of a commercially viable market-oriented biogas industry, to ensure the construction of 10,000 quality biogas plant in 10 provinces. While the biogas technology contributes to an annual reduction of GHG in the CO_2 level by 64,600-119,200 tons. The programme will ensure continues operation of all biogas plants installed and to maximise the benefits of the application of the bio-slurry. To develop the technical and promotional capacity for further wide-scale deployment of the biogas in Vietnam. Finally, to strengthen and facilitate the establishment of institutions for the continuous and sustainable development of the biogas sector [153].

To execute and drive the project, the Biogas project office (BPO) was established at the national and provincial level (PBPO). The BPO is responsible for coordinating and implementing activities such as promotion and marketing, subsidy disbursement and administration, quality management and technical training. The PBPO is responsible for all the activities of the biogas programme at the provincial level with strict compliance with the directive of the BPO.

In the implementation phase, the biogas programme developed a design that is used as a standard for the biogas plant [153, 165]. The fixed dome type digester selected by the programme has a size range of $4m^3$ to $16m^3$. The fixed dome digester adopted by the programme is called KT1 and KT2 respectively. The KT1 promoted by the Institute of Energy over 10 years was found to be very reliable [153]. The KT2 model was developed in the biogas project jointly done by Thailand and Germany [134].

The first phase of the programme commenced in 12 provinces out of the 64 provinces in Vietnam and was later extended to 20 provinces. The second phase of the biogas programme increases the number of participating provinces to 50 [153]. In the first phase, the programme achieved more than its target number of the biogas digester. The initial target of 12,000 biogas plants was achieved within 6 months and a further

6000 biogas plant was constructed raising the total number of constructed biogas plants to 18,000 [153, 164]. Furthermore, the programme started very slow during the early stages of the second phase, and this is due to poor management of the BPO. However, by the end of 2009, over 78,000 biogas plant was installed. The third phase of the programme started in 2016 and it is currently going (end in 2020). It is aimed the development of a sustainable market-oriented biogas sector in 45 provinces and cities. The provision of support for the construction of 100,000 biogas plant. By 2014, the number of biogas plant constructed is 145,000. 1,068 technicians have been trained in the province and district, and 1,668 masons have also been trained. The programme has trained more than 100,000 people in the use of biogas technology. It was awarded the 2006 Energy Global prize for outstanding contribution to reducing global warming, the 2010 Ashden award for sustainable energy and the 2012 Humanitarian award outstanding socio-economic and environmental impact [166] .

Like the biogas project in Nepal, the installation of the biogas plant in the Vietnam biogas project was done by masons who were registered and trained by the biogas programme. The mason is a subcontractor that was employed by the biogas technician in the District Agricultural Extension Centre (AEC) of the Provincial Department of Agriculture and Rural Development (DARD). The masons unlike their counterpart in Nepal did not register a company, rather they are self-employment. The masons are also responsible for the provision of biogas appliances such as biogas stoves and light, and this aspect is not monitored by the biogas technician.

The quality control is done by the district, provincial and national biogas offices. The technician from the district office checks the biogas plant after it is has installed, while biogas programme office performs quality checks on 2% of the biogas plant completed in the various province. Once the quality check is complete, details are sent to the provincial biogas programme division and then to the biogas programme division and the subsidy is released via the Vietnam post office [134]. A flat rate subsidy of $67 is applied for all digester size [166]. The middle level of the biogas

programme consists of the following activities; promotion of the biogas technology through mass media and local workshop, research and development in collaboration with universities, biogas user survey as a mean of obtaining carbon finance through the voluntary emission reduction market, and the provision of credit facilities. Biogas Programme Division handles most of the training initially, but later handed over the responsibility to the PBPD. The Provincial Biogas programme division employs an experienced mason to train new masons.

To ensure the programme performs effective, SNV provided the support, guidance, and funds required for a subsidy from DGIS. It worked in an advisory role by collaborating with the Ministry of Agriculture and Rural Development. It also ensures there is no overlap and duplicate of effort by persuading the ADB and World Bank to coordinate their biogas project with the biogas programme division. Despite this effort, the programme is negatively influenced by the lack of support from different ministries of the government. This is because many participating ministries are not inclined to support the programme. A key issue is the fund gap that was created when MARD could not secure the additional funding from KFW through the clean development mechanism from the sale of her carbon credit to the bank. An attempt was made with the Asia development bank regarding carbon financing of the biogas programme, but an agreement was not reached. However, carbon financing was sort in the voluntary Carbon market with Nexus. Financing of the biogas project by the poorest family has also been a major challenge of the biogas programme in Vietnam. As most poor family could not afford to install biogas giving the subsidy scheme in place [167].

2.3.5.2.3 National biogas programme of Rwanda

Rwanda national biogas programme was set up to meet the present challenge of reducing the dependence on the use of firewood, protect the soil and to improve agricultural activities, increase the employability of the

youths and women through the establishment of the vocational skill centre [156, 168]. The national biogas programme was aimed at developing, strengthen and facilitate a commercially viable and market-oriented biogas sector, increase the number of quality biogas plants to 15,000 while ensuring the sustainable operation of the biogas digester installed under the national biogas programme. Finally, to maximise the benefits of the digester in terms of the use of slurry [156, 168].

The national biogas programme of Rwanda is based on the strategy that in the provision of goods and service, the customer/ users is at the centre. The goods and service include pre-sale information, subsidy and credit scheme, biogas plant and appliances, users training, and after-sales service. The biogas programmes emphasised on the participation of private companies to provide an alternative for the users in terms of the reduction in the cost of the biogas plant while ensuring the minimum standard is achieved. This will lead to an increase in the demand side of the technology, thus ensuring long-term business opportunities for private companies. The national biogas programme also proposed a control strategy in which a minimum standard is required for the different goods and service to protect the reputation of the biogas technology as well as the user. An example of the control strategy is the adoption of a model plant and ensure the private construction companies meets the standard specified in the plant design during construction.

The promotion and marketing of the biogas technology focus on the population in the rural communities as well as among a small group of farmers. The strategy for promotion and marketing is that the customer is satisfied when the biogas plant is properly functioning. This is because a satisfied farmer is a better advocate of the biogas plant. Further, at the heart of the promotion of the biogas technology is the need to ensure the quality of service during the construction, operation and maintenance of the plant, and quality control regarding the appropriate size of the digester, [156] etc.

The promotional and marketing activities are performed collectively by the NBPO, DBPO, NGOs and the biogas construction companies.

The national domestic biogas programme adopted a subsidy scheme in addition to its promotional, marketing and extension activities. To ensure all potential users have access to the biogas plant, a flat rate subsidy was applied across the various districts. Also, to ensure quality standard, the access of subsidy was based on certain conditions; such as the installation of one plant per user (household), the biogas plant meets the size required for subsidy and the plant must have the approved design. The intending household is able to provide 20 kg daily, and there is availability of water, and the biogas plant must be constructed at safe distance from the house. The user must own land that can be used as collateral for obtaining loan. The user must have a percentage of the investment fund required for the digester construction or for upgrading the toilets [150, 156, 168]. He or she must be willing to cooperate and participate in the biogas programme. The subsidy provided can be accessed through the national biogas programme office (NBPO) and this is done once the NBPO has received the biogas plant completion forms and the sale contracts between the users (Household) and the construction company. The NDBP allow subsidy on three different sizes of the digester tank (4 m^3, 6 m^3 and 8 m^3). However, the recommended size for the biogas programme is the 6 m^3 [150]. The subsidy was initially provided by Germany Agency for Technical Cooperation (GTZ) and after 2011, the subsidy scheme was funded by the Rwanda Government with a budget of about $14.5 million.

Recognising the challenges facing the household in providing fund for the initial investment cost of the biogas plant. The NDBP and SNV partnered with a Rwandan microfinance bank to develop a credit scheme which allows the access to funds for the installation of the biogas plant. This credit scheme was provided with the support of Dutch Government Access to Energy Fund and the Netherland Development Finance Company. A 6.5 years agreement of 4 million euro was signed by BRP to provide a 3-yrs microfinancing scheme for eligible household [150].

As part of measures to ensure the overall success of the biogas programme and boost users (farmers) confidence in the biogas technology, a quality

control measurement is in place to ensure all construction companies meet the standard set for the construction of the biogas plant while ensuring competition in the biogas sector. Quality checks were performed to ascertain that the masons were giving proper training. Quality control was performed to check the quality the material of construction and biogas appliances as per the programme specification. Quality control check is performed on the dimension of the digester ensure it is as per the standard. Also, quality checks are done to ensure the proper piping and fitting of the gas appliances. Further, quality checks are performed to ensure the user (Household) have received the required training on the operation and maintenance of the biogas plant, and that biogas instructional manual is provided. After sale service quality checks were performed, and it is to ensure the service are provided as per the standard set by the NBPO. Also, the data obtained from the quality control check is used by the national biogas programme office to measure the performance of the construction companies and for the renewal of contract agreement. The data is used by the national biogas programme office to access the progress of the biogas programme, and to measure the performance of the biogas companies, to identify area for improvement. The quality control strategy of the programme was implemented through a partnership with the Centre for Innovation and Technology transfer of the Kigali Institute of Science and Technology and Tumba College of Technology [150].

After sale service is a crucial aspect of the biogas programme which is delivered by the mason teams and biogas company. It provides guarantees for the biogas plant. The biogas companies are required to visit the plant twice; the first visit is usually one year after construction to establish that the biogas plant is operating properly. The second visit is after 3 years to inspects the structure of the biogas plant. As part of the after-sales service, biogas companies are required to deposit the sum of $10 for guarantee in a special guarantee fund jointly operated by the national biogas programme office and biogas companies. The fund is reimbursed to the companies after the guarantee period has elapsed with no visible defects on the biogas plants and the maintenance reported is submitted to the programme office.

Also, the guarantee fund allows for another biogas companies to follow up on the after-sale service in event that the formal biogas companies fail to meet up the standard set by the programme office or have decided to pull out of the biogas programme.

2.3.5.2.4 Cambodia National Biogas Programme

The first digester was constructed in Cambodia in 1986, and by the year 2004, the total number of digesters built is 400. This digester is mostly made up of plastic material and were installed by 15 different organisations. Most of the digesters are in disuse or broken as the material of construction has a limited lifespan. Most of these digesters have failed because of the lack of support and ownership and the use of low skilled labour [169, 170].

The need to develop a viable biogas sector as an alternative to meet local demand for energy led to the collaboration between the government of Cambodia and SNV [170, 171]. A feasibility study was commissioned to assess the potential of biogas technology in the country with the aim to set up a national biogas programme in Cambodia. The findings of the feasibility study include; the formation of the national biogas office to coordinate and initiate various activities of the national biogas programme. The selection of the appropriate ministry to lead the programme. The Ministry of Agriculture, Forestry and Fisheries was selected [172]. The development of the strong biogas market through the implementation of quality control in every aspect of the programme starting from promotion, construction, after-sale services, and continuous research to ensure the standard required for the digester construction is achieved. The collaboration with the financial organisation to provide subsidy to the household and market strategy for adopting or sale of the biogas technology to the household. The development of local biodigester companies to ensure actual construction and follow up service is provided, and the continuous training of technicians and management support staff. The development of institutional capacity

necessary for the success of the national biogas programme through the capacity building and technical advice provide by the assistance of SNV.

The national biogas programme of Cambodia commenced in 2005, with a duration of 5 years. The first phase of the programme is aimed at the construction 17,500 quality biogas digesters in the selected province. The first phase of the programme will also ensure the digesters installed are continuously working. In the first phase of the biogas programme emphasis the improve in the application of effluent in agricultural practices. Further, the biogas programme will ensure the development of technical and promotional capacity for the biogas technology in every part of the country. Finally, to strengthen and facilitate the establishment of institutions required to sustain the development of the biogas programme.

The installation of the biogas plant was done by the biogas construction companies. They are involved in the direct marketing of the biogas plant and performs the after-sale activities. In addition to the biogas construction companies, there are mechanical workshops involved in the construction biogas appliances such as biogas stoves, gas pipes, gas taps, and water drains. The biogas companies also provide the biogas owner with manual and training in operation and maintenance of the biogas plant. According to the annual report of the national biogas programme, there are over 99 biogas companies involved in the biogas programme between 2006 and 2017. However, only 55 biogas companies are still active. This high rate of dropout of the BCEs is the key challenges of the biogas programme [148].

The National Biogas programme office provides technical and financial support, to the provincial programme offices. The provincial offices are responsible for programme monitoring and evaluation, research, and development. The provincial programme office also provides loan to farmers and coordinate the activities of the biogas programme at the provincial level. The national biogas programme office is also involved in the promotion and marketing of the biogas technology, training of masons and supervisor; the organisation of village workshops and small group meeting. At the provincial level, the Provincial Biogas programme office

(PBPOs) through its local offices in the Department of Agriculture promote and disseminate biogas technology locally. In addition, Community Economic Development Assistance Corporation (CEDAC), an NGO working collaboration with SNV/NBP have been involved in the extension service relating to the use of bio-slurry in 4 provinces [148]. The training of mason and supervisor was provided by Presh Kossmak Polytechnic institutes and the Cambodia-India Entrepreneurship Development Centre (CIEDC). Over 615 masons and 90 supervisors have been trained by these institutes. In 2011, People in Need (PIN) an NGO became part of the biogas programme and assisted the NBP to develop a permanent, market-oriented biogas sector that can sustain energy supply. It establishes a biogas digester user network where it is training 23 villagers. The biogas user networks are responsible for information sharing, provision of the plant parts, etc.

Quality management of the biogas programme is provided by the provincial and national supervisors. The quality check is done randomly to ensure the quality of construction, and after-sale service meets the standard set by the biogas programme. The quality of the operation and maintenance of the biogas plant are monitored. The programme develop and standardised two type of the fixed dome digesters, namely the Deenbandhu fixed dome design and the S1 design. The S1 design was made specifically for a low-income household [172].

The provision of subsidy was done through rural banks such as the ACLEDA and TPC. A fixed subsidy of $100 was applied for all size of the biogas digester installed and was later increased to $150. In addition, financing the biogas plant requires contribution from the farmer in cash or kind. Loan is provided at a fixed increase rate of 3 % for a period of 2 years. The loan is obtained from various sources such as the International Fund for Agriculture and Development (IFAD), Asia Development Bank and FMO the Netherlands development bank. Other sources of funding for the national biogas programme include revenue generated the sale of carbon credit through the voluntary carbon market [172].

The national biogas programme record success with the installation of 25,000 biogas plant. The programme is currently in its third phase (2016-2020). However, it has experienced some challenges. The government of Cambodia set a limit for borrowing, and this has made it difficult to obtain a loan. The process requires the provision of collateral as additional commitment and it lacked transparency. The national biogas programme also set a standard of owning livestock and at least £250 before a farmer can be part of the programme. The introduction of other models (Including the prefabricated fixed dome) of the biogas plant in the national programme lead to the issue relating to quality control, after-sale service, and warranty. Most biogas plants are in despair and they are not functioning. Further, the subsidy required to install the plant is more than what was set by the national biogas programme. The migration of people to the city and the sale of livestock by owners reduced the demand for the biogas plant. The changes in the internal policy of the national biogas programme limit the rate of deployment of the biogas technology. The number of biogas plant installed reduced when the SNV senior adviser left and the subsidy reduced by 30 % [148].

2.3.5.2.5 Tanzania National Domestic biogas programme

The national energy needs of Tanzania are fulfilled by the use of biomass, notably wood fuel. It accounts for 94% of the primary energy supply while hydropower, fossil fuel, biogas, coal, and other liquid biomass fuel account for the remaining. Low outputs of these traditional energy sources show that the economic activities in Tanzania are driven by low energy technologies. Especially in a rural area where there are limited transport system and outdated agricultural methods.

The use of biogas technology as an alternative energy source in Tanzania dates back to 1975. The small industries development organisation constructed 120 digester plant of the floating drum design. The promotion of the biogas technology started with organisations and NGOs such as the

Arusha Appropriate Technology institutes which operates in the Arusha region, and the MIGESADO operating in the Dodoma region of Tanzania. In 1983, the Centre for Agricultural Mechanization and Rural Technology took over the promotion of the biogas technology in the country. The led to the installation of 600 biogas plants in 1992 with the help of Germany Agency for Technical Cooperation (GTZ). GTZ participation in the biogas promotion by training masons on the construction of digester plants, including fixed dome and floating drum digester. Following the withdrawal of GTZ from the biogas extension scheme, government funding of the projects is not enough and the activities of CAMARTEC reduced. However, NGOs notably MIGESADO and FIDE continued to promote biogas technology digester, and a total of 2900 biogas plants were installed from 1997 to 2007. 1900 of the digester constructed are still in operation [113].

Despite the effort of the early organisations in the deployment of biogas technology. Its market penetration lagged behind countries in Asia notably Nepal, India, and China. The factors that limited the development of a robust biogas sector in Tanzania include the high investment cost as only the rich farmer could afford the digesters built by the various organisations. The digesters are very large, and the average volume of the digester installed was 16 m^3. Most families do not have the funds to make the initial investment for the construction of smaller digester and the service provided by the micro-finance organisation does not include loan for construction of biogas. The biogas technology was centred in the area that the central government directed. Further, CAMARTEC had most of their operating within the Arusha region, and this result in the dissemination of the technology in some parts of the country. The awareness of the benefits and cost of the biogas plant are known in the region where organisations like MIGESADO, CAMARTEC and ELCT operated. Technical skill, experience, and idea are isolated as there are lack of cooperation between the various actors (CAMARTEC, MIGESADO, etc.) and finally, lack of water for diluting the feedstock since Tanzania is mostly dry land characterised by seasonal drought [113].

In 2009, after an extensive feasibility study of the current state of the biogas sector in Tanzania, the national biogas programme of Tanzania was initiated under the Africa Biogas partnership programme. The programme is aimed at developing a commercially viable biogas sector in Tanzania, with the involvement of all level of Government organisation, Non-government organisation, and the private sector. The proposed duration of the programme is 10 years. In the first phase (2009-2013), the programme targeted the installation of 12,000 biogas plant. However, the number of digester installed at the end of the first phase was 8779, and the programme reached 10,000th biogas installation in September 2014. Building on the success of the first phase, the second phase of the programme commenced from 2014 to 2017 and it has a target of over 20,000 biogas digester [113].

2.3.5.2.6 Kenya National Biogas programme

The biogas technology was first introduced in Kenya by Mr. Tim Hutchinson in 1957 and in 1958, his company started mass production of biogas plant of the floating drum design. Between 1968 and 1986, the company constructed 160 biogas digesters in Kenya [45]. The digester producing organic fertiliser as its main product and biogas as a by-product [173].

In the mid-1980s, a Special Energy Programme was set up by the Kenya Ministry of Energy in collaboration with Germany development organisation GTZ to promotion the biogas technology. The India KVIC digester was adopted as the model design, because the material for construction is available locally and the presence of local steel companies. The number of biogas plant built was approximately 400 [173], consisting of 250 floating drum digester [45, 174] and 150 fixed dome digester. Further, the programme is aimed at training more technicians and equipping them with the knowledge and skill to set up companies to further promotion and disseminate the biogas technology. While the programme achieves the construction of 2,000 plants, the growth of the biogas technology was

hindered due to a lack of trust in the technology [45, 175]. This result from the lack of quality control during the construction of the plant and in the post-construction follow-up service., and the users lack the basic knowledge of how to operate and maintain the digester plant. The biogas programme experience failure due to lack of interest as users felt the feeding of the digester plant is a dirty job. Also, the biogas plant is expensive and not affordable to low income earner. Hence, some people decided to build their own digester instead of allowing construction companies to build it.

In 2007, the feasibility study of the Kenya biogas technology was recommended, under the biogas for better life programme. The aim is to identify the barriers as mentioned above and potential of biogas technology in Kenya. It was reported that Kenya have the potential to install more than 10,000 biogas plants in 10 years. And that the biogas market has not lived up to its potential as the private sector-led sale of the biogas plant is driven by a small group of technicians.

The outcome of the feasibility study in addition to the Kenya vision 2030, seeks to improve human resource development, creation of jobs, increasing energy access to the poor, and improvement in science and technology innovations. The Kenya national domestic biogas programme was established. The objective of the programme is to develop a commercially viable biogas sector through the partnership of various organisation such as government of Kenya, non-Government and the private sector. Increase the number of quality and operational domestic digester to 8000 in 4.5 years, and to ensure the biogas plant are still operating after the construction [138]. The Kenya domestic biogas programme is hosted by the Ministry of energy, which is the chair of the Kenya National biogas committee, while SNV provides the support needed to develop local experts and improve institutional capacity through knowledge transfer. The programme adopted the demand and supply approach used in the biogas programme in Asia. To implement the programme, the Kenya National Biogas Committee (KENBIC) selected the

Kenya National Federation of Agricultural Producer (KENFAP) as its implementing agent [138]. The sole responsibility of the KENFAP is to ensure commercial interaction between the end users of the biogas technology, biogas construction companies, and biogas service producers. And, this is achieved through coordination, capacity building, facilitation and monitoring of the various institutions need to successfully develop the biogas sector. The programme is organised such that every region of the country has a dedicated biogas office that liaises with the local organisations, farm group, etc. regarding the programme activities such as promotion and awareness of the biogas technology. Training and re-training of mason, technician, supervisors, and inspector. Registering of biogas companies and biogas service providers, construction of the biogas plant, quality control management, after sale services, subsidy disbursement, etc [138].

The strategy of the promotion and awareness activities incorporate biogas companies, financial institutions, local NGO such as the ABC-K, farmers association, etc. The promotional activities involve the sharing of the knowledge of the biogas technology through collaboration with media channels, the printing of polo shirt and caps, leaflets and the use of the annual farmer forum. Also, it leverages the relationship between mason and the end user household, and the use of words of mouth to promote the biogas technology. The promotion and awareness were schedule to avoid multiple visits to the potential client by different marketers, and the activities are recorded in a database to assist in identifying districts that has been covered. The promotional and awareness activities were also directed at women and youth, and this is to ensure more women are integrated into the biogas programme. The biogas programme also incorporate quality management to ensure that the biogas plant installed are of good quality and it is operating satisfactorily.

2.3.5.2.7 Institutional biogas programme of Ghana

The biogas technology began in Ghana in 1960 as a solution to the energy crisis. The first digester was installed in 1986 through the effort of the ministry of energy and the support of the Chinese Government [176], and another biogas digester was installed in hospital in 1994 [45]. More biogas plant was installed by the ministry of energy with support from the various international organisation. A recent report suggests that Ghana has the capacity to installation over 280,000 biogas plant [177], and the biogas plant has the capacity to produce 6000 cum per day of liquid fertilizer and boost agricultural production by 25%. A detailed study performed by the Kumasi Institute of Technology, Energy and Environment reported a biogas potential of 81,527 [177, 178], and the upper eastern region of Ghana has the capacity to install 34.34% of the biogas according to the feasibility study [177].

The biogas plants have been installed in various government and private sector institutions in Ghana by Biogas Technology Africa Ltd (BTAL). The company was founded by John Afari who has developed skills and expertise as a biogas engineer in Europe. The company built its first digester in a hospital in 1994. The digester built has a similar design to the KIST design. The volume of digester ranges from 10 m^3 to 600 m^3, and over 15 digester plant was successfully constructed by the company in 2008 [45]. The company offers training to its client on the operation and maintenance of the biogas plant and offers a one-year free repair or maintenance. All the biogas plant component used in the construction is purchased by BTAL to ensure the quality of the product [J, 2006 #3].

2.3.5.2.8 Bangladesh National Biogas programme

The first biogas plant of the floating drum design was constructed in the campus of a government-funded university in 1972. The Bangladesh Council of Scientific and Industrial Research (BCSIR) constructed another

floating drum digester in 1976. Further effort in the development of the biogas technology in Bangladesh leads to the construction of 260 digester plants consisting of the fixed dome and floating drum design by a government agency (EPCD) in 1981. The various organization in Bangladesh promotion the biogas technology within the same period and they include the Danish International Development Agency (DANIDA), Local Government Engineering Department (LGED), Department of livestock and the Grameen Bank. Also, local youths received training on the construct biogas plant by the Institute of Fuel Research and Development and a total of 126 biogas digesters were installed [179].

Prior to 2006, two biogas programmes started independently in Bangladesh, and it was organised by the Bangladesh Council of Scientific and Industrial Research, and the Local government engineering department. A total of 21,860 biogas plants were installed by BCSIR between 1995 and 2004 with the aid of subsidy provided by the government of Bangladesh, and LGED install over 1120 biogas plants between 1998 and 2003. 47 % of the plant installed were found to be operational, 32 % are partially operation and 21 % are not in operation. 83 % of the biogas digester is not properly fed and 50 % receives less than the required feeding. The biogas digester is not functioning properly because of the unavailability of feeding material, lack of operational and maintenance procedures, defects in the constructed plants and the inappropriate sizing of the digester plant [179].

Based on the number of plants installed it is considered that the potential for further development of the biogas technology in Bangladesh is highly Viable. Further, the development of biogas technology is encouraged by the availability of high-quality construction materials, a high number of farm animal (22.29 million) owned by 8.4 million households. In 1994, the Infrastructural Development Company Limited was formed by the government of Bangladesh using the funds provided by the World Bank. The company started promoting the biogas digester and installed over 4,500 biogas plant by the end of 2005. At the same time, the infrastructural

development company limited partnered with SNV after an extensive feasibility study to further develop the biogas project. The national biogas programme was aimed at the installation of 36.450 biogas plant for a period of 4 years (2006-2009), and to further develop the biogas technology and distribution in the rural area [179].

IDCOL as the implementation agency for the Bangladesh biogas programme collaborated with various government and NGO, such as Grameen Shaki, BCSIR, and BRAC who are already disseminating biogas technology to implement the national biogas programme [179, 180]. Training is provided for the mason by the partner organisation and the BPO. The digester model developed by BSCIR was modified by IDCOL and adopted for the biogas programme to ensure quality control and standard. The technicians in the BPO performed quality checks on half of the plant constructed by the partner organisation and follow up quality check is done on 20% of the plant after installation [179].

IDCOL is involved in the promotion of biogas and training of the staffs of partner organisations. The biogas programme stressed the importance of gender equality in biogas training as female masons are a key component of the promotion of biogas technology. The biogas plant components and gas appliance are manufactured by a separate organisation and the quality of the products undergo quality checks by IDCOL before it is distributed to the partner organisation. IDCOL monitors and evaluates the national biogas programme, and it is involved in the issuing and distributing of the subsidy and credits [179, 180]. A flat rate subsidy of 9000 BDT is applied to all sizes of the digester. Two types of subsidy are offered by Grameen Shaki; in the first subsidy, the client contributes his/her cash and pays 10% Service/Supervision charge during the construction of the biogas plant. The bank pays 75% of the cost of constructing the biogas plant at an interest rate of 8 %. In the second subsidy, 15 % upfront payment is paid by the client for the construction of biogas and receives a 5000 BDT subsidy for the biogas plant and a loan with a flat interest rate of 6% [180].

By 2015, the number of biogas installed by the programme is over 77,000. Some key challenge of the programme is the lack of feedstock as many biogas plants are not operational [180]. The lack of awareness on the use of the bio-slurry, and the market for bio-slurry are hurdle to the development of biogas technology.

2.3.5.2.9 Uganda National Biogas Programme

The interest in biogas technology began in 1972 in Uganda. However, very little has been achieved in terms of its dissemination. It was estimated that around 500 - 600 biogas plants were installed by various organisations involved in the promotion of the biogas technology [45, 136]. As part of the plan to provide energy for its people, the government of Uganda through its Ministry of Energy and Mines Development included biogas technology in its energy policy. Biogas technology have been promoted by a local group, Integrated Rural Development Initiatives (IRDI), though at a very low pace. SNV and HIVOS in collaboration with the government of Uganda agreed to set up a national biogas programme. In the first phase of the national programme which starts from 2009 through to 2013, the number of targeted biogas plant forecasted by the programme was 21,160. At the initial stages, the program will be implemented in selected districts in central, western and eastern Uganda, and 120 biogas plant was installed: 90 biogas demonstration plants and 30 regular biogas plant.

In Uganda, there are limit number of contractors and skilled masons, many of whom are registered in the city. Hence, specific attention is given to the development of skill mason and biogas construction enterprise in the rural areas through vocational training and business development. This involves the collaboration with local training institutes, and the inclusion of biogas technology in the school curriculum. Masons with the skill in the building of a house were selected based on their interest in biogas technology and are trained in the construction of biogas plant. The programme provided support for the different rural organisation such as the Uganda biogas

association, VEDCO, NOGAMU HIEFER UGANDA, etc. involved in the construction of biogas plant to strengthen their technical capacity. 5000 biogas plant was installed at the end of the first phase [136].

Biogas solution Uganda (BSU) was set up by the government of Uganda as the implementing agency for the second phase of the biogas programme. The aim been to install 13,000 biogas plants and to ensure that 61 % of the energy used in Uganda is renewable. Also, the programme is aimed at increasing access to affordable credit to improve the number of quality biogas plant installed and operating effectively. The installation of biogas plant reduces during the first quarter of the second phase following the withdrawal of subsidy. However, toward the end of 2014, there was a steady increase in the development of the sector through capacity building of the private construction companies and support from the partner organisation [181].

2.3.5.2.10 Biogas Technology in Nigeria

Biogas technology started in Nigeria in the early 80s, when a simple biogas plant was installed in the campus of Usman Danfodiyo University, Sokoto. Afterward, over 21 pilots' demonstration plants with capacity range from 10 m^3 – 20 m^3 were tested in various parts of the country [64, 65]. Within the period, the biogas technology performed in various institutions in Nigeria, with few pilot schemes set up, however, biogas technology has not spread into the general population. Although, in recent time biogas plants have been installed in some parts of the country through funding from companies and international organisation. One such company is Avenam link limited, that claimed to have installed over 15 medium to large scale biogas digester in various institutions across Nigeria [182]. However, the total number of biogas plant in Nigeria is still unknown.

The largest economy in Africa is Nigeria, and currently Nigeria is experiencing a rapid increase in urbanisation resulting from the boost in income from the discovery of petroleum [64]. The increase in the number of people relocating to the cities is estimated to increase by 49.52% in 2017

according to the report by Statista. The movement of people to urban areas is associated with increase in consumption and waste generation. The lack of adequate waste management strategy in most cities in Nigeria implies that waste generated are not properly disposed. The waste is combusted in open air or disposed in waterways, creating major health and environment problem. The application of anaerobic digestion technology in Nigeria is very limited. This is despite the potential of generating 25.53 billion m^3 of biogas, and 88.10 million tons of bio-fertilizer from 542.5 million tons of organic waste generated in Nigeria [64, 65]. Nigeria, the most populous country with the largest economy in Africa is faced with indiscriminate disposal of waste specifically municipal solid waste (MSW) and it result from poor governance, population growth, urbanisation, etc.[66, 67]. In Nigeria, the current practices in the disposal of solid waste involves burning in designated dumpsite across major cities. In Lagos, there are few recycle plants that recycles paper, plastic, and the other wastes are composted [67, 68]. In Rivers state, the solid waste management strategy is lacking [67], especially in Port Harcourt, the state capital where solid waste management practices have failed due to poor implementation, enforcement and lack of awareness of the waste management policy [69]. Salami et al [67] reported that 117,825 tonnes of waste is generated in Rivers State per month, and MSW makes up 44.2 percent of the total solid waste. The quantity of waste is based on the population of Rivers state in the 2006 census. Ogunjuyigbe et al [70] projecting that the amount of MSW generated in Port Harcourt is 284,446, and 293,548 tonnes in 2017 and 2018 respectively, and it is projected that in 2019, 302,942 tonnes of waste will be generated. This figure is based on the population of Port Harcourt obtained from the national population commission at the growth rate of 3.2 % and 0.86 kg/capita/day of waste generated.

Ogunjuyigbe et al [70], found that among the various technology assessed (landfill gas to energy, incineration, and anaerobic digestion), Anaerobic digestion offers a cost-effective means of generating electricity from MSW in Port Harcourt. Therefore, giving the enormous challenge of solid waste

disposal in Port Harcourt, the lack of solid waste disposal system in rural areas in Rivers State. This thesis is aimed at the application of anaerobic digestion as a waste treatment solution in Rivers State. Anaerobic digestion processes have been adopted in developing countries for the disposal of household and farm waste. Various designs of household or farm digester have been develop such as the fixed dome, floating drum and the plastic bag digester [45]. These digesters are operated at ambient temperature and are affected by the changes in the daily air temperature [71]. A comparison of the price of the digester reveals that the plastic bag digester is cheaper than fixed dome digester and floating drum digester, but has less durability. Like other digesters, plastic bag digester is buried underground [72], some designs of the plastic bag digester include a greenhouse cover [73]. Other designs of household digester have included a solar collector usually mounted on the cover of the digester [74-77]. However, with plastic bag digester, no study has explored the integration of solar collector and plastic bag digester. Hence, as a first step in the application of AD in Port Harcourt; this thesis will investigate the performance of various design of plastic bag digester.

2.3.5.3 Key Success of National Biogas programmes

Domestic biogas programme has been implemented in various parts of Asia and Africa. The aim has been to provide clean energy for cooking, lighting and to develop viable commercial biogas that is able to sustain the biogas technology and at the same time providing employment. The critical factor for the success of most of the programmes especially in Asia and some parts of Africa includes the commitment of the various national government. For example, the inclusion of the biogas technology in the government national plan in Nepal and Rwanda. In Nepal, the government subsidised the interest on the loan collected by household, and the exclusion of biogas systems and its accessories from value added tax. The introduction of quality control ensures that the biogas plant meets the expectation of the user and are fully functional. The quality control measure encourages various national programmes in parts of Asia and Africa to

adopt a suitable digester model. For example, the Cambodia biogas programme adopted and modified the deenbandhu model of the fixed digester. In Tanzania, the modified CAMARTEC digester design was adopted for the biogas programme. The approval of the design ensures the enforcement of quality standard regarding digester construction and the payment of subsidy. The training and re-training of masons, supervisors, and end users (Household) were equally important to the success of the biogas programme. This was achieved by the collaborations with various existing institutes in the countries. In Rwanda, the Kigali Institute of science and technology recorded success in the development of large-scale biogas plant by training prisons in the construction of the biogas, and this makes it easy to monitor and repair any parts of the biogas plant that is faulty. In the training of the user, specific attention was given to gender issue and more women were encouraged to participate in the programme and trained to construct, operate and maintain the biogas plant. The quality control checks also ensure that during the promotional stage of the biogas programme, the clients are given the relevant information to make the right decision to adopt the biogas plant. The quality control system or standard ensure strict compliance during the recruitment of partner organisation such as the biogas companies. MFI, etc. The provision of affordable finance from donor organisation such as SNV, HIVOS, national government, etc. ensure that the majority of the household could afford the installation of the biogas plant. This is in the form of subsidy to reduce the upfront investment cost of the biogas plant. Long term low-interest loans given to a household/farmer to complete the cost of construction and installation of the biogas plant.

The linking between the number of the households that have installed biogas plant and the development of capacity for the supply side is another key factor in the success of the biogas programme. This is because the number of biogas plant installed must correlate with the number of construction companies providing quality service and after-sale services. Further, the content of the capacity building for the supply side must be in

response to the recent changes or findings from research and development. For example, the training of the biogas companies in Vietnam to improve their business and marketing skills in response to research potential became important as the number of biogas constructed during the second phase of the biogas programme is not in synergy with the research potential. The following section will discuss details of the various types of domestic biogas plant used in various biogas programmes.

2.4 Domestic Biogas Plant

Different design of domestic digesters have been built in the various programme in Asia and Africa [42, 43, 45]. Most of the biogas plants lasted, especially those designs built in the programmes of China, India, and Nepal since the biogas technology began over 30 years ago. At the start of the programme, the digesters used were badly built as developers strive to make it easy to build, and the digesters affordable, reliable and sustainable. In time, through continuous sharing of knowledge, displace of designs and experimentation, several plants were built that are low cost and durable. Although some of the early digesters failed, a larger percentage of these plants are still in operation 20-30 years later [45].

The local digester is produced using diverse material, for example, plastic, brick, and concrete. An example of the digester made of brick is the Gol Ghar Godwon digester that was built by Captain John Garstin in 1786 in Patna, India. The digester has a base width of 125 m and it is 29 m high. A concrete digester was built in Rome around 128 AD, with an arch measuring 43.3 m, 21.7 m high and a based breadth of the length from the high. This digester is built to meet the cooking needs of households in various part of Asia has a size range of 7 m^3 to 20 m^3. However, the smaller size of 3 m^3 and 1 m^3 that utilises dung and food waste have been install [45, 60].

For a biogas plant to be suitable for local use, certain design criteria must be met such as the ability to retain slurry for a duration of time without

leakage of the slurry and gas. The biogas plant must not be expensive and should be erected with material that is available locally. It must be easy to operate and maintain. It should be easy to heat and insulate. The plant must be of good quality with no sign of failure, and the digester must be able to minimise the change in the operating temperature. Domestic digester must be able to withstand the pressure exerted by the slurry without leaking. Hence, the shape of most domestic biogas plants is cylindrical or hemispherical [45]. The various design of domestic biogas plant includes the fixed dome design, floating drum design and the bag digester or plug flow design.

2.4.1 Fixed dome digester

Fixed dome digester originated in China, and it is spherical in shape to withstand compression. The dome shape of the digester is built at an angle less than 100^{o}. The gas produced from the biochemical reaction inside the dome is collect via the principle of displacement. The level of the slurry in the dome is reduced as the gas produced cause a spill over of slurry into the reservoir pit. When the gas is collected in the external storage unit or used directly in a gas stove, the slurry is returned to the dome. The flow of slurry between the dome and the reservoir pit allow for mixing the slurry, thereby enhancing the gas produced. The difference between the pressure of the slurry in the reservoir and the main digester causes an increase in the pressure of the gas produced. This makes it easy for transporting the gas via smaller pipes and increase the amount of gas used in the burners. The drawback of the displacement principle is that biogas (methane) is a loss to the atmosphere since the reservoir pit is open as biodegradation process continued in the slurry, and this has raised concern regarding climate change caused by the release of greenhouse gases [45].

The original design of the fixed dome plant in figure 2.4 formed the basis of small-scale digester design used in the early biogas programmes in China and the ongoing biogas programmes in China. Also, the fixed dome design has been adopted in many biogas programmes in Asia and parts of Africa.

This has led to various modification of the original design, and examples include the Janata and Deenbandhu design used mostly in India and the GGC design in Nepal. Based on the design of the digester, different materials are used for its construction. The fixed dome and Janata designs can be made from either concrete or bricks, while brick is used to construct the Deenbandhu design. In a mountainous region such as Nepal, the use of local material such as broken stone and sand are used to make the GGC design [42, 43, 45].

The original fixed dome digester has a central concrete plug on the roof of the dome that can be removed to allow access to clean the digester after it has been used for a period. In the recent design, the central concrete plug is not included as it is difficult to seal off to prevent leaking of gas. This is corrected by opening the walls of the main digester to the displacement (reservoir) pit allowing for access to empty the digester. The digester is usually cleaned when the digester has issues relating to the presence of antibiotics and Inhibition of the bacteria [45]. The digester size varies depending on the region where it is installed, the exact number of people in the household and the availability of feedstock. In Asia, the size of digester varies between 4 and 150 m^3 [141, 183, 184]. In African, the digester sizes are about 6 m^3 [128]. However, in some parts of Africa, especially Nigeria where there is a cluster of houses in a particular location, the installation of community type digesters is preferable [185]. The digester has a life span of 20 years and requires skilled labour for proper installation.

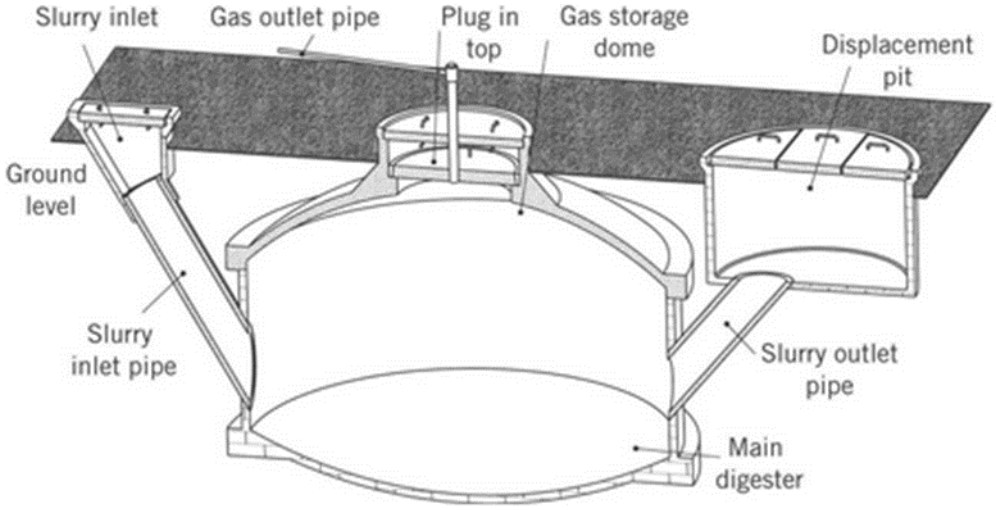

Figure 2.4 shows the diagram of the fixed dome digester [45]

2.4.1.1 Janta Fixed dome digester

This design of the fixed dome digester likes its floating drum design counterpart uses a masonry-lined underground pit. The underground pit is wider in the fixed dome compared to the floating drum and it has no central wall. In the design of this fixed dome digester, both the roof and floor of the digester is shaped like a dome, and its side wall is straight or slightly inclined outwards resulting in a cylindrical or cone shape. It is a fairly close copy of the original fixed dome digester, figure 2.5. In locations where the soil is less stable, the conical shape design is preferable. The input and output chamber of the digester is set using s pipe, which is made from either plastic or concrete. The formwork uses mud or metal in the construction of the dome to ensure the correct spherical shape, as any deviation from this shape will weaken the dome. In places where labour is cheap, the dome is made by filling the digester pit with mud and shape the top surface to form a mould. The mud is then removed when the dome has set. The material used for the construction of the floor, walls, and roof of the digester can be a combination of either brick and mortar, concrete blocks and mortar or from cast concrete. At the top of the dome, an access hole is made, and it is closed by construction two layers of the concrete ring that carries the

metal pipe used to remove the biogas. The space between the plug and the concrete ring is filled with wet clay to prevent leakage of biogas. The upper concrete ring is installed to reduce the rate of water evaporating from the wet clay. The input and output pipes are linked to the slurry mixing tank and the reservoir pit that is built over it.

2.4.1.2 Deenbandhu fixed dome digester

The Deenbandhu design is made from bricks and mortar, see figure 2.6, and its floor is laid with bricks to form a spherical shaped hole. At the top edge of the floor, bricks are laid horizontally to form the foundation of the dome. The foundation of the dome is made by laying bricks horizontally around the top edge of the ground. This digester design can be installed correctly by fitting a steel pin in the centre of the floor or slab. This helps to ensure the right circumference of the digester is obtained, and the brick is laid correctly. Each brick is placed one after the other in a circle to build the dome, and the edge of brick is placed such that it matches the mark on the guide. Mortar is used to hold the bricks that are laid at the lower rings of the dome. The brick in the higher ring are held together by means of a wood whose length is similar to that of the guide wood, and brick held in a rope is tied to it [45].

Like the Janata design, the top of the dome in the Deenbandhu design is open to allow access for emptying the digester. The opening can be closed using a pre-casting ring paced in between the last brick to seal off the whole structure. If no manhole is made at the top of the dome, a metal or wooden form is used to provide support for the brick laid to seal of the manhole. Further, the outlet space at the side of the dome extended to allow for cleaning and emptying the digester. The inlet and outlet pipes are fitted in the right position. The inlet pit and reservoir pit are built over inlet and outlet pipes.

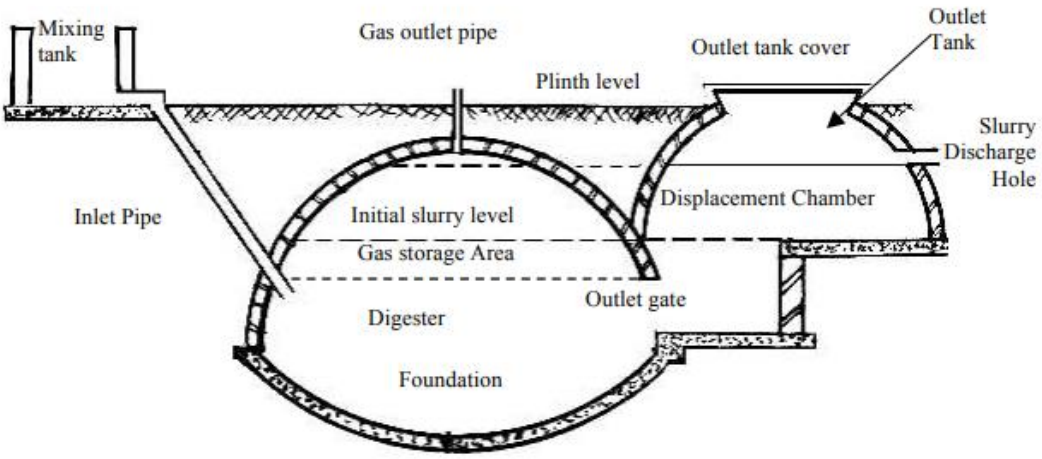

Figure 2.5 Show the diagram of the Deenbandhu fixed dome digester [186].

2.4.1.3 GCC fixed dome design

The design was developed in Nepal by the Gobar Gas Company. The floor of the digester has the shape of a dome. However, the flat floor design has been recommended due to the experience in use of floating drum digester. The floor and wall of the digester are built with bricks or stone masonry in a pit that is dug to the required size. Once completed, the soil is packed around the digester walls to provide support against hydraulic pressure building up in the digester pit. The dome is constructed by means of rigid material place on top of the hole formed after the pit is constructed [45].

Over time several modifications of the GGC-2047 digester was developed to address problems associated with the use of the digester. In the original design, it was found that because the compensation chamber is higher than the gas pipe in the dome; slurry enters and block the gas pipe after the gas is removed while the digester is continuously fed. The issue was resolved by lowering the compensation tank 20 cm below the dome. The slurry level in the digester was limited to 10 cm below the gas pipe. The lowering of the compensation chamber reduced the gas storage capacity of the digester,

and this means that not all the biogas produced escapes through the gas pipe as the pressure is not enough to force it out. The GGC digester was further modified by increasing the wide of the compensation chamber and lowering the minimum slurry level in the tank to ensure the gas displaces an equivalent amount of slurry (Volume) or more. Other modification done on the digester includes lower sloping of the floor of the digester to allow settling of the stones and non-degradable material to prevent blocking of the digester inlet.

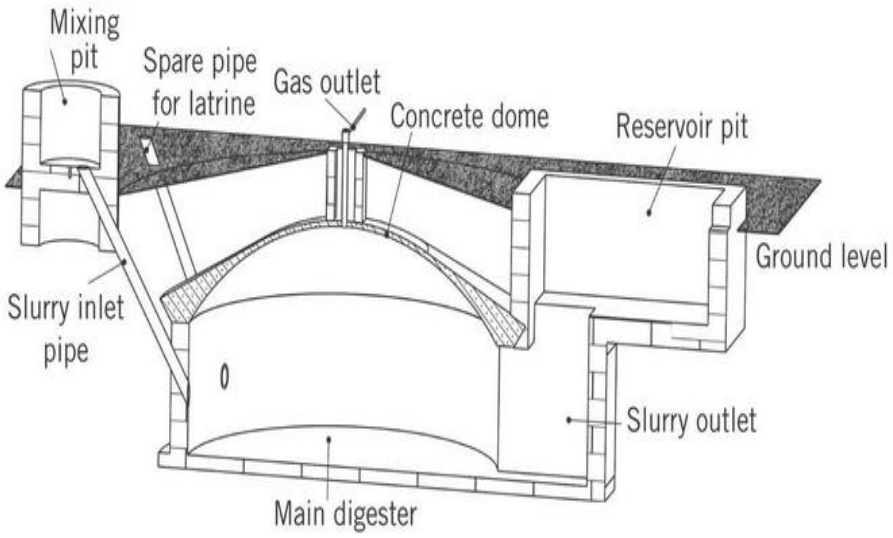

Figure 2.6 Show the DCC fixed dome design adapted from [45].

2.4.2 Floating Drum Digester

The float drum design was developed originally by Mr. J.J. Patel in Bombay, India. The unique feature of the digester design is the use of steel drum for the collection of the biogas produced. This steel drum makes it more expensive compared to other digester design. The floating drum design was deployed for wide use in India, following extensive publicity by Gobar Gas research institute in the 1970s, and the Khadi and Village Industries Commission (KVIC) in 1960 [42, 43, 45].

The design of digester has adopted by programmes in Nepal see figure 2.7. The digester is made from brick and masonry skill required is based on the skill available in the location. After digging the ground, a pipe is placed at the centre of the ground and a metal rod with a ring is attached to the pipe. The metal ring aids the lining of the bricks or stone so that the resulting shape of the pit is cylindrical. Then the soil is packed behind the brick after it has been fully built to provide additional support against the hydraulic pressure that will be exerted by the slurry inside the digester [45].

The inlet pipe which is made of either spun concrete, ceramic or plastic is placed close to the bottom of the digester, and a mixing pit where the feedstock and water are mixed is built over it. Directly opposite the inlet is a gap created on the digester wall that allows for the collection of effluent. The gas produces is collected in the steel drum that moves upwards, and down in response to the movement of the gas. The steel drum does not serve only as a storage for the gas produced, but its weight provides the pressure required to transport the gas through the pipeline to stove or external storage unit [42, 45]. Furthermore, the steel drum is fitted with metal bars which stirred the slurry and break scum, and the drum is mounted on a vertical central guide pipe. The below the central guide pipe is two layers of pipe arrange horizontally to provide support for the drum and prevent it from tipping over and jamming the walls of the digester. The main disadvantage of the floating drum design is that the steel corrodes easily as the external surface comes in contact with the slurry and the surrounding air. Hence, the steel drum needs to be coated with paint on a regular basis to avoid rust [42, 43]. The average size of the float drum design is 1.2 m^3 [125]. However, for small-medium scale, the digester volume varies from 5-15 m^3 [187]. The volume of 7.1 m^3 is used as the standard for the biogas programme in India and Nepal. It is used to provide enough gas to cook for a household with four to six cattle [154]. However, a larger volume of floating drum design has been built and are still in operation in some countries in Asia [45, 188, 189].

Different types of the floating drum digester have been developed, notably, the modified version of the KVIC model adapted to areas with high-water level. The design has a reduced deep and an increased wide, the walls of the digester are lined with brick such that the diameter at the bottom of the digester is different from the diameter at the top wall of the digester see figure 2.8 (i.e the walls are tapered). This is to ensure that the same size of the steel drum as the original KVIC model is used [45]. Floating-drum design is also made from plastic material to encourage further reduction in size and for the degradation of food waste. This plastic floating drum digester was developed by Appropriate Rural Technology Institute (ARTI) based in Pune and Maharashtra, India [45, 50, 190]. It consists of two water tanks of different size made from high-density polyethylene material that is welded together. The large size is the main digester and the small size is the gasholder see figure 2.9. The design of digester has been widely used in biogas programmes in China and India because they are very cheap and easy to transport.

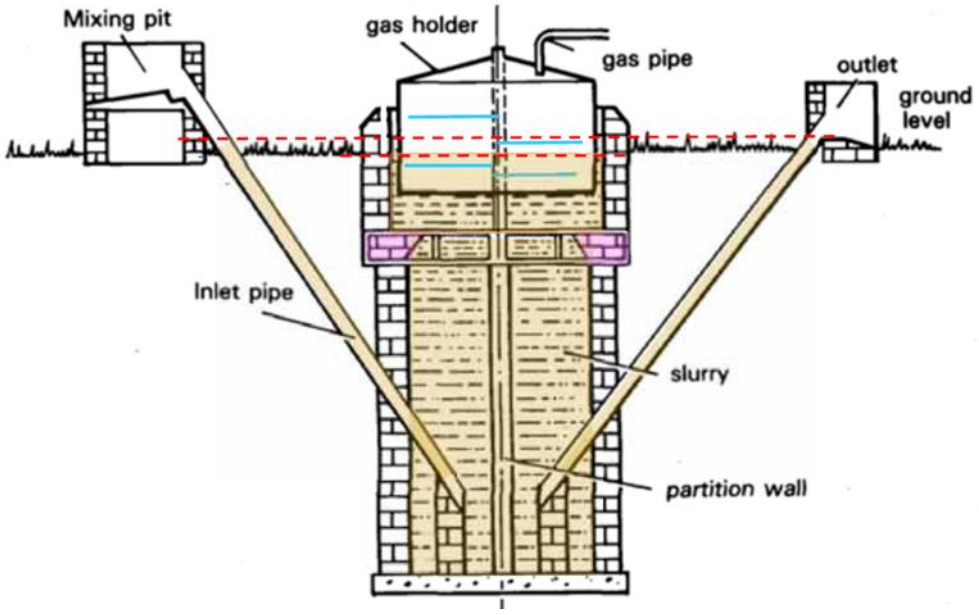

Figure 2.7 Shows the design of the floating drum digester [191].

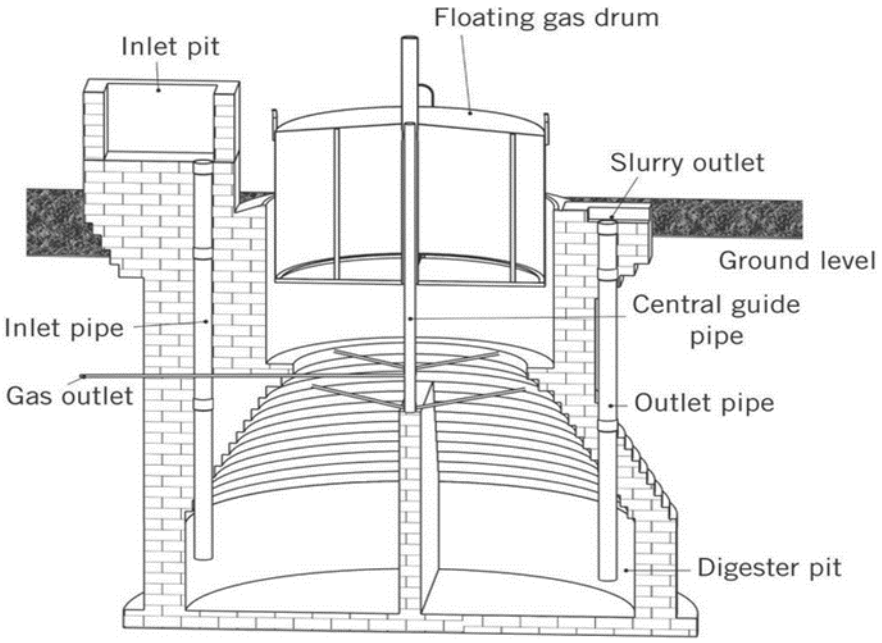

Figure 2.8 Modified floating drum digester for high water area [45].

Figure 2.9 floating drum design made from HDPE material [190].

2.4.3 Plastic bag digester

The number of designs of small-scale digester built over the years amount to several thousands or millions. In addition to this number, other designs such as the bag digester has been develop in the biogas programmes in various parts of Africa, Asia and South America [42, 192].

These digesters are made from polyethylene or polyvinyl chloride (PVC), and it consists of a long, narrow tank with average length to the wide ratio of 5:1 [42]. The diameter of the digester tubing varies from 800 mm to 2 m, and this is a function of the machine installed by the manufacturers. Usually, the material used in making the tubing is laid flat and folded into a roll. Therefore, the width of the tubing is half the circumference of the tune. The thickness of the plastic varies from 0.2 mm to 0.25 mm [45].

During the construction of the bag digester, two or three pieces of the plastic tubing are taking off the roll and cut to the required length. The plastics are then rolled together to form a tube made of two or three layers. This is to ensure that any damage on the outer plastic by sunlight, the tube is still protected and can maintain a tight gas seal. The volume and diameter of the bag digester determine the length of the plastic tubing [45].

Installing the bag digester requires careful digging of the ground to obtain the appropriate shape, length, and width so that when the slurry is feed into the bag digester it fits tightly into the trench. Further, the floor of the trench is dug at an inclined position from the inlet to the outlet to ease the flow of substrate from the inlet to the outlet under the influence of gravity. The digging of the trench is very important as it helps minimise fluctuation in the temperature overnight, especially in the cold mountainous region [42, 45]. Both ends of the tube are folded and held securely by means of rubber, and they are sealed with the inlet and outlet pipes by rubber bands. The inlet and outlet pipes have a length and diameter of 1000 mm and 150 mm respectively and are made of either plastic or ceramics. The gas produced is removed from the tube by cutting a small hole on the tube. The hole is sealed off to ensure no leakage of gas by installing a threaded PVC pipe

fitted with a rubber and plastic washer. The outlet gas pipe is connected to another flexible pipe running from the kitchen by means of a short rigid PVC pipe and glued.

In Latin America, other designs of the plastic bag digester has a shed or gable roof placed over the digester to provide insulation for the digester during the day and night [42, 43]. This also includes placing the bag digester under a greenhouse whose walls are of different height and are made from adobe material. The transparent cover and adobe walls of the greenhouse providing additional heating for the digester [73, 192, 193]. This bag digesters are made from a high-quality plastic material such as PVC, polypropylene and high-density polyethylene and the trenches are made with concrete or bricks [120, 194].

The covered lagoon is another design of bag digester, the surface of the lagoon is covered using high-density polyethylene, polypropylene, and fiber-reinforced flexible polymer geo-membrane. This design of digester is mainly used in the US and Thailand to treat slurry obtained from the animal husbandry operation. The main purpose of the cover is to reduce odour, induce anaerobic condition and for storage of the gas produced [45].

Generally, the plastic bag digester is easy to install, handle and are adapted to extreme conditions of low temperature in the mountainous region. The material can be transported easily to hilly areas. However, the material used in making the digester does not last and it has a life span of 2 -10 years [43]. Further, the material (polyethylene, etc.) is easily affected by sunlight, rodents, and birds looking for food. Hence it is usually recommended to cover the digester with grass matting to protect it. The dimension of the digester, trench, and roofed shed is generally a function of the location of the digester. At high mountainous region, the hydraulic retention time of the digester is between 60 - 90 days, and this implies that the volume of the digester and the dimension of the trench will increase.

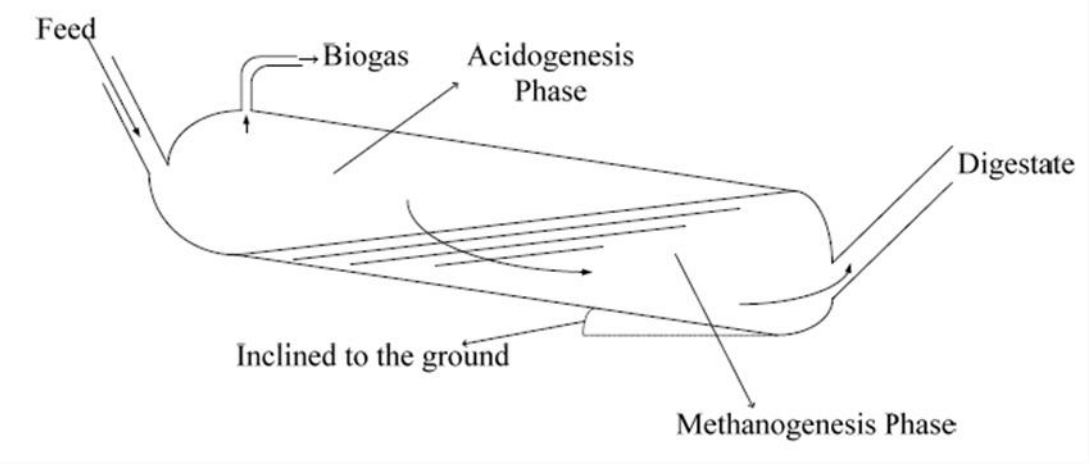

Figure 2.10 diagram of the plastic bag digester[43]**.**

Domestic digesters are unique in that they are buried underground and rely on the weather condition for the heating its contents. In the summer period, the digester performance very well and during winter it the performance is reduced.

2.5 Influence of weather condition on anaerobic digestion processes

The biochemical processes, physiochemical processes and dynamics of the anaerobic digestion process are influenced by the temperature. Therefore, it is best to operate the process in a controlled environment [195]. The fluctuations in the temperature of the anaerobic digestion process could be subject to a stepwise increase or decrease or it could be abrupt in the case of digester operated under passive heating [196-198].

Experimental reports have provided evidence that low biogas production is observed as the temperature drops below the mesophilic stage. Alvarez, Villca [199] Performed a semi-continuous experiment to investigate the influence of temperature. The solid content, hydraulic retention time and pressure on the bio-methane potential of cattle and llama manure were monitored and recorded. It was found that the temperature has the most impact on the production of methane, followed by hydraulic retention and solid content. Furthermore, it was observed that the methane yield of the

substrate considered was different and this can be attributed to the difference in the chemical content of the feedstock. The experimental study was performed in a control system operating at a different temperature. It did not consider the influence of the fluctuating temperature on the production of methane in high altitude regions as it is most characteristics of the location of the study. Also, the investigation of the impact of the pressure is very obvious, and should generally have no impact on the production of methane. In another study by Alvarez et al [198], a forced temperature fluctuation was employed in a laboratory experiment to determine the influence of the temperature on the biogas production and its methane content. The experiment was conducted initially at constant temperature and then later subjected to sudden forced temperature cycle changes of 12 hours digester operation at low or high temperature. The findings suggested that large amounts of biogas were produced at very high temperature during the first 12 hours of the cycle when the digester operated at high temperature. At low temperatures the digester, the amount of methane produced is low. This reduction in the methane flow rate is attributed to an inactive acidogenic state and the introduction of the large amount of feedstock.

The results of Alvarez, Villca [197] and Alvarez and Lidén [198] agrees that temperature has the most influence on the AD process. However, Alvarez, Villca [197] investigate the influence of Temperature on methane production at different operating temperature, and Alvarez and Lidén [198] investigated the impact of changes in the digester temperature. These studies were laboratory-based experimental in a controlled environment, and not field study that considers the influences of the uncontrolled weather conditions on the anaerobic digestion, since most small-scale digesters are operated at ambient temperature.

The unsteady nature of the ambient temperature results in a daily variation in the temperature of the anaerobic digestion process. During, the day the temperature is high while at night the temperature is low. Kalia and Kanwar [200] Investigated the temperature profile in fixed-dome and floating drum

digesters installed in a hilly location. The initial feeding of the digester occurred in the first month, and when the digester has attained steady sate, daily fed every morning commenced. Measurement of the slurry, feed, soil, gas and ambient temperature were taken. The study reveals slight variation in the temperature of the slurry as the biogas plant is installed underground. The same result was reported by Kalia and Kanwar [201], in their 10-year evaluation of the performance of the Janta-type fixed dome digester. The study also reveals that a decrease in methane production over the years is attributed to the formation lumps of digested slurry which settles in the digester.

The result agrees with the result of Kanwar and Guleri [202], whose one-year experimental study showed that biogas production is strongly influenced by the ambient temperature and the fluctuations between the seasons in the year. The digester was fed daily, the biogas measurements were taken twice a day. The ambient and digester temperatures are measured daily. Kalia [203] Compared the performance of different fixed-dome digesters (plug flow vs conventional fixed dome digester) and found that the plug flow digester produces 30 % more biogas than the conventional digester. The analysis of the digester temperature shows that the plug flow digester recorded higher slurry temperature than the conventional fixed dome digester. The plug flow digester was subject to a less variation to the environmental temperature as it inlet and outlet a further apart compared to the conventional digester.

These studies mainly focussed on the performance of anaerobic digesters in the hilly region and agrees that methane production is generally influenced by the weather conditions. However, Kalia [203] performed an assessment of the fixed dome plug flow digester in a cold hilly climate. Kalia and Kanwar [200], evaluated the impact of the environmental temperature on the performance of the fixed dome digester. Kanwar and Guleri [202] compared the performance of fixed digester made of a different material. Kanwar, Gupta [204] Compared the performance and cost of a modified fixed-dome digester against the conventional Deenbandhu type fixed-dome

digester. Kalia and Kanwar [201] Evaluated the impact of solid accumulation over time on the performance of the fixed-dome digester. A common limitation of these studies is the measurement and recording of the central (one-point) slurry temperature. A system operated unheated and unmixed will have spatial differences in the temperature of the slurry in the digester. The measurement of the slurry temperature at various depth could give a better representation of the slurry temperature in the digester.

Pham et al [205] investigate the factors affecting the temperature of the slurry and biogas production in small-scale digester in rural Vietnam. Four composite digesters were installed beneath the ground and the temperature measured at different depth (140 and 180 mm). Measurement of the air, soil, and mixing tank temperatures are taken at various depths (10,100, 140 and 180 mm). The study found that seasonal variation in the air temperature significantly influences the digester temperature, and the biogas production is dependent on the digester temperature. It was concluded that the main factors influence the temperature of the digester includes insulation, air temperature and temperature of the slurry in the mixing tank. This research project was part of the SUSANE biogas project funded by the Danish Ministry of Foreign Affairs.

Guo, Dong [206] Developed a mathematical model to assess the impact of the ambient temperature on the optimal operating conditions of the small scale digester. The model considered the heat demand of the digester, and it includes the heat required to raise the temperature of the influent and the heat given out by the effluent, heat losses from the digester bottom, walls, and top, and the heat loss by evaporation. Triplicate experiments were performed at various temperatures (38, 28 and 20 ^{o}C) and organic loading rates. The volume of methane production was measured. It was reported that net energy production is achievable when the ambient temperature is about 10 – 20 ^{o}C at a high loading rate of 4.6 - 5.4 kg ODM /m^{3}d. However, at temperatures lower than 10 ^{o}C, the net energy production is negative. This research received support from the China Scholarship Council and Sino-German project.

Gebremedhin, Wu [207] developed a thermal model of a plug flow digester that is built above ground, completely buried in the ground and partially buried in the ground. The models consist of heat gained from solar energy, hot water, and the heat losses from the mass flow in and out of the digester, circulating hot water in the pipe, heat losses through the floor and side walls of the digester and heat loss to the ambient air from the digester cover. It was validated by an experimental with two digesters, one uninsulated and the other insulated. The temperature, flow rate, and energy use are measured. It was found that less amount of energy is required to heat the digester during summer, and more energy is required to meet the heat demand in the winter or cold season.

Terradas-lll et al.[208] developed a mathematical model to simulate the temperature of an unheated, un-insulated fixed dome digester located in Hanoi, Vietnam. The model considered the impact of the soil characteristics, soil cover, ambient temperature and solar irradiation on the performance of the digester. The heat gained from solar energy absorbed on the surface of the digester. Heat losses from the liquid in the digester to the biogas, digester walls and floor, and digester cover. The thermal model also accounts heat losses when the soil is covered with snow or leaf in the estimation of the ground temperature. The model was validated by a field experiment with a digester identical to the digester in the model. It was found that the model predicted well the digester temperature and biogas production with some uncertainties. This research was part of the SUSANE research project, funded by the Danish Ministry of Foreign Affairs and Hivos.

2.6 Improvement of digester slurry temperature using a greenhouse

The need to improve the slurry temperature, especially during the cold periods led to the implementation of a greenhouse, with the aim of reducing daily temperature fluctuations. The implementation of the greenhouse has been extensively studied.

Ferrer, Garfí [71] investigated the performance of a psychrophilic anaerobic digester in regions with severe weather conditions. Field experiment involves two digesters operating at a hydraulic retention time of 60 -100 days in two locations. The study found that biogas production is possible at psychrophilic temperature with average methane production rate is 0.32 - 0.36%, and methane content of 60 - 63%. Further, the study concluded that using the greenhouse to cover the plastic bag digester reduces daily fluctuations in the slurry temperature. This research was performed in collaboration with various NGOs such as Intermediate Technology Development Group-Practical Action (ITDG-Peru), Engineers without Borders (ISF-Spain) and Green Empowerment (USA), etc. The financial support for the research was provided by the Centre for Development Cooperation (CCD-UPC), and the Catalan Agency for Development Cooperation.

Garfí, Ferrer-Martí [78] found that the slurry temperature in the digester varies between 22 – 23 ^{o}C using different greenhouse designs (dome roof and shed roof). The experiment was performed in the winter and summer periods, and the digester is fed with guinea pig manure. The research was carried out in collaboration with the various NGOs as stated in Ferrer et al (2011), and the same organisation provided the funding for the research.

Castano, Martin [209] reported the performance of small scale modified fixed dome digester cover with a greenhouse in Ohio state, US. The digester was operated at different stages corresponding to different organic loading rates. The results of the finding suggest an increase in biogas production during the summer when the slurry temperature is above 20 ^{o}C. The biogas production rate decreases during the winter when the slurry temperature is below 20 ^{o}C. The decrease in the slurry temperature is also attributed to the opening of the displacement tank, allowing the return of cold slurry. The partial covering of the digester with the greenhouse contributed to the decrease in the slurry temperature during the winter as cold air flows into the greenhouse. Thus, suggesting the importance of covering and insulating the displacement tank. The research received

support from the Ohio Agricultural Research and Development Centre, and funding from the Administrative Department of Science, Technology, and Innovation (COLCIENCIAS) and Universidad Technologica de Pereira.

Alternative methods of improving methane production from low-cost digester include the use of a biofilm carrier Martí-Herrero, Alvarez [120]. The research was performed in collaboration with the Caribbean and Latin American Biodigesters Net, and it received financial support from GTZ and HIVOS. The experimental work involves two digesters, one filled with biofilm and the other used as a reference digester. The digesters had the same operating conditions (i.e. the same loading rate and hydraulic retention time) and cow manure is used as the substrate. The results presented shows that the biofilm carrier separated the hydraulic retention time from the solid retention time, thus leading to an increase in the methane production against the reference digester. The use of biofilm could also limit the life span of the digester as over time the digester will require cleaning up and the disposal of the plastic ring used.

Mathematical modelling of the small-scale anaerobic digestion processes was develop to better understand the impact of the weather condition on the biogas production, the heat demand of the digester and the heat loss from the digester.

Perrigault, Weatherford [73] developed a mathematical model to evaluate the thermal performance of low-cost digester with a greenhouse in Peru. The model included the heat gained by the greenhouse cover, walls, greenhouse air, slurry, and the biogas. The heat losses to the surroundings and the ground via conduction, convection, and radiation. Using experimental data from a pilot low-cost plastic bag digester to validate the model. It was found that adjusting the thickness of insulation, it was possible to increase the slurry temperature above ambient temperature. The study concluded that the greenhouse acts as a solar collector receiving heat from the sun, and the greenhouse wall acts as thermal inertia by releasing stored heat during the night. The funding for the research was

provided by the Catalan Development Cooperation Agency, Centre for Development Cooperation, Endev-Bolivia program supported by GIZ,

In a similar study Weatherford and Zhai [210], used the same model to perform a parametric analysis of the effects of the insulation along the floor and side walls of the trench, cover transmissivity and digester material on the slurry temperature. It was concluded that the slurry temperature is positivity influenced by changes in the thickness of the insulation material, the orientation of the digester, and the amount of sunlight that is transmitted by the cover material. Also, it reveals that using a material that allows the transmission of the sunlight to the slurry is better to achieve a higher slurry temperature. From the results of Weatherford and Zhai [210] and Perrigault, Weatherford [73], it was observed that the thermal model showed the ability to represent the experimental data over a short period of time and it is considered that each element is at a single temperature. Further, both studies did consider heat transfer gradient in each component of the digester (except the slurry). However, Perrigault, Weatherford [73] seeks to explore the influence of geometry and material on the performance of the plastic bag digester in cold climate, and Weatherford and Zhai [210] explored some limitations of the work of Perrigault, Weatherford [73].

Kishore [211] developed a thermal model to explore the heat requirement of a fixed dome digester in a cold climate. The model included the evaporative, convective and radiative heat losses from the slurry surface. Heat losses by conduction from the floor and side walls of the digester. Also, the model considered the effect of external heating, such as the use of a greenhouse, biogas and the installation of insulation material. The study reveals that the use of biogas and greenhouse cover increases the slurry temperature slightly. But the individual approaches (use of only biogas or greenhouse) are not sustainable. It further concluded that insulation reduces the heat losses over the surface of the digester better than insulating the side walls.

Hassanein, Qiu [212] reported the use of a double greenhouse, an outer greenhouse cover and an inner greenhouse that covers the inlet of the

digester. Two underground digesters were examined, one with a greenhouse and the other without a greenhouse. The thermal model consists of the heat gained from solar energy on the greenhouse. The heat losses from the liquid surface to the ambient air, the digester floor and from the effluent leaving the digester. The experimental work was performed using the conditions in the model simulation. Measurements of digester, greenhouse and ambient temperature are recorded. It was found that with greenhouse the digester temperature is in the mesophilic regime most of the year, while without the greenhouse the digester achieves mesophilic in the summer. The results agree with the experiment but with some slight differences in the predicted temperature (0.34 ^{o}C). However, it was concluded that the design of the greenhouse is only effective for ambient temperature above -5^{o}C. Hence, suggesting the integration of a solar collector. This research was performed in Yangling, Xianyang and Shannxi, as part of the Northwest Biogas Research and Development project funded by the Ministry of Agricultural Department of Development and Planning, and the Chinese institutes for the Design, Planning, and Construction of Electric Power.

Similar, Hassanein, Zhang [213] integrated the solar collector with an underground digester cover with a greenhouse. The energy balance model developed included the heat supplied from the solar collector, heat gained from the influent substrate, the greenhouse and a supplementary electrical heater. The heat loss to the ambient air, influent, effluent and the floor of the digester. Also, the model was developed for normal clear weather condition as well as cloudy weather condition.

2.7 Improvement of digester slurry temperature using a solar collector

The heating of digesters with energy from the sun dates to the early 1980s in China. The success of the project led to various study on solar heating of anaerobic digesters Dong and Lu [214]. The solar collector is mounted on top of the digester. The hot fluid in the solar collector is transfer to the slurry via a pipe that run through the digester. The pipe is linked to the inlet

and outlet of the solar collector system. When the temperature in the solar storage tank is high, the valve open allowing hot water to flow through the heat exchange in the solar storage tank, thereby heating the slurry in the solar storage tank.

Alkhamis, El-khazali [215] developed a heat transfer model to investigate the design parameters for heating digester using solar collectors coupled with a heat exchanger. The model accounts for the useful energy gained from solar collectors, and the heat losses through the side, bottom, and top of the solar collectors. The experiment was performed using solar collectors in the laboratory made of less expensive materials. It was found that the digester temperature increases to 40 ^{o}C after 1 hour of operating the solar collector. Comparing the efficiency of the solar collector shows good agreement with the experimental values (61 % compared to 62 %).

Axaopoulos, Panagakis [74] investigated the impact of solar collectors on the temperature of the slurry in the digester, and the biogas production. An experimental study was performed by integrating an anaerobic digester buried underground with a solar collector. The digester was fed daily with manure slurry. The energy balance equation considered the heat gained from the solar collector, heat losses through the side wall of the solar collector, the back-heat loss, and the heat gained from the inlet manure. Heat losses from the manure surface inside the digester, and the heat losses through the digester wall and floor. It was revealed that the back-heat loss from the solar collector contributed to the maintenance of the digester temperature above the ambient temperature. The biogas temperature is influenced by the changes in the wind-speed and the total irradiance. The results obtained from the simulations agree well with the experimental evidence. The research was performed in Naxos, Island in Greece.

The result from Axaopoulos, Panagakis [74] and Alkhamis, El-khazali [215] agree that solar collector has positive impact on the performance of the digester buried underground. However, they differ in the design of the solar

collector, as the latter included an external heat exchange in the design while in the former, the solar collector is an integrated part of the digester.

El-Mashad, van Loon [75] examined the effects of preheating, insulation material and solar energy on the performance of a continuous stirred tank reactor in Egypt. In the experimental, two stirred tank reactors are operated at 55 ^{o}C and 60 ^{o}C, to attain steady state in the digester. The digesters were later subjected to daily temperature fluctuation, which causes a reduction in the methane production rate by 12 % (50 ^{o}C) and 20 % (60 ^{o}C). Fitting the experimental results into the model developed revealed that solar and insulation is effective for a small digester, and less effective for larger digesters. The study also found that the use of preheating is not economical for the biogas plant. The funding for the research was provided by the Egyptian ministry of higher education.

Unlike Axaopoulos, Panagakis [74] and Alkhamis, El-khazali [215], El-Mashad et al [75] explored the impact of pre-heater and insulation in addition to the solar energy on the methane production.

El-Mashad, van Loon [76] performed a similar experimental study to investigate the impact of different design of solar heating system on the performance of anaerobic digester. Two energy balance was developed: For the integrated system, the heat balance included; the heat gained from the solar collector, heat recovery, auxiliary heating. The heat losses through the back of the solar collector, between the slurry and the gas, losses to the surrounding and the pumping chamber. For the loose component, the heat balance did not consider the heat loss to the biogas and the losses to the pumping chamber. It was found that in each design of the solar heating system, the anaerobic digester has a net positive energy. Furthermore, it was suggested that the auxiliary heating does not have any significant impact on the thermal behaviour of the integrated system. However, a comparison of the systems show, that the loose system is better because it is cheap compared to the integrated system. Also, there are no particular differences in the impact of heat recovery on methane

production for both loose and couple systems. The Egyptian ministry of higher education provided financial support for this research.

Yiannopoulos, Manariotis [77] proposed a system consisting of a solar collector, digester and a heat storage tank. The model was developed to estimate the heat demand of the digester, consisting of the useful heat gained from the heat storage tank, heat loss to the surface of the insulator, heat loss to the surroundings and the losses from the pipe linking the digester and the storage tank. It was found that the solar collector was able to meet the heat demand of the digester for the different locations considered. The research was carried out in four different cities in Greece under the sponsorship of the Archimedes-EPEAK II Research program, and it was funded by the European Social Fund and Natural Resources.

In another study, a solar collector was used heat the digester built above ground Feng, Li [216]. In this novel approach, two experiments were performed. The first experiment was run in 7 batch digesters, three involves mono-digester and four co-digestion. In each experiment, the hydraulic retention time, feeding composition and digester temperature were varied. The second experiment was the semi-continues feeding of a mixture of feedstocks. The slurry, ambient, and heat storage temperatures were monitored as well as the biogas and methane production. The study reported an increase in the methane production during co-digestion, and an increase in the temperature of the slurry using the solar collector to provide heat. Also, the result of the experiment found that in the summer season, the temperature of the slurry increased to optimal mesophilic regime. In this hot month, the digester can be operated using feedstock with low degradability. However, during the cold months, it is advised to feed the digester with easily degradable organic matter. This research project was performed in Gaolan and Minqin Counties in China. The funding for the project was provided by the National High Technology Research and Development Program of China, Distinguished Young Scientists of Gansu Province, and Hongliu Outstanding Talents Projects of the Lanzhou University of Technology.

The study by Feng, Li [216] generally agrees with that reported by [74-76, 215] on the impact benefit of solar heating for anaerobic digester as well as the need to control the digester temperature. The distinguishing feature of the work by Feng, Li [216] is that the digester was built over ground and considers the impact of co-digestion in addition to temperature on the performance of the digester.

Further, the use of phase change heat storage material has been reported. Lu, Tian [217] developed a mathematical model to determine the heat demand of the digester system located in Anhui Province, in Central China. The research was funded under the National Key Technology Research and Development program, and funded by the National Natural Science Foundation of China. The model considers the heat loss from the digester, and the loss through the pipe connecting the digester and the heat storage tank. The size of the solar collector panel surface area and the storage tank volume are estimated. The required insulation material and thickness are determined. And it was found that when the solar fraction is 0.8, the 20 m^2 solar collector area and 3 m^3 heat storage volume could achieve the mesophilic slurry temperature in the winter. The determination of the suitable insulation material and thickness suggest that the use of 200 mm polyurethane is ideal for the digester system. However, some drawback of the study includes the assumption of a 5 ^oC ambient temperature during winter.

Similarly, Lu et al. [218] demonstrated that the impact of insulation of the heat storage tank with a phase change is an additional benefit. A thermal model was developed in fluent (v 3.3.26) to simulate the impact of a solar collector and heat storage on the digester temperature. It was validated with a laboratory study which uses an electric heater to supply hot water to a storage tank with paraffin wax placed between an internal and external polyurethane insulated material. The results obtained from both experimental studies agree with the simulated result as it shows that at air temperatures between 0 and 10 ^oC, the storage tank maintained the hot water temperature above 50 ^oC, thus providing a mesophilic temperature

in the digester. However, it was found that the simulation result overpredicted the water and paraffin temperature.

Lu, Wang [218] and Lu, Tian [217] demonstrated the impact of the phase change material in enhancing the digester temperature when integrated with the solar collector and heat storage tank. The difference is that the paraffin wax was the transfer fluid in the case of Lu, Tian [217], while in the study of Lu et al. [218] paraffin wax is used as the insulation material.

Youzhou, Pengfei [219] developed a solar collector heating pipe system to assess its impact on the anaerobic digestion of cow manure in winter. The thermal model developed considers the heat gained from the solar collecting pipe, the losses from the wall, floor and cover of the fermentation tank, and the heat exchanger. The model was validated with an experiment using the model conditions. The measurement of the methane yield, methane and carbon dioxide content, digester temperature, hot water temperature was recorded. The study found that the system was able to maintenance mesophilic temperature while achieving stable methane production. slurry temperature increased by 5 ^{o}C during the sunny day and decreases to 0.6 ^{o}C at night. Also. It was reported that during the day, there are no heat losses from the digester since it is surrounded by the heat collection system, while at night the digester losses heat. The project received grant and sponsorship from Special Fund for Agro-Research, Ministry of China, National Natural Science Foundation of China, and Science and Technology Open Cooperation project of Henan Province.

Simple heating of the digester with either solar energy or biogas has been reported to be unsustainable, especially during the cold season. Hence a sustainable way involves the combination of both heating sources. Rennuit and Sommer, [220] developed a decision support model to evaluate the heat demand of household biogas in Vietnam, considering the size of the digester plant, the number of pigs and the hydraulic retention time. The model includes the heat gained by the digester using solar and biogas. The results of the simulation show that a combination of solar and 10 % biogas will meet the heating demand of the digester while providing surplus biogas.

Further, to meet the heat demand, the digester must be operated a hydraulic retention time less than 40 days with a dilution rate of 1:3. The research was performed under the SUSANE Research Project with financial support for the Danish Ministry of Foreign Affairs.

2.9 Review of the various anaerobic digestion models

Mathematical models are a representation of reality. Models are applied to different situations with the aim of understanding the situation, design, control, troubleshooting and for optimisation of the situation. Here the model of the anaerobic digestion process is reviewed by looking at how the model was developed and its limitation.

2.9.1 Anaerobic digestion Model 1 (ADM1)

The ADM1 model was born out of the need to provide a more generalised model that takes into consideration many of the process stages in the anaerobic digestion process; with the focus on the understanding of the process dynamics for the design, operation and optimisation in the full scale [83]. Also, the model may serve as a tool for further improvement and validation of the anaerobic digestion process to achieve a better outcome. The model consists of two main reactions that occur in the digester, namely biochemical and Physiochemical reaction.

The model is used to describe the dynamics of 7 biomass groups, 12 soluble compounds, 5 particulate compounds, 19 biochemical reactions, 7 physicochemical reactions, and 3 gas-liquid transfer processes. The high number of parameters leads to the problem of parameter identification and structural weakness of the model. Anaerobic digestion model (ADM1) is unique in that it allows the description of the interactions between the various reaction (biochemical and physicochemical) and the hydrodynamic processes in one system (anaerobic digester).

In view of the comprehensive nature of the anaerobic digestion model. However, there are still processes and microbial species which are not covered in the model. This includes the solubilisation and precipitation processes, solid-liquid mass transfer process, etc. some species of the

model not include are sulphate and Nitrate species. Inhibition by long acid fatty acid is not included, the inhibition kinetics is assumed to be non-competitive, etc. the kinetics of disintegration and hydrolysis were simplified and represented by first-order kinetics. In the modelling of the process, only a few parameters are estimated while the majority of the parameters are assigned a default value, etc. Appels, Lauwers [221].

The following assumption is used in the ADM1 model:

- The complex particulate organic matter is homogenous, and it is disintegrated into Carbohydrate, protein, and lipids.
- The disintegration and extracellular hydrolysis steps consist of a complex process. Hence, the kinetic and biodegradability is lumped of the different processes are lumped.
- The extracellular processes are modelling using first-order kinetics.
- The rate equation is described using the substrate uptake rate. This is because it decouples the growth rate from the uptake rate and allows for variable yields.
- The biomass growth is implicit in the substrate uptake rate.
- The biomass decay rate is model using first-order kinetic and it is represented by a different set of equation.

2.9.2 Cardinal Temperature Kinetic model

The cardinal temperature model 1 with the inflection point is use to describe the growth of microorganism give a range of temperature [222, 223]. The model consists of three temperature such as minimum, optimum and maximum temperature. The minimum temperature describes the lowest temperature where the growth of the microbial population is limited, the maximum temperature where the growth of the microbial population is decreasing. An optimum temperature which corresponds to the exponential growth of the microbial population [222]. The model also lacks structural correlation between the parameter such as Uptakes rate, half-saturation constants, thus making the parameter estimation easy. Recently, it was

applied to investigate the effects of temperature fluctuations on the three stage of anaerobic digestion [223].

The model has some limitations, such as its inability to model the changes in the optimum uptake rate of the acidogenesis stages at temperatures between 12-30^{o}C. In addition, the affinity constant remained the same for the range of temperatures tested in the acidogenesis. Below 15^{o}C, the uptake rate of the methanogenesis was insignificant and the hydrolysis rate was very high. This is a consequence of using a substrate that is readily degradable (starch).

Furthermore, the cardinal temperature model 1 with a point of inflection has been used to predict the influence of the ambient temperature on domestic wastewater [224]. This model is explicitly implemented in the simplified three reaction, two population model of the anaerobic digestion process and it predicts well the degradation of the wastewater and the fluctuations in the methane production. In a similar study, the model has been accurately used to describe the growth of several algae species using the available data of growth response at high temperature. The study considered the effect of light and temperature [225] and predict well the effects of temperature and light on the cultivation of algae.

2.9.3 Simplified model of the anaerobic digestion processes

Several simplified models of the anaerobic digestion process have been developed to reduce the complexity in the measurement of the kinetic parameters and to allow for ease in the process monitoring and control. An example is the model by Bernard et al [84] which considers two a stage process of acidogenesis and methanogenesis. The model was originally based on the one population (reaction) model of Graef, [226], but it was modified to include a second bacteria population. Also, there are three reactions and two populations, where the hydrolysis stage consist of two parallel reactions [85] and a reaction in which the same bacteria is responsible for hydrolysis and acidogenesis [227].

The following assumption is used in the simplified two or three reactions, anaerobic digestion models:

- It was assumed that acetate and carbon dioxide are the only products of acidogenesis.
- The methane production is directly produced from the degradation of the acetate, and the estimated from the concentration of the bacteria, the stoichiometric and the kinetics of the methanogenic stage.
- The model considers the bacteria population characteristics to be homogeneous. To adequately predict that instability in the process, the acidic and alkalinity equilibrium terms were included in the model.
- It is assumed that the methane flows directly to the gas phase from the liquid phase.
- In modelling the total alkalinity of the system, it was assumed that since the substrate (wastewater) has a low pH.
- The inlet alkalinity is calculated from the inlet bicarbonate ion and the VFA ion concentrations, respectively. And the negligible concentration of hydroxide ion, hydrogen bicarbonate and carbonates ion.

The simplified models have been applied to simulate different problems identified in the literature, for example, it is been used as a tool for monitoring and controlling the anaerobic digestion processes, and the simulation of the wastewater treatment process where there is lack of available sensor. In the sequel, it has been used to compare the performance of the different reactor designs that treat solid waste [228] and the hydrolysis stage is modelled using the Contois kinetic equation. The model has some limitations in that it did not consider the dead biomass in the degradable organic matter. In addition, the total COD consists of the concentration of the influent organic matter and the VFA, thus the concentration of the biomass is not measured [84].

Chapter 3 Research Methodology

3.0 Introduction

The methodology developed for this thesis includes both modelling and experimental parts which are described in this chapter. The modelling work includes the thermal and biochemical model. The thermal model includes the models of the different designs of the plastic digester, the description of the various heat transfer equations, and the implementation in MATLAB. The biochemical models include one reaction, two reaction and three reaction anaerobic digestion models, and the temperature dependent kinetic model (Cardinal temperature model with point of inflection). The description of the various kinetic models, and the implementation of the biochemical models in Simulink. With the overall aim of developing a complete model consisting of thermal model linked to the biochemical model through the cardinal temperature model. This is a key novelty of the research work. The thermal model is used to test the performance of different designs of the plastic bag digester in different locations (Port Harcourt in Nigeria and Cuzco in Peru).

The methodology surrounding the gathering of experimental data obtained from Poggio, [81] is also described. The data was used for parameter estimation of the degradability coefficient, maximum update rate, half-saturation constants etc. The parameter estimation method and the sensitivity analysis are described and implemented in MATLAB.

3.1 Overview of the mathematical models

The research work is performed by modelling and simulation implemented in MATLAB/Simulink mathematical software. The mathematical model consists of the thermal, biochemical, and temperature dependent kinetic models, the parameter estimation method, and the sensitivity analysis. The thermal model describes the heat transfer occurring in the plastic bag digester buried underground and the heat transfer in the solar hot water system. The thermal model of the plastic bag digester is adapted from [73], see figure 3.2, and the solar collector model of the solar hot water system is adapted from [82]. The

thermal model of plastic bag digester was modified in the present study to account for the absence of greenhouse walls, see figure 3.1. The model of Dwivedi, [82] was modified to account for the absence of stratification in the solar storage tank, and it was integrated with the model of the plastic bag digester, see figure 3.3. This results in three designs of the plastic bag digester namely CASE 1: plastic bag digester without a greenhouse; CASE 2: plastic bag digester with a greenhouse; CASE 3: integration of the solar collector with the greenhouse plastic bag digester. These thermal models are linked with the biochemical model through the cardinal temperature model. The key contribution or novelty of the present study is the application of the complete model (thermal + cardinal temperature + biochemical) to investigate different designs of the plastic bag digester. Also, another novelty of the present study is the development of a numerical model of buried plastic bag digester covered with a greenhouse and integrated with a solar collector. This is because there are limited or no existing literature on the impact of solar collector and greenhouse on the performance of plastic bag digester.

These models are used to describe the physical processes of different designs of the plastic bag digester buried in the ground. The thermal models are used to simulate the performance of the different designs of the plastic bag digester given the location of the digester, solar radiation, wind speed, ambient temperature, digester geometry, and the properties of the construction materials. The model by Perrigault et al [73] has some limitations, such as the over-prediction of the temperature on one side of the greenhouse walls. The model did not include the inflow and outflow of the air inside the greenhouse in the energy balance equation of air inside the greenhouse. The model could not predict the absence of insulation material when the digester is continuously loaded over time as observed in the experimental study. This is because the digester expanded over time due to loading and shrinks the insulation material. However, the adaptation of the model in the present study is because it considers the key parameters, such as the solar radiation, wind speed, and the ambient temperature and it has been validated against experimental data [229]

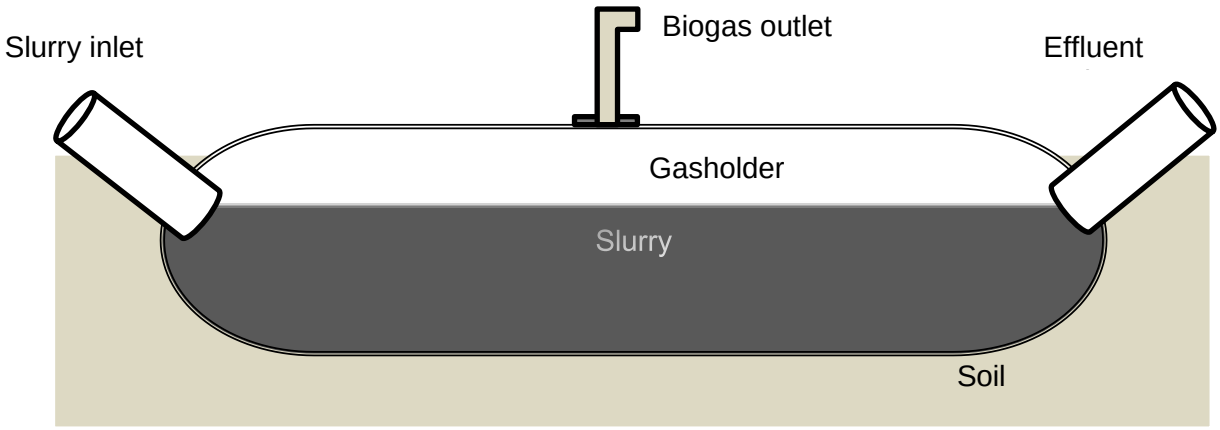

Figure 3.1 Schematic diagram of the plastic bag digester (CASE 1)

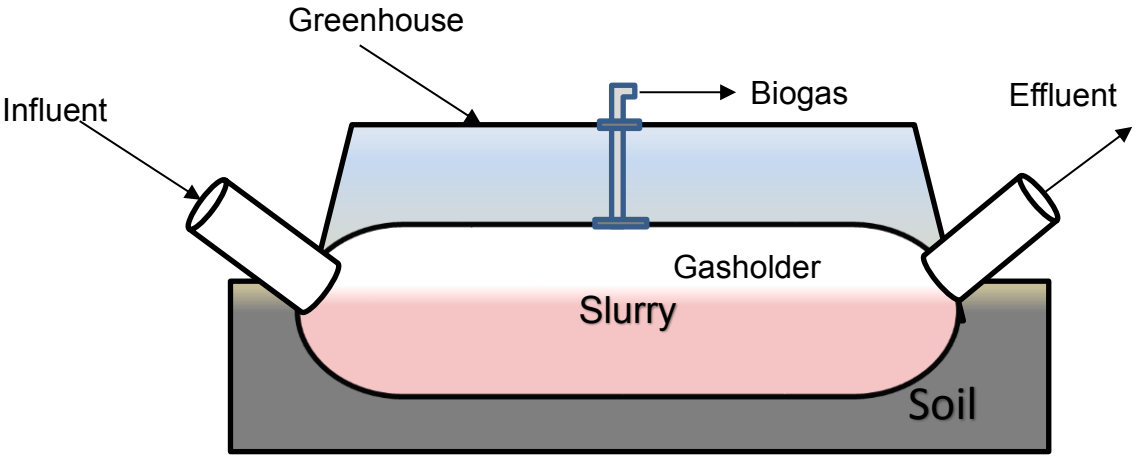

Figure 3.2 Schematic diagram of the plastic bag digester with greenhouse (CASE 2).

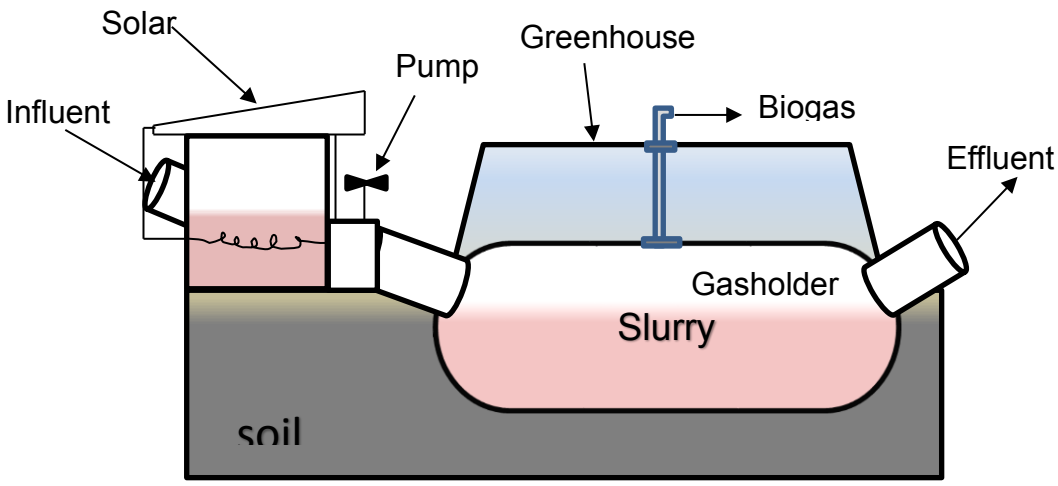

Figure 3.3 Schematic diagram of the plastic bag digester with greenhouse and solar hot water heating (CASE 3).

The biochemical model used in the research work is the simplified anaerobic digestion model and these consist of one, two or three reaction models mediated by two groups of micro-organism bacteria and archaea [84, 85]. In the one reaction model, the particulate organic matter degrades, and it is converted directly into methane. The two-reaction model consists of a first stage hydrolysis and second stage methanogenesis [84]. In the three-reaction model, the particulate organic matter is split into two fractions with different degradability and the second stage is methanogenesis where the soluble organic matter is converted to methane [85]. The hydrolysis stage is represented by the Contois kinetic, first-order, and Monod rate equation. The first order kinetic model is used to model the hydrolysis stage in anaerobic digestion processes to simplify the complex chain of reaction in the disintegration/ Hydrolysis stage [83], Contois kinetics is used in the present study because it considers the concentrations of the substrate and biomass, and the substrate to the biomass concentration ratio is used to either fix or adjust the degradation rate of the substrate [98]. The Contois kinetic model has been used extensively in the literature for describing the hydrolysis degradation of the particulate organic matter. For example, the degradation of raw compost material [230]. The methanogenic stage is described using the Haldane and Monod equations [84], Moser and Tessier equation [231]. It is

used in the present work because it expresses the growth limiting characteristics associated with the methanogenic stage at a very low concentration of volatile fatty acids and inhibitory effects of volatile fatty acid at high concentration.

The thermal model is linked to the biochemical model through the cardinal temperature model which is used as an input to describe the effect of the fluctuating temperature on the maximum uptake rate of the biochemical reactions, see figure 3.4. The temperature of the slurry obtained from the thermal model of the plastic bag digester is used to estimate the maximum uptake rate of both the hydrolysis and methanogenic stages. The cardinal temperature model (CTM1) is used in the present chapter because it can predict the kinetic behaviour of the microbes from the psychrophilic to the mesophilic temperature range. Also, the kinetic parameters employed in the CTM1 have been validated against experimental data [223].

The main limitation of the biochemical model is that they are a simplification of a complex microbiological system with 1000s of the species of bacteria competing for the same substrate and performing a variety of metabolic reaction. More specific limitation of the biochemical models includes; the exclusion of the inert component of the organic matter in the two reactions model. The lumping of the hydrolysis and acidogenesis stages in the hydrolysis reaction. The lumping of the acetogenic, hydrogenotrophic and aceticlastic stages into the methanogenesis stages. The cardinal temperature model is unable to estimate the hydrolysis rate constant and to predict the behaviour of the acidogenesis reaction below the temperature of 30 ^{o}C, the affinity constant of the acetic acid cannot be predicted at temperatures, less than 12 ^{o}C [223].

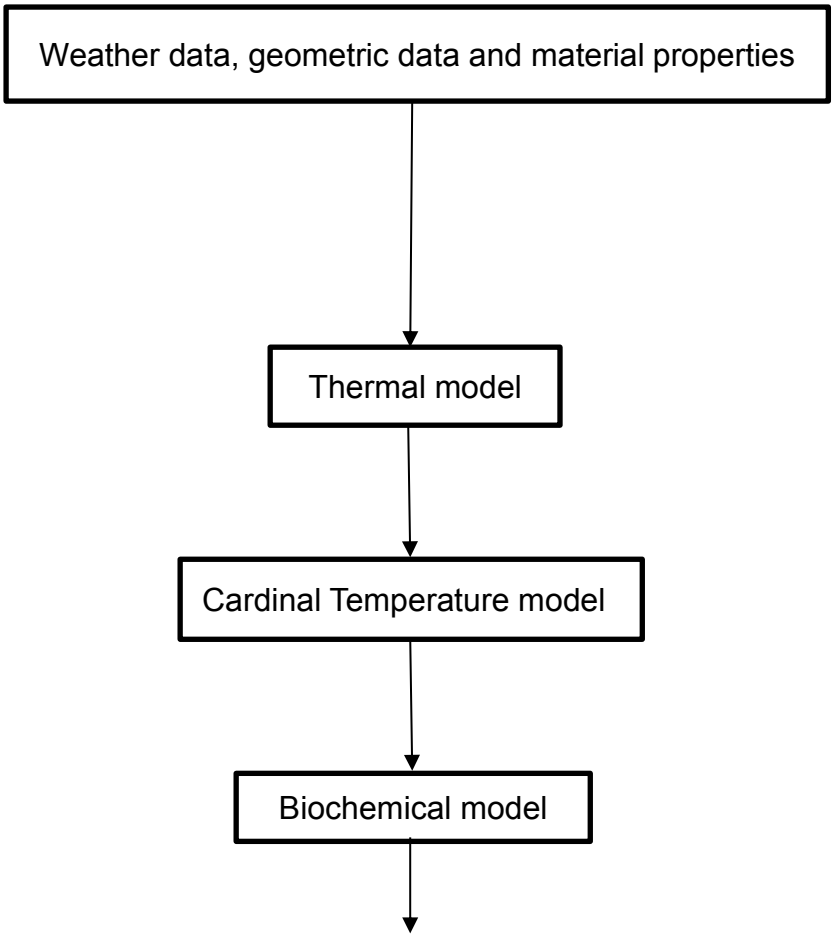

Figure 3.4 Schematic of the coupled model (thermal, biochemical and temperature dependent kinetic).

3.2 Description of Port Harcourt, Nigeria and Cuzco, Peru.

Two locations were chosen for the present study, Port Harcourt, Nigeria and Cuzco, Peru. Cuzco is located in south east Peru, in the Andes Mountains, with a total land area of 385.1 km^2 and it is about 3400 meter above sea level. It has an average annual minimum and maximum ambient temperature of 4.6 ^oC and 19.6 ^oC, average annual rainfall of 54.89 mm. The annual average insolation is 114KWh m^{-2}, and the yearly average wind speed is 3.48 ms^{-1}. Port Harcourt is the capital of River state, located in the southern part of Nigeria. It covers an area of 109 km^2, and it has an average high and low temperature of 30 ^oC and 22 ^oC. The average daily wind speed varies from 1.96 ms^{-1} to 2.5 ms^{-1}. The average daily solar energy varies between 3.5 Kwh in October to 4.4 Kwh in January. Between February and March of 2010, thermal data on digester installed in the field in the highlands of Peru and Bolivia, and in the laboratory in Cusco, Peru, was collected during a 7- week campaign [232].

3.3 Description of the various mode of heat transfer

Since an important aspect of this thesis relies on the predicting of temperature of various component within the plastic bag digester, a discussion of the different mode of heat transfer in the model is presented. Starting from the heat transfer by conduction, followed by heat transfer by convection and radiation. Finally, the section concludes with the discussion of the solar radiation absorbed on the surfaces of the digester component.

3.3.1 Conductive heat transfer coefficient

Conduction is a result of the vibration of the molecules or the atomic activity in a material where the molecules with a higher temperature have more energy than the molecules of lower temperature. It is generally associated with solid materials. The heat transfer by conduction can be described using the Fourier equation and it may be expressed as follows [233]:

$$q^{"} = -\lambda \frac{\partial T}{\partial x} \qquad (3.1)$$

where λ is the thermal conductivity of the material, $\frac{\partial T}{\partial x}$ is the temperature gradient along the material and $q^{"}$ is the heat flux through the material. The minus sign in the equation (3.1) is an indication of the direction of the heat flow. Furthermore, for steady state heat transfer by conduction, with a linear temperature gradient, the heat transfer equation can also be expressed as follows:

$$q'' = -\frac{\lambda}{l}(T_2 - T_1) \qquad (3.2)$$

where T_1 and T_2 are the temperatures at the ends of the material, and ⌊ is the thickness of the material. Furthermore, when a material is insulated, the Fourier rate equation for the heat conduction can be expanded to include the effects of the insulation in the computation i.e. the thermal conductivity of the insulation material and the thickness. The Fourier heat equation may be expressed as follows:

$$q = \frac{1}{\left(\sum_{i=o}^{n} \frac{\lambda}{l} A(T_1 - T_2)\right)} \qquad (3.3)$$

where $\sum \lambda/l$ is the summation of the thermal conductivity and the thickness of the conduction and insulation materials, and A is the cross-sectional area of the heat transfer surfaces (conduction and insulation materials). Additionally, the Fourier equation can be applied to model heat transfer in the soil, and this will be discussion in the following subsection.

3.3.1.1 Modelling Heat transfer by conduction in the soil

The Fourier model for the heat conduction can be applied to compute the heat transfer by conduction due to the seasonal variations in the soil conditions.

However, the temperature of the soil and its variation with depth with the variation in the weather conditions is discussed by Hillel [234]. The temperature profile in the soil with depth may be expressed as follows:

$$T_{gr}(z,t) = T_{gr,av} + A_o e^{-z/d} Sin\left[\frac{2\pi}{365}(t - t_o) - \frac{z}{d} - \frac{\pi}{2}\right] \qquad (3.4)$$

where for the case of infinite depth, i.e. $z = \infty$, and where the soil temperature remains constant at the $T_{gr,av}$, the mean average soil surface temperature at a depth $z = 0$. $Ae^{-z/d}$ is the amplitude of the temperature fluctuations at the depth z and it is smaller than the amplitude of the temperature fluctuation at the surface by a factor $e^{z/d}$. t_o is the time lag which describes an arbitrary starting point from the occurrence of the minimum temperature in the year, and $^{z}/_{d}$ is the time delay in the peak of the temperature of the soil. To model the temperature profile with depth, the damping depth d is estimated and it accounts for the decrease in the amplitude of the temperature at the depth z to a fraction of the amplitude in the temperature at the surface A_o. The damping depth is a function of the thermal properties of the soil and the frequency of the temperature fluctuations and may be expressed as follows:

$$d = \sqrt{2 * D_h * 3600 * {}^{2}/_{\omega}} \qquad (3.5)$$

where D_h is the thermal diffusivity of the soil and this is the ratio of the thermal conductivity of the soil to the volumetric conductivity and it is expressed as follows:

$$D_h = {}^{\lambda}/_{\rho C_p} \qquad (3.6)$$

where λ, ρ and C_p are the thermal conductivity, density and specific heat capacity of the soil, respectively, and the radian frequency $\omega = {}^{2\pi}/_{365}$.

The Fourier governing equation for heat transfer by conduction has been discussed and its application in the modelling of conductive heat transfer in the soil. The following paragraph demonstrate the application of the Fourier equation in the modelling of heat conduction through the walls of the plastic bag digester shown in figure (3.2). It is important to note that the same mode of heat transfer by conduction is applicable to figure (3.1) and (3.3).

In figure 3.2, the slurry in the digester exchanges heat via conduction with the ground (soil) through the digester side walls and the floor of the digester. The digester side walls, and floor are insulated. Hence to estimate the heat gain or loss through the digester side walls and floor, then equation (3.3) is applied. However, to estimate the heat loss or gain using equation (3.3), there is a need to estimate the temperature of the soil at the side walls of the digester and the soil temperature at the bottom of the digester. The soil temperature is a function of the soil characteristics and the weather condition. And is also a function of the depth of the soil which varies with time. Therefore, to estimate the variation of the soil temperature at different depths of the soil, equation (3.4) is applied, thus giving the average ambient temperature at the digester site.

3.3.2 Convective heat transfer

Convective heat transfer results from the motion of the fluid across a surface in the presence of a temperature gradient. The process is governed by the combined effect of diffusion and the bulk movement of the fluid, such as gases and liquid. Heat transfer by convection is modelled by the Newton law of cooling and it may be expressed as follows [233]:

$$q'' = h(T_2 - T_1) \qquad (3.7)$$

where $q^{"}$ is the heat flux, h is the heat transfer coefficient, and T_1 and T_2 are the temperatures of the surface of the material and the fluid, respectively. However, before modelling the convective heat transfer, the heat transfer coefficient must be determined, and this may be expressed as follows [235]:

$$h = N_{uL}\,{}^{\lambda}/_{L} \tag{3.8}$$

where N_{uL} is the Nusselt number and it is used to estimate the heat transfer coefficient for the different material's geometry. The Nusselt number relates to the convective heat transfer to the conductive heat transfer across the boundary of the material. It is a function of the Rayleigh number and the Prandtl number for fluid flow by natural convection. For the case of forced convection, where the fluid flow has a velocity u, the Nusselt number is a function of the Reynolds number and the Prandtl number [233, 235]. Mathematically, the Nusselt number may be expressed as follows:

$$N_{uL} = C(Re, Pr)^n \tag{3.9}$$

where C and n are constants. The indexes n describes the transition from the laminar flow regime to the turbulent flow regime. Equation (3.9) depends on the concentration of the flow over a solid surface and the orientation of the plate and it may be expressed as follows [233] :

$$N_{uL} = \begin{Bmatrix} 0.664Re^{1/2}Pr^{1/3} \\ 0.0360Re^{4/5}Pr^{1/3} \end{Bmatrix} \quad 2 * 10^5 < Re > 3 * 10^5 \tag{3.10}$$

For free convection, which is attributed to buoyancy, the Nusselt number may be expressed as follows:

$$N_{uL} = C(R_{aL}P_r)^n \tag{3.11}$$

For different material orientations, for example, for a vertical plate, the Nusselt number may be calculated using the formula [233] :

$$N_{uL} = \begin{Bmatrix} 0.68 + \frac{0.67R_{aL}^{1/4}}{\left(1+(0.492/Pr)^{9/16}\right)^{4/9}} \\ \left(0.825 + \frac{0.387R_{aL}^{1/6}}{\left(1+(0.492/Pr)^{9/16}\right)^{8/27}}\right)^2 \end{Bmatrix} \quad 10^9 \leq R_{aL} \geq 10^9 \tag{3.12}$$

Equation (3.12) is applicable to both laminar flow and turbulent flow, respectively. For a horizontal plate with an upper hot surface and a lower cold surface, the Nusselt number may be expressed as follows [233] :

$$N_{uL} = \begin{Bmatrix} 0.54R_{aL}^{1/4} & 10^4 \le R_{aL} \le 10^7 \\ 0.15R_{aL}^{1/3} & 10^7 \le R_{aL} \le 10^{11} \end{Bmatrix} \quad (3.13)$$

Also, for a horizontal plate with an upper cold surface and a lower hot surface, the Nusselt number may be expressed as:

$$N_{uL} = 0.27_{aL}^{1/4} \quad 10^5 \le R_{aL} \le 10^{10} \quad (3.14)$$

For plates inclined at an angle in the range $0 \le \theta \le 60^o C$, the same expression as for the vertical plate may be used. But, in the estimation of the Rayleigh number, the gravitational acceleration g should be replaced by $g \cos\theta$.

Also, for a horizontal rectangular cavity that is insulated from the surroundings with the upper and lower surfaces at different temperatures, the Nusselt number may be expressed as follows [233] :

$$\begin{Bmatrix} R_{aL} \le 5 * 10^4 \;\; h = {}^{\lambda}/_{L}, \;\; N_{uL} = 1 \\ 3 * 10^5 \le R_{aL} \le 7 * 10^9 \;\; N_{uL} = 0.069R_{aL}^{1/3}P_r^{0.074} \end{Bmatrix} \quad (3.15)$$

Furthermore, to solve for the Nusselt number, the Reynold number, Rayleigh number, and the Prandtl number, respectively, will be estimated. The Reynolds number is used to predict flow patterns in different fluid flows, and it relates the inertia force to the viscous force. It is used to determine whether a flow is laminar or turbulent, for a flow of fluid over a flat plate, the Reynolds number is used to describe the relationship between the fluid velocities, the

distance of the flow from the edge of the flat plate and the properties of the fluid (density and viscosity) and it is expressed as follows:

$$Re = \frac{\mu_\infty * L * \rho}{\mu} \tag{3.16}$$

where u_∞ is the fluid velocity, L is the characteristic length of the plate, ρ is the density of the fluid and μ is the dynamic viscosity of the fluid.

A thermal boundary layer exists when there is a difference in temperature between a surface and the fluid in motion. The thermal boundary layer is dependent on a unique number called the Prandtl number. It relates the momentum diffusivity to the thermal diffusivity, and it is a function of the fluid properties. It may be expressed as follows:

$$Pr = {\mu_\infty * C_p}/{\lambda} \tag{3.17}$$

where μ_∞ is the fluid velocity, C_p is the specific heat capacity of the fluid and λ is the thermal conductivity of the fluid.

The Rayleigh number is associated with a fluid flow driven by the buoyancy force and it is the product of the Grashof number and the Prandtl number, and it may be expressed as follows:

$$R_{aL} = \frac{g\beta(T_i - T_j)L^3}{\alpha_f v_f} = Gr * \mathrm{Pr} \tag{3.18}$$

where g is the gravitational acceleration, β is the temperature coefficient of the fluid, T_i is the temperature of the fluid, T_j is the temperature of the solid surface, L is the characteristic length of the geometry, α_f is the thermal diffusivity of the fluid, and v_f is the kinematic viscosity of the fluid.

3.3.2.1 Heat transfer by convection in the plastic bag digester

Thus far, the heat transfer by convection have been discussed, including its governing equation, modelling of the convective heat transfer based on the orientation of the material. The present section will demonstrate heat transfer by convection in the plastic bag digester without a greenhouse figure 3.1.

For the plastic bag digester without a greenhouse in figure (3.1), convective heat transfer occurs externally between the surrounding air and the digester tube. The digester tube is assumed to be a flat plate and the convective heat transfer coefficient of the surrounding air is estimated from the Nusselt number using equation (3.10). The heat transfer by convection between the digester tube and the surrounding air is calculated in equation (3.7).

Similarly, biogas gains or lose heat by convection with the digester tube and the slurry. Assuming the digester tube is a horizontal rectangular cavity with upper and lower surfaces at a different temperature. The characteristics distance between the slurry surface and the roof of the digester tube is equal to the average thickness of the gas. Equation (3.15) is applied to estimate the Nusselt number and the Rayleigh number, respectively, and the heat transfer by convection between the biogas and the digester tube is estimated by applying equation (3.7).

3.3.2.2 Heat transfer by convection in the plastic bag digester with a greenhouse

Additionally, the convective heat transfer equation is applied to description heat losses in various component of the plastic bag digester cover with a greenhouse. In Figure 3.2, the exchange of heat by convection occurs externally between the surrounding air and the greenhouse cover and the wall. Inside the greenhouse, the exchange of heat via convection occurs between the air inside the greenhouse, and the greenhouse walls, cover and the digester tube. Also, there is a convective heat exchange between the digester tube and the gas above the slurry. The digester tube is assumed to be a flat

plate and the convective heat transfer coefficient of the surrounding air is estimated from the Nusselt number using equation (3.10).

The air inside the greenhouse loses or gain heat by free convection by the two walls, the greenhouse cover, and digester tube. The estimation of the Nusselt number is based on the orientation of the greenhouse cover, two walls and digester tube, i.e. horizontal for the digester tube, vertical for the walls and titled for the greenhouse cover. The convective heat transfer coefficient in equation (3.8) is estimated from the Rayleigh number in equation (3.18) and the Nusselt number in equations (3.12) and (3.13), respectively, for the vertical surface (the walls) and Horizontal surface (digester tube). For the inclined surface (greenhouse cover) assumed to be a lower surface of a hot plate or lower surface of a cold plate, $gcos\theta$ is substituted for g in the Rayleigh equation (3.18).

The biogas gains or lose heat by convection with the digester tube and the slurry. The heat transfer coefficient in equation (3.4) is estimated, assuming the digester tube is a horizontal rectangular cavity with upper and lower surfaces at a different temperature. The characteristic length of the gas above the slurry is equal to the average thickness of the gas. Equation (3.15) is used to estimate the Nusselt number and the Rayleigh number, respectively.

3.3.3 Radiative heat transfer

Heat transfer by radiation is by means of electromagnetic waves, and it is due to the thermal energy of the material. When a body exchanges heat by radiation with an external body such as the sun, the amount of heat emitted or absorbed by the surface is expressed as follows [236]

$$q = \mathrm{A}\mathrm{h}_{\mathrm{r}}(T_2 - T_1) \qquad (3.19)$$

where A is the surface area and h_r is the radiative heat transfer coefficient which is modelled as follows (Duffie and Beckmann, 2013):

$$h_r = \sigma(T_2 + T_1)(T_2^2 - T_1^2) \Big/ \left(\frac{1}{F_{12}} + \frac{(1-\varepsilon_2)A_1}{\varepsilon_2 A_2} + \frac{1-\varepsilon_1}{\varepsilon_1}\right) \qquad (3.20)$$

where σ is the Stefan-Boltzmann constant, ε_1 and ε_2 are the emissivity of the two surfaces, A_1 and A_2 are the surface areas of the surfaces, for example, the Sun and Earth, and F_{12} is the view factor. The view factor is required to model the radiative heat transfer coefficient and it is defined as the percentage of the radiation emitted from a surface that is absorbed on another surface and it may be expressed as follows:

$$F_i = \frac{(1 + \cos(\omega))}{2} \qquad (3.21)$$

where F_i is the view factor and ω is the angle subtended at the surface.

Furthermore, when the difference in temperature between the sky and another surface is due to long-wave irradiation, then to model the heat transfer, the temperature of the sky is required. Assuming the sky to be a blackbody, the temperature of the sky may be expressed as follows [237]:

$$T_{sky} = 0.0552 T_{amb}^{1.5} \qquad (3.22)$$

Applying the equation of the heat transfer by radiation to the digester in Figure 3.2, there is an exchange of heat between the sky, greenhouse cover, and walls. On giving the temperature of the sky as a function of the ambient temperature in equation (3.22), the radiative heat transfer coefficient is calculated using equation (3.20) and the heat loss or gained by the surfaces (sky, greenhouse cover, and walls) is estimated using equation (3.19).

There is an exchange of heat by radiation between the greenhouse cover and the walls of the digester, and between the greenhouse walls as shown in

Figure 3.2. Also, heat loss or gain by radiation occurs between the digester tube and the greenhouse cover and walls, and then between the slurry and the digester tube. Similarly, equations (3.19), (3.20) and (3.21) are applied to solve for the view factor, the radiative heat coefficient, and the heat loss or gain by the surfaces (greenhouse cover, walls, digester tube, and slurry), respectively.

3.3.4 Solar heat absorbed

The amount of heat flux on a tilted surface is the sum of the beam and diffuse radiation falling directly on the surface as well as the radiation absorbed by the surface as a result of reflection [238]:

In Figure 3.2, the surfaces that absorb solar flux include the greenhouse cover, greenhouse walls, digester tube, and the slurry. However, the solar flux absorbed by the slurry is assumed to be negligible. The solar flux on these surfaces may be expressed as follows:

For the greenhouse cover,

$$S_c = \alpha_c A_c I_c \tag{3.23}$$

Where S_c is the solar energy that is absorbed by the greenhouse cover, A_c is the area of the cover, I_c is the amount of solar radiation on the surface of the greenhouse cover and α_c is the absorbance of the cover.

For the greenhouse walls, the solar heat flux on each side of the wall is given by:

$$S_{w2} = \alpha_{w2} A_{w2} I_{w2,out,T} + \tau_{w2} F_{w2} I_{w2,inT} \tag{3.24}$$

$$S_{w1} = \alpha_{w1} A_{w1} I_{w1,out,T} + \tau_{w1} F_{w1} I_{w1,in,T} \tag{3.25}$$

Where S_{w1} and S_{w2} are the solar energy absorbed by the greenhouse walls respectively, A_{w1} and A_{w2} are the area of the greenhouse wall 1 and wall 2, respectively. I_{w1} and I_{w2} are the amount of solar radiation on the surface of the greenhouse wall 1 and wall 2, respectively. F_{w2} and F_{w1} are the view factor for wall 1 and wall 2. α_{w1} and α_{w2} are the absorbance of the wall 1 and wall 2, τ_{w1} and τ_{w2} are the transmissivity of the walls, respectively.

For the digester tube:

$$S_t = \alpha_t A_t I_t F_t \tau_t \qquad (3.26)$$

where S_t is the solar energy absorbed on the tube, A_t is the area of the digester tube, I_t is the amount of solar radiation on the surface of the tube, F_t is the view factor of the digester tube, α_t is the absorbance of the digester tube, and τ_t is the transmissivity of the digester tube.

For the slurry:

$$S_s = \alpha_s A_s I_s F_s \tau_s \qquad (3.27)$$

where S_s is the solar energy absorbed on the tube, A_s is the area of digester tube, I_s is the amount of solar radiation on the surface of the tube, F_s is the view factor of the digester tube, α_s is the absorbance of the digester tube and τ_s is the transmissivity of the slurry.

3.4 Description of the energy balance in the various plastic bag digester design

The assumptions considered for the modelling of the heat transfer in the digester are as follows:

1. An energy balance is applied to each element of the digester and it is assigned a single temperature.

2. There is no stratification along with the depth inside the slurry.
3. The volumes of the gas above the column are constant and take the shape of a rectangle prism (trench).
4. There is no heat loss due to evaporation inside the digester and the mass flow rate of the biogas is not considered [211].
5. The heat generated due to the biochemical reactions is relatively small and hence neglected. This is because the reaction is endothermic and dissipated throughout the volume.
6. Digester tube transmissivity is not a function of the direction of the incident solar radiation.
7. For the plastic bag digester with greenhouse, the cover transmissivity is not a function of the direction of the incident solar radiation.
8. The inlet feed has the same properties as the slurry inside the digester, except for the temperature. This is to limit the amount of computation required.
9. The property of the soil is assumed to be uniform throughout its depth.
10. The soils temperature is constant, and it is not affected by the digester temperature [234].
11. There is negligible reflective solar radiation inside the system (digester).
12. There is negligible heat capacity for the digester gasholder and biogas.
13. The soil temperature varies sinusoidally with the annual frequency around an average value at all depth. At increasing depths, the oscillation of the temperature decreases with amplitude and increasing phase lags [234].

3.4.1 CASE 1: energy balance for the plastic bag digester without greenhouse

The plastic bag digester used in the present research is developed by [73], and the cross-sectional diagram of the digester is displaced in figure 3.5 below, showing the various digester components. In order to model the plastic bag without a greenhouse, the diagram is modified into figure 3.6 also showing below. In figure 3.6, the plastic bag digester has no walls and greenhouse. The components of the digester modelled are digester tube, slurry and biogas.

The heat transfer between the digester component were discussed in section 3.2.2.1

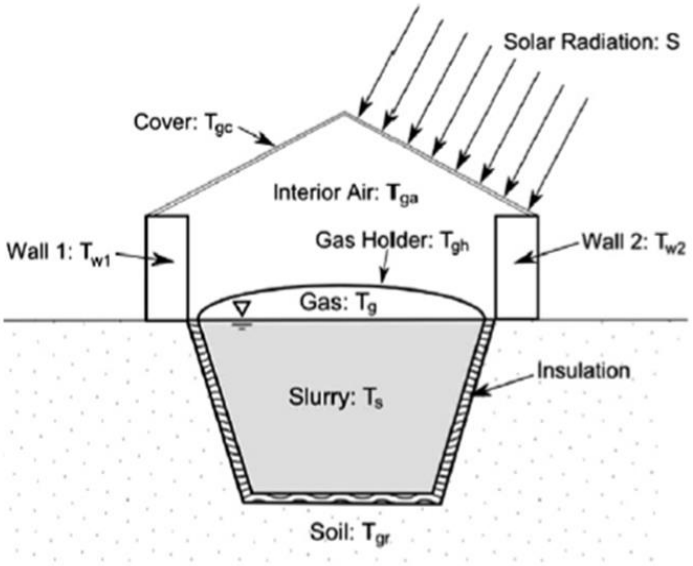

Figure 3.5 Cross-section of the diagram of the plastic bag digester with greenhouse [73].

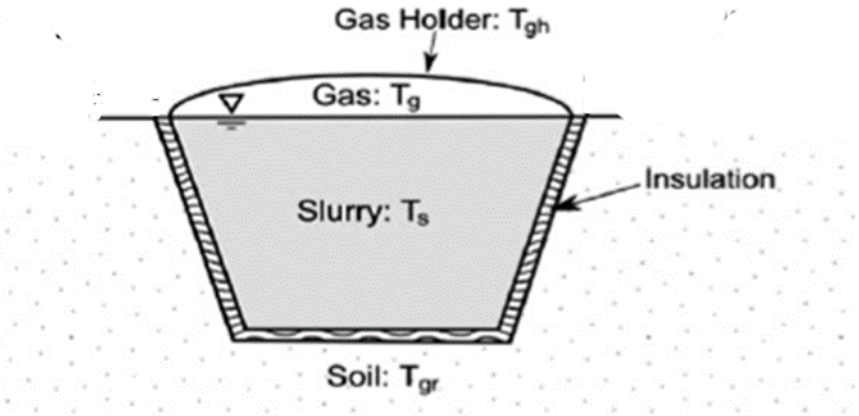

Figure 3.6 Cross-section of the diagram of the plastic bag digester without greenhouse wall and cover (modified from figure 3.5).

In Figure 3.6, the digester consists of three components representing the temperatures of the digester tube (t), the gas above the slurry (biogas), the

slurry (s), and the soil temperature. Additionally, the modelling of the temperature of the digester is represented by the diagram in figure 3.7 below.

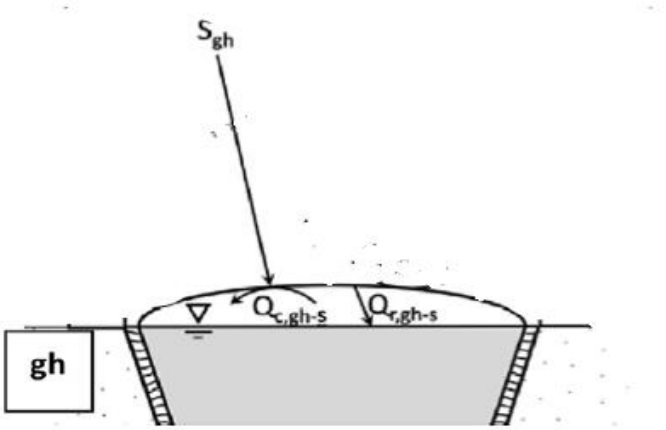

Figure 3.7 Show the scheme of the heat transfer in the digester tube.

Heat is lost or gain via convective and radiation between the digester tube and air, and between the digester tube and the slurry. The energy balance equation for the digester tube (Temperature T_t) is as follows:

$$0 = S_t + Q_{rd,t-s} + Q_{rd,t-sky} + Q_{rd,t-s} + Q_{air,c} \qquad (3.28)$$

where S_t has been defined in equation (3.26), section 3.2.4, $Q_{rd,t-sky}$ is the radiative heat losses between the digester tube and the sky, $Q_{rd,t-s}$ is the radiative heat transfer between the slurry and digester tube, and $Q_{Air,cnv}$ is the convective heat transfer between the external air and the digester tube.

The biogas exchange heat via convection with the digester tube and the slurry. The energy balance equation applied to solve the temperature T_g of the gas is as follows:

$$0 = Q_{cnv,t-g} + Q_{cnv,s-g} \qquad (3.28)$$

where $Q_{cnv,t-g}$ and $Q_{cnv,t-s}$ are the convective heat loss between the gas and the slurry, and between the gas and the digester tube.

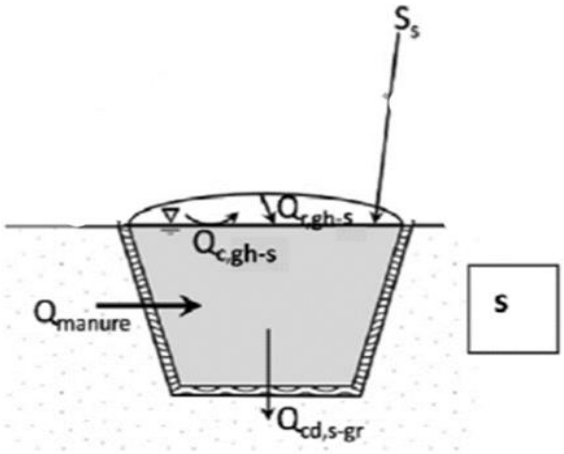

Figure 3.8 Show the scheme of the heat transfer in the slurry.

In figure 3.8, the slurry exchange heat via radiation with the digester tube, via convection with the biogas and the digester tube, and via conduction with the soil through the digester walls and the floors. Finally, the slurry gains or lose heat when it enters or exits the digester. The energy balance equation applied to solve the temperature of the slurry T_s, is as follows:

$$m_s C_{p,s} \frac{\partial T_s}{\partial t} = S_s + Q_{rd,t-s} + Q_{cnv,s-t} + Q_{con,s-gr} + Q_{in} \qquad (3.29)$$

where S_s has been defined in equation (3.27), $Q_{rd,t-s}$ and $Q_{cnv,t-s}$ are already defined in equation (3.28), $Q_{con,s-gr}$ is the conductive heat transfer between the slurry and soil, and Q_{in} is the heat exchange due to the mass flow of material in and out of the digester.

3.4.2 CASE 2: energy balance for the plastic bag digester with greenhouse

The scheme of the plastic bag digester with greenhouse has been presented in figure 3.5, section 3.4.1. The digester consists of the greenhouse cover (c), the greenhouse walls (w_1 and w_2), the air inside the greenhouse (a), the digester tube (t), gas (biogas) and the slurry (s). The heat transfer scheme for the modelling of each component of the digester is presented in figure 3.9.

The greenhouse cover exchange heat through radiation with the sky, the greenhouse wall, and the digester tube, and by convection, with the surrounding air and the air inside the greenhouse. The energy balance applied to solve the temperature of the greenhouse cover is as follows:

$$0 = S_c + Q_{rd,t-c} + Q_{rd,c-sky} + Q_{rd,w1-c} + Q_{rd,w2-c} + Q_{air,c} + Q_{cnv,a-c} \quad (3.30)$$

where $Q_{rd,t-c}$ is the radiative heat transfer between the greenhouse cover and the digester tube, $Q_{rd,c-sky}$ is the radiative heat transfer between the greenhouse cover and the sky, $Q_{rd,w1-c}$ and $Q_{rd,w2-c}$ is the radiative heat transfer between the greenhouse wall and the greenhouse cover, $Q_{air,c}$ is the convective heat transfer between the greenhouse cover and the air, and $Q_{cnv,a-c}$ is the convective heat transfer between the air inside the greenhouse and the greenhouse cover.

The air inside the greenhouse exchange heat by convection with the greenhouse cover, the greenhouse wall, and the digester tube. Also, it exchanges heat by radiation with the digester tube. The energy balance applied to calculate the temperature of the greenhouse gas is as follows:

$$0 = Q_{rd,t-a} + Q_{cnv,c-a} + Q_{cnv,w2-a} + Q_{cnv,w1-a} + Q_{cnv,t-a} \quad (3.31)$$

where $Q_{rd,t-a}$ is the radiative heat transfer between the air inside the greenhouse and the digester tube, $Q_{cnv,c-a}$ is the convective heat transfer between the air inside the greenhouse and the greenhouse cover, $Q_{cnv,w1-a}$ and $Q_{cnv,w2-a}$ is the convective heat transfer between the greenhouse walls and the air inside the greenhouse, and $Q_{cnv,t-a}$ is the convective heat transfer between the air inside the greenhouse and the digester tube.

The greenhouse walls loss or gain heat from the greenhouse cover, the digester tube, the sky, and the surrounding air. The energy balance to solve for the temperature $T_{w1}\ and\ T_{w2}$ of the greenhouse walls are as follows:

$$m_{w1}C_{p,w1}\frac{\partial T_{w1}}{\partial t} = S_{w1} + Q_{rd,w1-sky} + Q_{rd,c-w1} + Q_{rd,w2-w1} + Q_{rd,t-w1} + Q_{air,w1} + Q_{cnv,w1-a} \quad (3.32)$$

$$m_{w2}C_{p,w2}\frac{\partial T_{w2}}{\partial t} = S_{w2} + Q_{rd,w2-sky} + Q_{rd,c-w2} + Q_{rd,w1-w2} + Q_{rd,t-w2} + Q_{air,w2} + Q_{cnv,w2-a} \quad (3.33)$$

where $Q_{rd,w1-sky}$ and $Q_{rd,w2-sky}$ are the radiative heat transfer between the greenhouse walls and the sky, $Q_{rd,w1-c}$ and $Q_{rd,w2-c}$ has been defined in equation (3.30), $Q_{rd,t-w1}$ and $Q_{rd,t-w2}$ are the radiative heat transfer between the greenhouse walls and digester tube, $Q_{air,w1}$ and $Q_{air,w2}$ are the convective heat transfer between the greenhouse walls and the air. $Q_{cnv,w1-a}$ and $Q_{cnv,w2-a}$ has been defined in equation (3.31), $Q_{rd,w1-w2}$ and $Q_{rd,w2-w1}$ are the radiative heat transfer between the greenhouse walls.

The digester tube exchanges heat through radiation with the greenhouse cover, the greenhouse walls, and the slurry. It exchanges heat through convection with the slurry and the air inside the greenhouse. The energy balance equation applied to solve the temperature T_t of the digester tube is as follows:

$$0 = S_t + Q_{cnv,t-a} + Q_{rd,t-w1} + Q_{rd,t-c} + Q_{rd,t-w2} + Q_{rd,t-s} + Q_{cnv,t-s} \quad (3.34)$$

Where $Q_{rd,t-s}$ is the radiative heat transfer between the slurry and digester tube, and $Q_{cnv,t-s}$ is the convective heat transfer between the slurry and the digester tube.

For the gas (biogas) above the slurry, the heat lost or gained is by convection between the digester tube and the slurry. To solve for the temperature T_g of the gas, the following energy balance is applied:

$$0 = Q_{cnv,t-g} + Q_{cnv,s-g} \quad (3.35)$$

where $Q_{cnv,t-g}$ and $Q_{cnv,t-s}$ are the convective heat loss between the gas and the slurry, and between the gas and the digester tube.

The slurry exchanges heat through radiation with the digester tube, and via convection with the gas and with the soil through conduction in the digester wall and floor. The energy balance equation applied to solve the temperature of the slurry T_s, is as follows:

$$m_s C_{p,s} \frac{\partial T_s}{\partial t} = S_s + Q_{rd,t-s} + Q_{cnv,s-t} + Q_{con,s-gr} + Q_{in} \quad (3.36)$$

where $Q_{con,s-gr}$ is the conductive heat transfer between the slurry and soil, and Q_{in} is the heat exchange due to the movement of the slurry in and out of the digester, Q_{rd,t_s} and Q_{cnv,t_s} has been defined in equation (3.34).

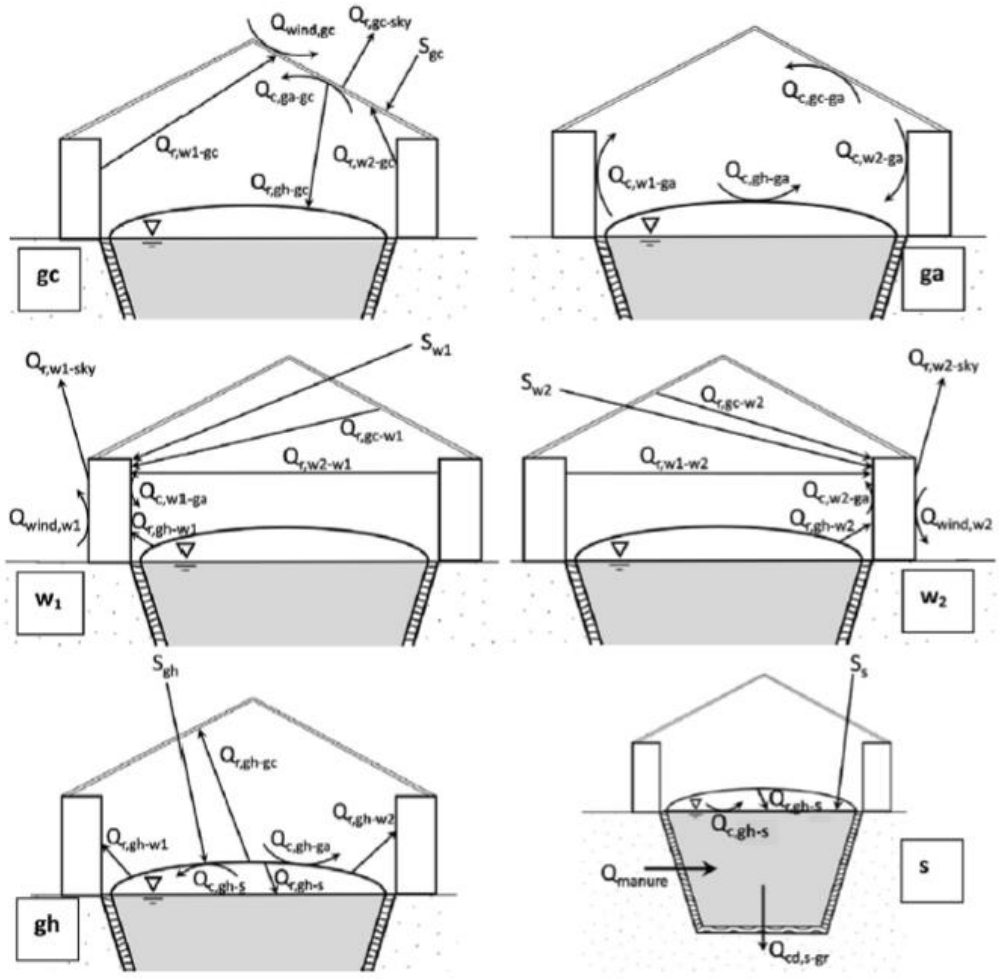

Figure 3.9 Show the scheme of the heat transfer in each component of the plastic bag digester (CASE 2).

3.4.3 CASE 3: energy balance for the solar domestic hot water storage system

The solar domestic hot water storage system is a unique type of heat exchanger that is used to convert the energy that is emitted by the sun into heat. It consists of a flat plate solar collector and a storage tank. The flat plate solar collector consists of the absorber plate, the tube fixed to the absorber plate from where fluid flow through the collector, the transparent cover and the collector box. CASE 3 is the modelling of the plastic bag digester as in CASE 2 coupled with a thermal model of the hot water storage system. Hot water

from the solar collector of the hot water system is used to heat the feed contained in the storage tank to the desire temperature. The hot feed (slurry) is transfer to the plastic bag digester through the outlet pipe of the storage tank that is connected to the plastic bag digester.

The assumption considered in the modelling of the solar domestic hot water storage system includes:

- The temperature drop across the cover thickness is negligible.
- Heat loss from the bottom of the collector and sidewall is negligible.
- The heat capacity of the storage tank material is negligible.
- There is no stratification inside the tank, hence the temperature of the fluid in the storage tank is uniform.

The energy balance equation that describes the heat absorbed by the solar panel is as follows, [236]:

$$A_c F_r [S - U_l(T_i - T_{amb})] = mC_p(T_l - \dot{T_o}) \qquad (3.37)$$

where A_c is the cross-sectional area of the collector, F_r is the collector heat removal factor, S is the solar energy absorbed on the solar surface, U_l is the overall heat transfer coefficient, $\dot{m}$ and C_p are the mass flow rate of the fluid in the collector and the specific heat capacity of the collector fluid, respectively, T_i, T_o, T_{amb} are the inlet and outlet temperature of collector fluid, and the ambient temperature, respectively.

The collector heat removal factor F_r is a key design parameter in the determination of the performance of the flat plate solar collector. It is defined as the actual useful heat gain when the temperature of the absorber plate is replaced with the inlet temperature of the collector fluid. It is a function of the flow rate of the heat transfer fluid and it is can be expressed as follows:

$$F_r = \frac{\dot{m}C_p}{A_c U_l}\left(1 - \exp\left(-\frac{A_c U_l F'}{\dot{m}C_p}\right)\right) \qquad (3.38)$$

where F' is the collector efficiency factor, other parameters in equation (3.38), has been defined in equation (3.37).

The overall heat transfer coefficient U consists of the heat loss from the top, bottom, and sidewalls of the flat plate solar collector. It is a function of the geometry of the solar collector panel. However, in the present study, it is assumed that heat loss from the bottom and sidewalls of the flat plate collector is negligible. Klein [239] developed an empirical expression for estimating the overall heat transfer coefficient from the top of the flat plate solar collector, and it is expressed as follows:

$$U_l = \left(\frac{N}{t_x} + \frac{1}{h_w}\right)^{-1} + \frac{t_y}{(t_w)^N + t_z - N} \qquad (3.39)$$

where the expressions for t_x, t_y, t_z and t_w are presented in the Appendix A.2. h_w is the convective heat transfer due to the wind speed, and N is the number of the glass cover.

The parameter S is estimated from the beam and diffuse solar irradiation on the surface of the collector panel in a matlab script, and the details can be found in the Appendix A.1.

For the storage tank, the heat delivered to the storage tank by the heat transfer fluid is lost to the surroundings through convection and radiation, by conduction with the walls and floor of the storage tank, and finally, heat is lost when the slurry enters and exits the storage tank. The energy balance for the solar storage tank can be expressed as follows:

$$m_s C_{ps} \frac{\partial T_s}{\partial t} = \left(mC_p(T_o \dot{-} T_i) - ((UA)_s(T_{amb} - T_s))\right) \qquad (3.40)$$

where m_s is the mass of the fluid in the storage tank, C_{ps} is the specific heat capacity of the fluid in the storage tank, A is the area of the storage tank, and U is the overall heat transfer coefficient of the storage tank.

3.5 Implementation of the Matlab model

3.5.1 Implementation of the plastic bag thermal model.

The thermal model of the plastic bag digester as described in section 3.3.2 was developed by Perigault et al [73] and it was implemented in MATLAB 2008, using the finite-difference method which is scripted in MATLAB. However, the disadvantage of the method is that the simulation did not make use of the inbuilt numerical tools in MATLAB, hence the errors in the simulation results was not estimated. In the present study, the thermal models (CASE 1, CASE 2) was rewritten in MATLAB 2015 so that it is solved using the inbuilt ordinary differential equation solver ode15s. The ode 15s uses the Runge-Kutta numerical method to solve the governing system of differential and algebraic equations in which the errors associated with one iteration is of the order five. From the energy balance equation presented in section 3.3, CASE 2 consist of a system of 3 ordinary differential equation and 4 algebraic equations, and CASE 1 consists of 1 ordinary differential equation and 2 algebraic equations.

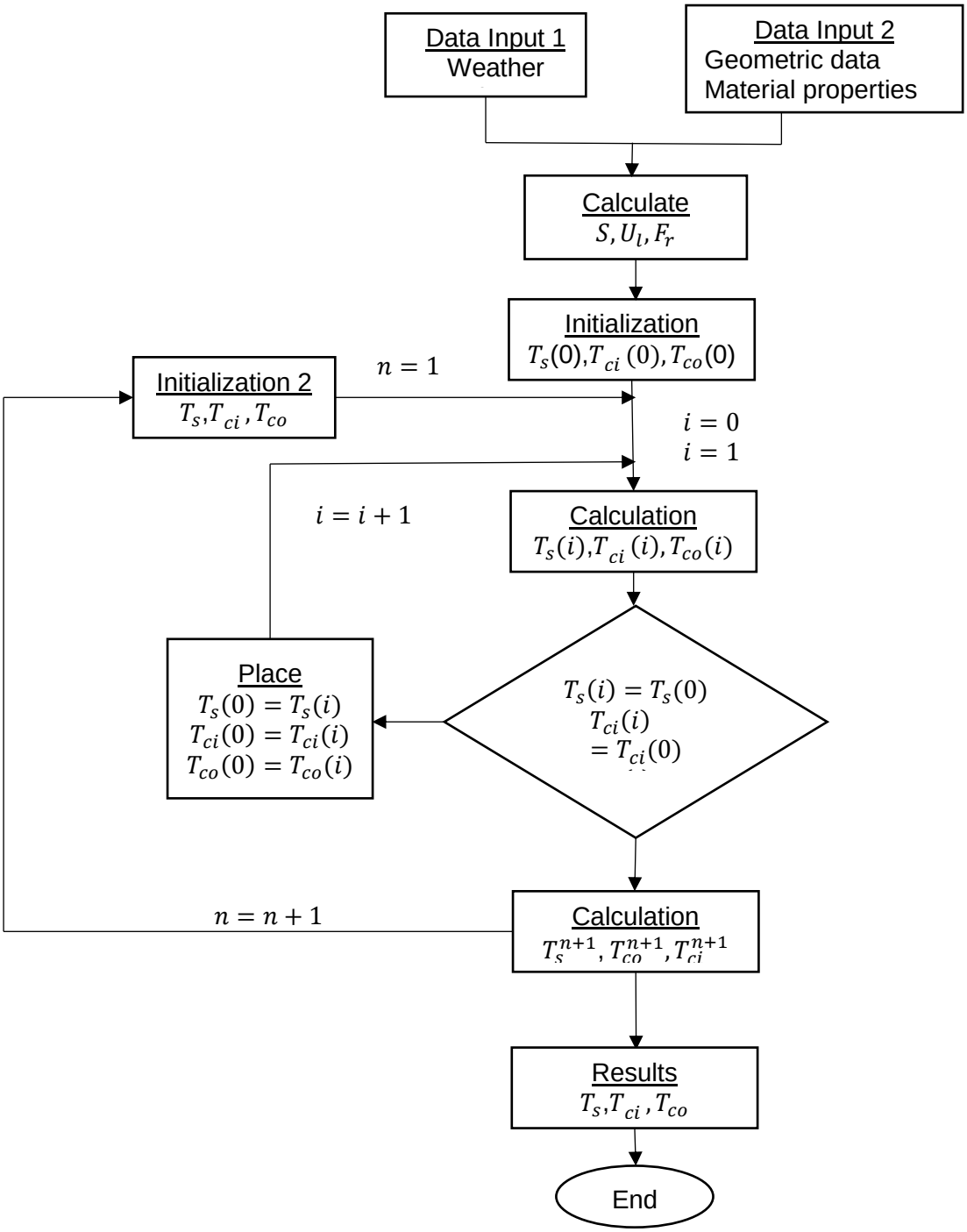

Figure 3.10 Shows the schematic of the thermal model of the plastic bag digester [73].

The operating scheme of the model involves loading the weather data, longitude and latitude of the location of the digester, digester geometric data, and material properties. The import data is used to arrange the weather data into months of the year, days of the year ad hour of the year. The longitude,

latitude, and orientation of the digester are input in cosine-theta, and the output is the cosine of the zenith angle. The property element arranges the geometric data and material properties in a matrix. The import data, digester orientation, and zenith angle are inputs used in the estimation of the direct, diffuse and total solar radiation from solar radiation data. The solar radiation data, the cosine of zenith angles, view factor and surface geometry are input used to estimate the solar radiation absorbed by each digester element (i.e. the amount of solar energy absorbed by the greenhouse cover, digester tube, greenhouse walls, and slurry). The intermediate is the amount of solar radiation on the surface of the digester components (cover, tube, and walls). The view factor and the surface geometry are input used in estimating the radiative, convective and conductive heat transfer coefficient of the digester components (cover, walls, tube, greenhouse gas, slurry, and biogas). The solar energy absorbed by the digester tube, greenhouse cover, slurry and greenhouse walls, the heat transfer coefficients and the ambient temperature are input in the estimation of the temperature of the digester components. The operating scheme of the thermal model of CASE 2 and CASE 1 is presented in figure 3.11 and 3.12. CASE 3 consists of CASE 2 and the solar hot water storage model. The description of the solar hot water storage tank model component of CASE 3 is presented in the following subsection.

3.5.2 Implementation of the solar collector model component of CASE 3.

The solar collector model is implemented in MATLAB/Simulink 2015a and it is solved using ode15s solver. The solar collector system consists of one differential equation and one algebraic equation. The solar collector model equations (3.37), (3.38), (3.39), (3.40) in section 3.3.3, are implemented in Simulink, while the input parameters are scripted in MATLAB.

The model parameters such as the collector area, inlet temperature of the collector fluid, Collector angle of tilt, thickness and heat conductivity of the storage tank, weather data (solar radiation, ambient temperature etc), latitude and longitude of the location, absorbance of the plate, plate efficiency factor

and transmittance are scripted in MATLAB. These parameters are used to calculate the hourly solar radiation on the surface of the solar collector, the overall heat transfer coefficient and the collector heat removal factor. The details of the MATLAB code can be found in Appendix B.1.

The energy balance equation for the solar domestic hot water system is implemented in the Simulink workspace. The model equation for the flat plate collector is implemented in the Simulink block named “collector”, the heat exchanger equation is implemented the Simulink block “exchanger”, and the storage tank model is contained in the Simulink block “solar storage model”. The simulation for the solar collector system is performed in two phases. The first phase is the initialisation stage, the model is simulated on an hourly basis for 365 days and the final temperatures of the storage tank, inlet and out temperature of the solar collector is obtained. The temperatures obtained are used as the initial condition for the second phase, and the simulation is repeated. The detail of the simulation process is presented in figure 3.10

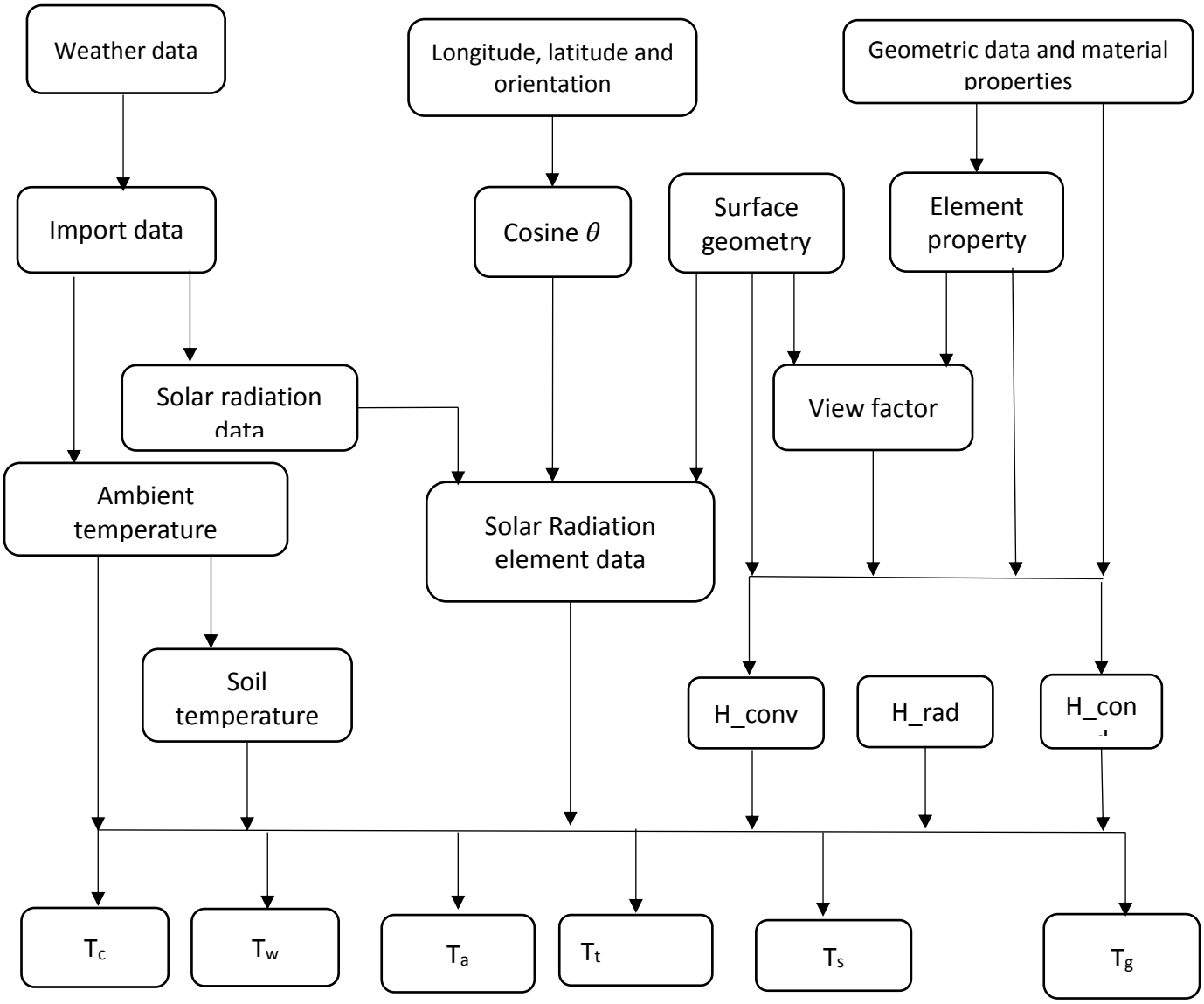

Figure 3.11 Show the operational scheme of the plastic bag model.

3.5.3 Model parameters and initial conditions

The parameters used in the thermal model (CASE 1, CASE 2 and CASE 3) includes the digester dimension, elevation of the digester above sea level, and the latitude and longitude of the location. The elevation, latitude, and longitude at Port Harcourt and Cuzco, are shown in table 3.1. The elevation above sea level, longitude and latitude of Cuzco is obtained from [73]. For Port Harcourt,

these values (elevation above sea level, longitude and latitude) were obtained from Google search. Also, the dimension of the digester, as well as the material properties, are presented in table 3.2 were obtained from [73]. Other model parameters used include the absorbance, emissivity, and transmissivity of the digester material and these are the same as the value used in [73] and present in table 3.3. The initial conditions of the temperature of the slurry, greenhouse cover, greenhouse walls, digester tube, the air inside the greenhouse and the biogas, are presented in table 3.4.

3.5.4 Input weather data

The weather data (solar irradiation, wind, and ambient temperature) used were collected from the National Renewable Energy Laboratory website and it is contained in the typical meteorological year (TM2) files. The TM2 files are a collation of the hourly weather data over a 10 years period for different location around the globe [240]. The data were converted to a readable format, exported and saved as a CSV file using the Autodesk Ecotect analysis tool. This was achieved by importing the weather file into the Ecotect workspace, and then using the Ecotect weather manager to read and separate the data into different columns corresponding to the direct and diffuse solar radiation, wind speed, ambient temperature. The data is stored in the following format; the month of the year, day of the month, day of the year and the hour of the year and it is saved in a Dat. File**.**

Table 3.1 Input data for the location of the digester [73] .

Parameters	**Values**
Orientation of digester	49^{o}
Inclination of digester	30^{o}
Elevation of digester in Cuzco	3800m
Latitude and Longitude of Cuzco	-13.513 and -71.976
Elevation in Port Harcourt	16m
Latitude and longitude of Port Harcourt	4.8156 and 7.0498

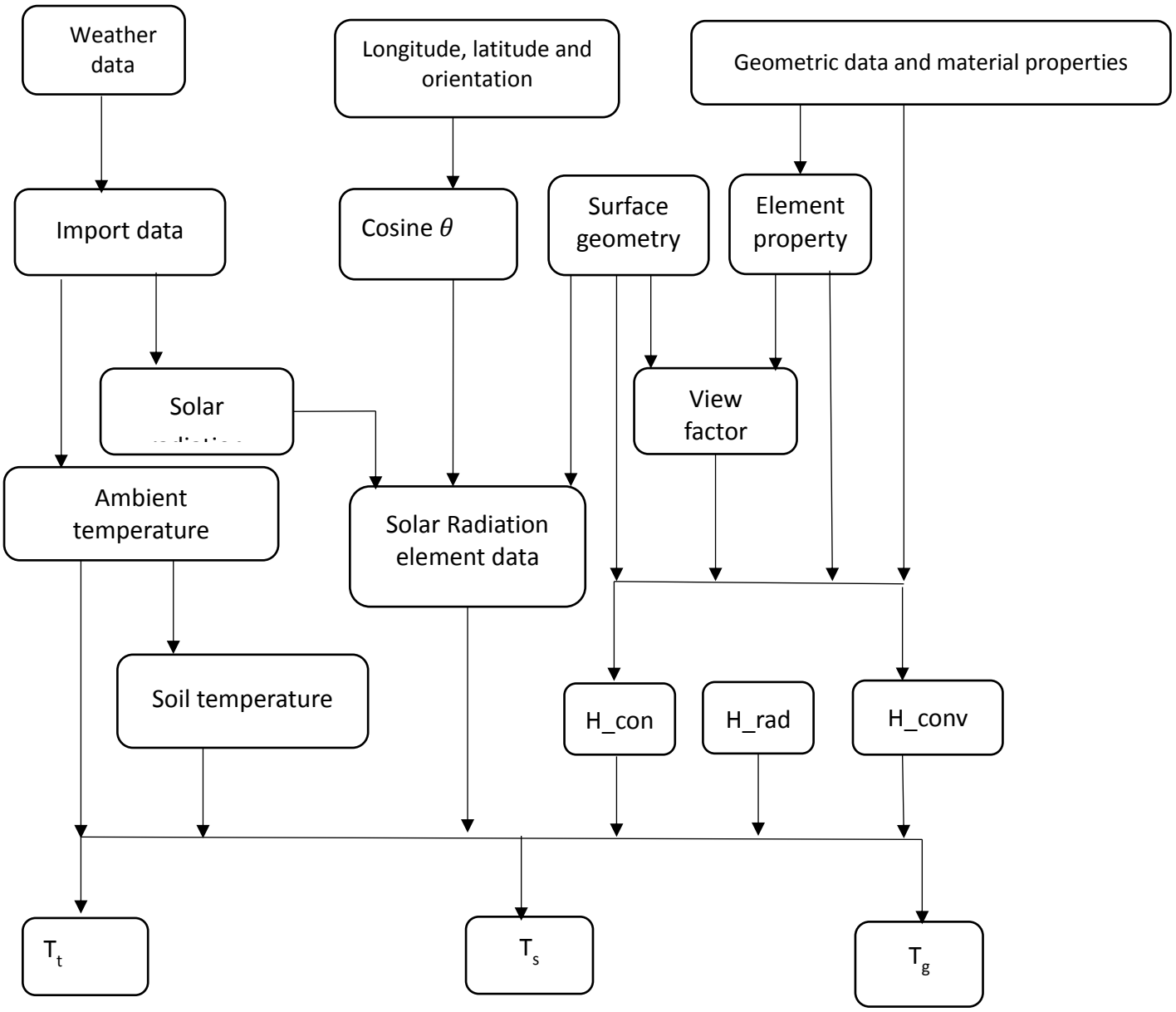

Figure 3.12 Operational scheme of the plastic bag digester (CASE 1).

Table 3.2 the dimensions of the digester and the digester material properties [73].

Parameters	Values
Thickness	
Upper insulation of digester	0.04
Lower insulation of digester	0.06
Base insulation of digester	0.08
Greenhouse cover	0.005
Digester tube	0.0025
Width	
Upper width of the digester	1.2
Sloping wall of the digester	0.23
Greenhouse adobe wall	0.3
The diameter of the digester tube	0.95
Height	
Trench (digester)	0.7
Wall1	0.5
Wall2	1.03
Other Parameters	
External length of the digester	5.6 m
Internal length of the digester	5 m
Thermal conductivity of straw	0.32 W/m^2K
Specific heat capacity of slurry	4180 J/kg K
Specific heat capacity of adobe	835 J/kg K
Thermal conductivity of adobe	1 W/m^2K
Daily mass feeding rate of slurry	40 kg

Table 3.3 Parameter used in the estimation of the radiative heat transfer [73].

Material	Absorbance	Emissivity	Transmissivity
Slurry	0.8	0.8	0
Geomembrane	0.8	0.8	0
Adobe wall	0.8	0.8	0
Greenhouse Cover	0.2	0.2	0.65

The parameters in table (3.1), were selected because the Cuzco and Port Harcourt represent region with two extreme temperature condition; one characteristic mostly by cold climate, while the other is mostly warm. Parameters in Table (3.2) are used because they represent the actual dimension of the

plastic bag digester built in Cuzco, and the data was measured during the construction of the digester [73]. Further, the parameters in table (3.3) are cited from [73] and the initial condition in table (3.4) is selected to ensure the thermal model (CASE 2) is able to reproduce similar results as in Perrigault et al [73], for the digester in Cuzco

Table 3.4 Initial condition of the temperature [73].

Parameters	**Values**
Slurry	18 ^{o}C
Greenhouse Cover	20 ^{o}C
Greenhouse walls	21 and 22 ^{o}C
Digester tube	23 ^{o}C
Greenhouse air	24 ^{o}C
biogas	22 ^{o}C

3.6 Description of the biochemical model

3.6.1 Mass balance and reaction kinetics

Recall that in section 3.1, an overview of the mathematic models used in the present research was discussed. The mathematical model consists of three biochemical models (1R, 2R, and 3R) in addition to the thermal models, and the temperature dependent model. The biochemical models are one population reaction model (1R), two population reaction model (1R) [228], and three population reaction model (3R) [85], which are modelled by applying the principle of conversation of mass which relates the amount of material entering and leaving the reacting system to the amount accumulated in the reacting system. This may be expressed mathematically as follows:

$$\frac{\partial M}{\partial t} = M_1 - M_2 \qquad (3.41)$$

where M_1 and M_2 are the mass flow rates of the material in and out of the system. For the individual reaction or stage of the anaerobic digestion process, the mass balance is expressed as follows:

$$\frac{\partial C}{\partial t} = D(C_i - C) + r_i \qquad (3.42)$$

where C_i and C are the inlet and outlet concentrations of the material, r_i is the net rate of production of component i.

The rate of the biochemical reaction (substrate uptake rates) in the anaerobic digestion processes has been described using different models. The simplified model of the anaerobic digestion system consists of two populations of micro-organisms. The rate of reaction for the first stage (hydrolysis/acidogenesis) is modelled using first order, Contois and Monod kinetic models. The Contois equation is expressed as:

$$r_h = \mu_{max} X_h \frac{X_o}{K_x X_h + X_o} \qquad (3.43)$$

where r_h the rate of the hydrolysis reaction, μ_{max} is the maximum specific growth of the hydrolytic biomass, K_x is the Contois half saturation constant and it is used to describe the ability of a microorganism to utilise a limited amount of substrate concentration for growth. X_o and X_h are the concentrations of the substrate and the hydrolytic biomass, respectively.

Similarly, the first order and Monod equations are expressed as:

$$r_h = k_{hyd} S \qquad (3.44)$$

$$r_h = \mu_{max} \frac{S}{k_s + S} X \qquad (3.45)$$

where r_h the rate of the hydrolysis reaction, μ_{max} is the maximum specific growth of the hydrolytic biomass, k_s is the half saturation constant, S and X are the concentrations of the substrate and the hydrolytic biomass, respectively. k_{hyd} is the first order rate constant.

In the second stage, or the methanogenesis reaction, the rate of reaction is modelled using the Monod and Haldane kinetic model [84], Moser and Tessier kinetic model [231]. The Haldane kinetic model considers the inhibitory influence of the VFA (volatile fatty acids). For modelling the methanogenesis stage, the Haldane kinetic model is expressed as follows [84]:

$$r_m = \mu_{max} X_m \frac{S}{K_s + S + {S^2}/{K_i}} \tag{3.46}$$

where r_m is the rate of the methanogenic reaction, μ_m is the maximum specific growth of the methanogenic biomass, K_s is the half saturation constant, K_i is the inhibition constant, and S and X_m are the concentrations of the substrate and the methanogenic biomass, respectively.

The Monod, Moser, and Tessier models are expressed as follows:

$$r_m = \mu_{max} \frac{S}{K_s + S} X_m \tag{3.47}$$

$$r_m = \mu_{max} \frac{S^\lambda}{K_s + S^\lambda} X_m \tag{3.48}$$

$$r_m = \mu_{max} \left(1 - e^{-\frac{S}{k_s}}\right) X_m \tag{3.49}$$

It should be noted that the equations (3.43), (3.44), (3.45), (3.46), (3.47), (3.48) and (3.49) are applicable for the modelling the uptake rate of the substrate at a constant temperature. However, for fluctuations in the digester temperature in the case of small-scale unheated digesters, the uptake rate of the substrate becomes a function of the digester temperature.

The anaerobic digestion process is, in general, affected by the presence of a high amount of ammonia or volatile fatty acid. These chemical compounds

reduce the activity of the microbial population, thereby limiting the process as well as the amount of biogas produced. In the modelling of the anaerobic digestion process [83], the effect of inhibition is included in the description of the degradation process and it is generally modelled as being uncompetitive inhibition. The inhibition of the biochemical process due to the presence of ammonia and VFA is considered and it is expressed as follows [83]:

$$I_N = \frac{1}{\frac{k_{i,N}}{N} + 1} \tag{3.50}$$

$$I_{vfa} = \frac{1}{\frac{k_{i,vfa}}{S} + 1} \tag{3.51}$$

Where I_N and I_{vfa} are the ammonia and VFA inhibition factor respectively. $k_{i,N}$ and $k_{i,vfa}$ are the inhibition constants for ammonia and VFA, respectively. N and S are the concentration of ammonia and VFA, respectively.

3.6.2 Temperature dependent kinetics

The temperature is a key parameter that affects the performance of any anaerobic system. However, it is rarely considered in a clear way in the modelling of anaerobic systems, since most anaerobic digestion systems are operated at a constant-controlled temperature. Further, for the anaerobic system in which the operating temperature is a function of the external variation in the ambient temperature, the influence of the temperature becomes essential in the modelling of such anaerobic systems. The temperature dependent kinetics provides the linking between the thermal model and the biochemical model. This is because it relates the slurry temperature and the uptake rate of the substrate by the micro-organism. The effects of the temperature on the kinetic parameter are modelled as follows [224]:

$$r = \mu_i(T) * X \quad (3.52)$$

where r the rate of the hydrolysis reaction, μ_i is the maximum specific uptake rate, X is the biomass concentration and T is the operating temperature.

To model equation (3.47), the cardinal temperature model is applied [241] and the reason for it being used in the present study have been explained in Section 3.1. The model defines three temperatures where there is a possibility of growth, the minimum temperature, the optimal temperature and the maximum temperature [222, 223] and it may be expressed as follows:

$$\mu_m = \mu_{opt} * \left(\frac{(T-T_{max})(T-T_{max})^2}{(T_{opt}-T_{min})[(T_{opt}-T_{min})(T-T_{opt})-(T_{opt}-T_{max})(T_{opt}+T_{min}-2T)]}\right) \quad (3.53)$$

where μ_m and μ_{opt} are the maximum growth rates of the microbial population and the optimum growth rate of the microbial population, respectively. T_{min} is the minimum temperature, T_{max} the maximum temperature and finally T_{opt} is the optimum temperature.

3.6.3 Mass balance analysis

The anaerobic digestion models applied are the one, two, and three reaction models derived from [84, 85]. In the one reaction model, the substrate degrades into methane and carbon dioxide in the hydrolysis stage. The two-reaction model consists of the Hydrolysis/Acidogenesis stage which produces acetate and carbon dioxide as the only product, while the methanogenesis stage involves the production of methane and carbon dioxide from the degradation of acetate.

In the three-reaction model, the influent organic matter is composed of two fractions; carbohydrate/lipids and protein, which degrade separately during the hydrolysis/acidogenesis reaction to acetate. The methanogenesis is the same for the two reactions and a schematic of the reaction pathway is presented in figure 3.12.

3.6.3.1 One reaction model

The 1R model is a generic mass balance involving the conversion of a single substrate (S_1) into methane and carbon dioxide by the action of a single population of microorganism (X_1). The dynamic model is described in the following equations:

$$k_1 S \rightarrow X_1 + k_2 CO_2 + k_3 CH_4 \quad (3.54)$$

$$q_m = k_3 r_1 \quad (3.55)$$

$$\frac{dX_1}{dt} = r_1 - DX_1 \quad (3.56)$$

$$\frac{dS_1}{dt} = k_1 r_1 + D\left(S_{1,in} - S_1\right) \quad (3.57)$$

3.6.3.2 Two Reaction model

The two-reaction model includes a single lumped particulate organic matter (S_1). The particulate organic matter is converted into VFA (S_2) by the action of the hydrolysis microorganism (X_1). The VFA (S_2) is further converted into methane and carbon dioxide in the methanogenesis stages by the action of methanogenic microorganism (X_2). The dynamic model of the two-reaction model is described thus:

- Hydrolysis/Acidogenesis:

$$k_1 S_1 \rightarrow X_1 + k_2 S_2 + k_4 CO_2 \quad (3.58)$$

- Methanogenesis:

$$k_3 S_2 \rightarrow X_2 + k_5 CO_2 + k_6 CH_4 \quad (3.59)$$

Solving for methane production, the mass balance in the liquid phase is applied. If ξ denotes the vector of the state variables, the mass balance may be written, in general, as follows:

$$\frac{\partial \xi}{\partial t} = Kr(\xi) - D\xi - Q + F \qquad (3.60)$$

The methane flow rate is obtained using equation:

Methane flowrate

$$q_m = k_6 r_2(\xi) \qquad (3.61)$$

where K is the stoichiometric ratio of the reactant and products of the biological reaction, D is the dilution rate, F is the inlet condition of the model variables, Q is the methane production rate and $\xi = [X_1, X_2, Z, S_1, S_2, C, N]$ is the vector of the model variables. In the matrix form, the mass balance is given as follows:

$$\xi = \begin{bmatrix} X_1 \\ X_2 \\ Z \\ S_1 \\ S_2 \\ C \\ N \end{bmatrix}, (3.62), \quad r(\xi) = \begin{bmatrix} \mu_1(\xi)X_1 \\ \mu_2(\xi)X_2 \end{bmatrix}, (3.63), K = \begin{bmatrix} 1 & 0 \\ 0 & 1 \\ -k_1 & 0 \\ k_2 & -k_3 \\ k_4 & k_5 \\ k_n & 0 \end{bmatrix}, (3.64),$$

$D = I_6 d$, (3.65)

$$F = \begin{bmatrix} 0 \\ 0 \\ DZ_{in} \\ DS_{1in} \\ DS_{2in} \\ DC_{in} \\ DN_{in} \end{bmatrix}, (3.66), Q = \begin{bmatrix} 0 \\ 0 \\ 0 \\ 0 \\ 0 \\ q_c k_6(\xi) \end{bmatrix} (3.67)$$

In the present model, the biochemical reaction and the mass balance is modified in order to consider the concentration of nitrogen.

3.6.3.3 Three Reaction model

The three-reaction model is similar to the two-reaction model except for the hydrolysis stage which includes a fractionation of the particulate organic matter into carbohydrates/fats (S_{1a}) and proteins (S_{1b}). The hydrolysis stage consists of two reactions, each producing VFA by the action of hydrolysis biomass (X_{1a}) and(X_{1b}):

- Hydrolysis:

Hydrolysis of Carbohydrates/lipids:

$$k_1 S_1 + k_2 NH_4^+ \rightarrow X_1 + k_3 S_3 + k_4 \qquad (3.68)$$

Hydrolysis of proteins:

$$k_5 S_2 \rightarrow X_2 + k_6 S_3 + k_7 NH_4^+ + k_8 CO_2 \qquad (3.69)$$

The methanogenic stage involves the conversion of VFA by the methanogenic population (X_2) to biogas which consists mainly of methane and Carbon dioxide:

- Methanogenesis:

$$k_9 S_3 + k_{10} NH_4^+ \rightarrow X_3 + k_{11} CH_4 + k_{12} CO_2 \qquad (3.70)$$

The general form of the mass balance in the liquid solution is as follows:

$$\frac{\partial \xi}{\partial t} = Kr(\xi) - D\xi - Q + F \qquad (3.71)$$

$$\xi = \begin{bmatrix} X_1 \\ X_2 \\ X_3 \\ Z \\ S_1 \\ S_2 \\ S_3 \\ N \\ C \end{bmatrix}, \text{ (3.72)}, r(\xi) = \begin{bmatrix} \mu_1(\xi)X_1 \\ \mu_2(\xi)X_2 \\ \mu_3(\xi)X_3 \end{bmatrix}, \text{ (3.73) } K = \begin{bmatrix} 1 & 0 & 0 \\ 0 & 1 & 0 \\ 0 & 0 & 1 \\ 0 & 0 & 0 \\ -k_1 & 0 & 0 \\ 0 & -k_5 & 0 \\ k_3 & k_6 & -k_9 \\ k_4 & k_8 & k_{12} \\ -k_2 & k_7 & -k_{10} \end{bmatrix}, \text{ (3.74) } F =$$

$$\begin{bmatrix} 0 \\ 0 \\ 0 \\ DZ_{in} \\ DS_{1in} \\ DS_{2in} \\ DS_{3in} \\ DN_{in} \\ DC_{in} \end{bmatrix}, \text{ (3.75) } Q = \begin{bmatrix} 0 \\ 0 \\ 0 \\ 0 \\ 0 \\ 0 \\ 0 \\ 0 \\ q_e(\xi) \end{bmatrix}, \text{ (3.76) } D = I_9 d \text{ (3.77)}$$

3.7 Implementation of the biochemical model

3.7.1 Description

The biochemical model was implemented in MATLAB 2015, and the numerical solution was provided by the inbuilt ordinary differential equation solver (ode15s). The ode 15s uses the Runge-Kutta numerical method to solve the system of differential and algebraic equations. The one reaction model consists of two different equation, each for the substrate degradation and microbial biomass, and 1 algebraic equation for the methane production. The two-reaction model is made up of 7 differential equations and 1 algebraic equation. The three-reaction model consists of 9 differential equations and 1 algebraic equation. The initial conditions, the kinetic parameters, and the stoichiometric coefficient, the flow rate of the feedstock, mass transfer parameters such as liquid-gas transfer rate and the Henry's Constant are scripted in a MATLAB and saved as init_contois. The parameters transformed into blocks in the Simulink environment as INIT, DFeed, K for initial condition, the flow rate of feedstock, stoichiometric coefficient, respectively.

The two-reaction model is implemented in Simulink as a block diagram link together and it saved as Bernard_model_contois. In the Bernard_model_contois, the rate of reaction (Haldane, Monod, first order, Contois, Tessier, and Moser) is executed in the Kinetic block. The effects of volatile fatty acid and ammonia on the rate of reaction is expressed in the Inhibition block. The methane production rate is estimated in the qm block, and the total carbon balance is estimated in the qc block. The transformation of the IS units of the methane produced from concentration to volume is done in the conversion block. The block diagram of the three-reaction model can be found in the Simulink file fractionation, see Appendix B.4. All other components of the three-reaction model are the same as that of the two-reaction model. The diagram of the cardinal temperature model implemented in the Simulink as Cardinal, see Appendix B.4.

3.7.2 Parameter values and initial conditions

The initial parameters used in the simulation of the biochemical model are listed in Section 3.5.1 and these are obtained from the literature [85, 228], see table 3.5, and the stoichiometric coefficients of the two and three reaction models are obtained from [84, 85], see table 3.6 (a) and (b). The parameter includes the stoichiometric parameters, which are calibrated to generate the parameters used in the simulation of the biochemical reaction in the present study. The details will be explained parameter estimation method in section 3.8. The initial condition for the simulation of the biochemical models (1R, 2R, and 3R) was obtained by a simple parameter estimation performed on a batch incubation of the inoculum. During the parameter estimation, it is assumed that the sum of the concentration of the particulate organic matter (S_1) and the hydrolytic (X_1) and methanogenic organisms (X_2) was measured in VS of the sample (14.4 kg m^{-3}). The methane production from the batch was then used to estimate the initial conditions which yield the following condition used in the semi-continuous simulation; S_1= 0.17 kg m^{-3}, X_1 = 7.75 kg m^{-3} and X_2= 6.48 kg m^{-3}.

Table 3.5 Kinetic parameter for the different kinetic models [220].

Parameter	**Value**	**Parameter**	**Values**
Contois		**First order**	
Maximum uptake rate	6.797d^{-1}	Hydrolysis constant	0.5 d^{-1}
Half-saturation constant	10.829	**Moser**	
Monod		Maximum uptake rate	0.0279 d^{-1}
Maximum uptake rate	1.19 d-1	Half-saturation constant	2.01g/L
Half saturation constant	0.021 d^{-1}	lamda	2.118
Haldane		**Tessier**	
Maximum uptake rate	1.19 d^{-1}	Maximum uptake rate	0.122 d^{-1}
Half saturation constant	0.021 d^{-1}	Half saturation constant	9.87 g/L
Inhibition constant	16.8 g/L	**Inhibition constant**	
		NH_3 inhibition constant	61 g/L
		VFA inhibition constant	1.5 g/L

Table 3.6(a) Stoichiometric coefficients and physiochemical parameters for the two-reaction model [75].

Parameters	**Values**
COD degradation yield	42.14
Yield of VFA produced	116.5 mmol/g
Yield of VFA consumed	268 mmol/g
Yield of CO_2 produced	50.6 mmol/g
Yield of CO_2 produced	343.6 mmol/g
Yield of CH_4 produced	453.0 mmol/g
Liquid-gas transfer rate	19.8 d^{-1}
Henry constant	34 mmol/L/atm
Pressure	1 atm

Table 3.6(b) Stoichiometric coefficient parameter for the three-reaction model [76]

Parameters	**Values**
Yield of sugar-lipid degradation	12.5 g COD/g COD
Yield of Ammonium ion consumed	6.2 mmol/ g COD
Yield of VFA produced	11.5 g COD/g COD
Yield of CO_2 produced	30 mmol/g COD
Yield of protein degradation	9.1 g COD/g COD
Yield of VFA produced	8.1 g COD/g COD
Yield of CO_2 produced	54 mmol/ g COD
Yield of Ammonium ion produced	30 mmol/g COD
Yield of VFA consumed	20 mmol/g COD
Yield of Ammonium ion consumed	6.2 mmol/g COD
Yield of CH_4 produced	30 mmol/g COD
Yield of CO_2 produced	20 mmol/g COD
The fraction of the Sugar-lipid content of microalgae	0.3 g COD/g COD
The fraction of the protein content of microalgae	0.4 g COD/g COD

Table 3.7 Substrate and biomass concentration of the different feedstocks (food waste, green waste and pig manure) [242].

State Variables	**Food waste**			**Green waste**			**Pig manure**
Model	**1R**	**2R**	**3R**	**2R**	**2R**	**3R**	
$X_{1,1a,1b,2}$	0	0	0	0	0	0	0
S_1	274	274	274	275	275	275	0
S_{1a}	N/A	N/A	440	N/A	N/A	392	317
S_{1b}	N/A	N/A	440	N/A	N/A	392	317
S_2	N/A	197.7	12.65	N/A	72.1	4.61	
N	N/A	0	0	N/A	0	0	0

3.8 Methodology for the operational strategy of small-scale digester

This section involves the description of the method used for the development of the framework for the operational strategy of small-scale anaerobic digesters, with the aim of predicting the maximum methane production rate,

minimum hydraulic retention time, and maximum loading rate or maximum dilution rate. The model (3R) in section 3.6.3.3 is used to simulate the biochemical reactions, and the biochemical processes include mono-digestion and co-digestion processes. The slurry temperature used in the framework is obtained from the thermal model of the plastic bag digester in section 3.3.2. The simulation starts by feeding the digester 0.0025 L L^{-1} day^{-1} of slurry for 180 days to achieve steady state, and stability methane production, then gradually the feeding rate is increase by 1.0025 L L^{-1} day^{-1}until the digester failure. The simulation is performed for a period of 1 year (365 days, 8760 hours).

In mono-digestion process, a script is written in MATLAB to estimate the maximum methane production rate and minimum hydraulic retention time giving the maximum and minimum slurry temperature, the feeding rate, kinetic parameters obtained from parameter estimation, table 4.5, and section 4.2.3.4.

The script run the simulation of the biochemical process at constant slurry temperature within the range of the maximum and minimum slurry temperature until the point of failure is achieve, and it estimate the maximum methane production rate and the minimum hydraulic retention time corresponding the specific slurry temperature. A total of 20 slurry temperature points is simulated. MATLAB script is also written to estimate the maximum loading rate or maximum dilution rate and maximum methane production before failure. Here, once the simulation has achieve failure in the digester (decrease in methane production). The script runs the simulation by varying the value of the dilution between a lower value and an upper value and estimate the maximum dilution rate and the corresponding maximum methane production.

For the co-digestion process, varying mixture of the feedstock are mixed, and like the mono-digestion process, the 3R model is simulated for 365 days, starting from a lower feeding rate (0.0025 L L^{-1} day^{-1}) and, gradually increase

by 1.0025 L L^{-1} day^{-1} until the digester failure. At a specific substrate mix ratio, the script is simulated, giving minimum and maximum slurry temperature to estimate the maximum methane production and minimum hydraulic retention time. To illustrate this, consider the substrate is mixed in the rate of 96 % green waste and 5 % food waste. The script runs the simulation at the mix ratio till the digester failure occurs at specific temperature points between within the maximum and minimum slurry temperature to estimate the corresponding maximum methane production and minimum hydraulic retention time. Further, to determine the maximum dilution rate or maximum loading rate before the point of failure, the MATLAB script simulated the performance of the digester by varying the dilution rate between an upper and lower limit at 95% green waste and 5 % food waste, to determine the corresponding maximum dilution rate and maximum methane production. The MATLAB script is presented in appendix A.3.

3.9 Experimental method and analysis

In this section a detail description of the experimental method and analysis used in the thesis is presented. The experimental work consists of batch and semi-continuous anaerobic digestion processes. The experimental method fits into the present thesis because it describes the degradation of substrate (food waste, green waste and pig manure) that are generated and used in the production of methane gas for cooking in rural communities of developing countries. The aim of the experimental work was to validate the biochemical model, and for calibration of the parameters used in the biochemical model. The experimental data were obtained from another publication [243].

3.9.1 Feedstocks

The feedstock used in the present study is food waste, green waste, and pig manure. The feedstock is measured based on volatile solid (VS) and Theoretical chemical oxygen demand (COD_{th}). The characteristics of the feedstock is present in table 3.8, and it is obtained from [81].

Table 3.8 The measured feedstock characteristics [81]

Characteristics	Unit	GW	FW	PM
TS	g/L	440	392	317
VS	g/L	275	274	242
ash	% of TS	34.88	10.27	11
C	% of TS	34.66	49.15	44.1
H	% of TS	4.50	7.65	5.2
S	% of TS	1.98	3.35	2.9
O	% of TS	23.95	33.1	36.7
COD_{th}	g COD/g VS	1.42	1.61	1.31
VFA	g COD/L	4.61	12.65	16.21

3.9.2 Batch experimental method

The batch experiments were performed in triplicate several (9) 600 ml laboratory digester, for the substrate and inoculum respectively, see Figure 3.13. The working volume of the digester is 350 and 500 ml, for the substrate and the inoculum, respectively. The digester was operated at the temperature of 37 ^{o}C by immersion in a hot water bath. The digester is agitated by means a vertical stirrer operated at 60 RPM, with a consecutive on/off cycles of 30 seconds each. The inoculum used in the experiment was obtained from a wastewater treatment plant operated at the mesophilic temperature. It was screened via a 0.5mm sieve and then incubated for 4 days in the bottles to ensure biodegradation of most of the remaining easily degradable organic matter, and it was sampled for analysis. The mass of the substrate added into the digester was estimated based on a defined inoculum to substrate ratio. A ratio of 2.5 $gVS_{inoculum}$ /$gCOD_{substrate}$ was selected. This is because the literature review of many BMP tests identified 2.0 $gVS_{inoculum}$/ $gCOD_{substrate}$ as a safe minimum threshold. Further, the choice of the inoculum to substrate ratio is because there is no accepted standardized ratio between the inoculum and substrate for batch biodegradation assays [81].

The digester headspace is purged with pure nitrogen after the substrate is added into the digester, to remove any remaining oxygen in the digester and ensure anaerobic condition. The carbon dioxide and hydrogen sulphide content of the produced gas is removed by scrubbing with 3M NaOH alkaline

solution. The volume of the scrubbed gas was measured through an AMPTSII system (Bioprocess Control), with a resolution of 10mL. Methane production is reported at STP (0 C and 1 bar) and it is calculated by assuming a scrubber efficiency of 98%, subtracting the concentration of the water vapour in the gas produce and by considering the overestimation in the biogas produced caused by the initial concentration of nitrogen in the headspace as detailed in [243, 244]. The experiment lasted for 60 days after initial feeding of the digester. The actual test performed in the batch experiment will be discussed in section 3.9.2.1 the actual measurement is the methane volume and methane flow rate.

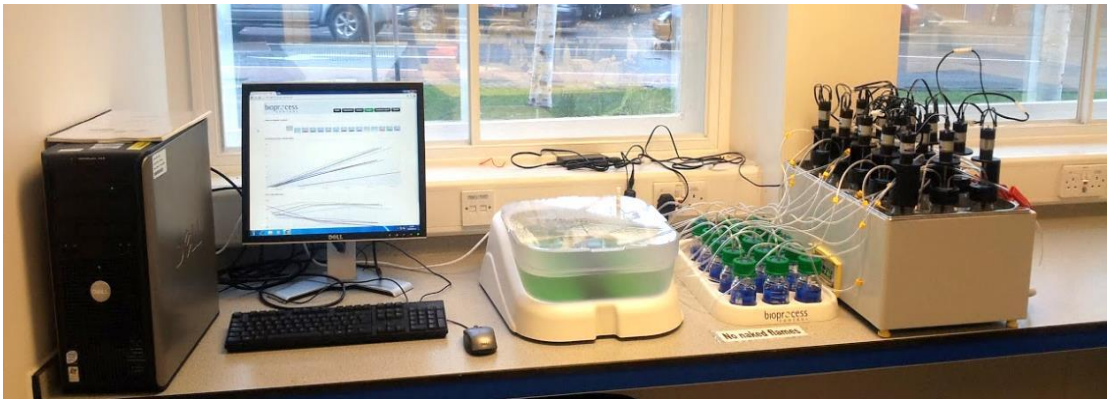

Figure 3.13 Photograph of the batch experimental setup, from the right to left: stirred batch reactors in the water bath, alkaline gas scrubbing systems, the multi-channel volumetric gas meter, and the software user interface [81].

3.9.2.1 Batch test conditions

The batch experiment involves two different tests performed, with different substrates and inoculum. The inoculum for test 1a was collected from an external digester, with sparse information about its operation. The inoculum for test 1b was a mixture of effluent withdraw from the digesters used in the semi-continuous test 2. In both tests, the inoculum was filtered through a 0.5 mm sieve and then incubated for 4 days in the reactor. The aim is to ensure the remaining readily degradable organic matter is digested. 3 different tests (Blank) were performed for each inoculum, and four standard tests was

performed each for food waste and green waste. Two standard tests were performed for pig manure [243].

3.9.3 Semi-Continuous experimental method

Anaerobic digestion is usually performed in a semi-continuous mode, see figure 3.14. The semi-continuous reactors were operated by intermittent batch feeding of a system whilst maintaining its volume as constant, achieved by removing a fraction of the digester content concurrent to feeding.

Segregated household GW and FW were collected at a local recycling centre (Todmorden, UK) and stored in the laboratory at a temperature of 5^{o}C. Within 24 hours, the samples were examined and large pieces of bone, plastic, metal, wood were removed to avoid damage to the homogenisation equipment and reduce sampling errors during the later analysis. The samples were then homogenised using a commercial food mincer and sampled for a physio-chemical analysis. The remainder of the biomass samples were stored in a freezer at a temperature of about -18 ^{o}C and thawed before feeding into the digesters.

The semi-continuous study of the production of biogas from GW and FW were performed in two 2-litre laboratory digesters. The temperature of the digester was maintained at 37 °C by immersion in a water bath and mixing was provided by a vertical stirrer operating at 60 RPM for 10s every minute. The inoculum for the experiment was obtained from a homogenised sample of laboratory digestate from other digestion experiments, which originated from a mesophilic digester treating primary and secondary sludge at a wastewater treatment plant.

The two digesters were fed chemical oxygen demand (COD) equivalent pulses of GW and FW over a period of 112 and 176 days, respectively, with a gradual increase in organic loading until failure of the process occurred. In the

case of GW, the experiment was terminated early due to excessive foaming in the digester. The methane production of the digesters was monitored continuously and samples for offline analyses were taken intermittently during the feeding operations [243].

The pulsed and irregular feeding of the experimental system is often used in AD research, especially for solids waste and in small scale digesters in the rural regions [120]. The digesters were fed 3 times a week for the first 80 days and subsequently, the digester is fed with an increased loading rate up to 5 times a week until the end of the experiment [243]. The methane flow rate and methane volume are the parameters measured in the experiment. The experiment is aimed at validating characteristics of food waste and green waste obtained from the batch test. This is done by comparing the quality of the fit of the experimental data and the values of the parameter obtained from the batch test [243].

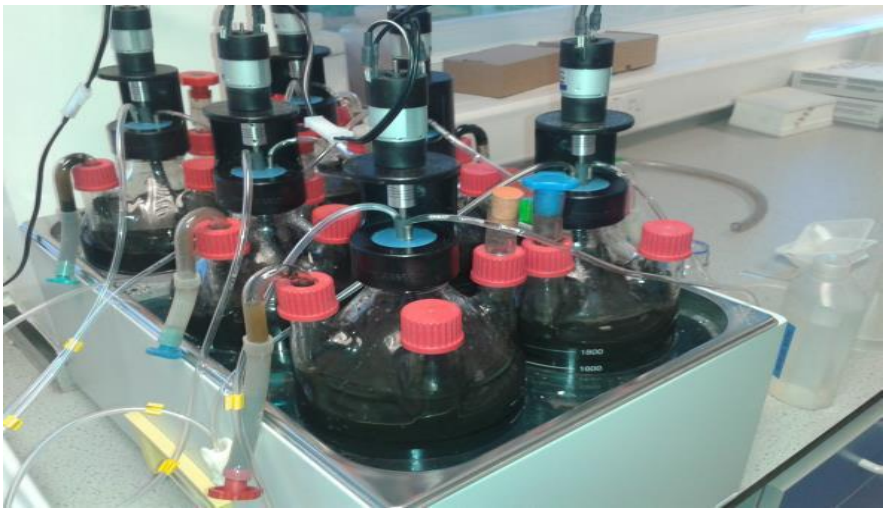

Figure 3.14 Photograph of the semi-continuous experimental set [243].

3.9.4 Analytical method

The total solids (TS) and volatile solids (VS) were measured as per standard method (APH, 2012). The concentration of the volatile fatty acids (VFA) was measured using an Agilent 7890A gas chromatograph, with a DB-FFAP

column of high polarity designed for the analysis of VFA columns, as per the manufacturer's guidelines. Elemental analysis was determined using an elemental analyser (Flash EA2000, CE Instruments) equipped with a flame photometric detector (Flash EA 1112FPD, CE Instruments). The theoretical chemical oxygen demand (COD_{th}) was calculated from the empirical formula obtained from the element analysis, considering the organic matter to be fully oxidised to carbon dioxide and water, with nitrogen being reduced to ammonia and sulphur oxidised to sulphuric acid. Methane content was measured with a Dynament premier infrared sensor, installed in the gas line, with data acquisition performed by an in-house programmed Arduino micro-controller.

3.10 Parameter estimation and sensitivity analysis

3.10.1 Parameter estimation

In anaerobic digestion processes, there is always a need to estimate the parameters of the model, as each process has its specific aim. Traditionally, the estimation of the parameters has been by the trial and error method. It involves a great deal of time, and the quality of the parameter values obtained is usually not guaranteed [241]. However, in recent years, optimization methods are developed to resolve the issues in the estimation of the parameters that occur in anaerobic digestion models as well as to determine the quality of the parameter. The first step in every optimization method is the selection of a cost function, which in this case is the methane flowrate for the semi-continuous process and methane volume for the batch processes. In the present study, the cost function is expressed as the sum of the square error between the biochemical model and experimental data points, and it is commonly used in the field of anaerobic digestion for parameter estimation [32, 245, 246]. The parameter estimation method is applied to the simplified AD models to assess their ability to reproduce the kinetics of methane production from anaerobic digestion of solid wastes. The parameter estimation technique uses the non-linear least square method as supplied with the optimisation toolbox in MATLAB (Mathworks, MA, USA). It involves a multi-start strategy employed where several different initial parameter sets were used to avoid the minimisation algorithm reaching a local minimum [241].

The parameter estimation was a tool used to fit the model with a rich experimental dataset, by considering several model structures, a combination of kinetic equations and simple inhibition description. And the closeness of the fit can be used to give an insight into the important phenomena exhibited by the AD system. The cost function is expressed as follows:

$$S(\theta) = min \sum_{t=1}^{n} \left(y_{\exp(t)} - y_{sim}(t, \theta) \right)^2 \qquad (3.78)$$

where S is the cost function, y_{exp} the value of the experimental measurement, y_{sim} is the predicted model results, θ is the estimated parameters of the model and n is the number of experimental measurement points. This cost function is implemented in Matlab 2015a.

Further, to measure the degree in the difference between the model results from the experimentally observed values, the root means square error (rRMSE) is used and this is expressed as follows:

$$rRMSE = 100 \frac{\sqrt{S/n}}{\sigma_{i,exp}} \qquad (3.79)$$

Where S and n are as defined in equation (3.78), n is the number of experimental data point and $\sigma_{i,exp}$ the mean of the experimental measured data.

After the best fitting parameters are estimation, their quality of fitness to the experimental data is determined. Generally, for experimental data with a large set of experimental data points, the Hessian matrix function is frequently used for estimating the uncertainty of a parameter. The standard errors are estimated as the square root of the absolute covariance matrix. The Hessian and standard error can be expressed as follows [245]:

E***rro***r! Bookmark not defined. $H(\theta)$

$$= \left\{\frac{\partial^2 \ell(\theta)}{\partial\theta_j \partial\theta_k}\right\} \tag{3.80}$$

$$SE = diag\left(abs\left(\sqrt{\left(H(\theta)\right)^{-1}}\right)\right) \tag{3.81}$$

Where $H(\theta)$ is the hessian matrix, $\ell(\theta)$ is the objective function to be minimised, θ is the eigenvalue of estimated parameters of the biochemical model, SE is the standard error associated with the parameters.

Applying the parameter estimation method to the batch test, the accumulated volume of the methane produced is used as the target measurement for both the inoculum and feedstock. The batch test was performed in triplicate Poggio, (2016), and each batch was treated as separate data and the parameters estimated from the blank (inoculum) test are the stoichiometric coefficient k_1, X_1 and X_3 in equation (3.68) and (3.70), see subsection 3.5.3.3, including the standard error associated with each parameter in equations (3.81). The final value of the parameters that are estimated is taken as the mean of the parameters estimated from each batch, and it is expressed as follows:

$$p_i = \frac{\left(\sum p_j\right)}{n} \tag{3.82}$$

The initial conditions of the feedstock (food and green waste, and pig manure) in the batch and continuous parameter estimation were derived from the values of the parameters estimated in the blank (Inoculum) test. It is assumed that the initial total COD into the reactor in the blank test consists of a concentration of the feedstock and microorganism. This can be expressed mathematically as follows:

$$COD_T = X_{1ini} + X_{3ini} + S_{1ini} \tag{3.83}$$

where X_{1ini} and X_{3ini} are the initial biomass (micro-organism) concentration of X_1 and X_3 in equations (3.68) and (3.69), Section, 3.5.3.2 and S_{ini} is the initial concentration of the substrate S_1 in equation (3.68). it should be noted that the initial concentration of X_1 is assumed to be equal to the X_2 in equation (3.70). This is because they are hydrolytic biomass. The 3R reaction model is used for the parameter estimation of the blank test since it consists of two separate hydrolysis reaction.

The initial substrate concentration of the inoculum is obtained as follows:

$$S_{1ini} = COD_T - X_{1in} - X_{2in} \tag{3.84}$$

The initial conditions in the standard test (substrate + inoculum) was estimated by multiplying the initial condition estimated from the blank test by the total volume of the inoculum and substrate and dividing by the volume of the inoculum or substrate. i.e. to estimate the new initial condition for the microorganism in the standard test, the total volume of reactor in the standard test is multiplied by the initial concentration of the microorganism estimate from the blank test divided by the volume of the inoculum. For the substrate, the initial conditions in the standard test is obtained by multiplying the initial concentration of the substrate in the blank test by the total volume of slurry in the reactor in the standard test and dividing by the volume of slurry. For each substrate (food waste, green waste, and pig manure), this is expressed as follows:

$$X_i = \frac{V_T * X_{ib}}{V_{jb}} \tag{3.85}$$

$$S_i = \frac{V_T * S_{ib}}{V_{js}} \tag{3.86}$$

V_T is total volume of the inoculum and slurry, V_{jb} is the volume of the inoculum, V_{js} is the volume of the substrate, S_{ib} is the initial concentration of substrate obtained from the parameter estimation of the blank test, X_{ib} is the initial concentration of microorganism obtained from the parameter estimation of the blank test. $X_i \; and \; S_i$ are the initial condition in the standard test.

For the substrate batch (Standard test) parameter estimation, the estimated parameters are the stoichiometric coefficient k_1 and uptake rate μ_1 of the hydrolysis reaction in equation (3.68), and the methane flow rate is used as the target measurement. Four different replicate batch tests were performed for the food waste and green waste, while for pig manure, the test was performed in duplicate. Again, each test is considered as a separate set of data and the parameter estimation methods in equations (3.78), (3.79), (3.80), (3.81) and (3.82) were applied to estimate all the parameters and the associated standard errors, see figure 3.15. For the operational scheme of the parameter estimation method and sensitivity analysis. The reason for restricting the parameter estimation to the parameters k_1 and μ_1 is because of the lack of adequate data.

In the case of the continuous experiment, the target measurement is the methane flow rate. The parameters estimation was performed for food waste and green waste using the two reactions and three reaction models. For the two-reaction model, the parameters estimated are the stoichiometric coefficient k_1, the uptake rates of hydrolysis and methanogenesis reactions μ_1 and μ_2, the half saturation constants k_x and k_s, and the inhibition constants due to the volatile fatty acid and ammonia k_{in} and k_i. For the three-reaction model, in addition to the parameters in the two-reaction model, the degradability of the carbohydrates/lipid and protein β_1 and β_2 were estimated.

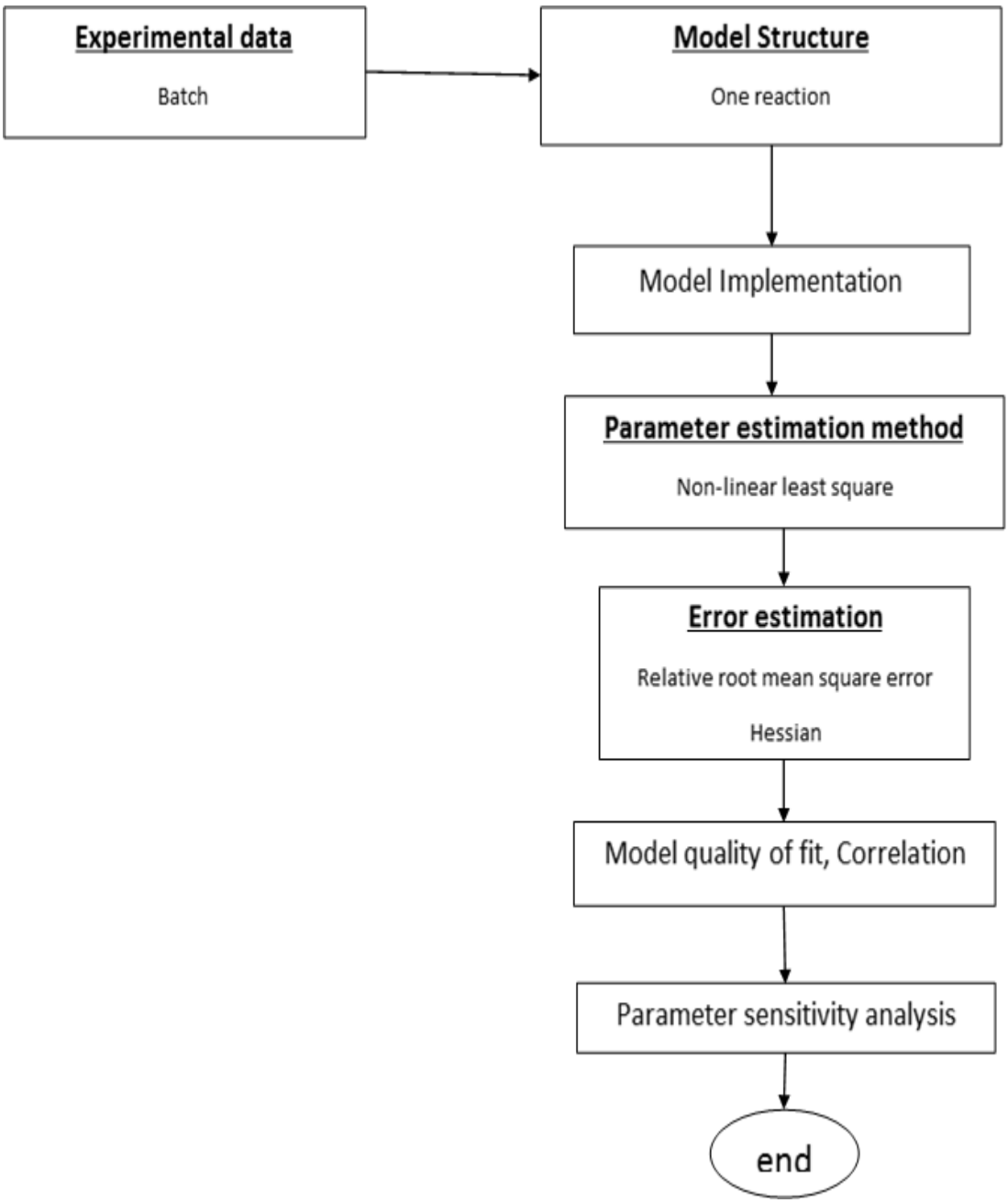

Figure 3.15 Shows the operational scheme for the parameter estimation procedure

It should be noted that in figure 3.15, the 3R model is used for the parameter estimation in the batch test. While all three model were used for the parameter estimation in the semi-continuous experiment. In the following section, the method of sensitivity analysis is discussed.

3.10.2 Sensitivity analysis

Sensitivity analysis is local in nature for anaerobic digestion system, and it is usually represented as the variation in the output signal with respect to the parameter. In this thesis, a local sensitivity analysis was performed with the aim of exploring the parameter space surrounding the optimum parameters obtained from the parameter estimation method. The result of the sensitivity analysis gives some insights into the relative important of each parameter at the chosen operating point. The sensitivity analysis is expressed as the average volume of methane produced in the batch experiment, while in the semi-continuous experiment it is expressed as the average of the methane flowrate and VFA concentration over the experimental period. It is expressed as follows [245]:

$$S_{i,j} = \frac{\partial X_j(p_i, t)}{\partial p_i} \tag{3.77}$$

Where $S_{ij}$the objective function of the sensitivity analysis is, X_j is the output of the model and p_i is the parameter of the model. The sensitivity analysis is performed on the following parameters in the semi-continuous experiment, such as the stoichiometric coefficient k_1, the uptake rates of hydrolysis and methanogenesis reactions μ_1 and μ_2, the half saturation constants k_x and k_s, and the inhibition constants due to the volatile fatty acid and ammonia k_{in} and k_i. k_{hyd} The first-order coefficient, λ the index of the substrate concentration. These parameters are found in equations (3.43), (3.44), (3.45), (3.46), (3.48) of section 3.51.

3.11 Conclusion

A detail description of the techniques used is presented in this chapter, starting with the description of the various heat transfer equations, and the thermal model of the different plastic bag digester designs (without a greenhouse, with a greenhouse, and with greenhouse and solar collector), and the implementation of these models in MATLAB. The description of the

various kinetic model and the simplified biochemical models (two and three reaction model) were presented as well as their implementation in MATLAB. Further, the chapter highlighted the novelty of the research work which is the linking of the thermal model to the biochemical model through the cardinal temperature and using the complete model to investigate the performance of the various designs of the plastic bag digester in different locations. The details of the experimental and analytical methods were discussed, and the method of the parameter estimation and sensitivity analysis was presented.

Chapter 4 Assessment and parameter estimation identification of simplified models to describe the kinetic of batch and semi-continuous biomethane production from anaerobic digestion of green waste, food waste, and pig manure.

4.1 Introduction

In this chapter, the results of simulation and parameter estimation of the kinetics of various feedstock using a simplified anaerobic digestion model are presented. This chapter is aimed at identifying the impact of the model structure, the choice of kinetic model and the influence of inhibition on the degradation of food waste and green waste. The simplified models can be classified in three ways; by the number of fractions that describe the complex organic matter, by the number of populations of microorganisms that catalyse the reactions, or by the number of biochemical reactions taking place with or without inhibition. Parameter estimation as a tool is used to fit the models to a rich experimental dataset using a number of model structures, combinations of kinetics and simple inhibition descriptions. The closeness of the fit can be used to give an insight into the important phenomena exhibited by the AD system as well as to assess the simplest model required to satisfactorily describe the digestion kinetics of complex solid wastes, such as food waste (FW), green waste (GW), and pig manure (PM). The batch and semi-continuous experimental data as obtained from another study [243], it consists of the methane flowrate, volume of methane produced, and in the case of Semi-continuous, the data on the concentration of VFA.

Model input such as COD of the substrate, VS of volatile fatty acid is estimated from the elemental analysis of substrates. It is assumed that the initial condition in the batch experiment consists of the concentration of substrate and the biomass (hydrolysis and methanogenic). The initial condition estimated from the batch parameter estimation is used as the initial condition for the calibration of the parameters for the semi-continuous experiment. The initial conditions for the kinetic parameter and stoichiometric coefficients were obtained from the literature [84, 85]. The materials and methods used in this chapter have been discussed in Chapter 3. Further, the inoculum used, and the procedure

of the Batch test are as described in [243] and two separate tests were performed for two sets of substrates.

4.2 Results and Discussion

4.2.1 Continuous Experimental Result

The two laboratory digesters were fed the equivalent OLR, on a COD basis, of GW and FW, respectively, which were characterised as presented in Table 4.1 including the calculation of COD_{th}. Despite the same OLR, the behaviour of the digesters, both in terms of the methane production rate and the mode of failure, were strikingly different due to the different compositions and degradability of the organic wastes. For the GW and FW fed systems, respectively the average methane production over the course of the experiment was 0.67 and 2.38 L day^{-1} and the specific methane production was 0.114 and 0.233 L g^{-1} COD_{added} (0.176 and 0.404 L g^{-1} VS_{added}).

The aim of the experiment was to produce rich kinetic data of the methane production rate and eventually failure of the system due to organic overload. However, in the case of GW, the system failed due to excessive foaming before there were any signs of organic stress (increased VFA, reduced specific methane production), at about day 110 and a maximum OLR of 5.52 g COD L^{-1} day^{-1} (experimental average 2.90 g COD L^{-1} day^{-1}). For the FW system, the organic failure of the system was observed with an increase in the VFA concentration to 18 g COD L^{-1} at day 160 and a reduction in the methane production despite continued, albeit reduced, organic loadings. The maximum and experimental OLR, in this case, were 15.03 and 5.15 g COD L^{-1} day^{-1}, respectively, and the experiment was terminated after 175 days. The methane production rate from the two systems is shown in figure 1 and this data forms the basis, and the sole input, for the parameter estimation and assessment of the model suitability. The number of data points was 4073 and 23644 for GW and FW, respectively, and it should be noted that although the data was collected by intermittent sampling for VFA, TS and VS, these did not form input into the parameter estimation method.

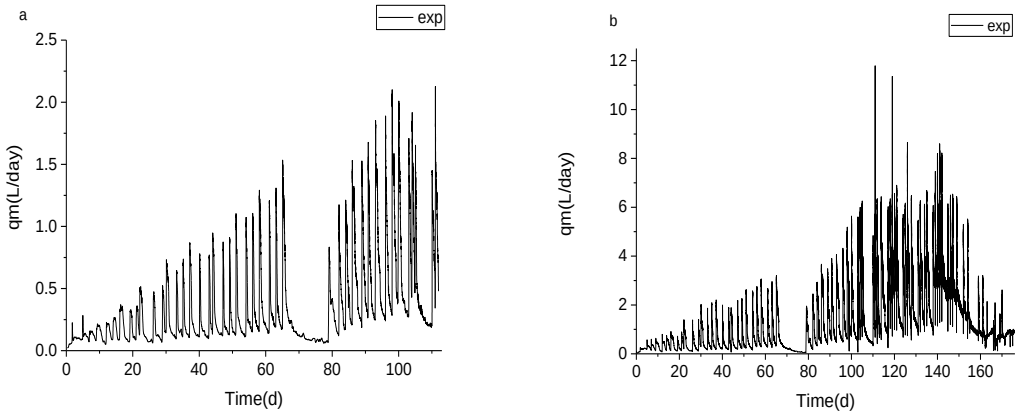

Figure 4.1 Experimental methane production for the digestion of (a) GW and (b) FW

Table 4.1 Measured feedstock characteristics.

Characteristic	Unit	GW	FW
TS	g L^{-1}	402	301
VS	g L^{-1}	275	274
Ash	% of TS	34.88	10.27
C	% of TS	34.66	49.15
H	% of TS	4.50	7.56
N	% of TS	1.98	3.35
S	% of TS	0.03	0.03
O	% of TS	23.95	29.64
COD_{th}	g COD g^{-1} VS	1.55	1.73
VFA	g COD L^{-1}	4.61	12.65

4.2.2 Parameter estimation using Semi-continuous experimental data.

The relative root mean square error (rRMSE) between the model output and the experimental data is used as the criteria for the assessment of the model's suitability to depict the experimental data. The model structure considered are 1R, 2R and 3R, and different reaction kinetics as discussed in Chapter 3. Assessing the impact of VFA and ammonia inhibition was applied to the cases

of the 2R and 3R models. The results of the 2R parameter estimation for each of the kinetic combinations are displayed in Tables 4.2 and 4.3 respectively. While the best fit parameter estimation for each model structure is shown in Table 4.4. The simulated methane production predicted by the best fitting case of each model is plotted against excerpts of the experimental data in figures 4.2 and 4.3 for GW and FW, respectively. It is important to state that the original model of Bernard et al., (2001) was modified to account for an additional state representing the ammonia concentration in the digester (N). This is included to allow the implementation of the ammonia inhibition in the model screening processes, since it is crucial phenomenon in the AD of solid waste, and this is novelty of the present study.

Table 4.2 rRMSE (%) between experimental and model data for the 2R model with combinations of kinetics and inhibition for AD of green waste (*Model chosen as suitable)

Inhibition	**Hydrolysis**	**Methanogenesis**			
		Monod	**Haldane**	**Moser**	**Tessier**
None	First order	22.6	N/A	*21.9	22.5
	Contois	22.6	N/A	21.9	22.7
	Monod	22.6	N/A	21.9	22.5
NH_3	First order	22.6	N/A	22.0	22.5
	Contois	22.6	N/A	22.0	22.5
	Monod	22.5	N/A	21.9	22.4
VFA	First order	22.5	22.2	26.8	22.5
	Contois	22.6	22.5	23.3	22.5
	Monod	22.5	22.2	21.9	22.4
VFA + NH_3	First order	22.5	22.3	21.9	22.5
	Contois	25.8	22.6	23.6	22.5
	Monod	22.5	22.3	21.9	22.5

Table 4.3 rRMSE (%) between experimental and model data for the 2R model with combinations of kinetics and inhibition for AD of food waste (*Model chosen as suitable).

Inhibition	**Hydrolysis**	**Methanogenesis**			
		Monod	**Haldane**	**Moser**	**Tessier**
None	First order	34.9	N/A	*34.6	34.8
	Contois	35.2	N/A	37.3	35.3
	Monod	38.1	N/A	34.6	34.8
NH_3	First order	37.0	N/A	33.6	35.2
	Contois	33.7	N/A	36.3	33.9
	Monod	36.9	N/A	33.6	35.0
VFA	First order	61.8	34.2	36.0	37.9
	Contois	35.2	29.5	30.4	29.0
	Monod	33.0	33.9	39.1	38.4
VFA + NH_3	First order	72.3	64.3	37.3	31.8
	Contois	27.9	27.2*	27.3	38.8
	Monod	28.2	28.1	32.1	37.7

4.2.2.1 1R model

Results obtained from the 1R model parameter estimation reveals that the Moser kinetic equation was most suitable for describing the GW methane production with an rRMSE of 23 %. Tessier, Contois, Monod and First-order kinetic equation gave an rRMSE of 23.5 %, 23.6 %, 23.6 % and 25.1 %, respectively. Similarly, for FW the best fit was the Contois kinetic equation with an rRMSE of 35.2%, whereas the rRMSE for the first-order, Tessier, Monod and Moser are 39.7 %, 38.1 %, 39.6 %, and 37.6 %, respectively. It is not easy to draw a strong conclusion from this since the results are not strongly dependent on the choice of the kinetic equation.

4.2.2.2 2R model.

Compared with the 1R model, the complexity of the model has been increased by the addition of the methanogenic reaction [84]. The hydrolysis stage was modelled using first-order rate kinetics [98],Contois kinetics [228], and Monod kinetics [75]. The methanogenic reaction was modelled using the Haldane kinetics with inhibition [75], Monod [228] ,Tessier kinetics and Moser kinetics

[231].The parameter estimation was performed, considering the condition of inhibition by VFA only, ammonia only and a combination of both inhibitions, and the effect of no inhibition on the kinetics of the processes.

4.2.2.2.1 Green waste

Considering the impact of inhibition on green waste (GW) degradation, first order/Moser kinetics and Monod/Moser kinetics are the best fit kinetic models with rRMSE of 21.9% when VFA is the only inhibitory substance. When ammonia is the only inhibitory agent, the best fit kinetic models are the Contois/Moser kinetics, First Order/Moser kinetics, and Monod/Moser kinetics models, with the relative root mean square error is 21.9%. When volatility fatty acid (VFA) and ammonia are present as the inhibitory agents in the reaction. Again, the best-fit kinetics models are the same as the case when only VFA is inhibiting the reaction. Further, considering the degradation of green waste in the absence of any inhibitory agent, i.e. the absence of VFA and ammonia Inhibition when, the best-fit kinetics models are the same as that obtained for ammonia inhibition only. Therefore, it can be concluded that the introduction of the inhibitory agent does not have any impact on the ability of the 2R model to describe the degradation of green waste.

The worst fit kinetic models from the parameter estimation procedure is the Contois/Tessier kinetic model and Contois/Monod kinetic model for VFA inhibition only, and the combination of VFA and ammonia inhibition, respectively. For the relative root mean square errors of both kinetics model see Table 4.1. Overall, for green waste, the best fit model is the first order and Moser kinetics. Although, relative root mean square errors reported is the same for the best fit kinetic models in all the categories. The choice of the best first kinetic model was based on the fact that in terms of the residual errors, the first order / Moser kinetics was better than all other kinetic model combination, and also because the hydrolysis rate is traditionally described using the first-order kinetic [83], and it has been validated experimentally [247] as well as for description of surface related processes [98].

Comparing the root mean square errors (rRMSE) between the 1R model and the 2R model shows only a small reduction in the minimum rRMSE to 21.9% from the value of 23.0% in the 1R model. Further, the result of the parameter estimation procedures produced low sensitivity to the types of reaction kinetics. This suggests that all kinetic rate equations could be used to accurately describe the physical process exhibited in the GW experimental data as shown in Table 4.2. The results also show no substantial advantage in the model fitting by introducing the two common forms of inhibition in the anaerobic digestion processes, namely ammonia and volatile fatty acid inhibitions. It can be derived that the tendency of inhibition by either species affecting the kinetics of biomethane production is doubtful at least by a mechanism that could be replicated by the equations (3.50) and (3.50) of Chapter 3. The low content of nitrogen measured in the feedstock, with respect to ammonia inhibition, the low biodegradability measured in the methane production data means that limiting the ammonia condition is extremely improbable in the green waste fed system. Regarding VFA inhibition, the concentration of VFA measured in the effluent from the green waste system was not up to 0.1 g COD L^{-1}, implying that most of the VFA in the digester where used up by the microorganisms.

4.2.2.2.2 Food waste

The 2R model was assessed for its suitability to reproduce the methane production of FW from the experimental data. As in the case of green waste, the impact of the presence or absence of inhibition in the reaction kinetics is considered. The 2R model could not replicate the methane production for the different combinations of kinetic models for hydrolysis and methanogenesis in the absence of inhibition. The minimum relative root mean square root (rRMSE) values obtained is 34 % - 38 % and it is similar to the values obtained from the 1R model for the food waste. When inhibition is included in the reaction kinetic models, it was found that in all case of inhibition by ammonia only, the kinetics model was not able to accurately reproduce the experimental data of the methane production. Again, the root mean square errors of the parameter estimation are within the range obtained when there is no inhibition

in the reaction kinetics. Regarding inhibition by volatile fatty acids (VFA), the results show a root mean square error 30 – 39 % in all combinations of the kinetic models with the exception of the Contois/ Tessier kinetic model and Contois/Haldane kinetic model where the root mean square error reduced to 29.6 %. Combining both forms of inhibition (volatile fatty acid and ammonia) and using Contois kinetics to represent the hydrolysis stage, while Monod, Haldane, Tessier, and Moser represent the methanogenic stage. It was found that the relative root mean square errors was further reduced to 27 % when the methanogenic stage is modelled by the Monod, Moser and Haldane kinetics. An exception is the Tessier Kinetic model with rRMSE of 39 %. Again, when Monod is used to representing the hydrolysis degradation processes, the relative root mean square error was 28 % for methanogenic degradation processes represented by the Monod and Haldane kinetics. While the Tessier and Moser kinetics give a relative root mean square value of 37.7 % and 32.1 %, respectively. Further, the parameter estimation using the first-order hydrolysis, and the Haldane, Monod, Moser, and Tessier for methanogenesis stage could not accurately replicate the methane production of the food waste trails. The relative root mean square errors were 64.4 %, 72.3 %, 37.3 % and 31.8 %, respectively.

The result of the parameter estimation of the food waste degradation expresses the potential weakness in the methodology since only the effects of the inhibition are presented to the minimisation algorithm in the methane production, and since both inhibition reactions have the same effect then it is difficult to distinguish between the effects of both in the sum of squares of the errors. In steady state conditions, the two forms of inhibition would be indistinguishable to the minimisation algorithm, however, the collection of rich kinetic data, by intermittent feeding, at least gives the algorithm a chance to distinguish between the two inhibition types since, due to the mechanistic nature of the model, the production and consumption kinetics of the NH_3 and VFA states are very different, thus leading to differing inhibition characteristics over time. Contois is selected as the best performing hydrolysis kinetics because it takes into consideration the impact of both substrate and

microorganism concentration in the control of the hydrolysis rate. This is very relevant when there are large changes in the organic loading rate, thus causing a deficiency in the first-order model of the hydrolysis, as is the case for the food waste trials. Furthermore, the Contois kinetic model showed its ability to replicate both the mass transfer limitation and the growth limiting condition during the period of high organic feeding rates [248]. Contois kinetics have been extensively employed to represent the hydrolysis stage of the anaerobic digestion process in the literature [249-251] and it agrees with the results of the present study. Further, Haldane type kinetic model has been extensively used for the modelling of the methanogenic stage of the anaerobic digestion process, since it incorporates the effects of inhibition by VFA.

4.2.2.2.3 Uncertainty of estimated parameters

The evaluation of the standard errors associated with the calibrated parameters shows there is an increase in the standard errors estimated in the 2R model (15.5 %) compared with the 1R model (11.3 %), in the case of GW. Whereas for FW, the errors remained relatively low, with a maximum of 1.2 %. The increase in the uncertainty in the parameters estimated for GW could indicate various related issues; the dataset is inadequate to confidently estimate the parameters or the number of parameters estimated and/or the model complexity leads to no distinct solution in the case where the parameters are co-correlated with the output data (over-parameterised). For FW, the low level of uncertainty in the parameter values can be explained; firstly, the richness of its dataset as it is larger than for GW both in terms of the length of the experiment and in the number of gas flow data points, giving that the methane production for FW is higher. Secondly, due to the complexity of the degradation kinetics. This is characterised by the shape of the methane flow rate after feeding which indicates some form of temporary inhibition of the methane production and also, in the period of severe inhibition caused by the organic failure of the system. These two factors mean that the dataset has rich information embedded in it, especially regarding the additional phenomena, which in turn ensures that errors associated with the parameters

remained low while the model complex model displays its ability to reproduce the experimental data increases as shown by the reduced rRMSE.

4.2.2.3 3R model.

The model complexity was further increased by the addition of a parallel hydrolysis reaction [85]. To refrain from comprehensive screening procedure, the 3R model was applied to the kinetic parameters of the best fitting kinetics combinations and inhibition models obtained from the 2R model study. There was no marginal improvement in the model fitting (rRMSE = 22.1 %) to the experimental data in the case of GW when compared with the 2R model with rRMSE of 21.9 %. This is observed in the best fit parameter shown in Table 4.5, where the optimum solution of the parameter estimation algorithm was found using only one of the two substrate fractions. This is established by the low value β_2 compared with β_1, and this means that the degradation of the predicted protein fraction had very little impact on the simulated methane production. This is depicted in figure 4.2, which shows 2R and 3R models are somewhat similar. Figure 4.2 also shows that using the model structure provided, the characteristics of the methane production cannot be better described with two particulate fractions degrading at different kinetic rates. This is in contrast with the results of [248] and [243] who reported the presence of different fractions of the organic matter consisting of readily degradable and slowly degradable constituents in a similar study investigating the degradation of green waste. Similarly, the standard errors associated with the parameter estimation for the 3R GW case are rather high (maximum 23.2 %). This indicates that the model is somewhat over-parameterised given the richness of the dataset. Hence, the increase in the uncertainty, in addition to no improvement in the goodness of fits indicates that the 2R or 1R model should be recommended. [243] reported similar results when comparing different fractionation models for the description of the degradation of green waste using similar experimental data. It was found that there was no difference in the quality of fit to the experimental dataset between the models with two particulate fraction, and one soluble fraction and the model with one and the model with two particulate fractions.

A direct contrast to the results for GW is the slight improvement in the model fit of the experimental dataset when comparing the 3R model with the 2R model (rRMSE =27.0 % c.f. 27.2 %). The additional improvement was linked with the prediction of two distinct particulate organic fractions as shown in the values of β_2 and β_1 (0.588 and 0.315). The effects of the particulate fractionation can be seen in the methane flow predicted by the 3R model. It shows a slight improvement in the fitting of the complex kinetic behaviour shown in the experimental data shortly after each feeding. The model behaviour can be related back to the Contois kinetic degradation of the two fractions which have different saturation constants. Increasing the complexity of the anaerobic digestion model for food waste degradation improves and gives a better description of the experimental dataset. This was reported in the study by Poggio, [243], where it was found that the model with two particulate and one soluble fraction was able to describe the behaviour of the experimental dataset under high and low organic stress. Again, Mottet, Ramirez [248] in their study on the degradation of waste activated sludge, found that methane production occurs in two stages. An initial spike of methane is produced, followed by a decrease but constant a methane production. Thus, suggesting there are two separate fractions of the influent degrading at different rates.

A significant aspect of anaerobic digestion modelling is the description of the methane production based on the characterisation of its substrate. It is interesting to note that the results of the present study, when compared to the conclusion drawn from the literature [85, 243, 248] agrees that the methane production is best described by the substrate which consists of different organic fractions. However, there is a difference in the characterisation of the substrates. Mairet, Bernard [85] propose a substrate fractionation consisting of three fractions; inert, protein and lump fraction consisting of carbohydrates and lipids. Mottet, Ramirez [248] Propose the substrate fraction consisting of two fractions: readily degradable and slowly degradable. These fractions are further fractionated into carbohydrate, protein, lipid and inert. Poggio, Walker [243] propose a substrate fractionation consisting of two fractions, a

particulate fraction which further consists of slowly and readily degradable fractions and a soluble fraction. Each fraction is further fractionated into inert, carbohydrate, protein and lipids. In the present model, the substrate fractionation is similar to Mairet, Bernard [85] with the exception of the inert fraction. This is to ensure consistency between the 3R model and the 2R model proposed by Bernard, Hadj-Sadok [84]. The standard errors linked with the parameters of the 3R model using the FW data remain low, with a maximum of 0.4 %. This is due to the richness of the dataset, as previously discussed, in section 4.2.2.2 and the use of the 3R model as well as the 2R model is recommended above the 1R model for the description of FW degradation.

4.2.3 Model description and goodness of fit

A detailed, but qualitative, examination of the fit between the different models and experimental data allows assessment of the phenomena that each model is able to reproduce and therefore some recommendations may be made. The best fitting model descriptions for each model structure and substrate, along with the parameters identified, are given in Table 4.5 and plots of the predicted methane production rate of all three models, along with the experimental data, are shown in figures 4.2 and 4.3 for GW and FW, respectively.

4.2.3.1 Start-up of the model fitting to the experimental dataset

All of the models investigated show a poor fit with the experimental data at the start of the experiment, namely during the period 0-15 days, see figures 4.2 (a) and 4.3 (a). This is likely to be due to the inoculum being disturbed during its collection, transport, and processing in the laboratory and also being poorly acclimatised to the chemical makeup of the new substrate (FW or GW) since the inoculum was originally sourced from a sewage sludge digester. Recent studies have argued the need for adequate monitoring and analysis of the microbial diversity for the purpose of gaining a better understanding of the complexity of the AD process since the current methods of analysis are lacking and/or are specific to a particular set of microorganisms [85, 252].

Generally, anaerobic microorganisms, especially methanogens, require a stable temperature for their continued effectiveness and a disruption of this state destabilises their overall activity in a new environment. Further, the contamination of the process by oxygen ingress during processing could also contribute to the poor model fit with the experimental data, particularly at the beginning of the experiment, and perhaps more importantly, during the development of a re-balancing of the microorganism populations caused by the new substrate composition [253]. The phenomena of temperature dependence, oxygen stress, and population acclimatisation are not modelled and therefore these complex behaviours cannot be captured by such simple models, and therefore, their use is not recommended for the simulation in the initial start-up phase of an AD system.

4.2.3.2 Model fitting of the green waste experimental dataset

The model fitting during the remaining phase of the GW experiments (figures 4.3(b)-(d)) is qualitatively better than at the start of the experiment. Presumably, this is because the experimental system is not experiencing the population shifts associated with acclimatisation and it is also not under stress for organic overload or inhibition. The differences between the 1 - 3 R models can be seen between days 20 - 70. The 3R model tends to fit well the experimental data, especially when there is a fall in methane production rate unlike the 1R and 2R models despite the similarity in the trend shown in the rRMSE results. For the period of no feeding, the 3R model could fit well the experimental data up till day 70, after which it showed a poor fit between days 70-78. This is contrary to the 1R and 2R reaction models which show a poor fit during the period of no feeding (days 65-78, figure 4.3(c)) when the methane production from the experimental data tails off much more slowly than any of the models predict. In the physical system, this phenomenon has two components: (i) the substrate contains a very slowly degradable fraction which can continue to release soluble matter over long periods of time and thus contributing to a long term, albeit low, production rate of methane, and, (ii) the death of microorganisms gives the living population a continuous (but dwindling) supply of fresh substrate. Whilst the first of these could be captured

by the 3R model, as was found in the FW results, the estimation method has not identified this as an optimal solution for GW. The latter of these phenomena cannot be captured by the 1 - 3R models as formulated in this work whereas this is included in the ADM1 where the decay of the microorganism populations is recycled back to the composite organic matter. Following the commencement of feeding days 80 - 112, an examination of the model fitness also shows better fitting than the less complex models (1R and 2R) till the point where the feeding stopped due to foaming in the digester.

Since the methane flow data for the GW experiment did not contain information relating to an organic overload event (in contrast to the FW experiment), the use of these models/parameters to predict the behaviour of a system in these conditions is not recommended. However, it is clear that the predominant failure mode for the GW digester was foaming, and the 1 - 3R GW models continue to fit well the experimental data until the repeated foaming events caused the experiment to be terminated. This shows the inadequacy of the simplified models to predict the complex phenomena that are outside of their scope.

4.2.3.3 Model fitting of food waste experimental dataset

The modelled methane flow rate during the ‘acclimatised’ period for the FW experiments is shown in figures 4.3(b) - (d). This shows distinct qualitative differences between the 1 - 3R models in their quality of fit to the experimental data, thus agreeing with the quantitative assessments described in Section 4.3.2. The 3R and 2R models appear to capture the collapse of methane production corresponding to an organic overload condition, and the accumulation of VFA and ammonia in the later parts of the experiment. However, the distinction between the 3R models from the 2R was in its ability to capture the characteristic ‘n’ shape in the degradation kinetics for the days following a feeding event and even during the long period without feeding during the days 65 - 71. This is because the parameter estimation algorithm identified a solution that described the FW with a rapidly and slowly degradable fraction ($\mu_{1,\,max}$ = 0.588 and 0.315, respectively).

Clearly, this is closer to reality than the single input fractions used for the 1R and 2R models since both shows characteristic exponential decay curves in the methane production rate after a feeding event which does not follow the experimental data. Again, the 3R model represents closely the physical system depicted by the experimental dataset because, at high loading rate, there is a decrease in the protein utilising microorganism. This leads to the accumulation of protein in the digester. For sugar, the degradation is faster due to an increase in the growth rate of sugar utilising microbial population [85].

4.2.3.4 Validation of the Model.

The model validation, the goodness of fit the between observed data and the model data was evaluated by estimating the coefficient of determination. In the case of green waste (GW), the model showed a strong correlation for all the models; r^2 = 0.91, 0.92 and 0.89, for 1R, 2R, and 3R respectively. While for food waste FW, the determination of coefficient is 0.70, 0.80 and 0.70, for 1R, 2R, and 3R, respectively. While the 3R model captured some key phenomena of the degradation of food waste degradation with a lower rRMSE. It did not show a strong correlation when checked against the experimental data. Further, it is interesting to note that the 2R model predicted well the concentration of the VFA in the system see Figure 4.5. This shows a good agreement in both the rise and fall in the VFA (or S_2). This gives some validation to the parameter set found in the 2R model for FW under organic/ammonia stress since the VFA data did not form part of the estimation method and its closeness of fit is purely down to the mechanistic nature of the model and the parameters estimated from the methane production.

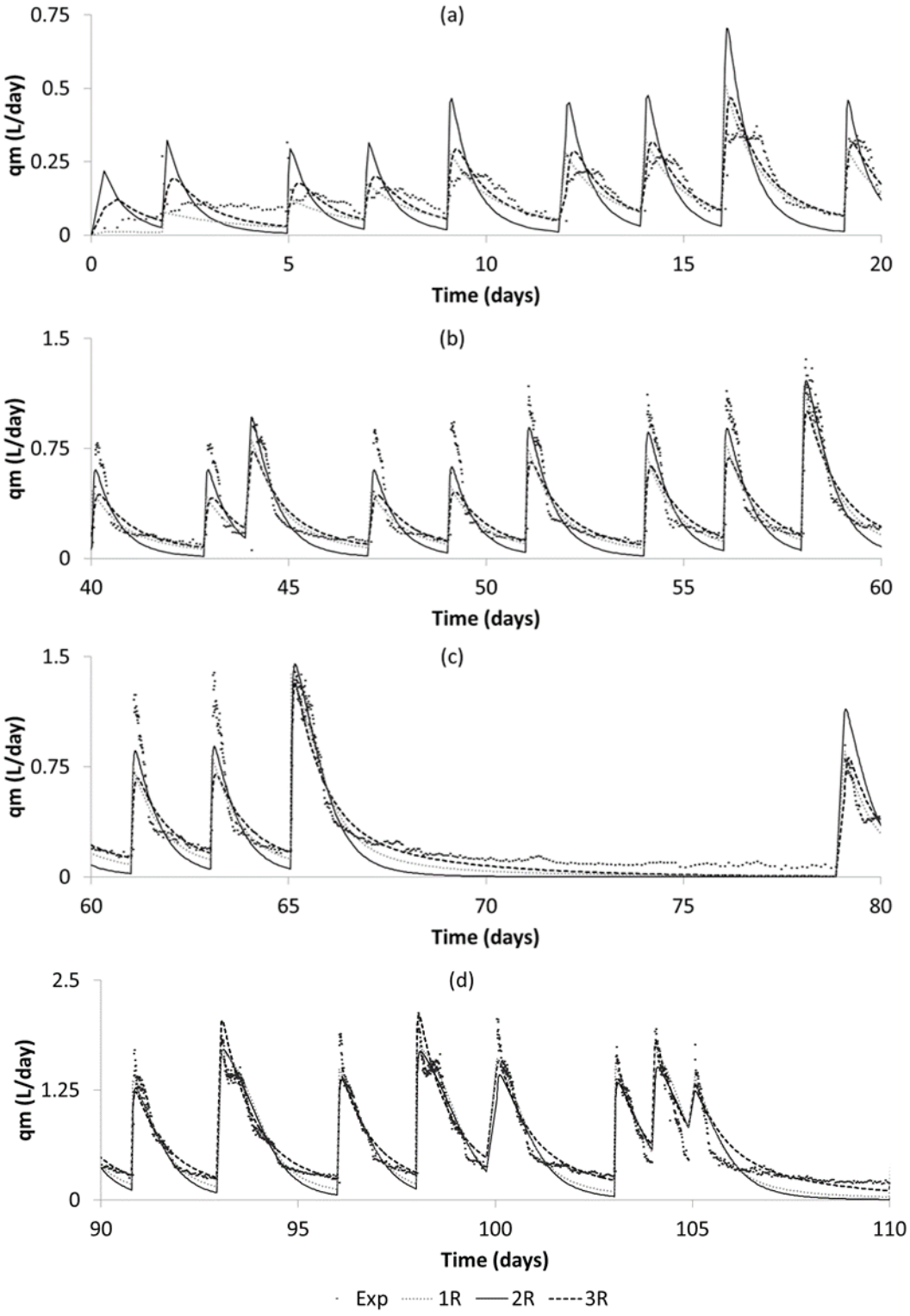

Figure 4.2 Methane flowrate for digestion of green waste showing the best fitting model combinations (1R, 2R, 3R) and experimental data for period (a) 0-20, (b) 60-80, (c)80-100, (d) 90-110 days.

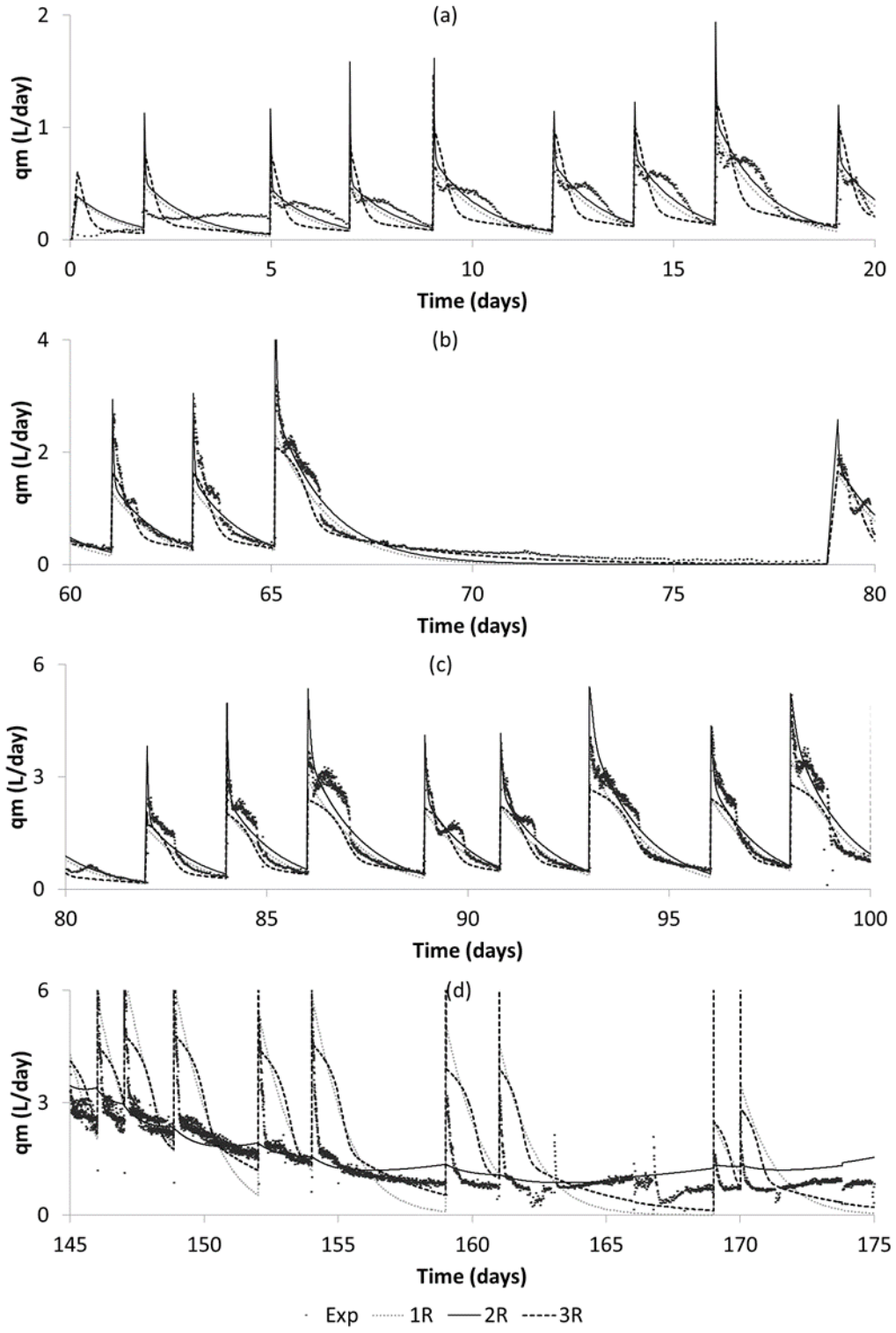

Figure 4.3 Methane flowrate for digestion of food waste showing the best fitting model combinations (1R, 2R, 3R) and experimental data for period (a) 0-20, (b) 60-80, (c)80-100, (d) 145-175 days.

Table 4.4 Parameter Values for GW and FW digestion for the best fitting models with 1R, 2R model.

Model	GW			FW		
1R	rRMSE (%)		23.0	rRMSE		35.2
	Kinetic		Moser	Kinetic		Contois
	Parameter	**Value**	**Std. Error (%)**	**Parameter**	**Value**	**Std. Error (%)**
	k_1	26.5	2.2	k_1	11.2	0.23
	$\mu_{1,max}$	0.279	6.5	$\mu_{1,max}$	0.136	1.18
	k_{s2}	9.87	11.3	k_{x1}	1.40	8.12
	λ	2.11	7.2			
2R	rRMSE		21.9	rRMSE		27.2
	Hydrolysis kinetic		1st order	Hydrolysis kinetic		Contois
	Methanogenesis kinetic		Moser	Methanogenesis kinetic		Haldane
	Inhibition		None	Inhibition		$VFA+NH_3$
	Parameter	**Value**	**Std. Error (%)**	**Parameter**	**Value**	**Std. Error (%)**
	k_1	38.2	2.5	k_1	15.0	0.25
	$k_{1,hyd}$	1.15	15.6	$\mu_{1,max}$	0.851	1.21
	$\mu_{2,max}$	0.0176	7.9	k_{x1}	15.3	0.73
	k_{s2}	280	14.2	$\mu_{2,max}$	0.128	0.23
	λ	2.14	7.8	k_{s2}	0.0364	1.04
				k_i	95.9	1.21
				$k_{i,N}$	138.3	0.13

Table 4.5 Parameter Values for GW and FW digestion for the best fitting models with 3R model.

rRMSE		22.1	rRMSE		27.0
Hydrolysis kinetic		1st order	Hydrolysis kinetic		Contois
Methanogenesis kinetic		Moser	Methanogenesis kinetic		Haldane
Inhibition		None	Inhibition		$VFA+NH_3$
Parameter	**Value**	**Std. Error (%)**	**Parameter**	**Value**	**Std. Error (%)**
β_1	0.486	2.4	β_1	0.588	0.01
β_2	0.0313	18.1	β_2	0.315	0.03
$k_{1a,hyd}$	3.19	18.2	k_{x1a}	6.60	0.32
$k_{1b,hyd}$	4.74	21.9	$\mu_{1a,max}$	0.653	0.40
$\mu_{2,max}$	0.0214	2.5	$\mu_{1b,max}$	0.487	0.21
k_{s2}	4.91	23.2	k_{x1b}	19.9	0.06
λ	3.12	8.3	$\mu_{2,max}$	0.141	0.00
			k_{s2}	0.0624	0.32
			k_i	5.95	0.42
			$k_{i,N}$	84.2	0.00

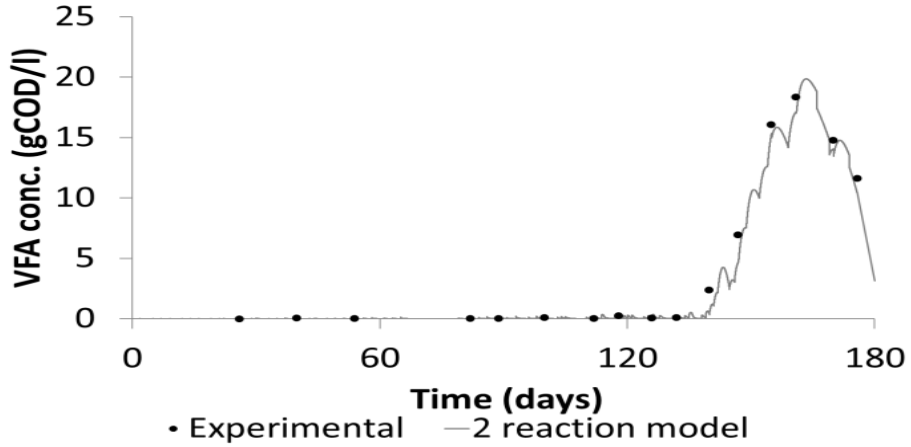

Figure 4.4 Model and experimental VFA data for degradation of FW with the 2R model.

4.2.3.5 Summary of model fitting

The models presented in this study have shown the ability to represent some of the major phenomena in anaerobic digestion, even though to variable degrees, and hence may be suitable for some modelling applications depending on the objectives. The 1R or 2R models are more desirable for the modelling of green waste degradation when comparing the quality of fit and parameter uncertainty, and it is not necessary to include inhibition of ammonia or VFA since the results show no improvement. A more complex 2R or 3R model, along with VFA and ammonia inhibition is suitable for the description of food waste degradation. These main results can be related back to both the characterisation work that was presented in table 4.2 and the known degradation characteristics of the two biomass feedstock samples used. Green waste contains a high fraction of non-degradable organic matter in the form of lignocellulose and relatively low nitrogen content which, when combined with the low degradability, leads to reduced ammonia release upon degradation compared with other feedstocks.

This means that neither the VFA inhibition, associated with organic overload conditions, nor the ammonia inhibition, associated with elevated ammonia concentrations, should be important phenomena in the degradation of GW in AD, which agrees with the results of this study. On the other hand, FW is

more degradable, contains a mixture of both rapidly (e.g. sugars, fatty acids) and slowly degradable components (e.g. cellulose, hemicellulose) and a higher degradable nitrogenous fraction which leads to higher concentrations of ammonia upon degradation. The combined result is that the degradation kinetics are more complex and that inhibition by both VFA and ammonia are important. Again, the physical model agrees with the modelling outcomes of this study. However, the characteristics of degradation of the feedstock cannot be predicted from the feedstock analysis given in table 4.2 alone since these only give some physical and chemical analysis and no information is presented here regarding the overall degradability and the associated rate of degradation, which both have a large impact on the AD process.

The applications of these models could be for online monitoring and control of AD processes due to the vastly reduced computational cost and effort relative to large complex models [84, 85] as well as the ease of recalibrating the dynamic state variables in real time. The models are flexible in that new state variables can easily be introduced based on the objectives of the modeller, e.g. if long term methane production (between feeding events) is of interest then a microorganism decay mechanism could be added. The limitations of these models have been elucidated here and they need to be understood before their application.

4.3.3.6 Sensitivity analysis

For AD systems, the sensitivity analysis is local in nature and it is usually presented as the variation in the output signal with respect to the parameters [245]. In this case, we have performed a local sensitivity analysis by exploring the parameter space surrounding the 'optimum' parameter set as located by the parameter estimation method (p_{opt}). Figure 4.5 shows the results obtained from the best fitting 2R models, for both FW and GW, with the sensitivity being expressed as the average of the methane flowrate (qm) and VFA concentration (S2) over the experimental period. In the case of GW, it was found that the degradation factor (K_1), the maximum uptake rate of VFA ($\mu_{2,max}$) and the index of the substrate concentration (λ) were the most influential parameters, while the solution was much less sensitive to the first-

order coefficient (K_{hyd}) and the half saturation (K_s). Similarly, for food waste, the parameters with the most significant influence on the solution were the ammonia inhibition constant ($K_{i,\,N}$), the VFA inhibition constant ($K_{i,\,vfa}$) and the uptake rate of VFA ($\mu_{2,\,max}$). The less sensitive parameters include the degradation factor, the uptake rate of the hydrolysis stage ($\mu_{1,\,max}$), the Contois half-saturation constant (K_x) and the half saturation constant for the VFA (K_s).

Further, to verify the results of the local sensitivity analysis, a global sensitivity analysis was performed using a Monte-Carlo method with the variation in each parameter being +/- 50% with a uniform probability distribution and 2000 sampling points. The results obtained are shown in Table 4.6 and are represented by correlation coefficients between the average methane flow and each parameter. Upon inspection, the analysis gives a similar outcome to the local analysis in terms of the relative sensitivity of the average methane flow rate to the parameter variations.

It is worth emphasising that in this Thesis, the model parameter(s) representing the overall stoichiometry of the first reaction step (k_1 in 1R and 2R models, β_1 and β_2 in 3R model) were included in the parameter estimation method, and this is in contrast with some other similar work [84, 85]. This can be easily justified by the outcome of sensitivity analyses, which shows that the model outputs have a high dependence on these parameters. Further, these parameters are largely dependent on the characteristics of the feedstock being digested since they must describe both the moisture content as well as the fraction of the organic material that is degradable. This implies that they should be considered, along with the kinetic parameters, to be feedstock specific.

Table 4.6 Global sensitivity analysis correlation coefficient (r^2) between parameter values and average methane flowrate for the best fitting two reaction model for FW and GW.

GW		FW	
Parameter	**r^2**	**Parameter**	**r^2**
k_1	-0.76	k_1	-0.40
$k_{1,hyd}$	0.03	$\mu_{1,max}$	0.04
$\mu_{2,max}$	0.30	k_{x1}	-0.08
k_{s2}	-0.15	$\mu_{2,max}$	0.60
λ	0.49	k_{s2}	0.04
		$k_{i,vfa}$	0.14
		$k_{i,N}$	0.47

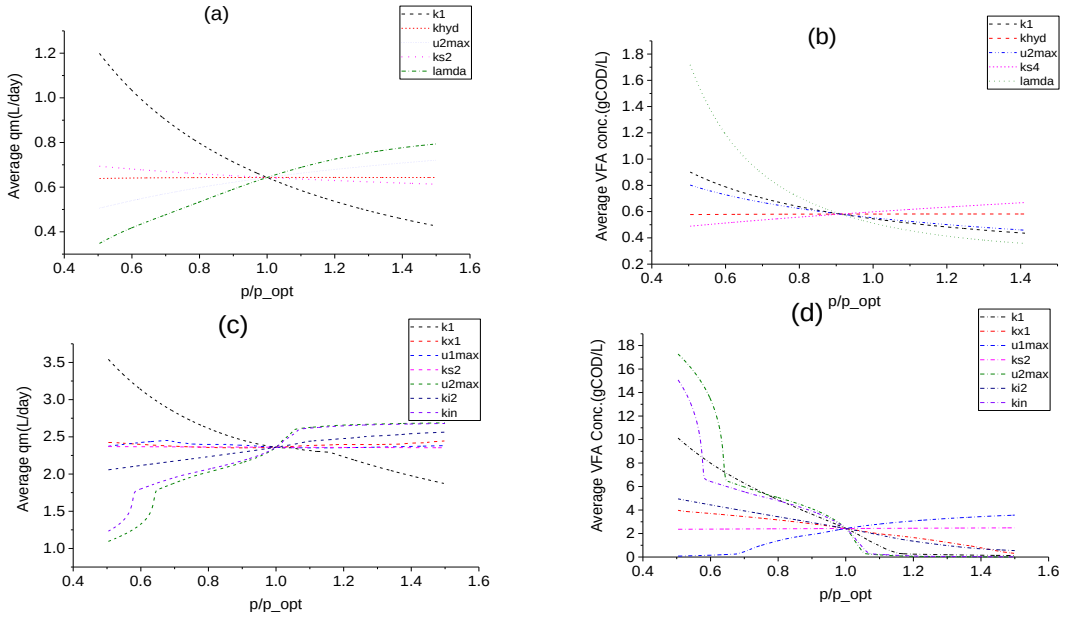

Figure 4.5 Local sensitivity analysis of the best-fit parameters set (p_opt±50%) for the simulation results of the average methane flow (q_m) and VFA concentration (S_2) over the whole experimental period for (a & b) GW and (c & d) FW.

4.2.4 Parameter estimation using batch experimental data.

Parameter estimation of the batch was performed using the 3R model. The batch experimental data consist of two separate tests; one for the inoculum (blank) and the standard test (inoculum + substrate). The blank test is

performed in triplicate (also known as experiment 1, 2 and 3 in the present study), and the inoculum is obtained from an external digester [81]. The standard test consists of batch test of green waste, food waste and pig manure.

4.2.4.1 Initial condition for the simulation

The estimation of the kinetic parameters of the biomass and its initial concentration was obtained from the parameter estimation of the blank test. Figure 4.6 (a) and (b) shows the model fitting of the experimental data of the methane production rate. The model was able to describe the degradation of the inoculum at the beginning of the experiment from day 0 to day 10, for experiment 1 and 2. While it fits well the dataset in experimental 3 up to day 25 and after day 25, the model did not fit well the experimental data, but it follows closely the methane production curves from the experimental data. The estimated kinetic parameter for the inoculum degradation and the initial biomass concentration is shown in table 4.7. The degradation coefficient k_1 for the inoculum is very small, thus suggesting only a fraction of the inoculum is degraded. This is expected as the inoculum has already been digested. Furthermore, the value of k_1 suggests that mostly the inoculum contains inert materials which do not degrade. In the 3R model, the total COD consists of the inoculum and substrate with different hydrolysis rate similar to the three reaction model of Mairet, Bernard [85] without any fractionation. Therefore, it did not take into consideration the inert content of the total COD of the inoculum, and this is a limitation of the model.

The 3R model considers different degradation pathways for the inoculum and substrate in the parameter estimation. Furthermore, the standard error obtained from the parameter estimation is very high for the initial concentration of the inoculum x_1 and x_2. This implies that there is less confidence in the estimated initial concentration of the inoculum in the batch test. The low confidence of the estimated inoculum concentration is a function of the poor quality of the experimental data used, as there is only a limited amount of data compared to the number of parameters estimated.

Table 4.7 Parameter values of 3R model and standard errors of the inoculum

Feed	Experiment	Estimated Parameters				Standard Error			
Inoculum		K_1	μ_1	X_1	X_2	K_1	μ_1	X_1	X_2
	1	1.04	0.31	7.29	7.57	2.19	0.55	39.10	39.10
	2	0.76	0.22	9.34	5.51	0.95	0.17	1.66	1.65
	3	0.78	0.21	8.02	6.83	0.99	0.24	27.00	27.00
Inoculum 2	1	0.82	0.08	19.01	10.81	0.53	0.04	161.00	161.00
	2	0.84	0.09	19.01	9.88	0.10	0.01	13.71	13.72
	3	0.74	0.10	19.94	10.73	0.12	0.01	22.61	26.62

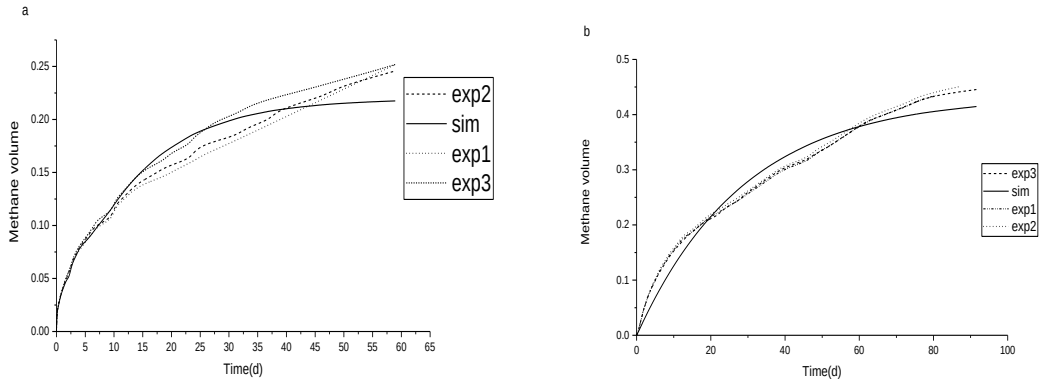

Figure 4.6 Volume of the methane production from 3R model (a) food waste and green waste inoculum, (b) pig manure inoculum.

4.2.4.2 Substrate Parameter estimation

Figure 4.7 shows the experimental data and simulated calibrated curve for the methane production in the batch test parameter estimation of pig manure, and table 4.7 presents the estimated parameter values and standard error of for each substrate. For the pig manure, the methane accumulated curve shows a better fitting of the model to the experimental dataset from 0-50 days. Thereafter, the 3R model predicts a lower methane production than the experimental dataset. The fitting of the model to the experimental data can be

quantified by the higher values as shown in table 4.8. Furthermore, the standard error estimated in both trials of the batch is very small, suggesting that data is sufficient to calibrate the parameters that describe the degradability of pig manure.

The degradation of food waste and green waste is displayed in figure 4.7, and it shows that in each batch trials, the experimental and simulated methane curve follows a similar pattern, with the model fitting the experimental data at the beginning of the experiment. The standard error of the estimated parameter of the food waste degradation is less than 50% in all the batches and this can be attributed to the 0.99 % correlation with the experimental data. For the case of green waste, the standard errors for the estimated parameter in batch 3 and 4 shows a value higher than 50 %, even though the correlation with the experimental data is high. It may be suggested that perhaps the Contois kinetic model is not suitable for the description of green waste hydrolysis degradation as it was also observed in the case of the semi-continuous experimental study.

The results of the volume of methane produced in figures 4.7 and 4.8 shows that the methane production reached a steady state faster with food waste, followed by pig manure and green waste. This is evident in the value of the estimated uptake rate of food waste, green waste, and pig manure, as shown in table 4.8. The difference in the uptake rate is attributed to the difference in the constituent of the feedstock. The methane production rate is higher for pig manure than from food waste and green waste, respectively. This is due to the difference in the total volume of substrate fed during the batch test. Also, given the same substrate to inoculum ratio of the food waste and green waste, there is a difference in the amount of methane produced. This difference in the volume of methane produced is because food waste is more degradable, has a higher fat content and lower water content compared to green waste. Furthermore, the degradability factor k_1 obtained from the parameter estimation of food waste, green waste and pig manure, revealed that the value of k_1 is very low for pig manure and food waste, compared to green waste. This is expected as the food waste is readily hydrolysed, and pig manure has been digested already, hence its low degradability. For green waste, the k_1

values estimated is higher, and this could possibly be a case of insufficient experimental data for the description of the degradation of green waste, and or the use of the Contois kinetic model is not sufficient to describe the hydrolysis of green waste.

Comparing the k_1 values estimated for green waste and food waste in the batch experiment to the values obtained from parameter estimation using the semi-continuous experimental data. In Section 4.2.3, the degradability factor k_1 predicted in the batch parameter estimation is low compared to the value of k_1 estimated in the case of the semi-continuous experiment, both substrates (FW and GW). The difference in the values could be due to the mode of operation of the batch and semi-continued test. The substrate is allowed more time in the batch system, implying an increase in the hydraulic retention time of the feedstock compared to the semi-continuous test. Also, in the batch experiment, the inoculum to substrate ratio is high, meaning a very small amount of substrate is added to the inoculum in the batch process compared to the feedstock.

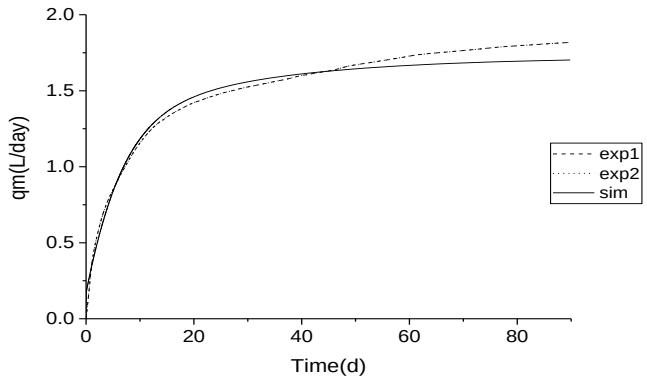

Figure 4.7 Shows the experimental and 2R model simulation of methane production for pig manure batch experiment.

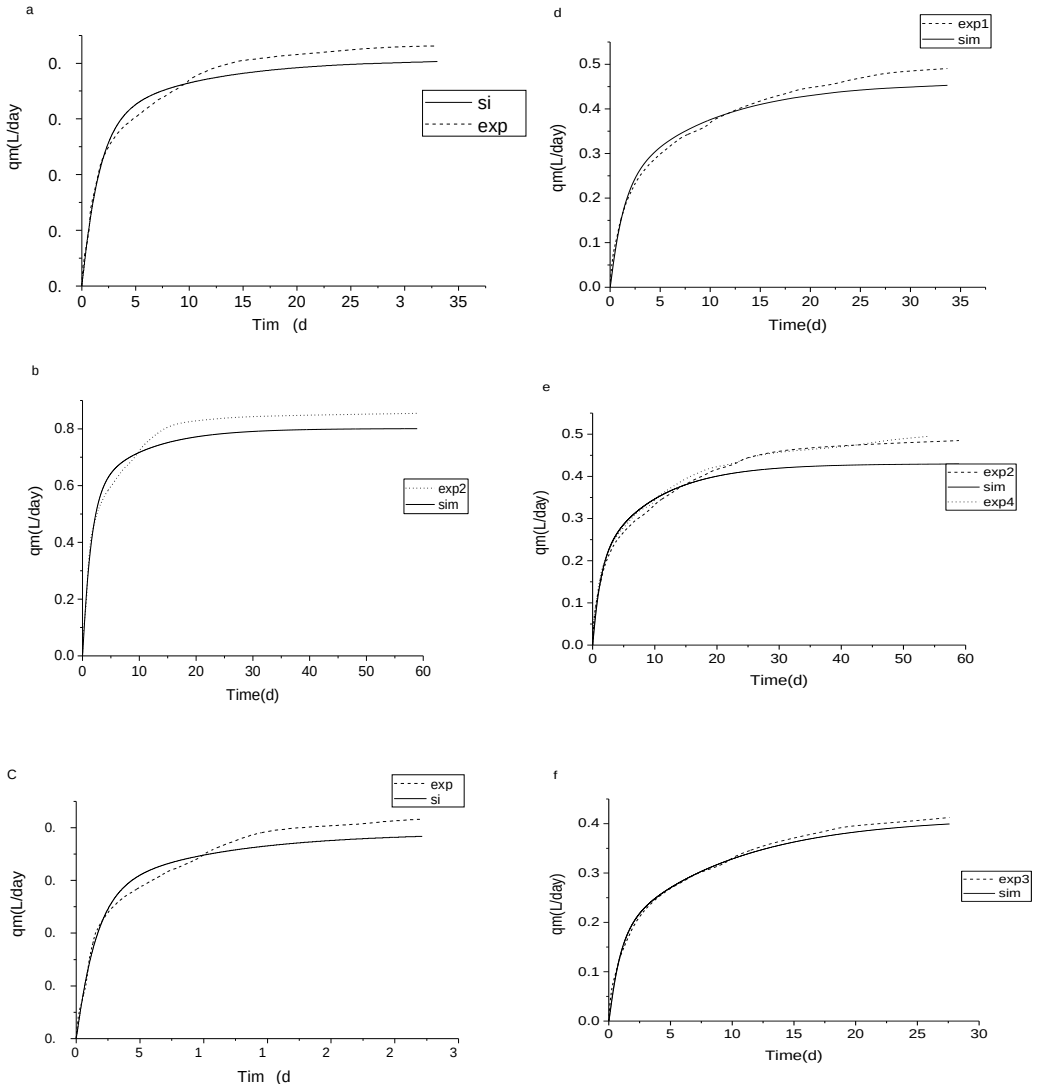

Figure 4.8 Result of the batch test experimental and simulated methane accumulation curve for food waste (a-c) and green waste (d-e) in the 3R model

Table 4.8 Results of the batch test parameter estimation, including standard errors.

Feeds	Experiment	Estimated Parameters		Standard Error		R^2
PM		K_1	μ_1	K_1	μ_1	
	1	0.22	0.05	2.03	1.00	99.0
	2	0.22	0.04	2.04	1.03	99.0
FW	1	0.26	0.16	6.27	9.44	99.0
	2	0.26	0.16	6.07	10.27	99.8
	3	0.26	0.16	5.72	9.41	99.9
	4	0.27	0.15	6.94	9.62	99.9
GW	1	0.68	0.07	47.02	16.95	99.01
	2	0.80	0.07	25.36	8.08	99.86
	3	0.88	0.08	85.06	25.09	99.93
	4	0.73	0.08	53.11	20.17	99.94

4.3 Conclusion

The main outcome of the Chapter reveals that anaerobic digestion models consisting of up to three biochemical reactions are able to fit well the experimental methane production from solid waste samples of both GW and FW with a minimum rRMSE of 22 % and 27 % over experimental periods of 112 and 176 days respectively. It was observed that the model structure, the number of biochemical reactions, and inhibition, plays a key role in the ability to accurately describe the experimental data, rather than the choice of the kinetic equation to determine the reaction rate. The results showed that either a one or two reaction model could fit well the experimental data for the case of GW, with no improvements from the addition of a third reaction or inhibition effects. However, for the case of FW, more complexity is required and increasing the number of reactions, as well as the inclusion of inhibition by VFA and ammonia improved the quality of fit. The two-reaction model was able to reproduce the elevated levels of VFA during a period of organic overloading. The estimated parameter from the batch test will be used as input to the biochemical model in Chapter 3.

Chapter 5 Performance of different designs of anaerobic digester

5.0 Introduction

This chapter is aimed at the determination of the thermal performance of different designs of the plastic bag digester installed in two different locations; Port Harcourt City, in Nigeria, and Cuzco, in Peru, respectively. The objective of this chapter is to determine the best digester design most suitable for Port Harcourt and Cuzco. This will be done by simulating the amount of methane produces from the different digester designs. The major contribution and novelty of the chapter is the comparison of the different designs of the plastic bag digester, and the integration of solar collector to a plastic bag digester. This is the first study based on the author's knowledge that explored the integrating a solar collector and plastic bag digester cover in a greenhouse. The details of the methodology of the development and implementation of the thermal and biochemical models are found in Chapter 3.

The dynamic equations of the mathematical model were implemented in both MATLAB and Simulink environment (MathWorks, MA, USA). The Thermal model is script in MATLAB, while the biochemical model is implemented in Simulink. The fourth order Runga-Kutta numerical method using the ode 15s solvers is used to solve the model equations with a maximum time step side of 0.01s.

5.1 Description of the digester designs

The first digester design consists of a plastic bag digester that is buried underground without a greenhouse to minimise heat losses. The digester tube absorbs solar energy from the sun to heat the slurry inside the digester. The second digester design consists of a plastic bag digester buried underground and is enclosed in a greenhouse. The solar energy absorbed on the greenhouse cover and adobe walls, is used to heat the slurry in the digester. The third digester design consists of a plastic bag enclosed in a greenhouse and a solar collector. In this design, the inlet of the plastic bag digester is modified into a tank, and on solar collector panel is mounted on the roof of the

tank. A heat exchanger pipe is installed inside the solar storage tank and it is connected to the inlet and outlet of the solar collector panel through an external pipe. Hot fluid from the solar collector panel flows through the heat exchanger pipe to heat the slurry in the solar storage tank. The solar storage tank is fed once every morning at 7 am with slurry, and the slurry remains in the storage tank until it is heated to the desired temperature before been discharged into the plastic bag digester. A controller is installed in the solar collector system to ensure that the slurry temperature in the solar storage tank is not above the desired set point temperature. In the present study, the control temperature is set at 55 ^{o}C and a sensor is installed in the solar storage tank to measure the temperature and relay to the controller. Once the slurry temperature is above the set point temperature, the controller stops the flow of hot water from the solar collector panel. When the slurry temperature is below the set point temperature, the flow of hot water resumes. A simple ON/OFF temperature controller is used in the present study, and the condition for the control of the flow rate of solar collector fluid is giving as:

$$\begin{matrix} T_s \geq T_{set\ point} \quad v_c = 0 \ ; \\ \sum T_s \leq T_{set\ point} \ ; \ v_c = 5.6e^{-06}\ m^3/_s \end{matrix} \qquad (6.1)$$

Where $T_{set\ point}$ is the desire control temperature in the solar storage tank, T_s is the temperature of the slurry in the solar storage tank, and v_c is the volumetric flow rate of collector fluid.

For the purpose of simplicity, the digester without a greenhouse is CASE 1, the digester with a greenhouse is CASE 2, and the digester with greenhouse and solar collector is CASE 3, see section 3.3, chapter 3. Further, it should be noted that CASE 3 (solar collector and plastic bag digester with a greenhouse) is for household use. Therefore, the design is made very simple to minimise cost. A simple valve is placed on the pipe that connects the solar storage tank to the plastic bag digester. This valve allows for the flow of the hot slurry into the plastic bag digester.

5.2 Result and Discussion

5.2.1 Performance of the solar collector tank

Solar energy has been used to reduce the cost of heating the anaerobic digester. In most cases, it has provided the required process condition that allows maximum productivity, while reducing the hydraulic retention time [74, 215]. The results of the simulation of the slurry temperature in the solar storage tank in Port Harcourt and Cuzco are presented in figure 5.1. The simulation is performed by setting a controlled temperature of 55 ^{o}C in the solar storage tank. In 1 hour, the slurry temperature in the solar storage tank is raised to 45 ^{o}C and 55 ^{o}C in Cuzco and Port Harcourt, respectively. It is expected that at the start of the simulation, there will be a decrease in slurry temperature in the solar storage tank. However, the model predicted the presence of solar radiation, hence the increase in the slurry temperature.

Figure 5.2 shows the hourly temperature of the slurry in the solar storage tank for a period of 10 days. It found that in both cities, the slurry temperature was fluctuating around the set point temperature of 55 ^{o}C. In Cuzco, the slurry temperature was below the setpoint temperature for the first 3 days. This is because the energy absorbed by the solar collector is very small, and the solar collector output temperature is 50 ^{o}C figure 5.2. The temperature of the slurry in the storage tank drops when the fresh slurry is fed into the digester, and the pump is switched on to allow the flow of hot water through the heat exchanger inside the solar storage tank. Once the temperature is equal or above the set point temperature (55 ^{o}C) the pump switches off. The important of the temperature control is to ensure that slurry temperature does not rise above the pasteurization temperature.

In literature, two types of the controller have been implemented to achieve the desired operating temperature in the storage unit or digester tank. The PID has been reported by Alkhamis et al [199] and Ouhammou et al [254]. The PID controller or differential is used in temperature control because of its sensitivity to input variation, the simplicity of the design parameter, and its ability to predict input perturbation. It is most use to control a 1 ^{o}C different in the desired temperature and the actual temperature of the system [199]. The

simple ON-OFF controller was reported by Dwivedi, [82]. The scheme of the ON-OFF controller is such that it allows the transfer of significant amount of heat recovered from the solar panel to storage tank. Therefore, in the present study, the ON-OFF controller is implemented to control the temperature in the solar storage tank figure 5.1.The concept of the ON/OFF scheme, involves the use of two temperature sensors, one at the outlet of the solar collector panel and the other at the storage tank. However, the drawback of the traditional ON-OFF controller is the inability to detect 1 ^{o}C difference in the temperature variation [233].

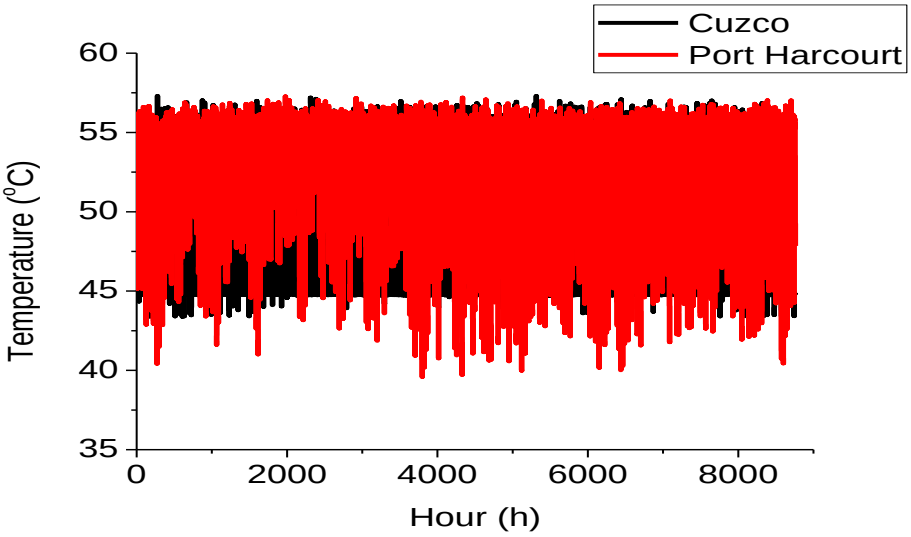

Figure 5.1 shows the hourly temperature of the slurry in the solar storage tank in Cuzco and Port Harcourt for 8760 hours (365 days).

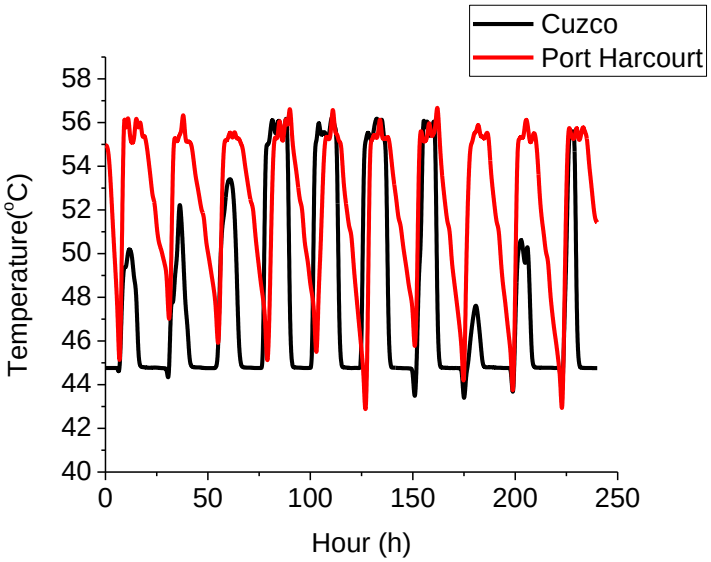

Figure 5.2 shows the hourly temperature of the slurry in the solar storage tank in Cuzco and Port Harcourt for 240 hours (10 days).

5.2.2 Performance of the different design of the plastic bag digester

In the section, the results of the simulation of the thermal performance of the different design of the plastic digester is presented, starting from the CASE 1, followed by CASE 2, and then CASE 3. The simulation was performed by investigating the impact of weather conditions such as ambient temperature, solar radiation, wind speed, longitude and latitude of location etc. The performance of the digester was compared to determine their suitability in two locations with different weather condition.

5.2.2.1 Plastic Bag digester without greenhouse (CASE 1)

The results of the simulation present the hourly slurry temperature in the digester installed in Cuzco and Port Harcourt over a period of 8760 hours (365 days), figure 5.3. The slurry temperature is above 10^{o}C with minimal fluctuation despite the fluctuation in the daily high and the low ambient temperature of 21 ^{o}C and 10 ^{o}C respectively. The slurry was able to maintain a temperature of 18 ^{o}C in the first 2 days figure 5.4, and this could be due to the solar energy received by the slurry. Figure 5.5 also shows that the slurry temperature increases from 18 ^{o}C to 24 ^{o}C in the month of January. The slurry

temperature remained within this range in the month of February, and a slight decrease in the slurry temperature within March and April (1417 - 2880 hours). In Cuzco, the winter season starts from May to September (2881 - 6552 hours). The low air temperature, lack of sufficient solar energy causes a further drop in the slurry temperature. The air temperature in the winter period has a maximum and minimum at 20.5 ^{o}C and -0.5 ^{o}C, figure 5.6. However, CASE 1 was able to maintain a slurry temperature between 10 ^{o}C to 15.5 ^{o}C. The average temperature of the slurry in the plastic bag digester within this period is 12.98 ^{o}C and the average air temperature is 10.68 ^{o}C. This is a 2.30 ^{o}C increase in the temperature of the slurry compared to the ambient air temperature. The plot of the hourly slurry temperature during the period demonstrates the effects of air temperature as the slurry temperature drops. Other factors that contributed to the fall in the slurry temperature includes the degree of heat exchanges between the digester and the air, soil temperature and the temperature of the inflowing slurry [205].

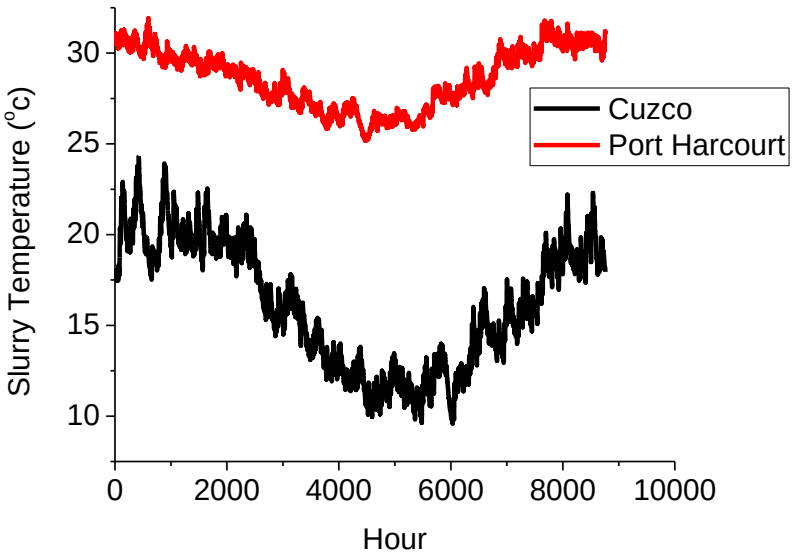

Figure 5.3 shows the plot of the slurry temperature in the plastic bag digester (CASE 1) in Cuzco and Port Harcourt.

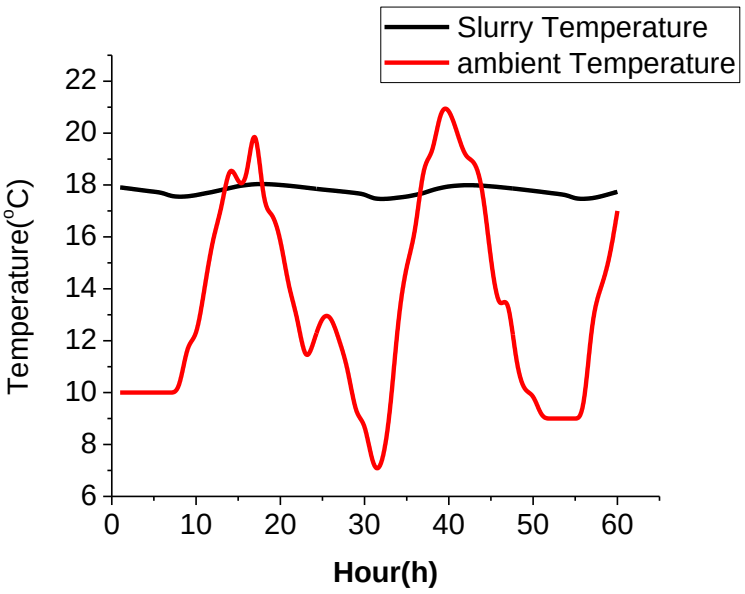

Figure 5.4 shows the profile of the slurry temperature in CASE 1 for 48 hours (2 days) in Cuzco.

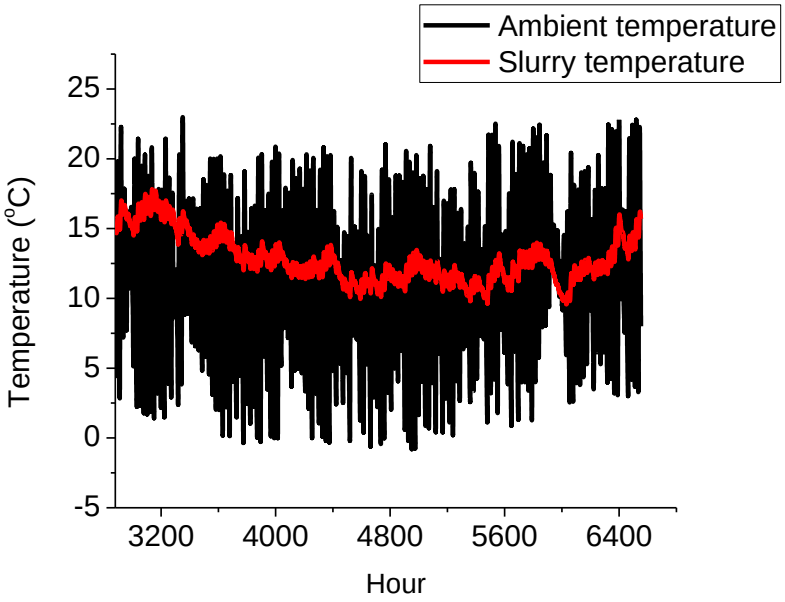

Figure 5.5 shows the slurry and ambient temperature in Cuzco.

To demonstrate further, the impact of season on the slurry, the monthly average slurry temperature presented in figure 5.6. The slurry temperature in the digester in the month of July is the lowest, and this corresponds to the coldest month in Cuzco. The warmest month in Cuzco is January, and the figure 5.6 shows that the highest slurry temperature in January. This change

in the digester slurry temperature due to seasonal changes has been reported by various authors in the literature [201, 255]. Pham, [234] reported that the month of August in the Northern hemisphere recorded the highest slurry temperature of 30 ^{o}C and lowest slurry temperature of 20 ^{o}C was reported in January. Tinarwo et al [256] reported a similar pattern in the slurry temperature as a direct result of the effects of changes in seasonal temperature. The average high and low slurry temperatures was 25.40 ^{o}C and 15.90^{o}C. In the present study, the average summer and winter temperature of the slurry in the digester is 20.44 ^{o}C and 11.61 ^{o}C for Cuzco.

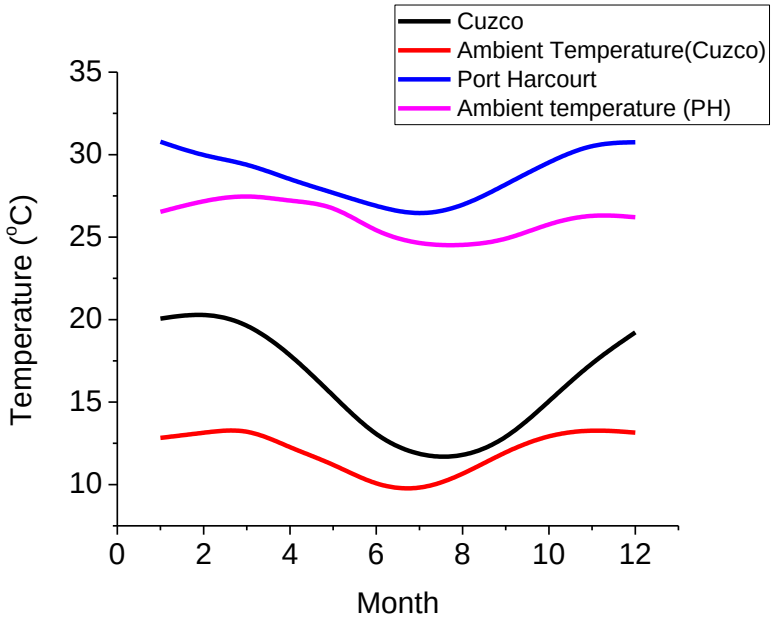

Figure 5.6 shows the monthly slurry and ambient temperature of the digester (CASE 1) in Cuzco and Port Harcourt.

Similarly, in Port Harcourt the profile of the slurry temperature in the digester is presented in figure 5.3. The slurry temperature is 30 ^{o}C between the month of November to February and it falls below 30 ^{o}C in the month starting from March to October. In Port Harcourt, the dry season starts from November to February and the wet season starts from March to October. In each season, the maximum and minimum ambient temperatures are in the range of 25.71 - 33.08 ^{o}C and 18.32 - 23.14 ^{o}C respectively [257]. Analysing the air temperature using the data in the present study, reveals that the maximum and minimum air temperature are within the range (26.42 - 30.40 ^{o}C and 22.39

- 24.57 ^{o}C) reported by Uko et al [257]. This high air temperature during the different season, and the mean monthly maximum and minimum air temperature of 31.29 ^{o}C and 21.80 ^{o}C ensures the plastic bag digester (CASE 1) maintain slurry temperature within the mesophilic regime (28.63^{o}C).

Further, it is observed that there is minimal fluctuation in the slurry temperature of the plastic bag digester installed in Port Harcourt. This is in comparison to the slurry temperature profile in Cuzco figure 5.6. The difference in the temperature profile is mainly due to the difference in air temperature and soil temperature in the locations [120, 208]. In general, in addition to the high air temperature, and the solar radiation, the digester slurry temperature was kept above the slurry temperature because the average biogas temperature above the slurry is high compared to the slurry temperature.

5.2.2.2 Plastic bag digester with greenhouse (CASE 2)

In the section the plastic bag digester installed was inside a greenhouse with an adobe wall. The profile of the slurry temperature in the digester is shown in figure 5.7. Comparing the temperature of the slurry obtained from the simulation of CASE 2 against CASE 1. There is a 3.49 ^{o}C increase in the temperature of the slurry in CASE 2 in Cuzco. In Port Harcourt, the temperature of the slurry in CASE 2 increased by 2.57 ^{o}C. This gain in the temperature of the slurry in CASE 2 is as a result of the heat gained or absorbed in the adobe walls, internal greenhouse air, greenhouse cover and biogas [73, 78].

The analysis of the slurry temperature against the ambient temperature is found in figure 5.8. The average slurry temperature in Port Harcourt is 31.2 ^{o}C, and the average ambient temperature in Port Harcourt is 26.1. This is 5.1 ^{o}C higher than the ambient temperature. In Cuzco, it was reported that the mean slurry temperature over the monitoring period (5 days) was 8.4 ^{o}C higher than ambient temperature [65]. It should be noted that the digester used in [65], is identical to the digester in the present study. The result of the simulation for one year gives an average slurry temperature of 19.64 ^{o}C in

Cuzco and the average ambient temperature in Cuzco is 12.04 ^{o}C. The temperature of the slurry in the digester in the present study is 7.6 ^{o}C higher than the ambient temperature. The difference in the results of the simulation of the plastic bag digester in Cuzco is explained by the experimental data used in the original paper [65]. The thermal model was calibrated to fit experimental data obtained for measurement of the slurry temperature in the field. Further, the analysis of the thermal performance of the plastic bag digester was done over a 5 days period in [65].

Similar studies reported a gain in the slurry temperature when the digester is covered by a greenhouse. Garfi et al [70] reported the temperature of the slurry in the plastic bag digester covered by a greenhouse. The mean slurry temperature was 20 ^{o}C, and it is 2.1 ^{o}C higher than the mean ambient temperature. Marti et al [120] reported that the temperature of the slurry has a mean value of 16.6 ^{o}C compared to the average air temperature of 8.5 ^{o}C. The same result was obtained by Marti et al [79] using similar digester designs. These digesters were installed about 3000 - 4000 meters above sea level. Also, the slurry temperature of household digester can be estimated from the ambient temperature [120] and the soil temperature [208]. In a warm and hot climate, soil temperature has been used to predict the slurry temperature as was reported by Terradas et al [208] . Marti et al [258] reported that the low-cost digester used in the treatment of slaughterhouse wastewater has a slurry temperature in the range of 26.8 - 28.5 ^{o}C, giving the maximum and minimum ambient temperatures of 28.2 ^{o}C and 20.2 ^{o}C. The results of these researchers agree with the result of the present study as the temperature of the slurry following the pattern of air temperature, but with minimal daily fluctuations. The maximum and minimum air temperature in Port Harcourt are 33.1 ^{o}C and 20.2 ^{o}C, while the temperature of the slurry in the digester is between 34.8 ^{o}C and 26.9 ^{o}C. However, note that the result of the thermal model of the plastic bag digester in Port Harcourt is modelled based and there is a need for a field experimental validation of the results.

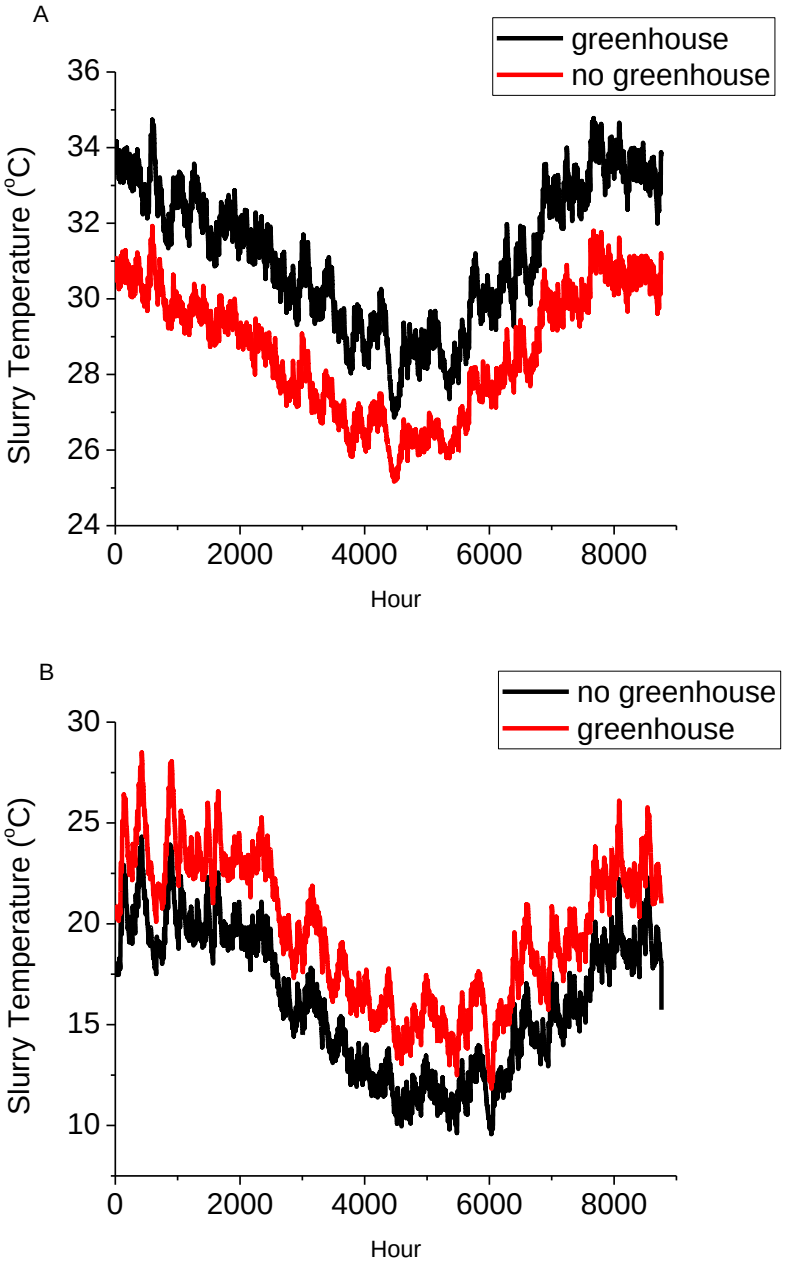

Figure 5.7 shows the slurry temperature of the digester design CASE 2 and CASE 1; (A) Port Harcourt, (B) Cuzco.

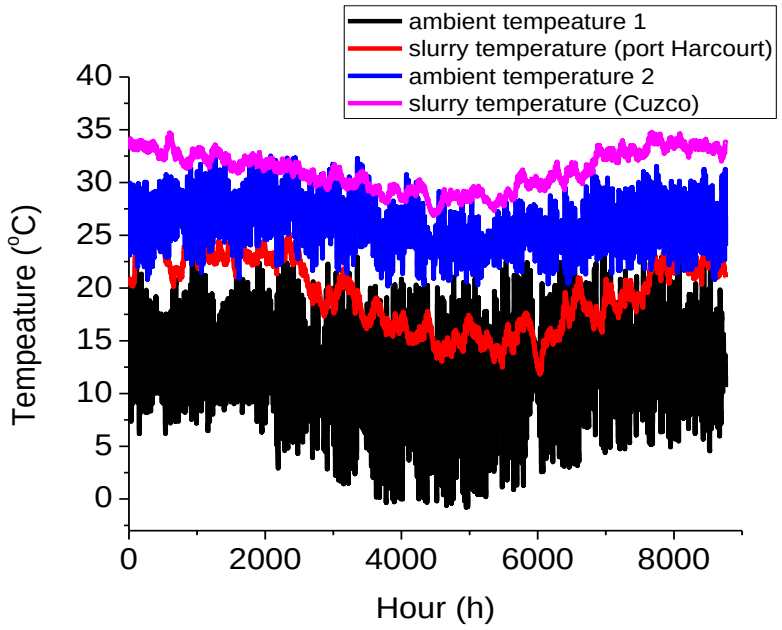

Figure 5.8 shows the slurry and ambient temperature for Cuzco and Port Harcourt.

5.2.2.3 Plastic bag digester in a greenhouse and solar collector (CASE 3).

In the energy balance of the slurry of CASE 2, it was assumed that the temperature of the slurry fed into the digester daily is at ambient, see equation 3.36, sub-section 3.3.2, Chapter 3. In the modelling of the plastic digester with a greenhouse, integrated with solar collector; the inlet slurry is heated in the solar storage tank before it is discharged into the plastic bag digester see figure 3.3, section 3.1, Chapter 3. The temperature of the slurry in CASE 3 in Port Harcourt, increase by 1.14 - 1.70 ^{o}C on an hourly basis and the mean slurry temperature is 32.68 ^{o}C see figure 5.9 (a). Compared to CASE 2, the temperature of the slurry increases by 1.48 ^{o}C (31.20 ^{o}C for CASE 2). Also, comparing with CASE 1, the temperature of the slurry in CASE 3 increase by 4.05 ^{o}C compared CASE 1, (28.63 ^{o}C). These slight increase in the slurry temperature in CASE 3 compared to CASE 2, may suggest that in Port Harcourt, the use CASE 3 is not useful. In Cuzco, figure 5.9 (b) shows the simulated temperature of the slurry in the plastic bag digester design (CASE 3). The temperature of the slurry increased by 6.2 ^{o}C and 9.7 ^{o}C compared to the slurry temperature in the other designs of the plastic bag digester (CASE

1 and 2). The mean temperature of the slurry in CASE 3 is 25.85 ^{o}C. This may suggest that the addition of extra energy (solar collector) to the plastic bag digester design may be feasible in Cuzco.

The profile of the slurry temperature in CASE 3 follows a similar pattern to the temperature of slurry in CASE 1 and CASE 2. There was an increase in the temperature of the slurry during the summer and a decrease in the temperature of the slurry during the winter or wet season. However, the temperature of the slurry in the digester in CASE 3 during the wet or winter season is higher than the slurry temperatures in CASE 1 and CASE 2 in this period. This is because the additional heating provided by the absorption of solar energy on the greenhouse in CASE 3 ensures the temperature of the slurry in CASE 3 is above 15 ^{o}C compared to the slurry temperature in CASE 2 (11.65 ^{o}C) in Cuzco. In Port Harcourt, the slurry temperature in this period for the different design of the digester is 28.33 ^{o}C, 26.86 ^{o}C, and 25.23 ^{o}C for CASE 3, CASE 2, and CASE 1 respectively.

Youzhou et al. [219] found that using an insulated solar collector pipe that is wrap around the digester; it is possible to raise the slurry temperature by 4.5 ^{o}C during a sunny day. However, the slurry temperature decreases by 0.8 ^{o}C and 0.4 ^{o}C at night and on a cloudy day due to lack of solar energy. Feng et al [216] proposed an over ground digester made from plastic material integrated with a solar collector system. The temperature of the slurry was maintained at 27 ^{o}C, and it was higher than the ambient temperature which varies between -10 ^{o}C - 0^{o}C. The slurry is heated to a suitable temperature before it is discharged into the digester similar to the procedure used in the present study.

A comparison of the slurry temperature of CASE 3 in Cuzco and the digester in Feng et al [216]; reveals that the mean temperature of the slurry in Cuzco is low than the temperature of the slurry reported by Feng et al [216].The difference could be in the effects of insulation on the digester slurry temperature. In Cuzco, it was reported that there was absence of straw insulation in the trench due to the expansion of the plastic bag digester as it accommodates more slurry [120]. Since, the same digester in Cuzco is used

in Port Harcourt, it is expect that there would be heat losses to the soil, which could reduce slurry temperature, however, the thermal model (CASE 3) predicted a higher slurry temperature compared to the temperature of the slurry reported by Feng et al [216].This could be due to difference in the ambient temperature, soil temperature, and solar radiation of the two location. Hassanein et al [212] reported the impact of solar heating on the performance of anaerobic digester. The digester is cover with a greenhouse to provide heating, and an internal greenhouse is install over the inlet tank, where the slurry is heated before it is transfer into the digester. The additional heat from the internal greenhouse ensure the slurry enters the digester at high temperature similar to the heating provide by the solar collector in the present study. The external digester helps to minimise the fluctuation in slurry temperature similar to the greenhouse in CASE 2 and CASE 3.

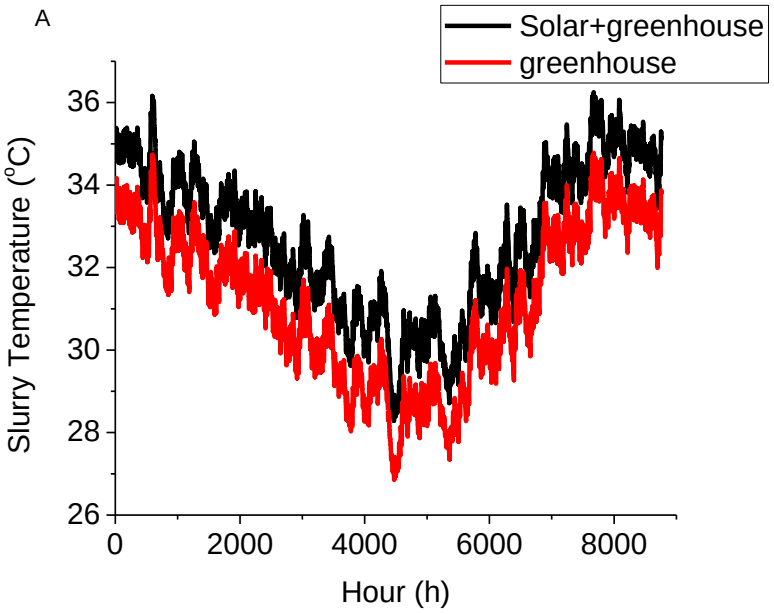

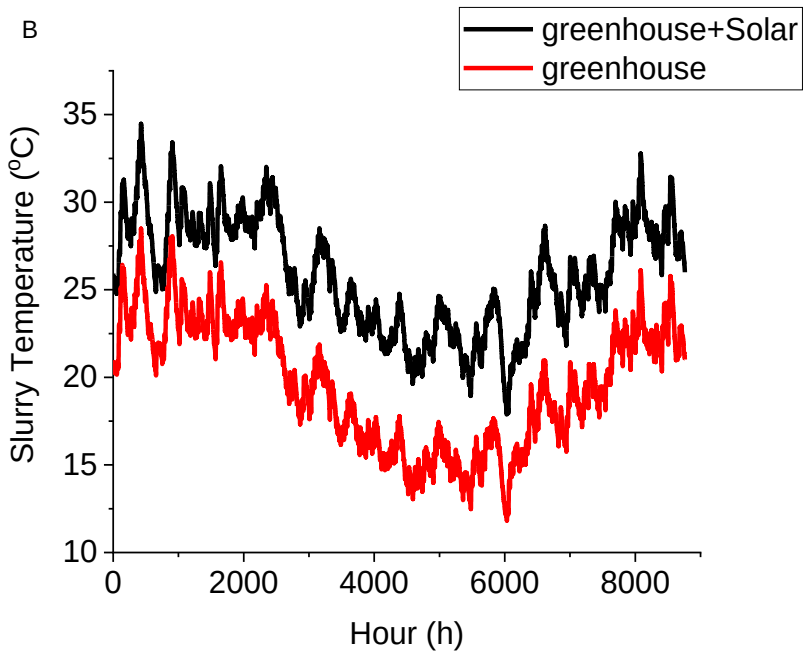

Figure 5.9 shows the slurry temperature of the digester design CASE 3 and CASE 2; (A) Port Harcourt, (B) Cuzco.

5.2.3 Evaluation of the methane production from the digester designs.

The thermal model of the plastic bag digester (CASE 1, CASE 2 and CASE 3) is simulated the slurry temperature as its output. The cardinal temperature model with the point of inflation [223] relates the operating temperature (in this case is the temperature of the slurry) to the uptake rate of the different stages of anaerobic digestion. The two population, two reactions model (2R model) is used to simulate the methane production. The impact of the weather condition on the methane production was simulated for the digester designs in Port Harcourt and Cuzco respectively. The dilution rate of 0.05 day^{-1} (organic loading rate of 20.93 kg COD/day) food waste is fed into the plastic bag digester daily.

The simulation of methane production from the different design of plastic bag digester is seen in figure 5.10. In Port Harcourt, there is little difference in the amount of methane produced, and as shown in the graph the methane production was stable with daily spikes of methane produce after fresh slurry enters the anaerobic digester. The spikes of methane produce after feeding is a characteristic of the readily degradable component of the food waste, as it

consist of readily degradable organic matter [242, 243]. Moreover, given that the slurry temperature reduces slightly in all the designs during the rainy season in Port Harcourt, the methane production is stable and was not affected by the slurry temperature. The thermal models (CASE 1, CASE 2 and CASE 3) predicts that the average methane production per litre of the digester volume is 0.345 – 0.476 m^3 m^{-3} day^{-1}. This results of the simulation of the methane production indicates that digester in CASE 3 is not useful in Port Harcourt.

In Cuzco, the methane production from the designs is influenced by the slurry temperature. The daily methane production is range from 0.207 m^3 m^{-3} day^{-1} in the CASE 1 to 0.287 m^3 m^{-3} day^{-1} in CASE 3. The results of the simulation suggested that the addition of extra heating source to the plastic bag digester in Cuzco is feasible. Furthermore, a comparison of the methane production in both locations reveals that the methane production is higher in Port Harcourt than in Cuzco. It is very important to highlight that the results of the present study are based on modelling and simulation of the plastic bag digester using a two-population biochemical reaction. However, there is need for further evaluation of the methane production from experimental study especially for the plastic bag digester installed in Port Harcourt.

A

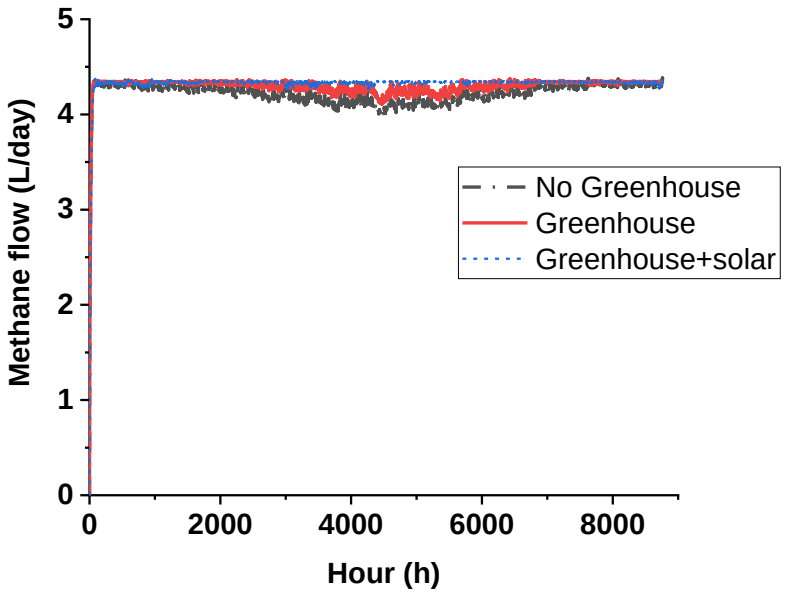

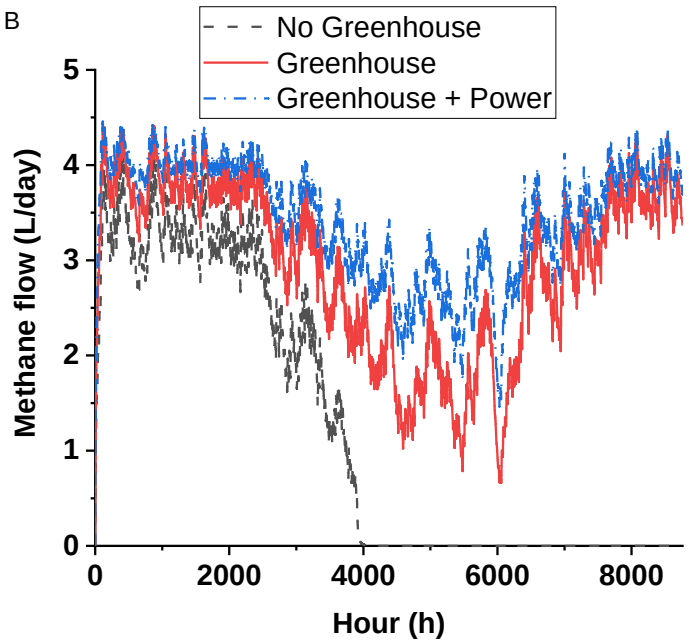

Figure 5.10 shows the methane production from the different design of the digester; (A) Port Harcourt, (B) Cuzco.

5.4 Conclusion

In this research work, the performance of different designs of the plastic bag digesters in two different locations was evaluated. The plastic bag digester consists of CASE 1: without greenhouse, CASE 2: plastic bag digester with greenhouse, and CASE 3: plastic bag digester with greenhouse and solar collector mounted on the inlet of the digester. Simulation of the thermal model of the digesters found a slightly or no significant increase in the slurry temperature in each design installed in Port Harcourt. In Cuzco, there is a significant difference in the slurry temperature in the different digester designs. CASE 3 has 4.2 ^{o}C increase in the slurry temperature compared to CASE 2, and 9.1 ^{o}C increase in slurry temperature compared CASE 1. The simulation of the methane production in each design reveals no difference in the average methane production (478 L L^{-1} day^{-1}) in Port Harcourt. In Cuzco, the methane production in CASE 1 is 207 L L^{-1} day^{-1} and 287 L L^{-1} day^{-1} in CASE 3. Therefore, the addition of an extra heating source to the plastic bag digester is not useful in Port Harcourt, but feasible in Cuzco. A further experimental study is required for the validation of the results of the simulation.

Chapter 6 Operational strategy of small-scale digesters

6.0 Introduction

This chapter is aimed at developing an operational strategy for small scale digester in different locations (Port Harcourt and Cuzco). The objective is to show how modelling can assist in developing an operating manual that highlights the best possible loading rate of the feedstock depending on the environmental conditions, digester operating temperature, and the availability of the feedstock. The thermal model of the plastic bag digester with greenhouse cover (CASE 2) simulate the slurry temperature. The model (CASE 2) is linking to the biochemical reaction model (3R model) by the temperature dependent kinetic model. This complete model is used to determine the maximum methane production and minimum hydraulic retention time.

6.1 Materials and Methods

The methodology developed in this section has been discussed in chapter 3, section 3.8.

6.1.1 Mathematical model

The equations depicting the dynamic variables of the mathematical model (thermal and biochemical models) were implemented in the MATLAB and Simulink environment (MathWorks, MA, USA). The thermal model of the plastic bag digester used in the chapter is CASE 2, see section 3.3.2, Chapter 3. The biochemical model used is the three-reaction model (3R model), equations (3.58) – (3.61) in section 3.5.3.2, Chapter 3. The kinetic models used are the Contois kinetic model for hydrolysis equation (3.43) and Haldane kinetic for methanogenic equation (3.46), see section 3.51. These kinetic models were applied to describe the degradation of food waste and pig manure. The First-order kinetic and Moser kinetic models are used to describe the degradation of green waste degradation, see equation (3.44) and (3.48) in section 3.5.1 Chapter 3. The thermal models (CASE 2) is used because it is the most suitable digester design in Port Harcourt and Cuzco, this is

explained later in chapter 6. The 3R model is applied in the present study together with the kinetic model described above, because it is best describes the degradation of food waste and green waste. The fourth order Runga-Kutta Numerical method using the stiff ode15s solver was employed to solve the mathematical model giving a maximum step size of 0.002 days.

6.2 Results and Discussion

6.2.1 Mono-digestion process

The anaerobic digestion process started with the digester operating at a low feeding rate for some days; thereafter, there is a step increase in the feeding rate until a point of failure is achieved, figure 6.1 (a). The minimum hydraulic retention time is calculated by extracting the maximum feeding rate, while the methane production corresponds to the maximum feeding rate is extracted from the curve. Figure 6.1 (a) and (b) shows the illustration of the basis of the model. The simulation is performed at a slurry temperature of 294 K (21^{o}C) and the feeding rate is constant until day 180 to achieve steady state before the step increase in the feeding rate from day 181, see figure 6.1 (b). The methane production increase to a maximum at day 284 and drops following further increase in the feeding rate. The MATLAB script extracts the two characteristic data points from the simulation; the maximum methane production rate of 4.47 L/day and the corresponding maximum dilution rate (before the failure) of 0.0222 day^{-1}, and this corresponds to a minimum hydraulic retention time of 44.87 days.

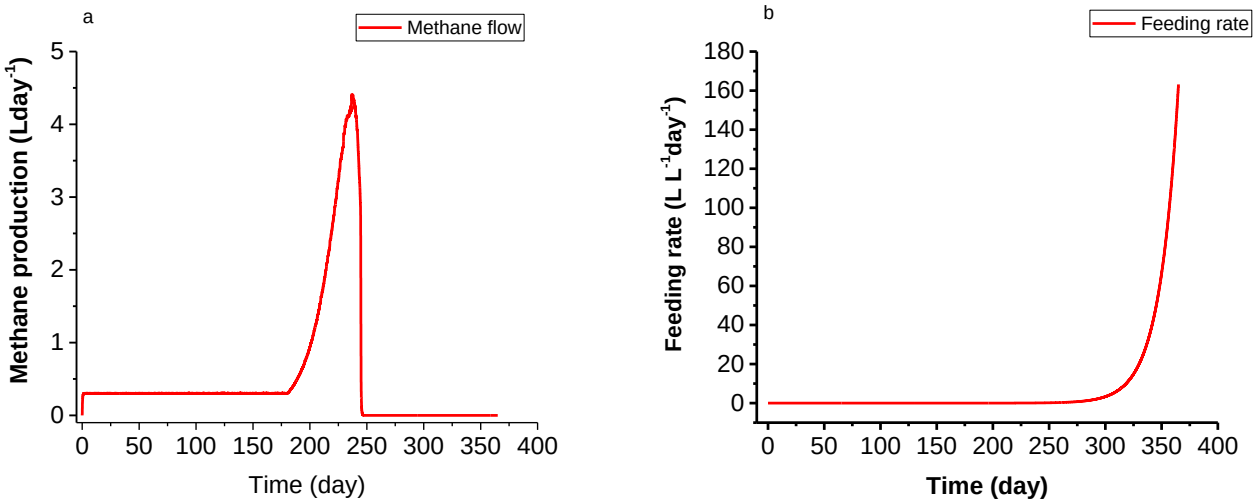

Figure 6.1 shows the methane flow rate (a) and feeding rate (b).

6.2.1.1 Maximum methane production and Hydraulic retention time at a varying slurry temperature.

The maximum methane production at various slurry temperature and loading rate for different feedstocks is shown in figure 6.2. It consists of 20 different points each corresponding to different digester (slurry) temperature of food waste, green waste and pig manure respectively. Using the MATLAB script, at the same slurry temperature, the maximum methane production rate estimated from the simulation of the MATLAB script is different for food waste, green waste, and pig manure. The result of the simulation shows that food has a higher biogas potential, compared to pig manure and green waste. The difference in the amount of methane produced from food waste, pig manure, and green waste is due the difference in their degradability see section 4.2.1, chapter 4. Food waste contains a higher amount of fats compared to pig manure and green waste. This agree with the report by Li et al [259], who reported higher methane production rate from feedstock with a high content of lipid. The significance of figure 6.2 and table 6.1 in practical terms is that it provides an estimation of the maximum methane production rate at specific slurry temperature. The maximum methane production rate increase as the temperature of the slurry approaches the optimum temperature for all substrates, figure 6.2. A further increase in the slurry temperature above the optimum mesophilic temperature, the maximum methane production began to decrease. This decrease in the maximum methane production rate at higher slurry temperature above the optimum mesophilic temperature is attributed to the cardinal temperature model used in describing the effects of temperature on the uptake rate of the microbial species [223, 224]. The cardinal temperature model defines an optimal temperature where microbial growth is rapid, a maximum and minimum temperature where there is a possibility of microbial growth [207]. The methanogenesis process is influenced by temperature, and the maximum uptake rate increase with temperature up to 35 ^{o}C, and lower when the temperature increase above 35 ^{o}C [207]. This

behaviour explains the decrease in the production of methane in the present study.

Figure 6.3 is the plot of the minimum hydraulic retention vs temperature (table 6.2) obtained from the simulation of the MATLAB script. It demonstrates the importance of hydraulic retention time as an operating parameter in anaerobic digester system. It can be deduced that when the slurry temperature is very low due to the impact of the environmental temperature, the hydraulic retention time requirement is increased to allow for enough time for the microorganism to utilise the feedstock in order to produce methane. The area inside the curve of the hydraulic retention time is considered safe for operating the anaerobic digester or the anaerobic digestion process in general. The importance of the hydraulic retention time could also be linked to the feed volume as well as the amount of organic matter added to the digester. Also, it helps in the sizing of the digester based on the feeding rate and the digester temperature [220]. As an illustration, in the degradation of pig manure at a slurry temperature of 296 K (23^{o}C). The minimum hydraulic retention time predicted by the 3R model is 13.55 days and the estimated organic loading rate is 0.8375 gCODm^{-3}d^{-1}. This means that the minimum hydraulic retention time cannot be lower than 13.55 days when pig manure is fed into the digester operating at 296 K (23 ^{o}C). Garfi et al [78] reported a hydraulic retention time of 75 days in a biogas digester treating pig manure at a slurry temperature of 23 ^{o}C, and organic loading rate of 0.6 kgVSm^{-3} d^{-1}. Therefore, the digester can operate effectively in cold weather condition by reducing the organic loading rate by 60 %. For food waste and green waste, the minimum hydraulic retention time predicted by the 3R model are 14.24 and 42.19 days respectively. Small-scale anaerobic digesters in cold climate are often not fed regularly [120]. This implies that there could be some flexibility in the amount of substrate fed into the digester. Thus, if the digester is not fed the previous day, the amount of feedstock fed into the digester the next day is double the amount of the previous day [120]. Doubling the amount of feedstock that is fed into the digester the next day increase the methane production. The feeding pattern was predicted by the 3R model, and this demonstrate that the

framework developed in the thesis can be used to give an insight on the feeding pattern for anaerobic digester system.

Generally, a reduced HRT has been recommended in the literature to maximum methane production [260, 261], improve the net energy production [261, 262], reduced the investment cost and the size of the digester [261]. However, in order to avoid washout of microbes and the failure of the anaerobic digestion process [261, 263], the generation time (or doubling time) of the slowest microbes must not be greater than the hydraulic retention time. This support the hypothesis of the present study which proposes that a particular minimum hydraulic retention time is required for process efficiency and stability. Figure 6.3 shows that the minimum hydraulic retention time increase as the temperature rose above 308 K (35 ^{o}C). Again, the possible explanation of this behaviour is that the cardinal temperature model applied predicted a decrease in the microbial activity when the temperature is above the optimal temperature [223, 224]. Therefore, the biochemical model (3R model) used in the present study predicted a higher minimum hydraulic retention time. The biochemical model predicted low methane production as the slurry temperature rose above the optimal temperature (35 ^{o}C). This is due to the increase in the amount of VFA and alkalinity in the digester as the hydraulic retention time increases.

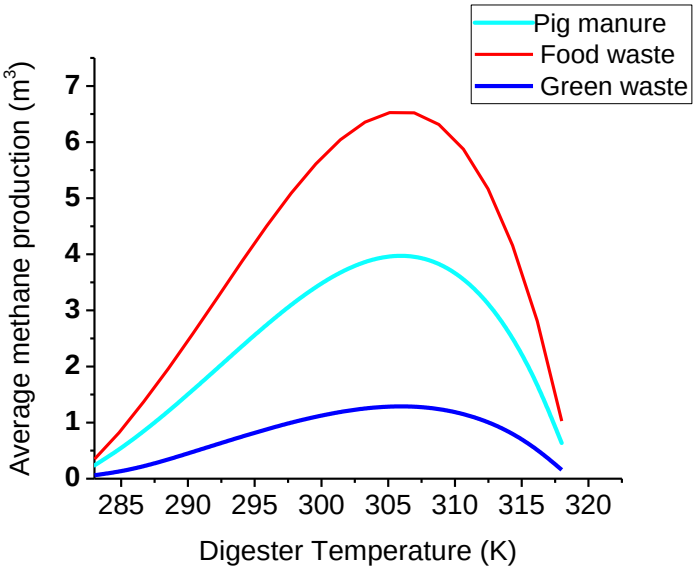

Figure 6.2 shows the maximum methane production for food waste, green waste and pig manure.

Table 6.1 shows the table of maximum methane production against digester operating temperature.

Digester Temperature (K)	Maximum Methane Production (L/L/day)		
	GW	FW	PM
283	0.061606	0.305828	0.222399
284.8421	0.120727	0.660603	0.443241
286.6842	0.201002	1.128938	0.727572
288.5263	0.298827	1.685652	1.065111
290.3684	0.409349	2.309405	1.442441
292.2105	0.527937	2.973493	1.842694
294.0526	0.650117	3.64869	2.248484
295.8947	0.771189	4.306579	2.643277
297.7368	0.886071	4.920273	3.011365
299.5789	0.98936	5.463807	3.337388
301.4211	1.075412	5.911303	3.605877
303.2632	1.13844	6.236299	3.800935
305.1053	1.172543	6.411265	3.905972
306.9474	1.171755	6.407214	3.903538
308.7895	1.130076	6.193297	3.77512
310.6316	1.041651	5.7363	3.500868
312.4737	0.90114	5.00003	3.059199
314.3158	0.704506	3.945667	2.426742
316.1579	0.450641	2.541406	1.582434
318	0.149089	0.828118	0.545124

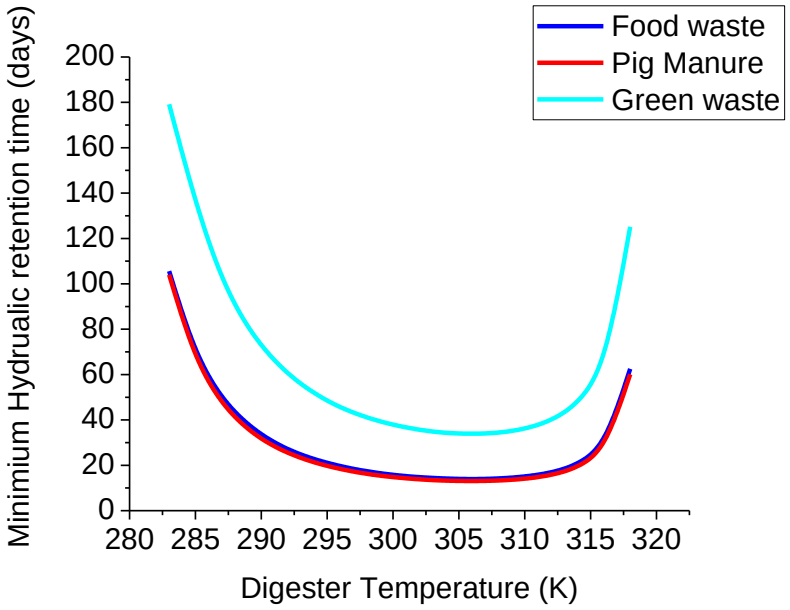

Figure 6.3 shows the minimum hydraulic retention time for specific temperature range.

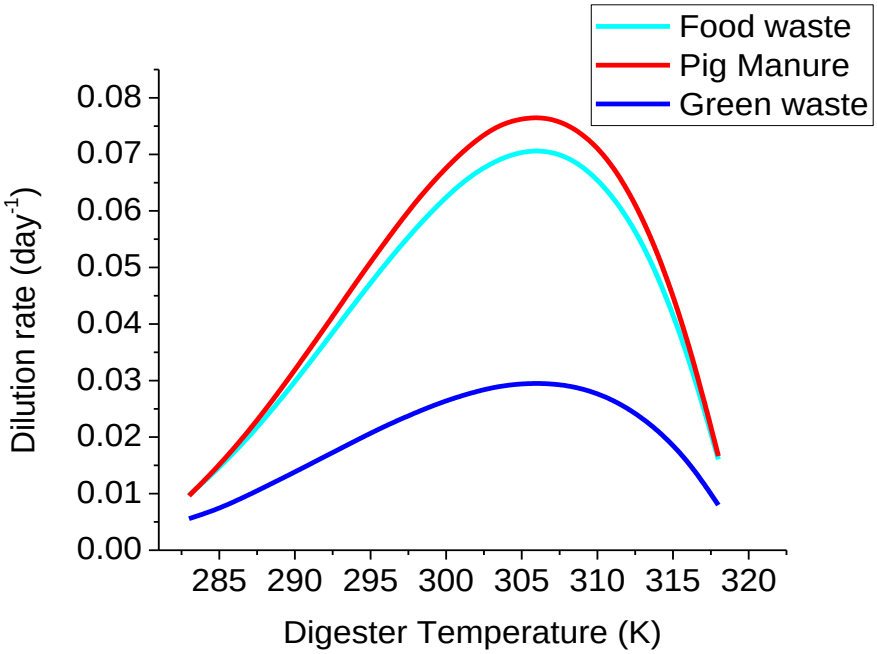

Figure 6.4 shows the maximum dilution rate as a function of slurry temperature methane flow rate (a) and feeding rate (b).

6.2.1.2 Operational Feeding strategy for mono-digestion

Here, the results of the simulation of the maximum performance of the anaerobic system before failure occurs is present. Figure 6.5 (a) and 6.5 (b) is the simulation of the digester system in Port Harcourt and Cuzco, respectively, and it is the plot of the methane production rate at varying dilution rate and slurry temperature. It shows in general that there are differences in the maximum feeding rate for different feedstock undergoing anaerobic degradation in different climates. The 3R model predicted that the maximum dilution rate of food waste in Port Harcourt and Cuzco are 0.062102 $days^{-1}$ and 0.0316 day^{-1}. Multiplying the dilution rate with the concentration of food waste, gives an estimate of the organic loading rate of 0.7671 $gCODm^{-3}day^{-1}$ and 0.389 $gCODm^{-3}day^{-1}$. The difference in the loading rate is due to the difference in the slurry temperature in the digester system in Port Harcourt and Cuzco, allowing greater organic loading rate in Port Harcourt before the process fails. The increase in daily ambient temperature in Port Harcourt, impacts positively on the digester slurry temperature, allowing a greater organic loading rate before process failure was reached. This is supported by the findings of Castano et al [209] which revealed that higher summer temperature allowed stable operation of the digester at a higher organic loading rate. In Cuzco, the result of the simulation found no difference in the optimal feeding rate estimated for food waste and pig manure (0.0316 day^{-1}) even though the methane produced differs (2.87 and 1.74 m^3). The difference in the methane produced is due to differences in the estimated organic loading rate of 0.389 $gCODm^{-3}day^{-1}$ and 0.358 $gCODm^{-3}day^{-1}$, as well as the difference in their degradability. Experimental analysis of the composition of the substrates found that food waste has a high COD compared to pig manure [243]. For green waste, the 3R model predicted the maximum dilution rate of 0.0396 day^{-1} and 0.0214 $days^{-1}$ when green waste is used as the substrate in the anaerobic digestion system in Port Harcourt and Cuzco. The corresponding organic loading rate of green waste in Port Harcourt and Cuzco is 0.663 gCOD m^{-3} day^{-1} and 0.356 gCOD m^{-3} day^{-1}. Similarly, the organic

loading rate of pig manure in Port Harcourt is 0.820 gCOD m^{-3} day^{-1} and 0.358 gCOD m^{-3} day^{-1} for Cuzco.

Figure 6.5 also depicts the range of safe operation of the digester to ensure the stability of the process. In Port Harcourt, the 3R model predicted that the digester has daily variation in the slurry temperature. It is possible to be safely operated at an organic loading rate below 0.767 gCOD m^{-3} day^{-1} , 0.82 gCOD m^{-3} day^{-1} and 0.663 gCOD m^{-3} day^{-1} for food waste, pig manure, and green waste respectively. Increasing the loading rate above this value, digester fails due to the washout of the microorganisms caused by an increase in hydraulic shock or increase in the organic content of the feed [253]. Figure 6.5 can be used as an operational template for meeting the demand of bio-methane produced in the rural bio-digester since it gives the digester operator the flexibility to load the digester based on the demand for bio-methane.

Going forward, the results of the simulation of biochemical model (3R model) to predict maximum feeding rate and methane production can be used to deduce in litres the maximum amount (volume) of slurry required to load the digester daily. The plastic bag diester used in the present study has a working volume of 2.5 m^3 [71]. Using food waste as the substrate, the model predicts a daily feeding of 0.0612 L L^{-1} day^{-1} in the digester system in Port Harcourt, and a daily feeding rate of 0.03155 L L^{-1} day^{-1} in Cuzco. Multiplying the values of the feeding rate by the working volume of the digester, the 3R model predicts that the daily volume of the slurry fed into the digester is 155 L day^{-1} in Port Harcourt, and 79 L day^{-1} in Cuzco. Similarly, for green waste, the maximum volumetric feeding rate at the dilution rate of 0.03959 $days^{-1}$ and 0.02137 $days^{-1}$ is 99 L day^{-1} and 53 L day^{-1}. The volumetric loading rate of pig manure in Cuzco is 79 L day^{-1} (0.03155 day^{-1}). The volumetric rate of the slurry feed into the digester in Cuzco in the present study is within the range volumetric loading rate (0.018-0.087 m^3) reported by Castano et al [209].

It should be noted that in the present study, a framework is developed that allows the prediction of the maximum organic loading rate for different

feedstocks required to maintain a stable digester operation in different locations. The digester system is simulated under variation of the daily slurry temperature, which is caused by the impact of changes in the weather condition such as ambient temperature, wind speed, solar radiation etc. The biochemical model (3R model) is simulated at constant loading rate for a period of time, then the feeding rate is increase until failure occurs. The maximum loading rate of the feedstock is estimated using the MATLAB code written in a script, the simulation estimates the methane production by varying the loading rate starting with a very lower value of the loading rate till an optimum value. While, the model developed in the present thesis is able to predict the maximum loading rate of the digester with daily variation in slurry temperature. It was unable to make a clear prediction or estimation of the loading rate requirement during the transition period between summer and winter period. Furthermore, there is a need for experimental validation of the results of the simulation since the present study is a model-based analysis of the safe operation of the household digester in a rural location.

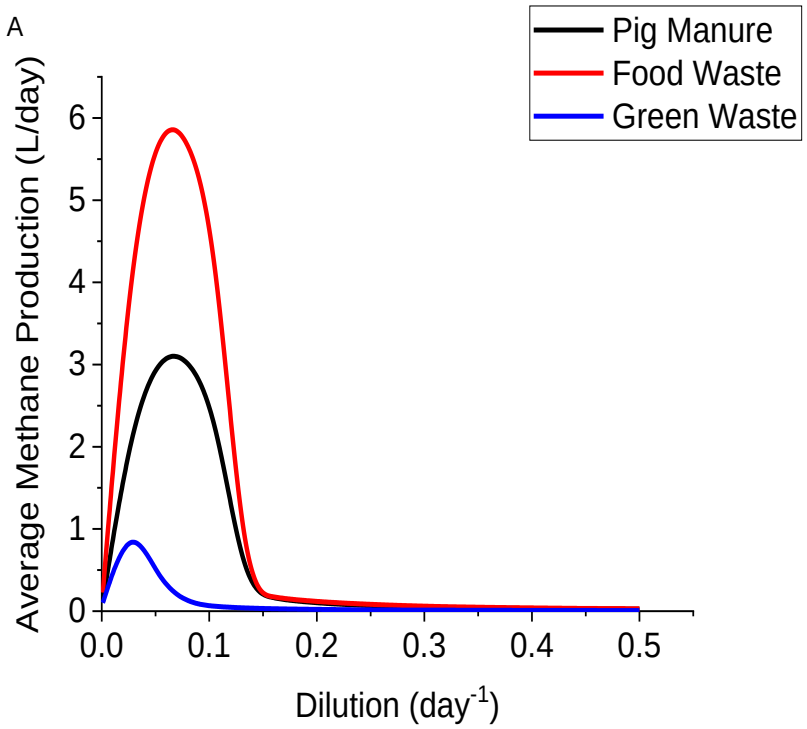

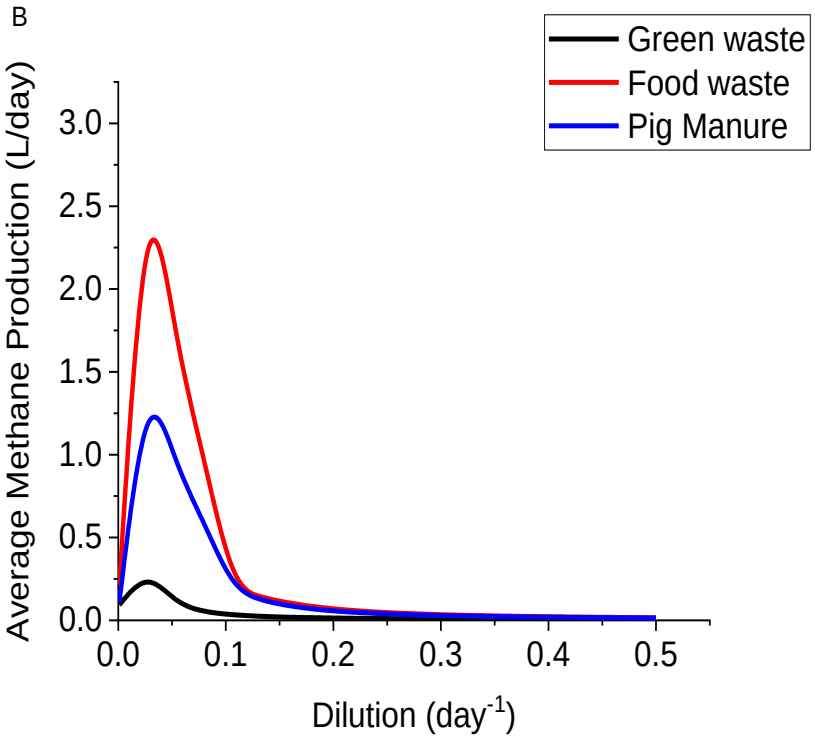

Figure 6.5 shows the plot of optimal dilution rate of the substrate in (A) Port Harcourt and (B) Cuzco

6.2.2 Co-digestion

Co-digestion of two or more substrates provides a balanced carbon to nitrogen ratio that ensures better process stability and promotes the activities of the methane producers [264]. However, there are instances of process failure due to overloading of the digester with high compound co-substrate, leading to increase organic acid production. In the present study, the result of the methane production and minimum hydraulic retention time for a co-digested mixture of the different substrate at different feed composition is shown in figure 6.6. Note that the methane production, and the minimum hydraulic retention time as shown in figure 6.6 can be represented in the same format as shown in figure 6.2. However, the number of different feed compositions makes this difficult to present and understand. The number of different feedstock combination is 21, and there are 20 different points simulated, each representing the slurry temperature or dilution rates.

6.2.2.1 Effect of feed composition and temperature on methane production

The impact of slurry temperature and different feed composition on the maximum methane production is presented. The 3R model predict the increase in the maximum methane production rate as the slurry temperature increase for a specific feed composition. And, at a specific slurry temperature changes in the feedstock ratio increases maximum methane production rate. In food waste and green waste co-digestion, the 3R model predicts that co-digestion of green waste (as the major substrate) with 5% of food waste increase the maximum methane production rate at constant slurry temperature. However, when food waste is used as the major substrate, and green waste is added at 5%, there is no significant improvement in the maximum methane production. The maximum methane production predicted by the model (3R model) for 95% green waste and 5% food waste is 1.32 m^3 compared to the predict of 0.98 m^3 for mono-digestion of green waste. Similarly, the 3R model predicted the maximum methane production for 95% food waste and 5% green waste is 5.36 m^3 against 5.47 m^3 for mono-digestion of food waste. Clearly, the model is predicting that addition of green waste to the substrate mix does not necessarily improve the methane production significantly, when food waste is the major substrate.

In the simulation of food waste and pig manure, the biochemical model (3R model) predict an increase in the maximum methane production rate when 5% of food waste is added to the slurry containing 95% of pig manure, and the methane flow increases as more food waste is added to the substrate mix. Again, when food waste is the major substrate, in the co-digestion feed, the maximum methane production rate increases slightly when 5% of pig manure is added. The maximum methane production rate becomes significant when the amount of pig manure added to the feed raise to 40%. Comparing the results of the maximum methane produced to the maximum methane produced in mono-digestion, co-digestion of different substrate increases the maximum methane production. The maximum methane production during the co-digestion of food waste and green waste at 10% concentration of co-

substrate is 5.51 m^3 (when food waste major substrate) and 3.69 m^3 (when pig manure is the major substrate). This is a 0.73% increase in the maximum methane production rate compared to mono-digestion of food waste, and 28.12% increase in the methane production rate compared to mono-digestion of pig manure. In the co-digestion of pig manure and green waste, the 3R model prediction is similar to the result of the co-digestion of food waste and green waste. The model reveals that mono-digestion of pig manure is much better, when pig manure is the major substrate in the feed. It is better to co-digested green waste (as major substrate) with pig manure.

The significance of the model prediction in a practical application is that it provides different scenarios for feeding that digester based on the intended desire or target of the digester operator. If the digester operator seeks to improve the amount of methane; the framework can be used to test different substrates combination or ratio that will improve the methane production. Mono-digestion of food waste is ideal for increasing the methane production rate, when food waste is the major substrate. For pig manure, co-digestion with more readily degradable food waste is ideal. Using green waste as a major substrate, co-digestion with food waste or pig manure will improve the methane production rate. If the operating condition or target of the digester is to ensure process stability and minimum souring of the digester, a co-digestion process is preferable compared to mono-digestion. Further, under the condition of low average slurry temperature in the digester due to seasonal changes in the weather condition, the model prediction of figure 6.6 provides an insight on the possible of co-digesting different substrates to enhance the digester methane production. At 13.53 ^oC (286.68 K), the 3R model predicts that the digester operator could either perform co-digestion of green waste and food waste at 60:30, when green waste is the major substrate to improve methane production or co-digestion of food waste and green waste at 60:30 (30% of green waste) to provide the carbon required to maintain the balance of nutrient to sustain microbial growth. The increase in methane production resulting from increase changes in the substrate ratio has been reported in the literature. Dennehy et al [265] found that the specific methane yield is the same when all three digesters are fed the same ratio of pig manure and food

waste (85:15) in the phase one of an experiment to investigate the impact of substrate ratio on methane production. Reducing the proportion of pig manure in the digester in phase two (63%) and three (40%) of the experiment increase the specific methane yield considerably. Co-substrate are broadly classified into carbohydrate, protein and lipid rich organic material, and it has been found that increasing the percentage of the lipid rich organic material in the substrate at high organic loading rate can have an antagonistic effect on the performance of the co-digestion process [266]. Silvestre et al [267] recorded more than 40% reduction in methane production, when the amount of grease added into the substrate (containing sewage sludge) increases from 27 to 37%. In addition to the increase in the methane production, the framework developed in the present study can aid the digester operator to (specific household anaerobic digester operator) identify the threshold for addition of co-substrate to reduce this antagonistic effect.

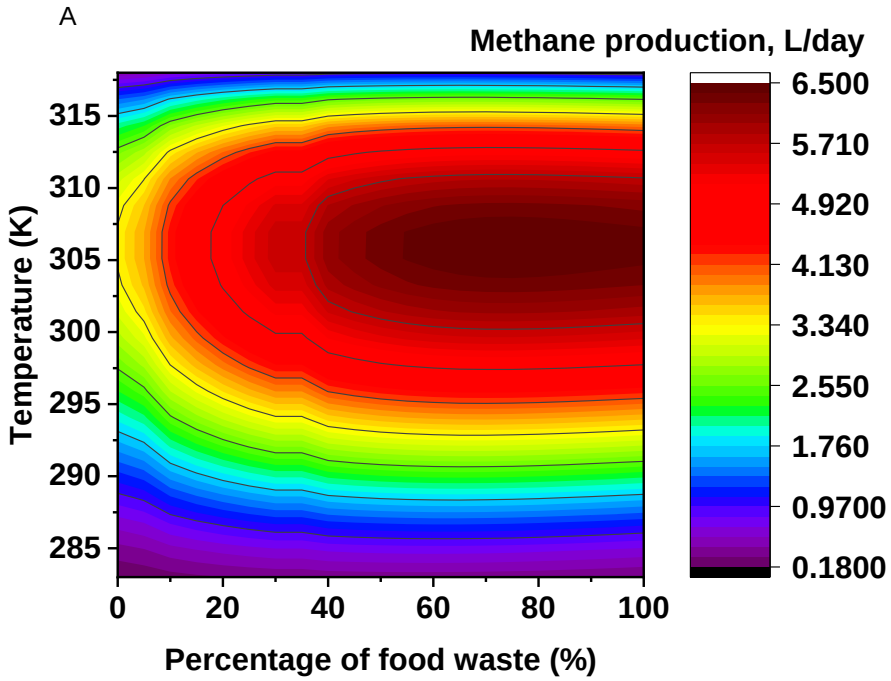

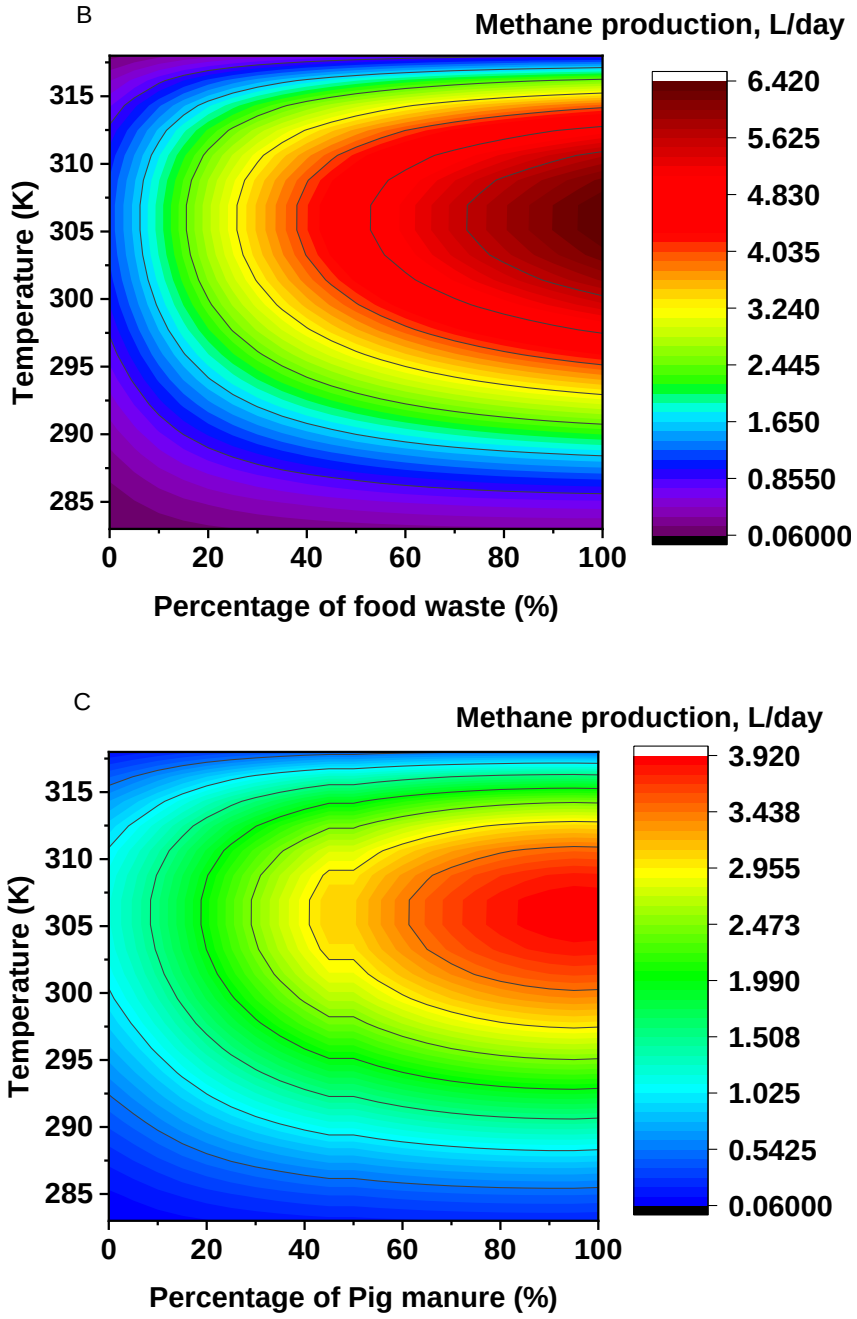

Figure 6.6 shows the maximum methane production at different feed composition (A) food waste and green waste, (B) food waste and Pig manure, (C) green waste and pig manure.

6.2.2.2 Effect of feed composition and temperature on the minimum hydraulic retention time

The simulation of the impact of different feed composition scenarios ad varying slurry temperature is presented in figure 6.7. The biochemical model

(3R model) predict a decrease in the minimum hydraulic retention time as the slurry temperature increase at constant feed composition. Also, at a specific slurry temperature, changes the relative percentage of each substrate in the feed stream reduces the minimum hydraulic retention time. For food waste and pig manure co-digestion, consisting of 80% pig manure and 20% food waste by volume, the 3R model predicts a minimum hydraulic retention time of 40.25 days when the average slurry temperature is 10 ^{o}C, and 11.71 days, when the average slurry temperature is doubled. The reduction in the minimum hydraulic retention time when the digester slurry temperature doubles is obvious, since it allows for an increase in the lipid rich organic content of the feed. However, at 10 ^{o}C, the 3R model predictions of the minimum hydraulic retention time is interesting. There is a slight decrease in the minimum hydraulic retention time, or it could be said that the minimum hydraulic retention time is within the same range. This is because increasing the percentage of food waste from 5% to 10%, the minimum hydraulic retention time decrease slightly from 42.30 days to 41.25 days. A further increase in the percentage of food waste from 25% to 35% reduced the minimum hydraulic retention time by 2.24%. One possible explanation of the model prediction is the addition of water to dilute the feedstock as the concentration of the co-substrate increase (food waste). Comparing the minimum hydraulic retention in the co-digestion process to mono-digestion process, the model predicts that co-digestion of two substrate allow for increasing organic loading. At 5% food waste and 95% pig manure, the minimum hydraulic retention time predicted by the model is 31.54 days against 56.37 days for mono-digestion of pig manure.

Also, the model predict that the minimum hydraulic retention can be reduced drastically or only slightly. This is the case for the co-digestion of food waste and green waste, where the estimated minimum hydraulic retention time reduced by 47.3% (110.75 days for mono-digestion of green waste and 58.30 days for co-digestion with food waste) when 5% of food waste is added to the substrate containing green waste. Increasing the relative amount of green waste in the feed containing food waste decreases the minimum hydraulic retention time slightly by 4.84 (64.34 days in mono-digestion of food waste

against 61.24 days for co-digestion of food waste 95%, and green waste 5%). Similar, the model prediction of the minimum hydraulic retention for pig manure and green waste is the same as the prediction for the co-digestion of food waste and green waste. 58.30 days for mono-digestion of pig manure, and 55.50 days when pig manure is co-digested with 5% of green waste, 110.77 days for mono-digestion of green waste against 64.34 days for co-digestion mixture consists of 5% pig manure.

The above results predicted by the model reveals that increasing the relative amount of co-substrate in the co-digestion feed mix allow for increase microbial activity in the case of 95% green waste and 5% food waste, due to availability of readily degradable organic matter in the food waste, or the addition of carbon to balance the nutrient required for microbial growth. Fjotoft et al [268] reported a decrease in the hydraulic retention time from 30.9 days to 25.9 days, when fish silage is co-digested with cow slurry. The fish silage was added for two reason: In the first instance, to balance the carbon to nitrogen ratio in the feed mix, since the cow slurry consist of dry organic matter and as such has a low pH. Secondly, to increase the methane production. Also, fish silage has high content of fats and protein, it is more degradable and can cause instability in the digestion process, which could lead to break down of the digester, and there is a recommended limit on the amount of fish silage that can be used as co-substrate [268]. The results of Fjotoft et al [268] agree with the prediction of the model which demonstrate the impact of co-digestion on the methane production and the need to understand the limitations in the operation of the digester.

A

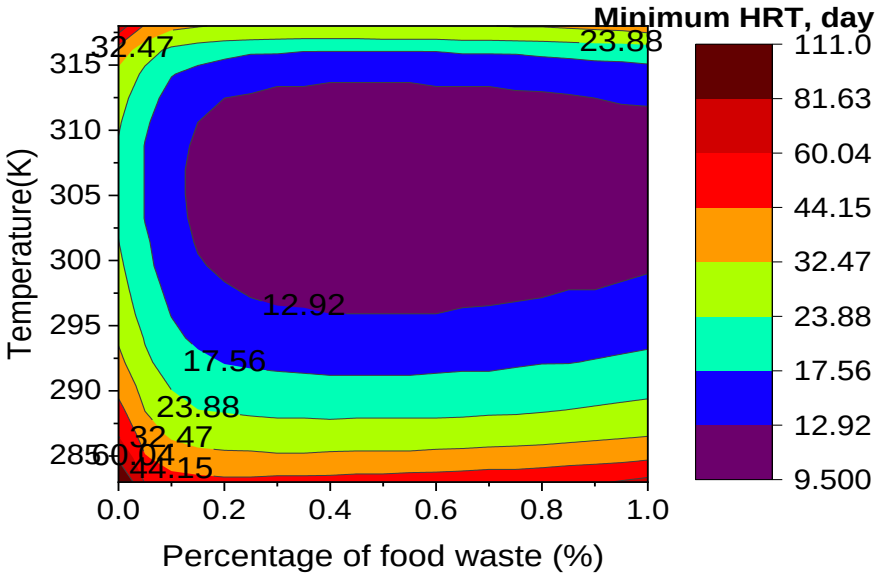
Minimum HRT, day
111.0
81.63
60.04
44.15
32.47
23.88
17.56
12.92
9.500
32.47
23.88
12.92
17.56
23.88
32.47
60.04
44.15
315
310
305
300
295
290
285
0.0
0.2
0.4
0.6
0.8
1.0
Temperature(K)
Percentage of food waste (%)

B

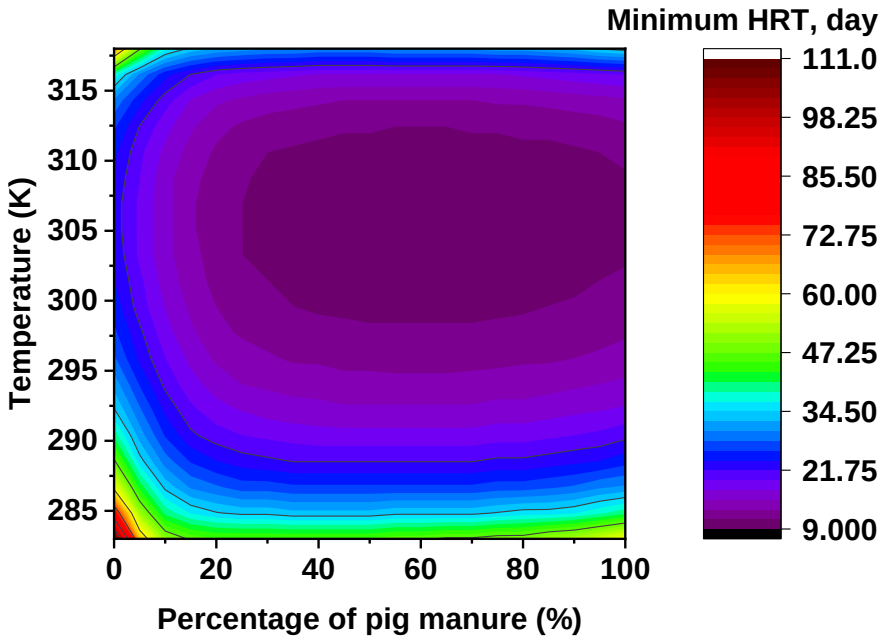
Minimum HRT, day
111.0
98.25
85.50
72.75
60.00
47.25
34.50
21.75
9.000
315
310
305
300
295
290
285
0
20
40
60
80
100
Temperature (K)
Percentage of pig manure (%)

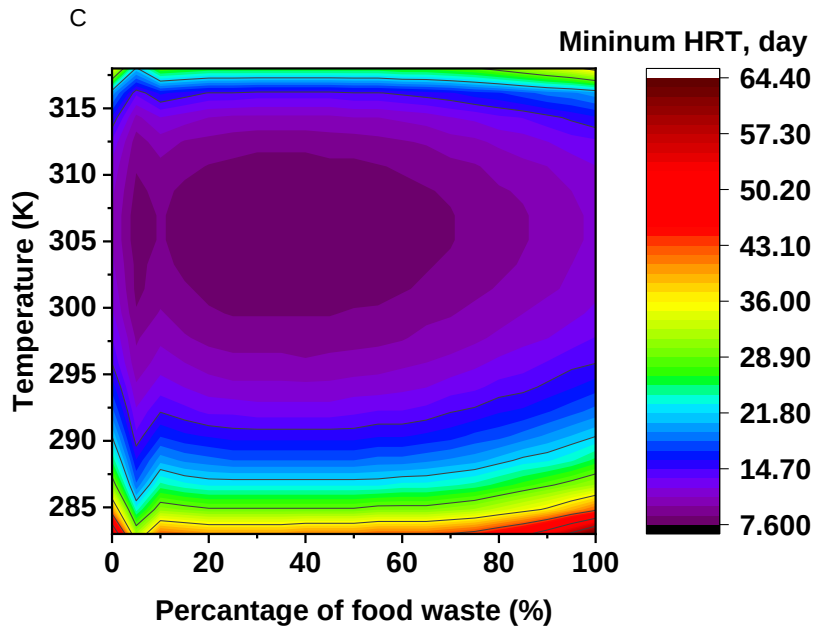

Figure 6.7 shows the minimum hydraulic retention time at different feed composition (A) food waste and green waste, (B) green waste and pig manure, (C) food waste and Pig manure.

6.2.2.3 Operational feeding strategy for co-digestion processes

In the section, the maximum methane production rate at different dilution rates and feed compositions before the failure of the digester in Cuzco and Port Harcourt respectively are presented in figure 6.8 and 6.9. As has been mentioned, the simulation of the 3R model, start by loading 0.0025 L L^{-1} day^{-1} of substrate over a period of days (180) to achieve steady state and gradually the loading rate is increased by 1.0025 L L^{-1} day^{-1} until failure occurs. The feeding rate at the point of failure is obtained from MATLAB script, and a sensitivity analysis is performed to vary the feeding rate between a lower bound and an upper bound to estimate the maximum organic loading rate and methane production at specific composition of the feedstock and average slurry temperature of the digester.

In Cuzco, Peru with an average slurry temperature of 295 K (19.9 ^{o}C), figure 6.8 shows the changes in the maximum dilution rate and organic loading rate as the volumetric load of co-substrate increase to 20 %. Above 20 %, the

organic loading rate changes, while the dilution rate remains the constant. In the co-digestion of green waste and food waste, the organic loading rates predicted by the 3R model when the volume of food waste in the feed increase by 5 %,10 %, 15 %, and 20 % are 0.283, 0.378, 0.417 and 0.496 g COD m^3 day^{-1} respectively. Above 20 %, the dilution rate remains the same at 0.0354 day^{-1}, however, the organic loading rate changes due to the increase in the concentration of food waste. Similarly, in the co-digestion of pig manure and green waste, the organic loading rate and feeding rate predicted by the 3R model is in the range of 0.20-0.4833 g COD m^3 day^{-1} and 0.0151-0.0314 day^{-1} respectively, when the concentration of pig manure in the feed increase from 5 - 25 %. Above 25 %, the maximum dilution rate remains constant, while the organic loading rate changes. In the co-digestion of food waste and pig manure, the model predict a constant maximum dilution rate of 0.0333 day^{-1} for different composition of the feedstock, however, the organic loading rate changes due to the increase in the concentration of food waste in the feed (0.380-0.395 g COD m^3 day^{-1}).

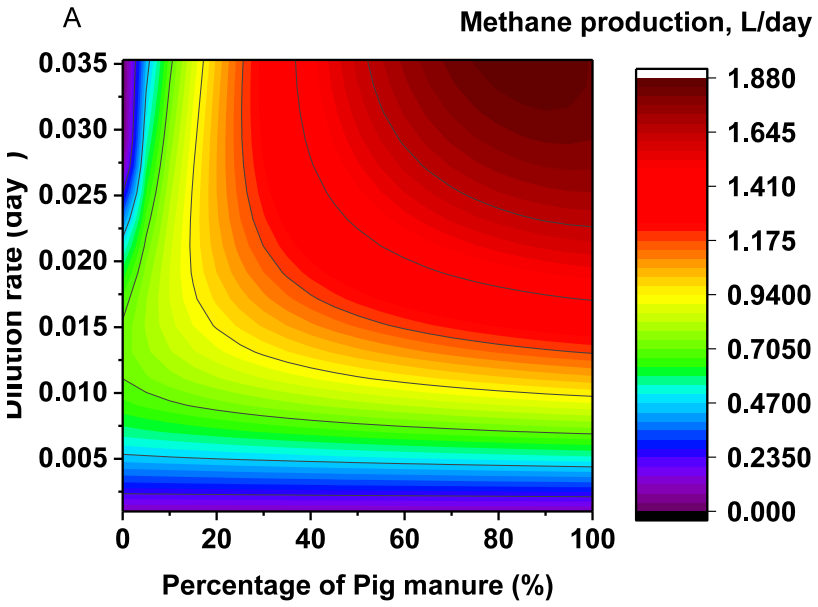

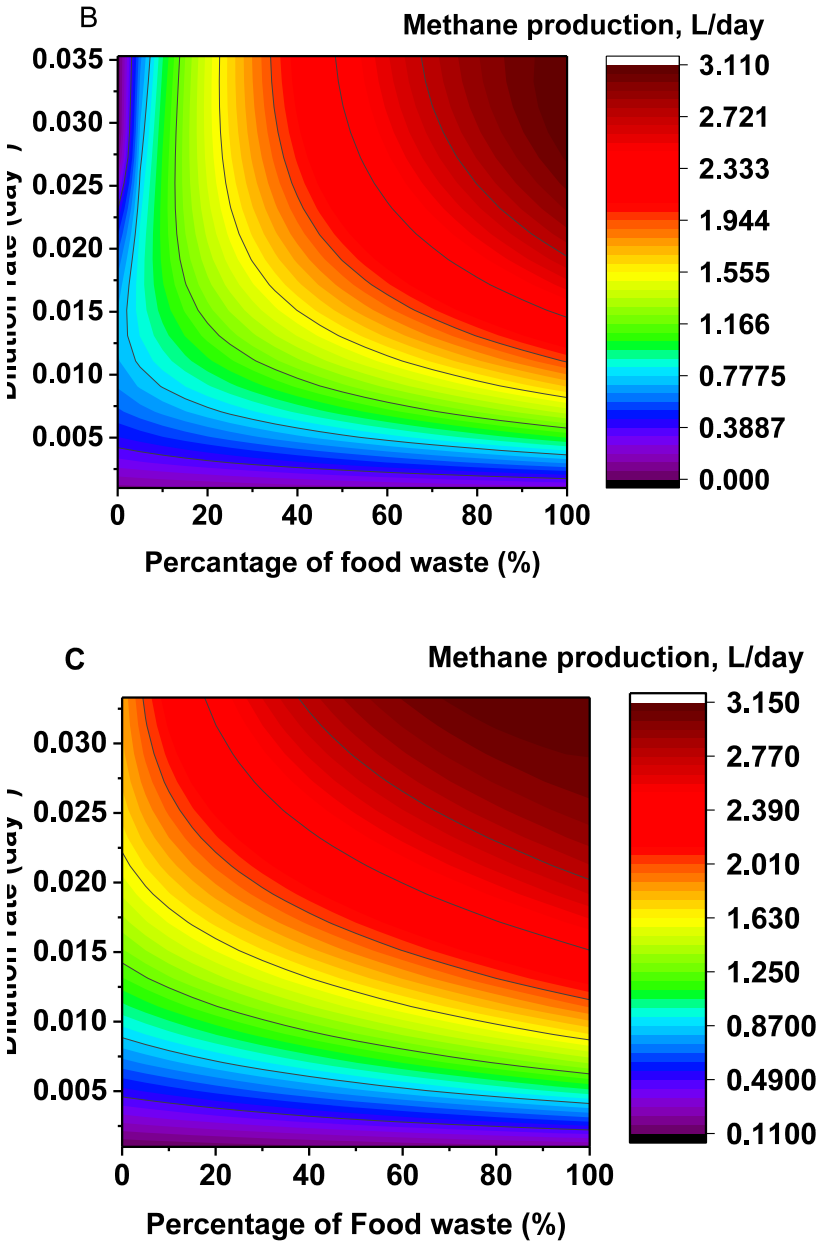

Figure 6.8 shows the maximum methane production different feed composition in the digester installed In Cuzco (A) green waste and Pig manure (B) green waste and food waste, (C) food waste and Pig manure.

In Port Harcourt, with an average digester slurry temperature of 306 K, the model (3R) predicts the maximum methane production as a function of the mix ratio of the substrates in the feeds and is presented in figure 6.9. In the co-digestion of green waste and pig manure, the organic loading rate is in the range of 0.467-0.812 g COD m^3 day^{-1} when the percentage of pig manure in substrate increase from 5 – 25 %. Above 25 %, the organic loading rate

increases, while the dilution rate remains the same at 0.056 day^{-1}. Similar behaviour was observed in the co-digestion of food waste and pig manure. The organic loading rate increased from 0.913 -1.25 g COD m^3 day^{-1} when the percentage of food waste is increased from 5 – 30 %. Increasing the composition of food waste in the substrate mix from 35 -50 %, the maximum dilution rate increased up to 0.110 day^{-1} and then remained constant. For co-digestion of green waste and food waste, the maximum organic loading rate predicted by the 3R model is 0.567 - 1.18 g COD m^3 day^{-1} when the percentage of food waste in the substrate mix is between 5 – 25 %. The maximum dilution rate is constant when the percentage of food waste in the substrate is in the range 30 - 40 %. When the percentage of food waste in the substrate is increased above 40 %, the maximum dilution rate predicted by the 3R model increased, and then it remained constant at 0.7702 day^{-1} when the percentage of food waste in the substrate is between 45 – 50 %. The maximum dilution rate for green waste and pig manure co-digestion is 0.056 day^{-1}, for food waste and pig manure, the maximum 0.110 day^{-1} for food waste and pig manure, and 0.077 day^{-1} for food waste and green waste. Therefore, it means that the digester is best operated below this threshold of dilution rates, to ensure process stability.

In the present study, the changes hydraulic stock load involves changes in the concentration of substrate as well as changes in the feeding rate. Therefore, it is expected that there will be a change in the maximum dilution rate as the total solid content of the substrate increases due to the addition of the co-substrate. However, the model predicted that the maximum dilution rate is the same when the percentage of co-substrate is above 20% or 25% suggesting that there is an increase in amount of water used in diluting the substrate before feeding.

It is interesting to note that this difference in the organic loading rate of the feedstock when the concentration of the co-substrate increase during anaerobic co-digestion, supports the hypothesis that the operation condition (organic loading rate) with respect to the feedstock used is different for the

same location (Port Harcourt in Nigeria, and Cuzco, in Peru). Additionally, the maximum organic loading rate of the same feedstock in a different location is different due to the difference in the slurry temperature. The organic loading rate of food waste and green waste is higher in Port Harcourt, Nigeria than in Cuzco, Peru. Thus, supporting the hypothesis that in a different location; the operation parameters (organic loading rate) of the digester is different, and it can be attributed to the difference in the operating temperature and the environment temperature. Also, the significance of the result is that it agrees with various results in the literature that suggests the lowering of organic loading rate during the winter and increasing the organic rate during the summer [71]. Port Harcourt and Cuzco represent two extremes of weather condition. While the latter has a low ambient temperature with a high daily fluctuation, the former has a high ambient temperature with minimal daily fluctuation. Also, figures 6.8 and 6.9, with table 6.2 and 6.3, can assist the digester operator in making a decision such as the estimate of the organic loading rate and the mixing ratio of the feedstock that required to produce a specific amount of methane.

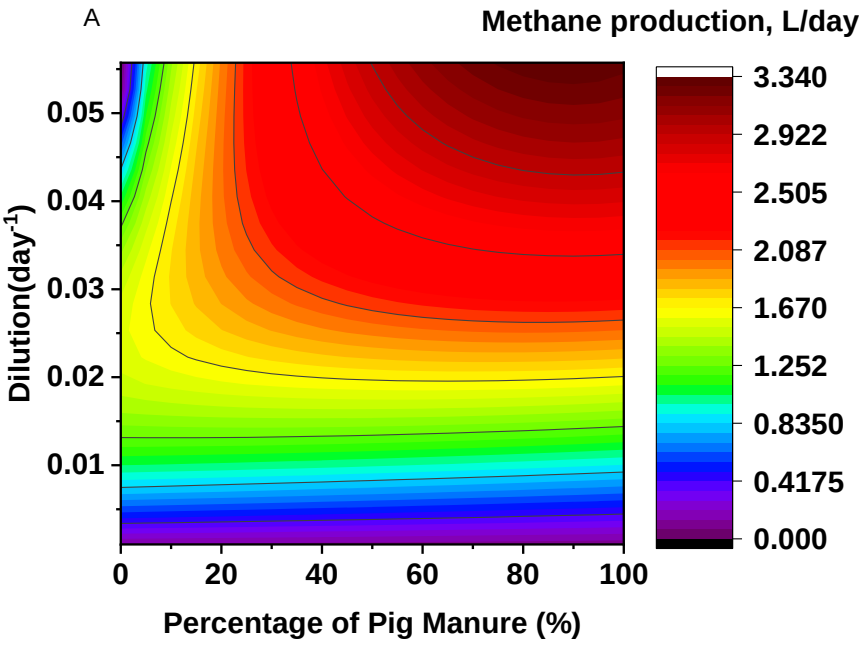

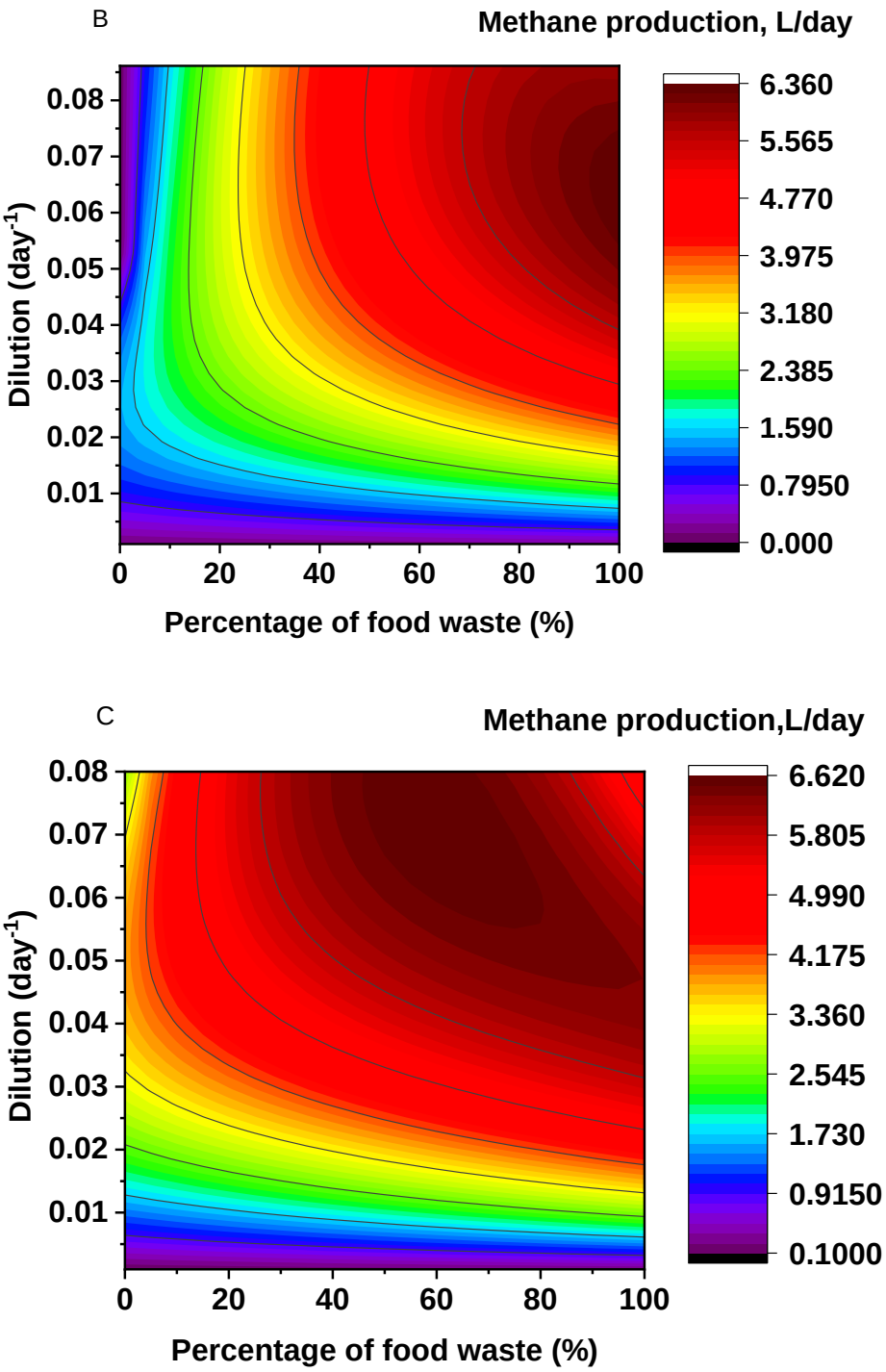

Figure 6.9 shows the maximum methane production for different feed composition in for the digester installed in Port Harcourt (A) green waste and Pig manure (B) green waste and food waste, (C) food waste and Pig manure.

Note that table 6.3 (a-c) shows that data used in plotting figure 6.9, and table 6.4 (a-c) shows the data used in plotting figures 6.8. Table 6.3 (a) is the data obtained from the simulation of co-digestion of pig manure and green waste, showing the variation of the composition of pig manure in the substrate at different dilution rate. Table 6.3 (b) is the data obtained from the simulation of co-digestion of food waste and pig manure, and table 6.3(c) is the data used in plotting figure 6.9 (B).

Table 6.2 shows the minimum hydraulic retention time versus the digester operating temperature.

Digester Temperature (K)	Minimum hydraulic retention time (day)		
	Food waste	Green waste	Pig manure
283	104.0455	179.19424	105.614
284.8421	68.77652	138.94883	71.22011
286.6842	49.48575	106.14207	51.75766
288.5263	37.80183	84.38179	39.93369
290.3684	30.05204	69.81333	31.90558
292.2105	24.86358	59.21863	26.39711
294.0526	21.09034	51.50016	22.5031
295.8947	18.43316	45.69021	19.66793
297.7368	16.43541	41.55927	17.53635
299.579	15.0242	38.37169	16.03061
301.4211	14.01091	36.1425	14.94945
303.2632	13.32925	34.55602	14.29324
305.1053	13.06597	33.87345	13.94121
306.9474	13.06597	33.87345	13.94121
308.7895	13.46288	34.7288	14.36471
310.6316	14.36471	36.87079	15.40358
312.4737	16.19132	40.94207	17.27592
314.3158	19.76627	48.75082	21.09034
316.1579	28.02522	65.4304	29.75376
318	60.11136	125.13177	62.55831

Table 6.3 (a) shows the table of the maximum methane production against dilution rate at varying pig manure concentration.

Dilution rate (day^{-1})	Maximum methane production at varying composition of pig manure (L/L/day)																				
	0	5	10	15	20	25	30	35	40	45	50	55	60	65	70	75	80	85	90	95	100
0.001	0.132	0.131	0.129	0.127	0.125	0.123	0.122	0.12	0.118	0.116	0.114	0.113	0.111	0.109	0.107	0.105	0.104	0.102	0.1	0.098	0.096
0.004	0.496	0.49	0.485	0.479	0.473	0.468	0.462	0.456	0.451	0.445	0.439	0.433	0.428	0.422	0.416	0.41	0.404	0.398	0.393	0.387	0.381
0.007	0.802	0.796	0.789	0.782	0.775	0.768	0.761	0.754	0.747	0.739	0.732	0.724	0.717	0.709	0.701	0.693	0.685	0.677	0.669	0.661	0.652
0.0101	1.054	1.05	1.045	1.04	1.034	1.029	1.023	1.016	1.01	1.003	0.996	0.989	0.981	0.974	0.966	0.957	0.949	0.94	0.93	0.921	0.911
0.0131	1.254	1.255	1.255	1.255	1.254	1.252	1.25	1.247	1.244	1.239	1.235	1.23	1.224	1.217	1.21	1.203	1.195	1.186	1.177	1.168	1.157
0.0162	1.404	1.415	1.424	1.432	1.438	1.443	1.447	1.449	1.451	1.451	1.45	1.449	1.446	1.442	1.438	1.432	1.426	1.419	1.41	1.401	1.391
0.0192	1.507	1.532	1.554	1.573	1.589	1.603	1.615	1.626	1.634	1.64	1.645	1.648	1.65	1.65	1.649	1.646	1.642	1.637	1.63	1.622	1.612
0.0222	1.564	1.609	1.648	1.681	1.711	1.737	1.76	1.779	1.796	1.81	1.821	1.831	1.838	1.843	1.845	1.846	1.845	1.842	1.837	1.83	1.821
0.0253	1.578	1.649	1.709	1.761	1.807	1.847	1.882	1.912	1.939	1.962	1.981	1.997	2.01	2.02	2.028	2.032	2.035	2.034	2.031	2.025	2.017
0.0283	1.55	1.655	1.742	1.816	1.88	1.936	1.985	2.028	2.065	2.098	2.125	2.149	2.169	2.185	2.197	2.206	2.212	2.214	2.213	2.208	2.2
0.0314	1.481	1.63	1.749	1.849	1.934	2.007	2.071	2.128	2.177	2.219	2.256	2.288	2.315	2.337	2.355	2.368	2.377	2.382	2.383	2.379	2.371
0.0344	1.375	1.58	1.736	1.863	1.971	2.063	2.143	2.213	2.275	2.328	2.375	2.415	2.449	2.477	2.5	2.518	2.531	2.538	2.541	2.538	2.53
0.0374	1.231	1.507	1.705	1.862	1.993	2.105	2.202	2.287	2.361	2.426	2.482	2.53	2.572	2.607	2.635	2.657	2.673	2.683	2.687	2.685	2.677
0.0405	1.052	1.419	1.661	1.85	2.005	2.137	2.251	2.35	2.437	2.512	2.578	2.635	2.684	2.725	2.759	2.786	2.805	2.817	2.823	2.821	2.811
0.0435	0.84	1.32	1.608	1.828	2.007	2.159	2.29	2.403	2.503	2.59	2.665	2.731	2.787	2.834	2.873	2.904	2.926	2.941	2.947	2.944	2.933
0.0466	0.594	1.217	1.551	1.8	2.003	2.174	2.321	2.449	2.56	2.658	2.743	2.817	2.881	2.934	2.978	3.012	3.037	3.053	3.06	3.057	3.043
0.0496	0.319	1.117	1.491	1.768	1.993	2.182	2.345	2.487	2.61	2.719	2.813	2.895	2.965	3.024	3.073	3.111	3.139	3.156	3.162	3.158	3.141
0.0526	0.068	1.023	1.431	1.734	1.979	2.186	2.363	2.518	2.653	2.771	2.875	2.964	3.041	3.106	3.159	3.2	3.23	3.248	3.254	3.247	3.227
0.0557	0.003	0.939	1.374	1.699	1.962	2.184	2.376	2.543	2.689	2.817	2.929	3.026	3.109	3.179	3.236	3.281	3.312	3.331	3.335	3.326	3.301

Table 6.3 (b) shows the table of the maximum methane production against dilution rate and varying feedstock composition.

Dilution rate (day^{-1})	Maximum Methane production at varying concentration of food waste (L/L/day)																				
	0	5	10	15	20	25	30	35	40	45	50	55	60	65	70	75	80	85	90	95	100
0.001	0.116	0.122	0.128	0.133	0.139	0.145	0.151	0.157	0.163	0.169	0.175	0.181	0.1869	0.193	0.199	0.205	0.211	0.217	0.223	0.228	0.234
0.004	0.455	0.478	0.501	0.524	0.547	0.569	0.592	0.615	0.638	0.661	0.683	0.706	0.729	0.752	0.775	0.797	0.82	0.843	0.866	0.888	0.911
0.007	0.776	0.815	0.853	0.892	0.93	0.968	1.006	1.044	1.082	1.12	1.158	1.196	1.2338	1.272	1.309	1.347	1.385	1.423	1.461	1.498	1.536
0.0101	1.08	1.133	1.186	1.238	1.29	1.342	1.394	1.446	1.498	1.549	1.601	1.652	1.7037	1.755	1.806	1.857	1.908	1.959	2.01	2.061	2.112
0.0131	1.366	1.433	1.499	1.564	1.63	1.694	1.759	1.823	1.887	1.951	2.014	2.078	2.1408	2.204	2.267	2.329	2.392	2.454	2.517	2.579	2.641
0.0162	1.635	1.714	1.793	1.871	1.948	2.025	2.101	2.176	2.251	2.326	2.4	2.474	2.5473	2.62	2.693	2.766	2.838	2.911	2.983	3.054	3.126
0.0192	1.886	1.979	2.07	2.16	2.248	2.335	2.422	2.507	2.592	2.676	2.76	2.843	2.9251	3.007	3.088	3.169	3.25	3.33	3.41	3.49	3.569
0.0222	2.121	2.227	2.33	2.43	2.529	2.627	2.723	2.818	2.911	3.004	3.095	3.186	3.276	3.365	3.454	3.542	3.629	3.715	3.802	3.887	3.972
0.0253	2.34	2.458	2.573	2.684	2.793	2.9	3.005	3.108	3.21	3.31	3.408	3.506	3.6017	3.697	3.791	3.884	3.976	4.068	4.159	4.249	4.338
0.0283	2.542	2.674	2.8	2.922	3.041	3.157	3.27	3.38	3.489	3.595	3.699	3.802	3.9036	4.003	4.102	4.199	4.295	4.39	4.483	4.576	4.667
0.0314	2.729	2.873	3.012	3.144	3.273	3.397	3.517	3.635	3.749	3.861	3.971	4.078	4.1831	4.286	4.388	4.487	4.585	4.682	4.777	4.87	4.963
0.0344	2.9	3.058	3.208	3.352	3.489	3.621	3.749	3.873	3.993	4.109	4.223	4.334	4.4416	4.547	4.65	4.751	4.85	4.947	5.041	5.134	5.225
0.0466	3.432	3.654	3.857	4.043	4.216	4.379	4.531	4.675	4.811	4.94	5.062	5.178	5.2883	5.393	5.492	5.585	5.674	5.757	5.836	5.909	5.978
0.0496	3.528	3.769	3.986	4.184	4.366	4.536	4.694	4.842	4.981	5.112	5.234	5.35	5.4584	5.56	5.656	5.745	5.828	5.904	5.975	6.04	6.098
0.0526	3.61	3.871	4.103	4.313	4.505	4.681	4.845	4.997	5.138	5.27	5.393	5.507	5.6135	5.712	5.803	5.886	5.963	6.031	6.093	6.147	6.194
0.0557	3.678	3.961	4.209	4.431	4.632	4.815	4.984	5.14	5.284	5.416	5.539	5.651	5.7546	5.849	5.935	6.012	6.08	6.14	6.191	6.232	6.265
0.0587	3.733	4.038	4.303	4.537	4.748	4.939	5.113	5.272	5.417	5.551	5.672	5.783	5.8824	5.972	6.052	6.121	6.181	6.23	6.269	6.297	6.314
0.0618	3.773	4.104	4.386	4.633	4.854	5.052	5.231	5.393	5.541	5.674	5.794	5.902	5.9977	6.082	6.155	6.216	6.266	6.303	6.329	6.342	6.341
0.0648	3.801	4.158	4.459	4.719	4.95	5.155	5.339	5.505	5.653	5.786	5.905	6.01	6.1011	6.179	6.245	6.297	6.336	6.361	6.372	6.367	6.347
0.0739	3.804	4.255	4.616	4.92	5.182	5.409	5.608	5.782	5.934	6.065	6.177	6.27	6.3458	6.403	6.443	6.463	6.465	6.446	6.405	6.34	6.247
0.077	3.78	4.266	4.65	4.969	5.241	5.476	5.68	5.857	6.01	6.14	6.249	6.338	6.4074	6.457	6.487	6.496	6.484	6.448	6.388	6.299	6.177
0.08	3.744	4.268	4.675	5.01	5.293	5.536	5.744	5.924	6.077	6.206	6.312	6.397	6.4599	6.501	6.521	6.518	6.491	6.439	6.357	6.243	6.09

Table 6.3 (c) shows the table of the maximum methane production against dilution rate and feedstock composition (Food waste and green waste)

Dilution rate (day^{-1})	Maximum methane production at varying composition of food waste (L/L/day)																				
	0	5	10	15	20	25	30	35	40	45	50	55	60	65	70	75	80	85	90	95	100
0.001	0.11056	0.117	0.123	0.129	0.135	0.142	0.148	0.154	0.16	0.166	0.173	0.179	0.185	0.191	0.197	0.203	0.21	0.216	0.222	0.228	0.234
0.004	0.41901	0.444	0.469	0.494	0.518	0.543	0.568	0.592	0.617	0.642	0.666	0.691	0.715	0.74	0.764	0.789	0.813	0.838	0.862	0.887	0.911
0.007	0.68612	0.73	0.774	0.818	0.861	0.904	0.947	0.99	1.032	1.074	1.117	1.159	1.201	1.243	1.285	1.327	1.369	1.411	1.453	1.494	1.536
0.0101	0.91227	0.977	1.041	1.104	1.166	1.228	1.289	1.349	1.409	1.469	1.528	1.587	1.646	1.705	1.763	1.822	1.88	1.938	1.996	2.054	2.112
0.0131	1.09787	1.187	1.272	1.355	1.437	1.517	1.596	1.674	1.751	1.828	1.903	1.979	2.054	2.128	2.202	2.276	2.349	2.423	2.496	2.568	2.641
0.0253	1.44335	1.677	1.877	2.058	2.227	2.386	2.538	2.685	2.827	2.965	3.1	3.232	3.361	3.489	3.615	3.739	3.861	3.982	4.102	4.22	4.338
0.0283	1.43256	1.723	1.961	2.171	2.363	2.543	2.714	2.877	3.034	3.186	3.334	3.478	3.619	3.757	3.893	4.027	4.158	4.288	4.416	4.542	4.667
0.0314	1.38374	1.743	2.022	2.262	2.479	2.68	2.869	3.048	3.22	3.385	3.546	3.701	3.853	4	4.145	4.287	4.427	4.564	4.699	4.832	4.963
0.0344	1.29726	1.74	2.063	2.335	2.577	2.799	3.006	3.201	3.387	3.565	3.737	3.902	4.063	4.22	4.373	4.522	4.668	4.811	4.952	5.09	5.225
0.0435	0.81606	1.63	2.095	2.464	2.78	3.063	3.321	3.56	3.785	3.997	4.198	4.39	4.574	4.751	4.921	5.086	5.245	5.398	5.547	5.692	5.832
0.0496	0.31546	1.508	2.063	2.492	2.854	3.174	3.463	3.729	3.975	4.206	4.424	4.629	4.825	5.01	5.187	5.357	5.518	5.673	5.821	5.963	6.098
0.0526	0.06735	1.444	2.038	2.493	2.876	3.213	3.517	3.795	4.051	4.291	4.515	4.726	4.926	5.115	5.294	5.464	5.625	5.779	5.924	6.063	6.194
0.0557	0.003	1.38	2.007	2.488	2.891	3.244	3.56	3.849	4.115	4.362	4.593	4.809	5.012	5.203	5.383	5.553	5.714	5.865	6.007	6.14	6.265
0.0587	8.14E-04	1.318	1.974	2.476	2.897	3.265	3.594	3.894	4.168	4.422	4.658	4.878	5.084	5.277	5.457	5.626	5.784	5.932	6.069	6.197	6.314
0.0618	8.14E-04	1.26	1.938	2.46	2.898	3.279	3.62	3.928	4.211	4.471	4.712	4.935	5.143	5.336	5.516	5.684	5.838	5.981	6.113	6.233	6.341
0.0648	8.45E-04	1.206	1.901	2.44	2.892	3.286	3.637	3.954	4.243	4.509	4.754	4.98	5.189	5.383	5.561	5.726	5.877	6.014	6.138	6.249	6.347
0.0678	8.74E-04	1.156	1.863	2.416	2.881	3.285	3.646	3.971	4.266	4.537	4.785	5.013	5.223	5.416	5.593	5.754	5.9	6.031	6.147	6.247	6.333
0.0709	9.00E-04	1.11	1.825	2.389	2.865	3.279	3.648	3.98	4.281	4.555	4.806	5.036	5.246	5.438	5.611	5.768	5.909	6.032	6.139	6.228	6.299
0.077	9.45E-04	1.028	1.748	2.328	2.82	3.25	3.632	3.975	4.285	4.565	4.82	5.051	5.259	5.446	5.613	5.76	5.886	5.992	6.077	6.139	6.177
0.08	9.62E-04	0.991	1.71	2.294	2.792	3.228	3.615	3.962	4.275	4.558	4.813	5.044	5.251	5.435	5.597	5.738	5.856	5.952	6.024	6.071	6.09

Table 6.4 (a) shows the table of the maximum methane production against dilution rate and feedstock composition (Food waste and green waste) in Cuzco, Peru.

Dilution rate (day^{-1})	Maximum Methane production at varying composition of food waste (L/L/day)																				
	0	5	10	15	20	25	30	35	40	45	50	55	60	65	70	75	80	85	90	95	100
0.001	0.10803	0.114	0.12	0.127	0.133	0.139	0.145	0.151	0.157	0.163	0.17	0.176	0.182	0.188	0.194	0.2	0.206	0.212	0.219	0.225	0.231
0.003	0.2984	0.317	0.336	0.354	0.372	0.391	0.409	0.427	0.445	0.463	0.482	0.5	0.518	0.536	0.553	0.571	0.589	0.607	0.625	0.643	0.661
0.005	0.452	0.484	0.516	0.547	0.578	0.608	0.638	0.668	0.698	0.727	0.757	0.786	0.815	0.844	0.873	0.902	0.93	0.959	0.988	1.016	1.045
0.007	0.57014	0.618	0.664	0.709	0.752	0.795	0.837	0.878	0.919	0.959	0.999	1.039	1.078	1.117	1.156	1.195	1.234	1.272	1.31	1.348	1.386
0.009	0.65407	0.721	0.783	0.842	0.899	0.954	1.008	1.061	1.112	1.163	1.213	1.263	1.311	1.36	1.408	1.455	1.503	1.55	1.596	1.643	1.689
0.0111	0.70513	0.795	0.877	0.952	1.023	1.091	1.156	1.22	1.282	1.342	1.402	1.46	1.517	1.574	1.63	1.686	1.74	1.795	1.849	1.902	1.955
0.0131	0.72463	0.845	0.947	1.039	1.125	1.206	1.283	1.357	1.429	1.499	1.567	1.634	1.699	1.763	1.826	1.889	1.95	2.01	2.07	2.129	2.188
0.0151	0.71387	0.871	0.998	1.108	1.209	1.303	1.392	1.477	1.558	1.636	1.713	1.787	1.859	1.93	1.999	2.067	2.133	2.199	2.263	2.327	2.389
0.0171	0.67387	0.879	1.032	1.161	1.277	1.384	1.484	1.579	1.669	1.756	1.839	1.92	1.999	2.075	2.149	2.222	2.293	2.362	2.43	2.497	2.562
0.0191	0.60533	0.872	1.052	1.201	1.332	1.451	1.562	1.666	1.765	1.859	1.949	2.036	2.12	2.201	2.279	2.356	2.43	2.502	2.573	2.641	2.708
0.0212	0.50848	0.853	1.061	1.229	1.374	1.506	1.627	1.74	1.847	1.948	2.044	2.136	2.224	2.309	2.391	2.47	2.547	2.621	2.692	2.762	2.829
0.0232	0.3825	0.826	1.061	1.247	1.407	1.55	1.681	1.802	1.916	2.023	2.125	2.221	2.314	2.402	2.486	2.567	2.645	2.72	2.791	2.86	2.926
0.0252	0.22874	0.794	1.054	1.257	1.43	1.584	1.724	1.853	1.974	2.086	2.193	2.293	2.388	2.479	2.565	2.648	2.726	2.8	2.871	2.938	3.001
0.0272	0.07853	0.759	1.043	1.261	1.446	1.61	1.758	1.894	2.02	2.138	2.249	2.352	2.45	2.543	2.63	2.713	2.79	2.864	2.932	2.996	3.056
0.0292	0.01113	0.725	1.027	1.259	1.455	1.628	1.784	1.926	2.058	2.18	2.294	2.4	2.5	2.594	2.681	2.763	2.84	2.911	2.977	3.037	3.091
0.0313	0.0012	0.691	1.009	1.253	1.459	1.639	1.802	1.95	2.086	2.212	2.328	2.437	2.538	2.633	2.72	2.801	2.876	2.944	3.006	3.061	3.109
0.0333	4.43E-04	0.658	0.988	1.243	1.457	1.645	1.813	1.966	2.106	2.235	2.354	2.464	2.566	2.661	2.747	2.827	2.899	2.964	3.021	3.069	3.109
0.0353	3.99E-04	0.627	0.967	1.229	1.451	1.644	1.818	1.975	2.118	2.25	2.371	2.482	2.584	2.678	2.764	2.841	2.91	2.971	3.022	3.063	3.093

Table 6.4 (b) shows the table of maximum methane production against dilution rate and feedstock composition (Food waste and Pig manure) in Cuzco, Peru.

Dilution rate (day^{-1})	Maximum Methane production at varying composition of food waste (L/L/day)																				
	0	5	10	15	20	25	30	35	40	45	50	55	60	65	70	75	80	85	90	95	100
0.001	0.10803	0.114	0.12	0.127	0.133	0.139	0.145	0.151	0.157	0.163	0.17	0.176	0.182	0.188	0.194	0.2	0.206	0.212	0.219	0.225	0.231
0.003	0.2984	0.317	0.336	0.354	0.372	0.391	0.409	0.427	0.445	0.463	0.482	0.5	0.518	0.536	0.553	0.571	0.589	0.607	0.625	0.643	0.661
0.005	0.452	0.484	0.516	0.547	0.578	0.608	0.638	0.668	0.698	0.727	0.757	0.786	0.815	0.844	0.873	0.902	0.93	0.959	0.988	1.016	1.045
0.007	0.57014	0.618	0.664	0.709	0.752	0.795	0.837	0.878	0.919	0.959	0.999	1.039	1.078	1.117	1.156	1.195	1.234	1.272	1.31	1.348	1.386
0.009	0.65407	0.721	0.783	0.842	0.899	0.954	1.008	1.061	1.112	1.163	1.213	1.263	1.311	1.36	1.408	1.455	1.503	1.55	1.596	1.643	1.689
0.0111	0.70513	0.795	0.877	0.952	1.023	1.091	1.156	1.22	1.282	1.342	1.402	1.46	1.517	1.574	1.63	1.686	1.74	1.795	1.849	1.902	1.955
0.0131	0.72463	0.845	0.947	1.039	1.125	1.206	1.283	1.357	1.429	1.499	1.567	1.634	1.699	1.763	1.826	1.889	1.95	2.01	2.07	2.129	2.188
0.0151	0.71387	0.871	0.998	1.108	1.209	1.303	1.392	1.477	1.558	1.636	1.713	1.787	1.859	1.93	1.999	2.067	2.133	2.199	2.263	2.327	2.389
0.0171	0.67387	0.879	1.032	1.161	1.277	1.384	1.484	1.579	1.669	1.756	1.839	1.92	1.999	2.075	2.149	2.222	2.293	2.362	2.43	2.497	2.562
0.0191	0.60533	0.872	1.052	1.201	1.332	1.451	1.562	1.666	1.765	1.859	1.949	2.036	2.12	2.201	2.279	2.356	2.43	2.502	2.573	2.641	2.708
0.0212	0.50848	0.853	1.061	1.229	1.374	1.506	1.627	1.74	1.847	1.948	2.044	2.136	2.224	2.309	2.391	2.47	2.547	2.621	2.692	2.762	2.829
0.0232	0.3825	0.826	1.061	1.247	1.407	1.55	1.681	1.802	1.916	2.023	2.125	2.221	2.314	2.402	2.486	2.567	2.645	2.72	2.791	2.86	2.926
0.0252	0.22874	0.794	1.054	1.257	1.43	1.584	1.724	1.853	1.974	2.086	2.193	2.293	2.388	2.479	2.565	2.648	2.726	2.8	2.871	2.938	3.001
0.0272	0.07853	0.759	1.043	1.261	1.446	1.61	1.758	1.894	2.02	2.138	2.249	2.352	2.45	2.543	2.63	2.713	2.79	2.864	2.932	2.996	3.056
0.0292	0.01113	0.725	1.027	1.259	1.455	1.628	1.784	1.926	2.058	2.18	2.294	2.4	2.5	2.594	2.681	2.763	2.84	2.911	2.977	3.037	3.091
0.0313	0.0012	0.691	1.009	1.253	1.459	1.639	1.802	1.95	2.086	2.212	2.328	2.437	2.538	2.633	2.72	2.801	2.876	2.944	3.006	3.061	3.109
0.0333	4.43E-04	0.658	0.988	1.243	1.457	1.645	1.813	1.966	2.106	2.235	2.354	2.464	2.566	2.661	2.747	2.827	2.899	2.964	3.021	3.069	3.109
0.0353	3.99E-04	0.627	0.967	1.229	1.451	1.644	1.818	1.975	2.118	2.25	2.371	2.482	2.584	2.678	2.764	2.841	2.91	2.971	3.022	3.063	3.093

Table 6.4 (c) shows the table of maximum methane production against dilution rate and feedstock composition (Pig manure and green waste) in Cuzco, Peru.

Dilution rate (day^{-1})	Maximum Methane production at varying composition of Pig manure																				
	0	5	10	15	20	25	30	35	40	45	50	55	60	65	70	75	80	85	90	95	100
0.001	0.10803	0.108	0.109	0.109	0.109	0.11	0.11	0.11	0.111	0.111	0.111	0.112	0.112	0.112	0.113	0.113	0.113	0.113	0.114	0.114	0.114
0.003	0.2984	0.3	0.302	0.304	0.306	0.308	0.31	0.312	0.314	0.315	0.317	0.319	0.32	0.322	0.324	0.325	0.327	0.328	0.33	0.331	0.333
0.005	0.452	0.458	0.463	0.468	0.473	0.478	0.482	0.487	0.491	0.495	0.499	0.503	0.507	0.511	0.515	0.518	0.522	0.525	0.528	0.531	0.534
0.007	0.57014	0.581	0.592	0.602	0.612	0.621	0.63	0.638	0.646	0.654	0.661	0.668	0.675	0.681	0.687	0.693	0.699	0.705	0.71	0.715	0.72
0.009	0.65407	0.674	0.693	0.71	0.726	0.741	0.755	0.769	0.781	0.793	0.804	0.815	0.825	0.835	0.844	0.853	0.861	0.868	0.876	0.882	0.889
0.0111	0.70513	0.738	0.767	0.794	0.818	0.841	0.861	0.881	0.899	0.916	0.931	0.946	0.96	0.973	0.985	0.997	1.007	1.017	1.026	1.035	1.043
0.0131	0.72463	0.775	0.818	0.857	0.891	0.922	0.95	0.977	1.001	1.023	1.044	1.063	1.081	1.097	1.113	1.127	1.14	1.152	1.163	1.173	1.182
0.0151	0.71387	0.788	0.849	0.901	0.947	0.988	1.024	1.058	1.089	1.117	1.143	1.167	1.189	1.209	1.227	1.244	1.259	1.273	1.285	1.296	1.306
0.0171	0.67387	0.781	0.863	0.93	0.989	1.04	1.086	1.127	1.165	1.199	1.23	1.259	1.285	1.308	1.33	1.349	1.366	1.382	1.395	1.406	1.416
0.0191	0.60533	0.758	0.863	0.947	1.019	1.081	1.136	1.185	1.23	1.27	1.307	1.34	1.37	1.397	1.421	1.443	1.462	1.478	1.492	1.503	1.512
0.0212	0.50848	0.721	0.852	0.954	1.039	1.112	1.176	1.234	1.285	1.331	1.373	1.411	1.445	1.475	1.502	1.525	1.546	1.563	1.577	1.588	1.595
0.0232	0.3825	0.677	0.835	0.953	1.051	1.135	1.209	1.274	1.332	1.384	1.431	1.473	1.51	1.543	1.573	1.598	1.619	1.637	1.65	1.66	1.665
0.0252	0.22874	0.63	0.812	0.947	1.057	1.151	1.233	1.306	1.371	1.428	1.48	1.526	1.567	1.603	1.634	1.661	1.683	1.7	1.713	1.72	1.723
0.0272	0.07853	0.583	0.787	0.936	1.058	1.162	1.252	1.332	1.402	1.465	1.521	1.571	1.615	1.654	1.687	1.714	1.737	1.754	1.765	1.77	1.768
0.0292	0.01113	0.539	0.76	0.923	1.055	1.167	1.265	1.351	1.427	1.495	1.556	1.609	1.656	1.696	1.731	1.759	1.781	1.797	1.807	1.808	1.802
0.0313	0.0012	0.5	0.734	0.907	1.048	1.169	1.273	1.365	1.447	1.519	1.583	1.639	1.689	1.731	1.767	1.796	1.818	1.832	1.839	1.837	1.824
0.0333	4.43E-04	0.465	0.708	0.89	1.039	1.166	1.277	1.374	1.46	1.536	1.604	1.663	1.715	1.759	1.795	1.824	1.845	1.858	1.862	1.855	1.836
0.0353	3.99E-04	0.434	0.683	0.872	1.027	1.16	1.276	1.378	1.469	1.548	1.619	1.681	1.734	1.78	1.817	1.845	1.865	1.876	1.877	1.864	1.837

6.3 Conclusion

The present study demonstrates the ability of the mathematical model (thermal and Biochemical) to predict the operating conditions of individual substrates as well as the operating condition for co-digestion of different substrates. It found that the organic loading rate (dilution rate) differs for different feedstock and for different mix ratio of co-digestion feedstock. For mono-digestion, the organic loading rate of pig manure is higher than food waste and green waste. However, food waste produced more methane than pig manure and green waste. During co-digestion, the addition of co-substrate increases the organic loading rate and reduces the hydraulic retention time. The digester operational parameters (organic loading rate and HRT) are different in different locations (Port Harcourt and Cuzco). The digester can achieve stability when the organic loading rate and hydraulic retention time are below the values of the optimum loading rate and above the minimum hydraulic retention time.

Chapter 7 General Discussion of Results chapters

This chapter presents a comprehensive discussion of the outcome of the result chapters in the present thesis. The chapter starts with the general discussion of the results of chapter 4, followed by the general discussion of the outcome of chapter 5, and finally the general discussion of the outcome of results chapter 6 is presented.

Anaerobic digestion models have been applied to describe the degradation of feedstocks. In chapter 4, the degradation of food waste and green waste in a semi-continuous experiment was presented. Using the one population anaerobic digestion model represented by the hydrolysis stage, and applying different kinetic rate equations, the one reaction model described the degradation of food waste and green waste with a relative root mean square errors (rRMSE) in the range of 35.2 -39.6 % and 23 - 25.1 % respectively.

Increasing the complexity of the model was done by introducing the methanogenic stage, volatile fatty acid and ammonia in the anaerobic digestion model (two reaction model, 2R). There was an improvement in the quality of fit of the model result against the experimental result. The improvement in the quality of fit is related to the reduction in the rRMSE of the parameter estimation. In the case of two reaction model, rRMSE was 21.9 % and 27.2 % for the best bit kinetic models of green waste and food waste degradation. The key difference between the fitness of both models to the experimental data is the presence of the methanogenic stage in the 2R model which resulted in better modelling of the behaviour of the experiment data especially with regards to the methane production. There was, however, a distinction between the 2R model description of food waste and green waste degradation; the 2R model requires the inclusion of

inhibition (volatile fatty and ammonia) in the description of food waste degradation to ensure the better quality of fit to the experimental data. In green waste degradation, the 2R model fits well the experimental data with or without inhibition. The difference is also because food waste has more soluble organic matter than green waste, and this is seen in the value of k_1 (Reactions coefficient for hydrolysis) (38.2 for green waste vs 15.0 for food waste). These values of k_1 was different from 42.14 reported by Bernard et al [84], and it is due to differences in the method of estimating k_1.In Bernard et al. [84], k_1 was estimated from the measurement of the biomass concentration, while k_1 is determined from the parameter estimation method in the present study and this is important because its describes the extent of degradability of the feedstocks..

In the simulation of the digestion of food waste and green waste, the three reactions model (3R) reveals the importance of substrate characterisation in the anaerobic digestion processes. In this model (3R) the parameter estimation approach found a minimisation solution that was not intended in the mechanistic structure of the 3R model, but led to a better fitting solution, and this was to fractionate the feedstock into a rapidly and slowly degradable fraction. The fitness of the model to the experimental data is better than that of the 2R and 1R models, as the 3R model is able to describe the initial rapid production of methane followed by a slow production of methane due to the presence of fast hydrolysed fraction and a slowly hydrolysed fraction of the substrate fed into the digester. The concept of fast and slow hydrolysed fraction has been the topic of discussion in the literature, e.g. Siegrist [247] observed that rapid production of gas occurs within an hours of feeding, and this is followed by a prolong biogas production [247] [246]. Generally, a substrate consists of particulate and soluble fractions which degrade at different rate. The soluble substrate is utilized quickly by the microorganism such that the rate of degradation is dependent on the biomass concentration and their

respective uptake rates. The particulate fraction is complex, and it is hydrolysis limiting since its degradation rate is described by the first order hydrolysis kinetic coefficient [98]. The particulate fraction consists of particle of different sizes, which have varying content of lignin. This makes it easy to further distinguish substrate fractions into readily and slowly degradable fractions.

The results of the biochemical model reveal the importance of the model structure in the description of the degradation. The more complex the structure of anaerobic digestion model, the better its ability to describe or fit experimental data. This is true as the degradation of green waste was better described when the complexity of the ADM1 model was increase from a single particulate fraction to a one particulate and one soluble fraction, and the degradation of food waste is best described using model structure with two particulates [243]. Mottet et al [248] reveal that using a new structure consisting of two hydrolysable fractions, the modified AMD1 was able to describe the degradation of sludge and biogas production in a continuous digester.

The first order hydrolysis coefficient obtained for the different fractions of the green waste was 3.19 d^{-1} and 4.74 d^{-1}. These are different from the literature reported values e.g. (1.57 and 0.192 d^{-1}) for two particulate fractions; 0.68 and 0.136 d^{-1} for two particulate and one soluble reported for green waste in Poggio, [243]. The difference in the values of the first order hydrolysis coefficient in the present study is because 3R model is a simplified anaerobic digestion model which tend to describe the complex microbial activities. Also, in Poggio, [243], the first order hydrolysis rate is calibrated by the ADM1 model which could led to a more accurate description of the degradation of the substrate [83, 243]. For food waste, the hydrolysis rate is represented by the Contois kinetic, and the values reported in the present study are 0.653 d^{-1} and 0.487 d^{-1} ($\mu_{1a.max}$ and

$\mu_{1b.max}$). The $\mu_{1a.max}$ is within the range 0.2-6.797 d^{-1} reported by [269-271] for the description of the hydrolysis stage using Contois Kinetics.

Anaerobic digesters are often heated to reduce the daily fluctuations in the slurry temperature and increase biogas production. The development of heating systems that use solar water heating, greenhouse and biogas to heat pilot or small-scale anaerobic digesters has been presented by several authors [74, 76, 212, 213, 272, 273], and [76]. In Chapter 5 of the present research work, different designs of the plastic bag digester were tested in different locations (Port Harcourt and Cuzco), using input such as the solar radiation, wind speed, air temperature, material of construction, etc. The design of the AD system that was studied included a simple biogas digester (CASE 1), biogas digester with a greenhouse cover (CASE 2), and the biogas digester in a greenhouse, coupled with a solar heating system (CASE 3). The simulation shows that the different designs of the plastic bag digester (CASE 2, and CASE 3) adding the greenhouse and solar collector have an influence on the average slurry temperature, minimises daily fluctuation in the slurry temperature compared with the fluctuation in air temperature. In Port Harcourt, biogas digester (CASE 1) has a slurry temperature above 20 ^{o}C, which is enough for biogas production year-round. Lansing et al [72] reported slurry temperature was above 20 ^{o}C in the plastic bag digester installed in warm climate (Costa Rica), which has an average temperature of (24 ^{o}C). Lansing et al [72] agree with the results of the present study, that installing anaerobic digester underground in warm climate has a positive impact of the digester slurry temperature. Similar results were observed in the Cuzco, with the slurry temperature is above 9.5 ^{o}C all years around, demonstrating the thermal inertia of the slurry in the digester. Marti et al [274] investigated the application of low cost AD digester for the treatment of fruit and vegetable waste in Cochabamba, Bolivia. The digester used is a different design of plastic bag digester without external heating source (solar water and

greenhouse). The mean slurry temperature reported by Marti et al [274] shows 4.1 ^{o}C higher than the mean ambient temperature. The mean slurry temperature in the present, is 4.3 ^{o}C higher than the mean ambient temperature. In a similar study, performed in Cochabamba, Bolivia, three plastic bag digesters connected in series were applied in the treatment of slaughterhouse wastewater. Investigation of the slurry temperature found that it was the same as the mean maximum ambient temperature during the summer period [258]. The weather condition in Cochabamba is similar to that Cuzco, since both cities are located in Mountainous region which is characteristised by high fluctuation in the ambient temperature. The digester is made of the dark geomembrane material which is able to absorb solar radiation to keep the slurry temperature above the minimum ambient temperature. Also, the increase in the slurry temperature is as a result of insulation of the digester, which helps to minimise heat losses to the soil. Weatherford et al [229] reveals that the thickness of insulation material and the tube material (material used in making the plastic bag digester) are among factors that positively influence the slurry temperature.

In Cuzco, the biogas digester (CASE 2) has a minimum slurry temperature of 11.8 ^{o}C in Cuzco. Hassanian et al [212], compared two designs of digester; in the first design, the digester had two greenhouse cover, an inner greenhouse cover use to heat the feed in the inlet tank and an external greenhouse over the digester. The second design is a digester without heating source, and both design of the digester was buried underground. Hassanien et al [212] found that the minimum slurry temperature in the digester with greenhouse is above 9.8 ^{o}C over one-year period compared to the digester without greenhouse which has a minimum slurry temperature that is less than 8 ^{o}C. Therefore, it can be concluded from the results of the present study and literature that the addition of an external heating source such as greenhouse has a positive impact of the performance of the digester.

Combined solar water and greenhouse heating of biogas digester can minimise temperature fluctuation in different weather conditions [213]. For the system investigated by Hassanien et al in Central China [213], it was found that the difference between the slurry temperature on a cloudy day and cloudless day varies between 1-2 ^{o}C, when the digester is slurry is heated using a combination of solar heating, greenhouse and an auxiliary DC Heater. This is comparable with the results of the (CASE 3) predicted a low variation in the slurry temperature 0.5-1 ^{o}C, and the temperature of the slurry predicted during the cold season is 13 ^{o}C. The average temperature in Xianyang during the cold months is -1.6^{o}C compared to 0 ^{o}C in Cuzco. In Port Harcourt, the digester design (CASE 3) has slurry temperature in the range of 28 and 32 ^{o}C during the coldest month of the year, and an average slurry temperature of 36.8 ^{o}C in summer. For the digester system investigated by [275], it was found that the slurry temperature is below 37 and 39 ^{o}C during the coldest month of the year, and in the summer the temperature of the slurry did not exceed 39 ^{o}C. The average ambient temperature in Port Harcourt is 26 ^{o}C compared to the mean ambient temperature of 21 ^{o}C in Nancy, Eastern France [275]. It is expected that giving the high ambient temperature in Port Harcourt, the greenhouse cover and solar water heating in the digester design CASE 3, and the fact that slurry in the solar storage tank is heating above 45 ^{o}C before it is discharged into the main digester, the temperature of the slurry in the main digester should have increased considerable to the optimal mesophilic temperature. However, this was not the case as the slurry temperature in digester CASE 3 increase by 1.48 ^{o}C. It is noteworthy, to state that the digester design in Heirz et al [275] is the fixed dome digester buried in a cogeneration unit. Hot water from the cogeneration unit is used to heat the slurry through the heat exchange installed in the digester tank, the slurry is mixed regular using a mixer inside on the top side of the digester walls, and the top of the digester is cover with an EPDM material, which acts as a greenhouse. However, in the present study, the digester

CASE 3 is made of plastic material, heated external hot water storage unit attached to the inlet of the digester and it is operated unmixed. Additionally, it is important to state that despite the different in the design of the digester and the type of material used. The combination of different external heating source contributed significantly to the performance of anaerobic digester.

Digester operating temperature, hydraulic retention time and the feedstock composition are key parameters for anaerobic digestion processes. In chapter 6, a framework was developed to predict the maximum methane production rate, minimum hydraulic retention time, and the maximum organic loading rate.it was found that increasing the slurry temperature corresponds to a reduction in the minimum hydraulic retention time under which the digester system could sustainably operate, corresponding to an increase in the maximum biogas production and organic loading rate. This trend continued until 37 ^{o}C. The methane production increases up to a maximum at 37 ^{o}C and decreases as the slurry temperature increase about 37 ^{o}C. The optimal methane production is predicted in the model is because the cardinal temperature model used in the modelling the impact of slurry temperature of the uptake rate of the substrate has an optimum growth rate at 37 ^{o}C [223].

For digesters installed in cold climates (Cuzco), it is was found that the reduced slurry temperature leads to increase in the minimum hydraulic retention time, and consequently a lower maximum biogas production, when compared to warmer climates (Port Harcourt). Also, with respect to the substrates used, the model (3R) found that the minimum hydraulic retention time are different for different substrate. For example, at a slurry temperature of 10 ^{o}C (283 K), the predicted minimum HRT for green waste is 150 days, and the minimum HRT of food waste and pig manure is 80 days. The difference is in the substrate characteristics, where food waste

and pig manure with more degradable organic matter allow for increase in the OLR compared to green waste.

The amount of substrate added to the digester influences the HRT, and for different feed combination at the same operating temperature, the minimum HRT is different due to the difference in the organic strength and digestion characteristics of the feedstock. This allows for increasing in OLR when the operating temperature is reduced, as in the case of green waste co-digester with food waste, and pig manure co-digester with food waste. The weather condition in different location affects the slurry temperature, and consequently the operation of the digester. In Cuzco, the feeding rate of the feedstock charged into the digester is different from the feeding rate of the digester in the Port Harcourt. 0.496 kg COD m^3 day^{-1} (0.397 kg VS m^{-3} day^{-1}) is reported in the present study as the organic optimal organic loading rate in Cuzco, this value is within the range reported in several reported 0.26-0.44 Kg VS m^{-3} day^{-1} [197, 276]. 0.812 kg Vs m^{-3} day^{-1} (is optimal organic loading rate in Port Harcourt, and this value is within the range reported for biogas digester installed in temperate regions [209]. The difference in the organic loading rate in Port Harcourt and Cuzco provides insights into the impact of the different environmental temperature (summer and winter) on the performance of anaerobic digester. Further, it implies that when the digester heating is provided by the environmental condition, the digester operating condition will differ in different climates due to the difference in the ambient temperature which has an impact of the digester temperature.

Chapter 8 Conclusion and Future work

8.0 Conclusions

This chapter present the summary of the conclusion of the research work undertaken in this thesis. It starts with the conclusion of the assessment and parameter identification of methane production from food waste, green waste and pig manure, the thermal performance of the different design of plastic bag digester, and the operational strategy of small-scale anaerobic digestion process. Then suggestions will be made for area of improvement on various aspects of the thesis and future work.

In this thesis, the description of the degradation of solid waste using a simplified model of anaerobic digestion model was explored with a focus on the structure of the model, reaction kinetics and the impact of inhibition detailed in chapter 4. The results of the study found that the structure of the model had a significant impact on the ability of the model to describe the degradation of solid wastes. For food waste degradation, the inclusion of inhibition in the reaction kinetics played a significant role in the model's ability to describe methane production. Increasing the complexity of the model increases the quality of fit to the experimental dataset. One or two reaction model was able to fit the experimental dataset for green waste, with no observable difference in the model fitting for the three-reaction model. Green waste degradation can be described with/without inhibition. A comparison of the stoichiometric coefficient (k_1) obtained from parameters estimation found that the values are different for batch and continuous anaerobic processes. The value of k_1 for food waste degradation ob batch parameter estimation is 0.2601. In the continuous experiment, the value is $k_1 = 11.2$, for the 1R model. $k_1 = 15.0$, for 2R model; $k_{1a,\ hyd} = 6.60$, and $k_{1b,\ hyd} = 19.9$ for 3R model. Similarly, in green waste degradation, the value of k_1 is 0.7734 in the batch parameter estimation. While, the values obtained from the continuous parameter estimation are

k_1= 26.5 for the 1R model, k_1= 38.2 for 2R model, $k_{1a,\ hyd}$ = 3.19 and $k_{1b,\ hyd}$ = 4.74 for 3R model respectively. From the aforementioned, it was concluded increasing complexity of AD model leads to better description of the degradation of organic waste.

In Chapter 5, the performance of different design of the plastic bag digesters in Port Harcourt, Nigeria, and Cuzco, in Peru was explored. Three cases were modelled; CASE 1: the plastic digester without greenhouse, CASE 2: the plastic bag digester with greenhouse, and CASE 3: The plastic bag digester with greenhouse and solar collector mounted on the inlet of the digester. The key outcome of the simulation of the thermal model of the plastic digester is that CASE 3 is not useful in Port Harcourt, But feasible in Cuzco. This is because there is no significant difference in temperature between CASE 2 and CASE 3. The mean temperature of the slurry in CASE 3 and CASE 2 are 32.7 ^oC and 31.2 ^oC in Port Harcourt, respectively. In Cuzco, the temperature of the slurry is 25.85 ^oC and 19.65 ^oC in CASE 3 and CASE 2, respectively. The result also shows a 3.3 ^oC increase in the slurry temperature in CASE 2 and 4.5 ^oC increase in slurry temperature in CASE 3, compared to the temperature of the slurry in CASE 1. The average temperature of the slurry in CASE 1 for both locations (Port Harcourt and Cuzco) are 28.80 ^oC and 16.31 ^oC respectively. The simulation of the methane production in each case reveals no difference in the average methane production (478 L L^{-1} day^{-1}) in Port Harcourt. Whilst in Cuzco, the methane production in CASE 1 is 207 L L^{-1} day^{-1} and 287 L L^{-1} day^{-1} in CASE 3. Therefore, the addition of an extra heating source to the plastic bag digester is not useful in Port Harcourt, but it is feasible in Cuzco.

In chapter 6, the operational strategy of a rural digester was investigated to determine the maximum methane production, hydraulic retention time, and the organic loading as a function of feedstock and weather condition. The results of the simulation found that the organic loading rate is different for the substrates in different locations. For the mono-digestion processes, the

organic loading rate of food waste, green waste, and pig manure are 0.766 g COD day^{-1} (0.062 day^{-1}), 0.663 g COD day^{-1} (0.0396 day^{-1}), and 0.820 g COD day^{-1} (0.0723 day^{-1}) in Port Harcourt. In Cuzco, the organic loading rate of food waste, green waste, and pig manure is in the range of 0.356 - 0.395 g COD day^{-1}, corresponds to a dilution rate of 0.214-0.032 day^{-1}. Therefore, the maximum OLR for the substrates are different giving the same slurry temperature. Consequently, the minimum HRT is reduces and it is different for each substrate giving their maximum OLR. In the co-digestion process, it was found that maximum OLR and dilution rate increase as the percentage of the co-substrate added increase. However, when the percentage of co-substrate is above 20 % - 30 %, the dilution rate remains the same, while the maximum OLR increase, and this is possible because of the addition of easily degradable organic matter. The maximum OLR of the food waste and green waste co-digestion is different in Port Harcourt (0.912 g COD day^{-1}) and Cuzco (0.394 g COD day^{-1}). For co-digestion of green waste and pig manure, the maximum OLR is 0.766 g COD day^{-1} in Port Harcourt and 0.468 g COD day^{-1} in Cuzco. For food waste and pig manure co-digestion the maximum OLR is 1.303 g COD day^{-1} in Port Harcourt, and 0.484 g COD day^{-1} in Cuzco. Therefore, it can be deduced that the composition of feedstock has a significant impact on the operational parameter (Maximum OLR and minimum HRT) in co-digestion processes, and the digester can be operated safety below the maximum OLR and Minimum HRT.

8.2 Future Work

8.2.1 Improvement of the biochemical models

The outcome of the description of food waste and green waste degradation show some inadequacies in the ability of the simplified model to explain continuous production of methane, especially during periods of low or zero

biomass feeding. The structure of the model needs improvement. The biochemical models could also be extended to include the effect of moisture content, and micronutrients on the degradation of organic matter. Further, the future work includes the validation of the complete biochemical model using experimental data (Thermal, biochemical and temperature dependent kinetic models). This because necessary as the individual models has been validated individually, and it place a limitation on the confidence in the quantitative outputs of the model.

8.2.2 Improvement and future work on the strategy of anaerobic digestion model.

Following the detailed work in Chapter 6 of this thesis, there is need for improvement in the methods used in order to make the outcome more realistic and this includes:

- The use of another temperature dependent kinetic model such as Arrhenius kinetic to model the effects of temperature on the kinetic parameters. In chapter 6, the temperature range in the evaluation of the minimum hydraulic retention time and the maximum organic loading rate is between 5 and 45 ^{o}C.
- An improvement to the method will be to determine the maximum slurry temperature in summer and winter and apply this temperature range to determine the maximum organic loading of the digester.
- The improvement of the biochemical method by including substrate fractionation for both mono-digestion and the co-digestion process is very crucial. This will aid in understanding the best blend of the feedstock based on the percentage fraction of carbohydrate, protein, and fats. Field experimental validation of the modelling result is very important, especially in Port Harcourt.

8.2.3 Improvement and future work for solar assisted anaerobic digestion processes.

In the modelling of CASE 3 (solar and greenhouse), the solar heating is operated using a simple OFF/ON control system to control the temperature in the solar storage tank at 55 ^{o}C. In the storage tank, it was assumed that the entire content is fully mixed. This is not the case as most domestic biogas systems in practice are not completely mixed. Improving the modelling of the solar collector system will require the inclusion of control to regulate the flow of hot water especially in the winter. This is crucial as it will increase the amount of how water flowing through the heat exchanger. Modelling of a stratified tank is an improvement to the present study as it will give a better understanding of the impact of the solar collector and greenhouse on the overall performance of the plastic bag digester.

Another improvement that can be made in the modelling of the digester is the determination of optimal angle of inclination of the solar collector, and the greenhouse. This is because angle of inclination is a function of the latitude of a location. Potential future research will involve an experimental validation of the thermal model all the design (CASE 1, 2 and 3) in Port Harcourt, Rivers State. Also, since it has been establish the higher temperature can be achieve using external heating source like the solar heating system. A future research could involve exploring the two-stage anaerobic digestion process, for application in domestic biogas technology. In the two-stage anaerobic digestion process, CASE 3 is used, and anaerobic digestion process is allowed in the solar storage tank before its content is discharge into the main digester.

Appendix A

A.1 estimation of the solar radiation of the solar panel

```
%% Matlab program for maximum tilt angle for given solar configuration
%% Solar data input data for SDHW
%% function [Q]=A_max_tilt_radaition_july11()

clc;clear;

% Opening commands for files. Input_1 contains three colums,viz direct,
%diffuse and ambient temperature
fid1=fopen('input_1.txt');
% Reading commands parameters
a=fscanf(fid1,'%g',[3,8760]);
direct_solar=a(1,:)';
diffuse_solar=a(2,:)';
temp_amb=a(3,:)';
%windspeed=a(4,:)';
% L_1=[(1:1:8760);a(5,:)]'; %Normal load profile in % of total hot waster demand
% L_2=[(1:1:8760);a(6,:)]'; %RAND load profile in % of total hot water demand

%Tank parameters
V1=80;Va=0.8*V1;Vb=0.2*V1;
```

```
%Tank UA
UA_upper=0.72;UA_lower=0.008; UA_hot=UA_upper+UA_lower;
%UA=0.728;

%initial condition of the storage tank C
int_con=10;

%%Basic input for mathematical modelling of solar plate collector
% Latitude and Longitude of the location in radian
lat=0.98; longitude=0.1;
%Absorption, transmittance and ground reflectance coefficients
alpha=0.95; tau=0.87;rho=0.6;
% Area of the flat plate collector, sq.m
area=2.8;
%Room temperature where panel is kept, C
RTa=10;

%% Calculation of overall het transfer coefficient, U, W/(sq.mK)
%% Number of glass cover
N=1;
% plate to plate spacing,mm
pp=25;
%plate & glass emittance
ep=0.95; eg=0.88;
%Ambient temperature, degree C
amb_T=mean(temp_amb)+273.15;
%Mean plate temperature, degree C
mean_Tp=30+273.15;
% Collectir tilt, degree
```

```
tilt=45;
%Wind Heat transfer coefficient, W/(sq m C)
h_wind=15;
%Stefan_Boltzman constant
sb_c=5.67e-8;

%Calculation of some other parameters
f=(1+0.089*h_wind-0.1166*h_wind*ep)*(1+0.07866*N);
C=520*(1-0.000051*tilt^2);
e1=0.430*(1-100/(mean_Tp));

%Overall heat transfer coefficient, W/(sq m C)
U_1=((N/((C/mean_Tp)*((mean_Tp-amb_T)/(N+f))^e1)+1/h_wind))^-1;
U_2=sb_c*(mean_Tp+amb_T)*(mean_Tp^2+amb_T^2);
U_3=(ep+0.00591*N*h_wind)^-1+((2*N+f-1+0.133*ep)/eg)-N;
%u=1.1*(U_1+U_2/U_3);
U=0.1;
%% Data for solar panel and heat exchanger
% plate efficiency factor
F1=0.85;
% Flow rate of fluid in flate plate collector, kg/s and heat capacity ,J/kg-K
mc=50/(area*3600); cp=3800;
% Dimeansional collector mass flow rate
mcc=mc*cp/(area*U*F1);
% Solar plate collector flow factor
F2=mcc*(1-exp(-1/mcc));
% Heat removal factor of solar plate collector
Fr=F1*F2;
%Flow rate of water in flate plate collectir, kg/s ans heat capacity,j/kg-k
```

```
mw=119;%*load_profile_normal;
cp_w=4184;
%% Basic input for mathemactical modelling of heat exchanger inside the storgae tank
%% Effectiveness of heat exchanger
effect_HX=0.8;
%Heat exchanger penalty in SDHW
Frr=Fr*((1+(1/mcc)*((1/effect_HX)-1))^(-1));

I_dir_hourly = [];
I_diff_hourly = [];
I_ground_hourly = [];
I_tot_hourly = [];

%% This block calculate the tilt angle for maximum value of total solar radiation falling on collector
 for k=1:1:20
    %tilt(k)=k*pi/40;
    tilt(k)=0.785398;
    for j=1:1:365
        days(j)=j;
        for i=1:1:24
            t(i)=i;
            %Declination angle, radian
            d_declin(i)=(pi/180)*(23.5*(sin((pi/180)*((360*(284+days(j)))/365)))));
            % Factor B
            B(i)=(pi/180)*(360*(days(j)-81)/364);
            % Factor E
            E(i)=9.87*sin(2*B(i))-7.35*cos(B(i))-1.5*sin(B(i));
            %Local solar time, hour
            lst(i)=t(i)+((4*(0-5.5))+E(i))/60;
```

```
        %Hour angle, radian
        h_angle(i)=(pi/180)*(15*abs(12-lst(i)));
        %Solar elevation angle, radian
        sol_elv(i)=asin((cos(lat))*(cos(h_angle(i)))*(cos(d_declin(i)))+(sin(lat))*sin(d_declin(i)));
        %Solar azimuth angle, radian
        sol_azim(i)=acos(((sin(lat))*(cos(h_angle(i)))*(cos(d_declin(i)))-(cos(lat))*(sin(d_declin(i))))/cos(sol_elv(i)));
        % Direct component of Solar radiation, kJ/hr-sq.m
        I_dir(i)=(direct_solar(i+(j-1)*24))*((cos(sol_elv(i)))*(cos(sol_azim(i)))*(cos(tilt(k)))+(sin(sol_elv(i)))*sin(tilt(k)));
        % Diffuse component of solar radiation, kJ/hr-sq.m
        I_diff(i)=(diffuse_solar(i+(j-1)*24))*(1+sin(tilt(k)))/2;
        %Diffuse component solar radiation from ground, KJ/hr-sq.m
        I_ground(i)=rho*((direct_solar(i+(j-1)*24)))*(1-sin(tilt(k)))/2;
        % Total solar radiation on flat palte collector, Kj/hr_sq.m
        I_tot(i)=I_dir(i)+I_diff(i);


    end
    I_dir_daily(j) = mean(I_dir);
    I_diff_daily(j)= mean(I_dir);
    I_ground_daily(j)= mean(I_ground);
    I_tot_daily(j)= mean(I_tot);

    I_dir_hourly = [I_dir_hourly I_dir];
    I_diff_hourly = [ I_diff_hourly I_diff];
    I_ground_hourly = [I_ground_hourly I_ground];
    I_tot_hourly = [I_tot_hourly I_tot];
end
heat_rate(i)=(1000/3600)*area*Fr.*((I_tot(i)).*tau*alpha-U*(100-amb_T));
```

end

A.2 the expressions of t_x , t_y, t_w and t_z in equation in (3.39) of chapter 3

$$t_x = \frac{1}{\frac{C}{T_{mp}}\left(\frac{T_{mp} - T_a}{N + f}\right)^e}$$

$$t_z = \frac{2N + f - 1 + 0.133e_p}{e_g}$$

$$t_y = \sigma\left(T_{mp} + T_a\right)\left(T_{mp}^2 + T_a^2\right)$$

$$t_w = e_p + 0.00591Nh_w$$

Where N is the number of glass cover, T_{mp} is the mean plate temperature, T_a is the ambient temperature, e_g is emittance of the glass cover, e_p is the emittance of plate, $e = 0.43(1 - (\frac{1}{T_{pm}})$,

$f = \left(1 + 0.089h_w - 0.116h_we_p\right)(1 + 0.07866N)$, $C = 520(1 - 0.0005\beta^2)$

A.3 Matlab scripted used for developing operational protocol for small scale digesters.

A.3.1 Matlab script for predicting the maximum methane production and maximum dilution before point of failure.

```
figno = 1;
noparams = 11;
points =20;
globalpoints = 2000;
paramp = zeros(points,noparams);

% p_opt = sdo.getParameterFromModel('Bernard_model_Contois',{'Tslurry'});
% p_opt.Value=285; % Temperature in kelvin
% p_opt.Minimum=283;
% p_opt.Maximum=306;
% p=p_opt;
Tslurrymin = 283;
Tslurrymax = 312;
%
% Dmin = 0.002;
% Dmax = 0.005;

% % creating an experiment using one of the simulation data; in the my case
% % the feeding rate Dfeedin.
qf = 1.0025; % feed increase per day
qi = 0.0005; % initial q per day
qid = 100* qi; % initial q per day 1% pulse
```

```
for timegas = 1:60;
Dfeedin (timegas,:) = [timegas qi];% continuous feeding
%Dfeedind (timegas,:)= [timegas ; qid];% daily feed (1% of day ~ 15 minutes)
end

for timegas = 61:5000
Dfeedin (timegas,:) = [timegas qi*qf^(timegas-61)];% continuous feeding
%Dfeedind (timegas,:)= [timegas ; qid*qf^(timegas-61)];% daily feed (1% of day ~ 15 minutes)
end


Exp=sdo.Experiment('Bernard_model_Contois');
% Exp.InputData = timeseries(Dfeedin, Timegas);

methaneflow=Simulink.SimulationData.Signal;
methaneflow.Name = 'methaneflow';
methaneflow.BlockPath = 'Bernard_model_Contois/conv';
methaneflow.PortType = 'outport';
methaneflow.PortIndex = 1;
% methaneflow.Values = timeseries(gasrate,timegas);

% Dmax = zeros(points,noparams);
% Mmax = zeros(points,noparams);

Mav = zeros(points,noparams);

%  a=-0.1;
```

```
%MAXIMUM LOADING RATE AND METHANE FLOWRATE (LOCAL SENSTIVITY)
 for x = 1:noparams;
%  a = a+0.1;
%  F = [0 0 a*zin+(1-a)*zin_C a*s1in a*s2in+(1-a)*s2in_C a*cin+(1-a)*cin_C a*nin+(1-a)*nin_C (1-a)*s3in]';

  for  y= 1:points


        Tslurry = [0 Tslurrymin + (y-1)*(Tslurrymax-Tslurrymin)/(points-1)];


%       Dfeedin = [0 Dmin + (y-1)*(Dmax-Dmin)/(points-1)];

      Exp=sdo.Experiment('Bernard_model_Contois');
      % Exp = setEstimatedValues(Exp);
      Simulator = createSimulator(Exp);
      Simulator = sim(Simulator, 'ReturnWorkspaceOutputs', 'on', 'SrcWorkspace', 'base');
      SimLog = find(Simulator.LoggedData,get_param('Bernard_model_Contois','SignalLoggingName'));
      methaneflowsim=find(SimLog,'methaneflow');


%       for n = 1: max(size(methaneflowsim.Values.Data)-1)
%          if(methaneflowsim.Values.Data(n)<methaneflowsim.Values.Data(max([n-10 1])) && methaneflowsim.Values.Time(n)>60)
%          tfail = methaneflowsim.Values.Time(n);
%          break
%          end
%       end

      tsr = resample(methaneflowsim.Values, timegas);
```

```
        Mav(y,x) = mean(tsr.data);
        Mav(y,x) = mean(tsr.data(35041:43800));
        paramp(y,x) = Dfeedin(2);


 end
 end

Dmaxn = Dmax/max(max(Dmax));
HRTmin = 1./Dmax;
figure(1)
hold
for n=1:noparams
    plot(paramp(:,n),Mav(:,n));
    %axis([0 4 0 10]);
    title('average methane production');
    legend('methaneflow');
    grid;
end
hold off

% figure(2)
% hold
% for n=1:11
%     plot(paramp(:,n),HRTmin(:,n));
%     %axis([0 4 0 0.10]);
%     title('Minimum HRT');
%     legend('hydrualic retention');
%     grid;
```

```
% end
% hold off
```

A.3.1 Matlab scripted for predicting the maximum methane production and minimum hydraulic retention time.

```
figno = 1;
noparams = 1;
points =20;
globalpoints = 2000;
paramp = zeros(points,noparams);

% p_opt = sdo.getParameterFromModel('Bernard_model_Contois',{'Tslurry'});
% p_opt.Value=285; % Temperature in kelvin
% p_opt.Minimum=283;
% p_opt.Maximum=306;
% p=p_opt;
Tslurrymin = 283;
Tslurrymax = 318;

% creating an experiment using one of the simulation data; in the my case
% the feeding rate Dfeedin.
qf = 1.005; % feed increase per day
qi = 0.0025; % initial q per day
```

```
qid = 100* qi; % initial q per day 1% pulse

for timegas = 1:60;
Dfeedin (timegas,:) = [timegas qi];% continuous feeding
%Dfeedind (timegas,:)= [timegas ; qid];% daily feed (1% of day ~ 15 minutes)
end

for timegas = 61:1825
Dfeedin (timegas,:) = [timegas qi*qf^(timegas-61)];% continuous feeding
%Dfeedind (timegas,:)= [timegas ; qid*qf^(timegas-61)];% daily feed (1% of day ~ 15 minutes)
end


Exp=sdo.Experiment('Bernard_model_Contois');
% Exp.InputData = timeseries(Dfeedin, Timegas);

methaneflow=Simulink.SimulationData.Signal;
methaneflow.Name = 'methaneflow';
methaneflow.BlockPath = 'Bernard_model_Contois/conv';
methaneflow.PortType = 'outport';
methaneflow.PortIndex = 1;
% methaneflow.Values = timeseries(gasrate,timegas);

Dmax = zeros(points,noparams);
Mmax = zeros(points,noparams);



%MAXIMUM LOADING RATE AND METHANE FLOWRATE (LOCAL SENSTIVITY)
  x = 1:noparams;
```

```
  for  y= 1:points

        if (x == 1) % in case you want to do multiparameter analysis
           Tslurry = [0 Tslurrymin + (y-1)*(Tslurrymax-Tslurrymin)/(points-1)];
        end

        Exp=sdo.Experiment('Bernard_model_Contois');
        % Exp = setEstimatedValues(Exp);
        Simulator = createSimulator(Exp);
        Simulator = sim(Simulator, 'ReturnWorkspaceOutputs', 'on', 'SrcWorkspace', 'base');
        SimLog =
find(Simulator.LoggedData,get_param('Bernard_model_Contois','SignalLoggingName'));
        methaneflowsim=find(SimLog,'methaneflow');



        Mmax(y,x) = max(methaneflowsim.Values.Data);
        m = find ((methaneflowsim.Values.Data)== max(methaneflowsim.Values.Data));
        tfail = methaneflowsim.Values.Time(m);
        Dmax(y,x) = Dfeedin(floor(tfail),2);
        paramp(y,x) = Tslurry(2);


 end


Dmaxn = Dmax/max(max(Dmax));
HRTmin = 1./Dmax;
```

```
figure(1)
for n=1
    plot(paramp(:,n),Mmax(:,n));
    %axis([0 4 0 10]);
    title('Maximum methane production');
    legend('methaneflow');
    grid;
end

figure(2)
for n=1
    plot(paramp(:,n),HRTmin(:,n));
    %axis([0 4 0 0.10]);
    title('Minimum HRT');
    legend('hydrualic retention');
    grid;
end
```

Appendix B
Thermal modelling of the different design of digester

B.1 Digester design CASE 1

```
%This program allows you to calculate the temperatures of every element of
%the biodigester for any day of the year, any hour of the day.
%The first phase is the initialization of the initial conditions to
%take into account the thermal inertia of certain elements of the digester.
%The second phase is the program itself.
%
%_____________________________________________________________________________%


%tic;
%Coordinates of the study site in Port Harcourt
% z=16; %Altitude of the study site
% theta=4.8156; %Latitude always between +90° and -90°
% Longitude=7.0498;
%Coordinates of the study site in Cuzco
z=3800; %Altitude of the study site
theta=-13.5125; %Latitude always between +90° and -90°
Longitude=-71.975833;
m_load=40; %total mass of the slurry addition
%Orientation and inclination of the biodigester and greenhouse roof
    omega=49; %orientation from south (West is +)
    beta=0; %inclination of the roof in degrees
%Initialization of the geometric parameters
```

```
    %Compositen of the biogas
    PerCH4=0.6; %percentage CH4 in the biogas by volume
    PerCO2=0.4; %percentage CO2 in the biogas by volume
    %Thicknesses (m)
    Th_insUpper=0.04; %thickness of upper insulation on both sides of the trench
    Th_insLower=0.06; %thickness of lower insulation on both sides of the trench
    Th_insBase=0.08; %thickness of insulation at the base of the trench
    Th_cover=0.5e-3; %thickness of the plastic cover
    Th_tube=2.5e-3; %thickness of the digester plastic
    %Widths (m)
    W_trTop=1.2; %Upper width of the trench
    W_trSide=0.23; % relative (horizontal) width of the sloping walls of the trench
    W_ww=0.3; %cross-sectional width of the adobe walls
    D_tube=1.5*2/pi; %diameter of the biodigester tube
    %Heights (m)
    H_tr=0.7; %Height of the trench
    k_straw=0.32;

    usevergilwind=0;  % Don't use Vergil wind as measured specific data to Peru project (set to 1
if required)
    datfile='Cuzco2010.Dat';
    CoverTransmissivity=0.65;
    Slopes = 1;
    if Slopes == 1
        H_w1 = 0.5;
        H_T = 1.03;
    else
            H_w1 = 0.5;
            H_T = 1.03;
    end
```

```
    %Lenths (m)
    L_ext=5.6; %Exterior length of the digester including the greenhouse
    L_int=5; %Length of the interior of the digester (length of the trench)

%Materials of each element
    MatAir='Air'; %Material of the outdoor the air
    MatCover='Agrofilm'; %Material of the cover
    MatAirInt='Air'; %Material of the interior air
    MatWall1='Adobe'; %Material of Wall1
    MatWall2='Adobe'; %Material of Wall2
    MatTube='Geomembrane'; %Material of the digester tube
    MatBiogas='Biogas'; %Material of the Biogas
    MatSlurry='Slurry'; %Material of the slurry
    MatSoil='Soil'; %Material of the soil
    MatInsul='Straw'; %Material of insulation


%Calculations of all other geometric parameters and introduction of the
%properties of the materials used
[ELEMENT,MATERIAL]=PropElement(k_straw,CoverTransmissivity,L_ext,L_int,H_w1,H_T,Slopes,W_trTop,W_w
w,H_tr,W_trSide,Th_cover,Th_tube,D_tube,Th_insBase,Th_insUpper,Th_insLower,PerCH4,PerCO2,MatAir,Ma
tCover,MatAirInt,MatWall1,MatWall2,MatTube,MatBiogas,MatSlurry,MatSoil,MatInsul);

disp('loading weather data...');
%Load ambient temperature and radiation data
[T_amb_C,Windspeed,TotalHorizontalSolarRadiation,DiffuseHorizontalSolarRadiation,DirectNormalSolar
Radiation,Month,DayOfMonth]=ImportData(datfile);
[T_max,T_min,Tt_max,Tt_min,Tavg,I]=TempAmbientMaxMin(T_amb_C);
```

```
% %Load wind speed data
% disp('loading wind speed data...')
% V = NaN(1,365);
%
% %updated by Vergil to include hourly wind speed data rather than daily, and divided all values
by 16 to normalize to Kayra.  (16 is March Average for SPZO divided by my study period average)
% for i=1:8760
%     if i<=744; %january hours
%         V(i)=20*10/36;
%     elseif 744<i && i<=1416; %february hours
%         V(i)=18*10/36;
%     elseif 1416<i && i<=2160; %march hours
%         V(i)=18*10/36;
%     elseif 2160<i && i<=2880; %april hours
%         V(i)=16*10/36;
%     elseif 2880<i && i<=3624; %may hours
%         V(i)=18*10/36;
%     elseif 3624<i && i<=4344; %june hours
%         V(i)=16*10/36;
%     elseif 4344<i && i<=5088;%july hours
%         V(i)=16*10/36;
%     elseif 5088<i && i<=5832; %august hours
%         V(i)=20*10/36;
%     elseif 5832<i && i<=6552; %september hours
%         V(i)=20*10/36;
%     elseif 6552<i && i<=7296; %october hours
%         V(i)=22*10/36;
%     elseif 7296<i && i<=8016; %november hours
%         V(i)=22*10/36;
%     elseif 8016<i && i<=8760; %december hours
```

```
%         V(i)=20*10/36;
%     end
% end
% V = V/16;
% %load wind data from study period (March 13, 1:00PM - March 30, 10:00AM
% %2010) (only if we're using Cuzco2010):
% %if strcmp(datfile,'Cuzco2010.dat')
% if usevergilwind == 1;
%   load('kayranew.mat')
%   V(1717:2122) = kayranew.wspeed(194:end); %insert wind speed data into V vector
% end
% disp('wind speed imported successfully')


%Introduction and differentiation of the walls and tube
disp('initializing geometry...')
% [surfacedescriptube,Ntube,wtube]=SurfaceGeometry(ELEMENT,'Tube');
% [surfacedescripwall1,Nwall1,wwall1]=SurfaceGeometry(ELEMENT,'Wall1');
% [surfacedescripwall2,Nwall2,wwall2]=SurfaceGeometry(ELEMENT,'Wall2');

surfacedescriptube=0;
Ntube=0;
wtube=0;


%Precalculate Total Solar Radiation incident on the elements of the digester (only need to run
this when geometry changes):
disp('calculating solar radiation. . .')
HOUR=1;
for day=1:365
```

```
    for hr=1:24
%         S_Cover(day,hr) =
SolarRadiationElementData(MATERIAL,Slopes,ELEMENT,DirectNormalSolarRadiation(day,hr),DiffuseHorizo
ntalSolarRadiation(day,hr),'Cover',theta,omega,day,hr,surfacedescripcover,Ncover,wcover);
%         S_Cover_H(HOUR) = S_Cover(day,hr);
%         S_Wall1(day,hr) =
SolarRadiationElementData(MATERIAL,Slopes,ELEMENT,DirectNormalSolarRadiation(day,hr),DiffuseHorizo
ntalSolarRadiation(day,hr),'Wall1',theta,omega,day,hr,surfacedescripwall1,Nwall1,wwall1);
%         S_Wall1_H(HOUR) = S_Wall1(day,hr);
%         S_Wall2(day,hr) =
SolarRadiationElementData(MATERIAL,Slopes,ELEMENT,DirectNormalSolarRadiation(day,hr),DiffuseHorizo
ntalSolarRadiation(day,hr),'Wall2',theta,omega,day,hr,surfacedescripwall2,Nwall2,wwall2);
%         S_Wall2_H(HOUR) = S_Wall2(day,hr);
        S_Tube(day,hr) =
SolarRadiationElementData(MATERIAL,Slopes,ELEMENT,DirectNormalSolarRadiation(day,hr),DiffuseHorizo
ntalSolarRadiation(day,hr),'Tube',theta,omega,day,hr,surfacedescriptube,Ntube,wtube);
        S_Tube_H(HOUR) = S_Tube(day,hr);
        hr=hr+1;
        HOUR=HOUR+1;
    end
    day=day+1;
end

% save('SolarRadGeom.mat', 'S_Cover', 'S_Wall1', 'S_Wall2', 'S_Tube');
%load('SolarRadGeom.mat');



%Precalculate view factors for each element of the digester (only need to
%run this when geometry changes).
```

```
disp('calculating viewfactors...');

%populate a struct with values for view factors which can be called later
% VF.Tube_Wall1 = ViewFactor(ELEMENT,'Tube','Wall1');
% VF.Tube_Cover = ViewFactor(ELEMENT,'Tube','Cover');
% VF.Tube_Wall2 = ViewFactor(ELEMENT,'Tube','Wall2');
% VF.Wall1_Cover = ViewFactor(ELEMENT,'Wall1','Cover');
% VF.Wall1_Wall2 = ViewFactor(ELEMENT,'Wall1','Wall2');
% VF.Wall1_Tube = ViewFactor(ELEMENT,'Wall1','Tube');
% VF.Wall2_Cover = ViewFactor(ELEMENT,'Wall2','Cover');
% VF.Wall2_Wall1 = ViewFactor(ELEMENT,'Wall2','Wall1');
% VF.Wall2_Tube = ViewFactor(ELEMENT,'Wall2','Tube');
% VF.Cover_Wall2 = ViewFactor(ELEMENT,'Cover','Wall2');
% VF.Cover_Tube = ViewFactor(ELEMENT,'Cover','Tube');
% VF.Cover_Wall1 = ViewFactor(ELEMENT,'Cover','Wall1');
% VF.Tube_Slurry = ViewFactor(ELEMENT,'Tube','Cover');
% VF.Slurry_Tube = ViewFactor(ELEMENT,'Slurry','Tube');
% save('VF.mat','VF')
 load('VF.mat')


%INITIALIZATION-----------------------------------------------
disp('initializing temperatures...')
% T_c = NaN(51,1);
T_t = NaN(51,1); %
% T_aint = NaN(51,1); % Temp air internal
T_g = NaN(51,1); % Temp biogas?
h_rad_c_sky = NaN(51,1);
h_conv_c_wind = NaN(51,1);
```

```
% T_w1 = NaN(365,24);
% h_rad_w1_sky = NaN(365,24);
% h_conv_w1_ext = NaN(365,24);
% T_w2 = NaN(365,24);
% h_rad_w2_sky = NaN(365,24);
% h_conv_w2_ext = NaN(365,24);
T_s = NaN(365,24);
h_cond_s_grSide = NaN(365,24);
h_cond_s_grBase = NaN(365,24);

%Initial Temperatures (K)
    %Elements with thermal mass
%     T0_w1=21+273;
%     T0_w2=22+273;
    T0_s=18+273;
    %Elements without thermal mass
%     T0_c=20+273;
    T0_t=23+273;
%     T0_aint=24+273;
    T0_g=25+273;

%Iterations over one year to initialize the temperatures
    %Elements with thermal mass
%     T_w1(1,1)=T0_w1;
%     T_w2(1,1)=T0_w2;
    T_s(1,1)=T0_s;
    %Elements without thermal mass
%     T_c(1)=T0_c;
    T_t(1)=T0_t;
%     T_aint(1)=T0_aint;
```

```
    T_g(1)=T0_g;

Exit=0;
Exit2=0;
H=0;


%initialize for speed:
T_grSide = NaN(1,365);
T_grBase = NaN(1,365);
T_amb_K = NaN(365,24);
T_sky = NaN(365,24);
HOUR = NaN(1,8760);
T_amb_K_H = NaN(1,8760);
T_sky_H = NaN(1,8760);

% Tc = NaN(365,24);
Tt = NaN(365,24);
% Taint = NaN(365,24);
Tg = NaN(365,24);
% Sc = NaN(365,24);
St = NaN(365,24);
hrad_c_sky = NaN(365,24);
hconv_c_wind = NaN(365,24);

% Tc_H = NaN(1,8760);
Tt_H = NaN(1,8760);
% Taint_H = NaN(1,8760);
Tg_H = NaN(1,8760);
% Sc_H = NaN(1,8760);
```

```
St_H = NaN(1,8760);
hrad_c_sky_H = NaN(1,8760);
hconv_c_wind_H = NaN(1,8760);
V=NaN(1,8760);

Losses_rad_c_sky_H = NaN(1,8760);
Losses_rad_c_sky = NaN(365,24);
Losses_c_wind_H = NaN(1,8760);
Losses_c_wind = NaN(365,24);

%store the data in a vector [hour of the year]
% T_w1_H = NaN(1,8760);
% T_w2_H = NaN(1,8760);
T_s_H = NaN(1,8760);
% h_rad_w1_sky_H = NaN(1,8760);
% h_conv_w1_ext_H = NaN(1,8760);
% h_rad_w2_sky_H = NaN(1,8760);
% h_conv_w2_ext_H = NaN(1,8760);
h_cond_s_grSide_H = NaN(1,8760);
h_cond_s_grBase_H = NaN(1,8760);


%Calculate the heat losses to the exterior
% Losses_rad_w1_sky_H = NaN(1,8760);
% Losses_rad_w1_sky = NaN(365,24);
% Losses_conv_w1_ext_H = NaN(1,8760);
% Losses_conv_w1_ext = NaN(365,24);
% Losses_rad_w2_sky_H = NaN(1,8760);
% Losses_rad_w2_sky = NaN(365,24);
% Losses_conv_w2_ext_H = NaN(1,8760);
```

```
% Losses_conv_w2_ext = NaN(365,24);
Losses_cond_s_grSide_H = NaN(1,8760);
Losses_cond_s_grSide = NaN(365,24);
Losses_cond_s_grBase_H = NaN(1,8760);
Losses_cond_s_grBase = NaN(365,24);

Month1 = NaN(1,8760);
DayOfMonth1 = NaN(1,8760);
disp('starting simulation. . .')
for d=1:365 % loop days of the year
    d1=d;
    tic
    [T_grSide(d),T_grBase(d)]=TempSoil(MATERIAL,ELEMENT,d,Tt_max,Tt_min,Tavg,I);
    T_amb_K(d,1)=T_amb_C(d,1)+273;
    T_sky(d,1)=0.0552*T_amb_K(d,1)^1.5;


    for h=1:23
        H=(d-1)*24+h;
        HOUR(H)=H;

        T_amb_K(d,h+1)=T_amb_C(d,h)+273;
        V(H)=Windspeed(d,h);
        T_sky(d,h+1)=0.0552*T_amb_K(d,h)^1.5; %Temperature of
        T_amb_K_H(H)=T_amb_K(d,h);
        T_sky_H(H)=T_sky(d,h);

        i=2;
```

```
%
[T_c(i),h_rad_c_sky(i),h_conv_c_wind(i)]=TempCover(Slopes,MATERIAL,ELEMENT,DirectNormalSolarRadiat
ion,DiffuseHorizontalSolarRadiation,V(H),z,theta,omega,d,h,T_amb_K(d,h),T_aint(i-
1),T_w2(d,h),T_t(i-1),T_w1(d,h),T_c(i-1),surfacedescripcover,Ncover,wcover,S_Cover(d,h),VF);

[T_t(i)]=TempTube(MATERIAL,ELEMENT,DirectNormalSolarRadiation,DiffuseHorizontalSolarRadiation,V(H)
,z,theta,omega,d,h,T_amb_K(d,h),T_t(i-1),T_s(d,h),T_g(i-
1),surfacedescriptube,Ntube,wtube,S_Tube(d,h),VF);
%         T_aint(i)=TempAirInt(MATERIAL,ELEMENT,z,theta,T_c(i-1),T_aint(i-
1),T_w1(d,h),T_w2(d,h),T_t(i-1));
        T_g(i)=TempBiogas(T_t(i-1),T_s(d,h));

        while ((abs(T_t(i)-T_t(i-1))>1)||(abs(T_g(i)-T_g(i-1))>1))&&(Exit==0)
            i=i+1;

%
[T_c(i),h_rad_c_sky(i),h_conv_c_wind(i)]=TempCover(Slopes,MATERIAL,ELEMENT,DirectNormalSolarRadiat
ion,DiffuseHorizontalSolarRadiation,V(H),z,theta,omega,d,h,T_amb_K(d,h),T_aint(i-
1),T_w2(d,h),T_t(i-1),T_w1(d,h),T_c(i-1),surfacedescripcover,Ncover,wcover,S_Cover(d,h),VF);

[T_t(i)]=TempTube(MATERIAL,ELEMENT,DirectNormalSolarRadiation,DiffuseHorizontalSolarRadiation,V(H)
,z,theta,omega,d,h,T_amb_K(d,h),T_t(i-1),T_s(d,h),T_g(i-
1),surfacedescriptube,Ntube,wtube,S_Tube(d,h),VF);
%             T_aint(i)=TempAirInt(MATERIAL,ELEMENT,z,theta,T_c(i-1),T_aint(i-
1),T_w1(d,h),T_w2(d,h),T_t(i-1));
            T_g(i)=TempBiogas(T_t(i-1),T_s(d,h));

            if i>50
                Exit=1;
            end
```

```
        end
        %Initialization of the variables for the iterations,
        %keeping the results obtained before
        Exit=0;
%         T_c(1)=T_c(i);
        T_t(1)=T_t(i);
%         T_aint(1)=T_aint(i);
        T_g(1)=T_g(i);

        %Store the data in a matrix [day,hour]
%         Tc(d,h)=T_c(1);
        Tt(d,h)=T_t(1);
%         Taint(d,h)=T_aint(1);
        Tg(d,h)=T_g(1);
        hrad_c_sky(d,h)=h_rad_c_sky(i);
        hconv_c_wind(d,h)=h_conv_c_wind(i);

        %Store the data in a vector [hour of the year]
%         Tc_H(H)=T_c(1);
        Tt_H(H)=T_t(1);
%         Taint_H(H)=T_aint(1);
        Tg_H(H)=T_g(1);
        hrad_c_sky_H(H)=h_rad_c_sky(i);
        hconv_c_wind_H(H)=h_conv_c_wind(i);

        %Calculate the heat loss to the exterior
%         Losses_rad_c_sky_H(H)=hrad_c_sky_H(H)*ELEMENT(5,2)*(Tc_H(H)-T_sky_H(H));
%         Losses_rad_c_sky(d,h)=Losses_rad_c_sky_H(H);
%         Losses_c_wind_H(H)=hconv_c_wind_H(H)*ELEMENT(5,2)*(Tc_H(H)-T_amb_K_H(H));
%         Losses_c_wind(d,h)=Losses_c_wind_H(H);
```

```
        %Calculate the temperatures of the elements with thermal mass
%
[T_w1(d,h+1),h_rad_w1_sky(d,h+1),h_conv_w1_ext(d,h+1)]=TempWall1(MATERIAL,ELEMENT,DirectNormalSola
rRadiation,DiffuseHorizontalSolarRadiation,V(H),z,theta,omega,d,h+1,T_t(1),T_c(1),T_amb_K(d,h+1),T
_aint(1),T_w2(d,h),T_w1(d,h),surfacedescripwall1,Nwall1,wwall1,S_Wall1(d,h),VF);
%
[T_w2(d,h+1),h_rad_w2_sky(d,h+1),h_conv_w2_ext(d,h+1)]=TempWall2(MATERIAL,ELEMENT,DirectNormalSola
rRadiation,DiffuseHorizontalSolarRadiation,V(H),z,theta,omega,d,h+1,T_t(1),T_c(1),T_amb_K(d,h+1),T
_aint(1),T_w1(d,h),T_w2(d,h),surfacedescripwall2,Nwall2,wwall2,S_Wall2(d,h),VF);

[T_s(d,h+1),h_cond_s_grSide(d,h+1),h_cond_s_grBase(d,h+1)]=TempSlurry(MATERIAL,ELEMENT,z,theta,h+1
,m_load,T_t(1),T_s(d,h),T_g(1),T_grSide(d),T_grBase(d),T_amb_K(d,h+1),VF);

        %store the data in a vector [hour of the year]
%         T_w1_H(H)=T_w1(d,h);
%         T_w2_H(H)=T_w2(d,h);
        T_s_H(H)=T_s(d,h);
%         h_rad_w1_sky_H(H)=h_rad_w1_sky(d,h);
%         h_conv_w1_ext_H(H)=h_conv_w1_ext(d,h);
%         h_rad_w2_sky_H(H)=h_rad_w2_sky(d,h);
%         h_conv_w2_ext_H(H)=h_conv_w2_ext(d,h);
        h_cond_s_grSide_H(H)=h_cond_s_grSide(d,h);
        h_cond_s_grBase_H(H)=h_cond_s_grBase(d,h);

        %Calculate the heat losses to the exterior
%         Losses_rad_w1_sky_H(H)=h_rad_w1_sky_H(H)*ELEMENT(5,3)*(T_w1_H(H)-T_sky_H(H));
%         Losses_rad_w1_sky(d,h)=Losses_rad_w1_sky_H(H);
%         Losses_conv_w1_ext_H(H)=h_conv_w1_ext_H(H)*ELEMENT(5,3)*(T_w1_H(H)-T_amb_K_H(H));
%         Losses_conv_w1_ext(d,h)=Losses_conv_w1_ext_H(H);
```

```
%          Losses_rad_w2_sky_H(H)=h_rad_w2_sky_H(H)*ELEMENT(5,4)*(T_w2_H(H)-T_sky_H(H));
%          Losses_rad_w2_sky(d,h)=Losses_rad_w2_sky_H(H);
%          Losses_conv_w2_ext_H(H)=h_conv_w2_ext_H(H)*ELEMENT(5,4)*(T_w2_H(H)-T_amb_K_H(H));
%          Losses_conv_w2_ext(d,h)=Losses_conv_w2_ext_H(H);
        Losses_cond_s_grSide_H(H)=h_cond_s_grSide_H(H)*ELEMENT(5,7)*(T_s_H(H)-T_grSide(d));
        Losses_cond_s_grSide(d,h)=Losses_cond_s_grSide_H(H);
        Losses_cond_s_grBase_H(H)=h_cond_s_grBase_H(H)*ELEMENT(5,8)*(T_s_H(H)-T_grBase(d));
        Losses_cond_s_grBase(d,h)=Losses_cond_s_grBase_H(H);

        Month1(H)=Month(d);
        DayOfMonth1(H)=DayOfMonth(d);

    end
    h=24;

    H=(d-1)*24+h;
    HOUR(H)=H;


    V(H)=Windspeed(d,h);
    T_amb_K(d,h)=T_amb_C(d,h)+273;
    T_sky(d,h)=0.0552*T_amb_K(d,h)^1.5;
    T_amb_K_H(H)=T_amb_K(d,h);
    T_sky_H(H)=T_sky(d,h);

    i=2;

%
[T_c(i),h_rad_c_sky(i),h_conv_c_wind(i)]=TempCover(Slopes,MATERIAL,ELEMENT,DirectNormalSolarRadiat
```

```
ion,DiffuseHorizontalSolarRadiation,V(H),z,theta,omega,d,h,T_amb_K(d,h),T_aint(i-
1),T_w2(d,h),T_t(i-1),T_w1(d,h),T_c(i-1),surfacedescripcover,Ncover,wcover,S_Cover(d,h),VF);

[T_t(i)]=TempTube(MATERIAL,ELEMENT,DirectNormalSolarRadiation,DiffuseHorizontalSolarRadiation,V(H)
,z,theta,omega,d,h,T_amb_K(d,h),T_t(i-1),T_s(d,h),T_g(i-
1),surfacedescriptube,Ntube,wtube,S_Tube(d,h),VF);
%     T_aint(i)=TempAirInt(MATERIAL,ELEMENT,z,theta,T_c(i-1),T_aint(i-
1),T_w1(d,h),T_w2(d,h),T_t(i-1));
    T_g(i)=TempBiogas(T_t(i-1),T_s(d,h));

    while ((abs(T_t(i)-T_t(i-1))>1)||((abs(T_g(i)-T_g(i-1))>1))&&(Exit2==0))
        i=i+1;

%
[T_c(i),h_rad_c_sky(i),h_conv_c_wind(i)]=TempCover(Slopes,MATERIAL,ELEMENT,DirectNormalSolarRadiat
ion,DiffuseHorizontalSolarRadiation,V(H),z,theta,omega,d,h,T_amb_K(d,h),T_aint(i-
1),T_w2(d,h),T_t(i-1),T_w1(d,h),T_c(i-1),surfacedescripcover,Ncover,wcover,S_Cover(d,h),VF);

[T_t(i)]=TempTube(MATERIAL,ELEMENT,DirectNormalSolarRadiation,DiffuseHorizontalSolarRadiation,V(H)
,z,theta,omega,d,h,T_amb_K(d,h),T_t(i-1),T_s(d,h),T_g(i-
1),surfacedescriptube,Ntube,wtube,S_Tube(d,h),VF);
%         T_aint(i)=TempAirInt(MATERIAL,ELEMENT,z,theta,T_c(i-1),T_aint(i-
1),T_w1(d,h),T_w2(d,h),T_t(i-1));
        T_g(i)=TempBiogas(T_t(i-1),T_s(d,h));

        if i>50
            Exit2=1;
        end
    end
    %Initilization of the variables for teh iterations, keeping the
```

```
    %last results obtained before
    Exit2=0;
%     T_c(1)=T_c(i);
    T_t(1)=T_t(i);
%     T_aint(1)=T_aint(i);
    T_g(1)=T_g(i);

    %Store the results in a matrix [day,hour]
%     Tc(d,h)=T_c(1);
    Tt(d,h)=T_t(1);
%     Taint(d,h)=T_aint(1);
    Tg(d,h)=T_g(1);
    hrad_c_sky(d,h)=h_rad_c_sky(i);
    hconv_c_wind(d,h)=h_conv_c_wind(i);

    %Store the results in a vector [hour of the year]
%     Tc_H(H)=T_c(1);
    Tt_H(H)=T_t(1);
%     Taint_H(H)=T_aint(1);
    Tg_H(H)=T_g(1);
    hrad_c_sky_H(H)=h_rad_c_sky(i);
    hconv_c_wind_H(H)=h_conv_c_wind(i);

    %Calculate the heat losses with the exterior
%     Losses_rad_c_sky_H(H)=hrad_c_sky_H(H)*ELEMENT(5,2)*(Tc_H(H)-T_sky_H(H));
%     Losses_rad_c_sky(d,h)=Losses_rad_c_sky_H(H);
%     Losses_c_wind_H(H)=hconv_c_wind_H(H)*ELEMENT(5,2)*(Tc_H(H)-T_amb_K_H(H));
%     Losses_c_wind(d,h)=Losses_c_wind_H(H);

    %Store the results in a vector[hour of the year]
```

```
%     T_w1_H(H)=T_w1(d,h);
%     T_w2_H(H)=T_w2(d,h);
    T_s_H(H)=T_s(d,h);
%     h_rad_w1_sky_H(H)=h_rad_w1_sky(d,h);
%     h_conv_w1_ext_H(H)=h_conv_w1_ext(d,h);
%     h_rad_w2_sky_H(H)=h_rad_w2_sky(d,h);
%     h_conv_w2_ext_H(H)=h_conv_w2_ext(d,h);
    h_cond_s_grSide_H(H)=h_cond_s_grSide(d,h);
    h_cond_s_grBase_H(H)=h_cond_s_grBase(d,h);

    %Calculate the losses to the exterior
%     Losses_rad_w1_sky_H(H)=h_rad_w1_sky_H(H)*ELEMENT(5,3)*(T_w1_H(H)-T_sky_H(H));
%     Losses_rad_w1_sky(d,h)=Losses_rad_w1_sky_H(H);
%     Losses_conv_w1_ext_H(H)=h_conv_w1_ext_H(H)*ELEMENT(5,3)*(T_w1_H(H)-T_amb_K_H(H));
%     Losses_conv_w1_ext(d,h)=Losses_conv_w1_ext_H(H);
%     Losses_rad_w2_sky_H(H)=h_rad_w2_sky_H(H)*ELEMENT(5,4)*(T_w2_H(H)-T_sky_H(H));
%     Losses_rad_w2_sky(d,h)=Losses_rad_w2_sky_H(H);
%     Losses_conv_w2_ext_H(H)=h_conv_w2_ext_H(H)*ELEMENT(5,4)*(T_w2_H(H)-T_amb_K_H(H));
%     Losses_conv_w2_ext(d,h)=Losses_conv_w2_ext_H(H);
    Losses_cond_s_grSide_H(H)=h_cond_s_grSide_H(H)*ELEMENT(5,7)*(T_s_H(H)-T_grSide(d));
    Losses_cond_s_grSide(d,h)=Losses_cond_s_grSide_H(H);
    Losses_cond_s_grBase_H(H)=h_cond_s_grBase_H(H)*ELEMENT(5,8)*(T_s_H(H)-T_grBase(d));
    Losses_cond_s_grBase(d,h)=Losses_cond_s_grBase_H(H);

    %Calculate the temperatures of the elements with thermal mass from the first hour of
    %the following day if we are not on the last day of the year
    if d~=365
        T_amb_K(d+1,1)=T_amb_C(d+1,1)+273;
        T_sky(d+1,1)=0.0552*T_amb_K(d+1,1)^1.5;
```

```
%
[T_w1(d+1,1),h_rad_w1_sky(d+1,1),h_conv_w1_ext(d+1,1)]=TempWall1(MATERIAL,ELEMENT,DirectNormalSola
rRadiation,DiffuseHorizontalSolarRadiation,V(d+1),z,theta,omega,d+1,h,T_t(1),T_c(1),T_amb_K(d+1,1)
,T_aint(1),T_w2(d,h),T_w1(d,h),surfacedescripwall1,Nwall1,wwall1,S_Wall1(d,h),VF);
%
[T_w2(d+1,1),h_rad_w2_sky(d+1,1),h_conv_w2_ext(d+1,1)]=TempWall2(MATERIAL,ELEMENT,DirectNormalSola
rRadiation,DiffuseHorizontalSolarRadiation,V(d+1),z,theta,omega,d+1,h,T_t(1),T_c(1),T_amb_K(d+1,1)
,T_aint(1),T_w1(d,h),T_w2(d,h),surfacedescripwall2,Nwall2,wwall2,S_Wall2(d,h),VF);

[T_s(d+1,1),h_cond_s_grSide(d+1,1),h_cond_s_grBase(d+1,1)]=TempSlurry(MATERIAL,ELEMENT,z,theta,h+1
,m_load,T_t(1),T_s(d,h),T_g(1),T_grSide(d),T_grBase(d),T_amb_K(d+1,1),VF);
    elseif d==365
        %Initialization of the temperatures of the elements with thermal mass
        %for the next calculatetions
        T_amb_K(1,1)=T_amb_C(1,1)+273;
        T_sky(1,1)=0.0552*T_amb_K(1,1)^1.5;

%
[T_w1(1,1),h_rad_w1_sky(1,1),h_conv_w1_ext(1,1)]=TempWall1(MATERIAL,ELEMENT,DirectNormalSolarRadia
tion,DiffuseHorizontalSolarRadiation,V(1),z,theta,omega,1,h,T_t(1),T_c(1),T_amb_K(1,1),T_aint(1),T
_w2(d,h),T_w1(d,h),surfacedescripwall1,Nwall1,wwall1,S_Wall1(d,h),VF);
%
[T_w2(1,1),h_rad_w2_sky(1,1),h_conv_w2_ext(1,1)]=TempWall2(MATERIAL,ELEMENT,DirectNormalSolarRadia
tion,DiffuseHorizontalSolarRadiation,V(1),z,theta,omega,1,h,T_t(1),T_c(1),T_amb_K(1,1),T_aint(1),T
_w1(d,h),T_w2(d,h),surfacedescripwall2,Nwall2,wwall2,S_Wall2(d,h),VF);

[T_s(1,1),h_cond_s_grSide(1,1),h_cond_s_grBase(1,1)]=TempSlurry(MATERIAL,ELEMENT,z,theta,h,m_load,
T_t(1),T_s(d,h),T_g(1),T_grSide(d),T_grBase(d),T_amb_K(1,1),VF);
    end
if d==182
```

```
    disp('25%')
end
    Month1(H)=Month(d);
    DayOfMonth1(H)=DayOfMonth(d);
    %toc
end

%xlswrite('SimulacionInicializacion.xls', [Month1' DayOfMonth1' HOUR' T_amb_K_H' T_sky_H' Tc_H'
Taint_H' T_w1_H' T_w2_H' Tt_H' Tg_H' T_s_H' Sc_H' Losses_rad_c_sky_H' Losses_c_wind_H'
Losses_rad_w1_sky_H' Losses_conv_w1_ext_H' Losses_rad_w2_sky_H' Losses_conv_w2_ext_H'
Losses_cond_s_grSide_H' Losses_cond_s_grBase_H']);
%time1=toc;
%No need to initialize the temperatures without thermal mass
%we'll just use the results from the last iteration

disp('50%')

Exit=0;
Exit2=0;
H=0;
%tic;
for d=1:365
    d2=d;
    [T_grSide(d),T_grBase(d)]=TempSoil(MATERIAL,ELEMENT,d,Tt_max,Tt_min,Tavg,I);
    T_amb_K(d,1)=T_amb_C(d,1)+273;
    T_sky(d,1)=0.0552*T_amb_K(d,1)^1.5;

    for h=1:23
        H=(d-1)*24+h;
        HOUR(H)=H;
```

```
        T_amb_K(d,h+1)=T_amb_C(d,h)+273;
        V(H)=Windspeed(d,h);
        T_sky(d,h+1)=0.0552*T_amb_K(d,h)^1.5;
        T_amb_K_H(H)=T_amb_K(d,h);
        T_sky_H(H)=T_sky(d,h);

        i=2;

%
[T_c(i),h_rad_c_sky(i),h_conv_c_wind(i)]=TempCover(Slopes,MATERIAL,ELEMENT,DirectNormalSolarRadiat
ion,DiffuseHorizontalSolarRadiation,V(H),z,theta,omega,d,h,T_amb_K(d,h),T_aint(i-
1),T_w2(d,h),T_t(i-1),T_w1(d,h),T_c(i-1),surfacedescripcover,Ncover,wcover,S_Cover(d,h),VF);

[T_t(i)]=TempTube(MATERIAL,ELEMENT,DirectNormalSolarRadiation,DiffuseHorizontalSolarRadiation,V(H)
,z,theta,omega,d,h,T_amb_K(d,h),T_t(i-1),T_s(d,h),T_g(i-
1),surfacedescriptube,Ntube,wtube,S_Tube(d,h),VF);
%         T_aint(i)=TempAirInt(MATERIAL,ELEMENT,z,theta,T_c(i-1),T_aint(i-
1),T_w1(d,h),T_w2(d,h),T_t(i-1));
        T_g(i)=TempBiogas(T_t(i-1),T_s(d,h));

        while ((abs(T_t(i)-T_t(i-1))>1)||(abs(T_g(i)-T_g(i-1))>1))&&(Exit==0)
            i=i+1;

%
[T_c(i),h_rad_c_sky(i),h_conv_c_wind(i)]=TempCover(Slopes,MATERIAL,ELEMENT,DirectNormalSolarRadiat
ion,DiffuseHorizontalSolarRadiation,V(H),z,theta,omega,d,h,T_amb_K(d,h),T_aint(i-
1),T_w2(d,h),T_t(i-1),T_w1(d,h),T_c(i-1),surfacedescripcover,Ncover,wcover,S_Cover(d,h),VF);

[T_t(i)]=TempTube(MATERIAL,ELEMENT,DirectNormalSolarRadiation,DiffuseHorizontalSolarRadiation,V(H)
```

```
,z,theta,omega,d,h,T_amb_K(d,h),T_t(i-1),T_s(d,h),T_g(i-
1),surfacedescriptube,Ntube,wtube,S_Tube(d,h),VF);
%             T_aint(i)=TempAirInt(MATERIAL,ELEMENT,z,theta,T_c(i-1),T_aint(i-
1),T_w1(d,h),T_w2(d,h),T_t(i-1));
            T_g(i)=TempBiogas(T_t(i-1),T_s(d,h));

            if i>50
                Exit=1;
            end
        end
        %Initialization of the variables for teh iterations, keeping                    o the
        %the last results obtained before
        Exit=0;
%         T_c(1)=T_c(i);
        T_t(1)=T_t(i);
%         T_aint(1)=T_aint(i);
        T_g(1)=T_g(i);

        %Store the data in a matrix [day,hour]
%         Tc(d,h)=T_c(1);
        Tt(d,h)=T_t(1);
%         Taint(d,h)=T_aint(1);
        Tg(d,h)=T_g(1);
        hrad_c_sky(d,h)=h_rad_c_sky(i);
        hconv_c_wind(d,h)=h_conv_c_wind(i);

        %%Store the data in a vector
%         Tc_H(H)=T_c(1);
        Tt_H(H)=T_t(1);
%         Taint_H(H)=T_aint(1);
```

```
        Tg_H(H)=T_g(1);
        hrad_c_sky_H(H)=h_rad_c_sky(i);
        hconv_c_wind_H(H)=h_conv_c_wind(i);

        %Calculate the losses of heat to the exterior
%         Losses_rad_c_sky_H(H)=hrad_c_sky_H(H)*ELEMENT(5,2)*(Tc_H(H)-T_sky_H(H));
%         Losses_rad_c_sky(d,h)=Losses_rad_c_sky_H(H);
%         Losses_c_wind_H(H)=hconv_c_wind_H(H)*ELEMENT(5,2)*(Tc_H(H)-T_amb_K_H(H));
%         Losses_c_wind(d,h)=Losses_c_wind_H(H);

        %Calculate the termperatures of the elements with thermal mass
%
[T_w1(d,h+1),h_rad_w1_sky(d,h+1),h_conv_w1_ext(d,h+1)]=TempWall1(MATERIAL,ELEMENT,DirectNormalSola
rRadiation,DiffuseHorizontalSolarRadiation,V(H),z,theta,omega,d,h+1,T_t(1),T_c(1),T_amb_K(d,h+1),T
_aint(1),T_w2(d,h),T_w1(d,h),surfacedescripwall1,Nwall1,wwall1,S_Wall1(d,h),VF);
%
[T_w2(d,h+1),h_rad_w2_sky(d,h+1),h_conv_w2_ext(d,h+1)]=TempWall2(MATERIAL,ELEMENT,DirectNormalSola
rRadiation,DiffuseHorizontalSolarRadiation,V(H),z,theta,omega,d,h+1,T_t(1),T_c(1),T_amb_K(d,h+1),T
_aint(1),T_w1(d,h),T_w2(d,h),surfacedescripwall2,Nwall2,wwall2,S_Wall2(d,h),VF);

[T_s(d,h+1),h_cond_s_grSide(d,h+1),h_cond_s_grBase(d,h+1)]=TempSlurry(MATERIAL,ELEMENT,z,theta,h+1
,m_load,T_t(1),T_s(d,h),T_g(1),T_grSide(d),T_grBase(d),T_amb_K(d,h+1),VF);

        %Store the data in a vector [hour of the year]
%         T_w1_H(H)=T_w1(d,h);
%         T_w2_H(H)=T_w2(d,h);
        T_s_H(H)=T_s(d,h);
%         h_rad_w1_sky_H(H)=h_rad_w1_sky(d,h);
%         h_conv_w1_ext_H(H)=h_conv_w1_ext(d,h);
%         h_rad_w2_sky_H(H)=h_rad_w2_sky(d,h);
```

```
%         h_conv_w2_ext_H(H)=h_conv_w2_ext(d,h);
        h_cond_s_grSide_H(H)=h_cond_s_grSide(d,h);
        h_cond_s_grBase_H(H)=h_cond_s_grBase(d,h);

        %Calculate the heat losses to the exterior
%         Losses_rad_w1_sky_H(H)=h_rad_w1_sky_H(H)*ELEMENT(5,3)*(T_w1_H(H)-T_sky_H(H));
%         Losses_rad_w1_sky(d,h)=Losses_rad_w1_sky_H(H);
%         Losses_conv_w1_ext_H(H)=h_conv_w1_ext_H(H)*ELEMENT(5,3)*(T_w1_H(H)-T_amb_K_H(H));
%         Losses_conv_w1_ext(d,h)=Losses_conv_w1_ext_H(H);
%         Losses_rad_w2_sky_H(H)=h_rad_w2_sky_H(H)*ELEMENT(5,4)*(T_w2_H(H)-T_sky_H(H));
%         Losses_rad_w2_sky(d,h)=Losses_rad_w2_sky_H(H);
%         Losses_conv_w2_ext_H(H)=h_conv_w2_ext_H(H)*ELEMENT(5,4)*(T_w2_H(H)-T_amb_K_H(H));
%         Losses_conv_w2_ext(d,h)=Losses_conv_w2_ext_H(H);
        Losses_cond_s_grSide_H(H)=h_cond_s_grSide_H(H)*ELEMENT(5,7)*(T_s_H(H)-T_grSide(d));
        Losses_cond_s_grSide(d,h)=Losses_cond_s_grSide_H(H);
        Losses_cond_s_grBase_H(H)=h_cond_s_grBase_H(H)*ELEMENT(5,8)*(T_s_H(H)-T_grBase(d));
        Losses_cond_s_grBase(d,h)=Losses_cond_s_grBase_H(H);


    end
    h=24;

    H=(d-1)*24+h;
    HOUR(H)=H;

    T_amb_K(d,h)=T_amb_C(d,h)+273;
    V(H)=Windspeed(d,h);
    T_sky(d,h)=0.0552*T_amb_K(d,h)^1.5;
    T_amb_K_H(H)=T_amb_K(d,h);
    T_sky_H(H)=T_sky(d,h);
```

```
    i=2;

%
[T_c(i),h_rad_c_sky(i),h_conv_c_wind(i)]=TempCover(Slopes,MATERIAL,ELEMENT,DirectNormalSolarRadiat
ion,DiffuseHorizontalSolarRadiation,V(H),z,theta,omega,d,h,T_amb_K(d,h),T_aint(i-
1),T_w2(d,h),T_t(i-1),T_w1(d,h),T_c(i-1),surfacedescripcover,Ncover,wcover,S_Cover(d,h),VF);

[T_t(i)]=TempTube(MATERIAL,ELEMENT,DirectNormalSolarRadiation,DiffuseHorizontalSolarRadiation,V(H)
,z,theta,omega,d,h,T_amb_K(d,h),T_t(i-1),T_s(d,h),T_g(i-
1),surfacedescriptube,Ntube,wtube,S_Tube(d,h),VF);
%     T_aint(i)=TempAirInt(MATERIAL,ELEMENT,z,theta,T_c(i-1),T_aint(i-
1),T_w1(d,h),T_w2(d,h),T_t(i-1));
    T_g(i)=TempBiogas(T_t(i-1),T_s(d,h));

    while ((abs(T_t(i)-T_t(i-1))>1)||(abs(T_g(i)-T_g(i-1))>1))&&(Exit2==0)
        i=i+1;

%
[T_c(i),h_rad_c_sky(i),h_conv_c_wind(i)]=TempCover(Slopes,MATERIAL,ELEMENT,DirectNormalSolarRadiat
ion,DiffuseHorizontalSolarRadiation,V(H),z,theta,omega,d,h,T_amb_K(d,h),T_aint(i-
1),T_w2(d,h),T_t(i-1),T_w1(d,h),T_c(i-1),surfacedescripcover,Ncover,wcover,S_Cover(d,h),VF);

[T_t(i)]=TempTube(MATERIAL,ELEMENT,DirectNormalSolarRadiation,DiffuseHorizontalSolarRadiation,V(H)
,z,theta,omega,d,h,T_amb_K(d,h),T_t(i-1),T_s(d,h),T_g(i-
1),surfacedescriptube,Ntube,wtube,S_Tube(d,h),VF);
%         T_aint(i)=TempAirInt(MATERIAL,ELEMENT,z,theta,T_c(i-1),T_aint(i-
1),T_w1(d,h),T_w2(d,h),T_t(i-1));
        T_g(i)=TempBiogas(T_t(i-1),T_s(d,h));
```

```
        if i>50
            Exit2=1;
        end
    end
    %Initialize the variables for teh iterations, keeping the
    %last results obtained before
    Exit2=0;
%     T_c(1)=T_c(i);
    T_t(1)=T_t(i);
%     T_aint(1)=T_aint(i);
    T_g(1)=T_g(i);

    %Store the data in a matrix [day,hour]
%     Tc(d,h)=T_c(1);
    Tt(d,h)=T_t(1);
%     Taint(d,h)=T_aint(1);
    Tg(d,h)=T_g(1);
    hrad_c_sky(d,h)=h_rad_c_sky(i);
    hconv_c_wind(d,h)=h_conv_c_wind(i);

    %Store the data in a vector [hour of the year]
%     Tc_H(H)=T_c(1);
    Tt_H(H)=T_t(1);
%     Taint_H(H)=T_aint(1);
    Tg_H(H)=T_g(1);
    hrad_c_sky_H(H)=h_rad_c_sky(i);
    hconv_c_wind_H(H)=h_conv_c_wind(i);

    %Calculate the losses of heat to the exterior
%     Losses_rad_c_sky_H(H)=hrad_c_sky_H(H)*ELEMENT(5,2)*(Tc_H(H)-T_sky_H(H));
```

```
%     Losses_rad_c_sky(d,h)=Losses_rad_c_sky_H(H);
%     Losses_c_wind_H(H)=hconv_c_wind_H(H)*ELEMENT(5,2)*(Tc_H(H)-T_amb_K_H(H));
%     Losses_c_wind(d,h)=Losses_c_wind_H(H);
%
    %Store the data in a vector [hour of the year]
%     T_w1_H(H)=T_w1(d,h);
%     T_w2_H(H)=T_w2(d,h);
    T_s_H(H)=T_s(d,h);
%     h_rad_w1_sky_H(H)=h_rad_w1_sky(d,h);
%     h_conv_w1_ext_H(H)=h_conv_w1_ext(d,h);
%     h_rad_w2_sky_H(H)=h_rad_w2_sky(d,h);
%     h_conv_w2_ext_H(H)=h_conv_w2_ext(d,h);
    h_cond_s_grSide_H(H)=h_cond_s_grSide(d,h);
    h_cond_s_grBase_H(H)=h_cond_s_grBase(d,h);

    %Calculate the losses of heat to the exterior
%     Losses_rad_w1_sky_H(H)=h_rad_w1_sky_H(H)*ELEMENT(5,3)*(T_w1_H(H)-T_sky_H(H));
%     Losses_rad_w1_sky(d,h)=Losses_rad_w1_sky_H(H);
%     Losses_conv_w1_ext_H(H)=h_conv_w1_ext_H(H)*ELEMENT(5,3)*(T_w1_H(H)-T_amb_K_H(H));
%     Losses_conv_w1_ext(d,h)=Losses_conv_w1_ext_H(H);
%     Losses_rad_w2_sky_H(H)=h_rad_w2_sky_H(H)*ELEMENT(5,4)*(T_w2_H(H)-T_sky_H(H));
%     Losses_rad_w2_sky(d,h)=Losses_rad_w2_sky_H(H);
%     Losses_conv_w2_ext_H(H)=h_conv_w2_ext_H(H)*ELEMENT(5,4)*(T_w2_H(H)-T_amb_K_H(H));
%     Losses_conv_w2_ext(d,h)=Losses_conv_w2_ext_H(H);
    Losses_cond_s_grSide_H(H)=h_cond_s_grSide_H(H)*ELEMENT(5,7)*(T_s_H(H)-T_grSide(d));
    Losses_cond_s_grSide(d,h)=Losses_cond_s_grSide_H(H);
    Losses_cond_s_grBase_H(H)=h_cond_s_grBase_H(H)*ELEMENT(5,8)*(T_s_H(H)-T_grBase(d));
    Losses_cond_s_grBase(d,h)=Losses_cond_s_grBase_H(H);

    %Calculate the temperatures of the elements for the first hour of the following day
```

```
    %if we're not on the last day of the year
    if d~=365
        T_amb_K(d+1,1)=T_amb_C(d+1,1)+273;
        T_sky(d+1,1)=0.0552*T_amb_K(d+1,1)^1.5;

%
[T_w1(d+1,1),h_rad_w1_sky(d+1,1),h_conv_w1_ext(d+1,1)]=TempWall1(MATERIAL,ELEMENT,DirectNormalSola
rRadiation,DiffuseHorizontalSolarRadiation,V(d+1),z,theta,omega,d+1,h,T_t(1),T_c(1),T_amb_K(d+1,1)
,T_aint(1),T_w2(d,h),T_w1(d,h),surfacedescripwall1,Nwall1,wwall1,S_Wall1(d,h),VF);
%
[T_w2(d+1,1),h_rad_w2_sky(d+1,1),h_conv_w2_ext(d+1,1)]=TempWall2(MATERIAL,ELEMENT,DirectNormalSola
rRadiation,DiffuseHorizontalSolarRadiation,V(d+1),z,theta,omega,d+1,h,T_t(1),T_c(1),T_amb_K(d+1,1)
,T_aint(1),T_w1(d,h),T_w2(d,h),surfacedescripwall2,Nwall2,wwall2,S_Wall2(d,h),VF);

[T_s(d+1,1),h_cond_s_grSide(d+1,1),h_cond_s_grBase(d+1,1)]=TempSlurry(MATERIAL,ELEMENT,z,theta,h+1
,m_load,T_t(1),T_s(d,h),T_g(1),T_grSide(d),T_grBase(d),T_amb_K(d+1,1),VF);
    end

    Month1(H)=Month(d);
    DayOfMonth1(H)=DayOfMonth(d);
if d==182
    disp('75%')
end
end
disp('100%')

format bank;
% disp('Convection Tube to Wind:')
% mean(Losses_t_wind_H)
disp('Conduction Slurry to Base:')
```

```
mean(Losses_cond_s_grBase_H)
disp('Conduction Slurry to Sides:')
mean(Losses_cond_s_grSide_H)
% disp('Convection Wall1 to Wind:')
% mean(Losses_conv_w1_ext_H)
% disp('Convection Wall2 to Wind:')
% mean(Losses_conv_w2_ext_H)
% disp('Radiation Tube to Sky:')
% mean(Losses_rad_t_sky_H)
% disp('Radiation Wall 1 to Sky:')
% mean(Losses_rad_w1_sky_H)
% disp('Radiation Wall 2 to Sky:')
% mean(Losses_rad_w2_sky_H)

% disp('Solar Radiation on Cover:')
% mean(S_Cover_H)
% disp('Solar Radiation on Wall 1:')
% mean(S_Wall1_H)
% disp('Solar Radiation on Wall 2:')
% mean(S_Wall2_H)
disp('Solar Radiation on Tube:')
mean(S_Tube_H)


%time2=toc;
```

B.2 Digester design CASE 2

```
%_____________________________BIODIGESTER_____________________________%
%This program allows you to calculate the temperatures of every element of
%the biodigester for any day of the year, any hour of the day.
%The first phase is the initialization of the initial conditions to
%take into account the thermal inertia of certain elements of the digester.
%The second phase is the program itself.
%
%_____________________________________________________________________%


%tic;
%Coordinates of the study site
z=3800; %Altutude of the study site
theta=-13.5125; %Latitude always between +90° and  -90°
Longitude=-71.975833;
m_load=40; %total mass of the slurry addition
%Orientation and inclination of the biodigester and greenhouse roof
    omega=49; %orientation from south (West is +)
    beta=30; %inclination of the roof in degrees
%Initialization of the geometric parameters
    %Compositen of the biogas
    PerCH4=0.6; %percentage CH4 in the biogas by volume
    PerCO2=0.4; %percentage CO2 in the biogas by volume
    %Thicknesses (m)
    Th_insUpper=0.04; %thickness of upper insulation on both sides of the trench
    Th_insLower=0.06; %thickness of lower insulation on both sides of the trench
    Th_insBase=0.08; %thickness of insulation at the base of the trench
```

```
    Th_cover=0.5e-3; %thickness of the plastic cover
    Th_tube=2.5e-3; %thickness of the digester plastic
    %Widths (m)
    W_trTop=1.2; %Upper width of the trench
    W_trSide=0.23; % relative (horizontal) width of the sloping walls of the trench
    W_ww=0.3; %cross-sectional width of the adobe walls
    D_tube=1.5*2/pi; %diameter of the biodigester tube
    %Heights (m)
    H_tr=0.7; %Height of the trench
    k_straw=0.32;

    usevergilwind=0;   % Dont use Vergil wind as measured specific data to Peru project (set to 1
if required)
    datfile='Cuzco2010.dat';
    CoverTransmissivity=0.65;
    Slopes = 1;
    if Slopes == 1
        H_w1 = 0.5;
        H_T = 1.03;
    else
            H_w1 = 0.5;
            H_T = 1.03;
    end

    %Lenths (m)
    L_ext=5.6; %Exterior length of the digester including the greenhouse
    L_int=5; %Length of the interior of the digester (length of the trench)

%Materials of each element
    MatAir='Air'; %Material of the outdoor the air
```

```
    MatCover='Agrofilm'; %Material of the cover
    MatAirInt='Air'; %Material of the interior air
    MatWall1='Adobe'; %Material of Wall1
    MatWall2='Adobe'; %Material of Wall2
    MatTube='Geomembrane'; %Material of the digester tube
    MatBiogas='Biogas'; %Material of the Biogas
    MatSlurry='Slurry'; %Material of the slurry
    MatSoil='Soil'; %Material of the soil
    MatInsul='Straw'; %Material of insulation



%Calculations of all other geometric parameters and introduction of the
%properties of the materials used
[ELEMENT,MATERIAL]=PropElement(k_straw,CoverTransmissivity,L_ext,L_int,H_w1,H_T,Slopes,W_trTop,W_w
w,H_tr,W_trSide,Th_cover,Th_tube,D_tube,Th_insBase,Th_insUpper,Th_insLower,PerCH4,PerCO2,MatAir,Ma
tCover,MatAirInt,MatWall1,MatWall2,MatTube,MatBiogas,MatSlurry,MatSoil,MatInsul);

disp('loading weather data...');
%Load ambient temperature and radiation data
[T_amb_C,TotalHorizontalSolarRadiation,DiffuseHorizontalSolarRadiation,DirectNormalSolarRadiation,
Month,DayOfMonth]=ImportData(datfile);
[T_max,T_min,Tt_max,Tt_min,Tavg,I]=TempAmbientMaxMin(T_amb_C);

%Load wind speed data
disp('loading wind speed data...')
V = NaN(1,365);
```

```
%updated by Vergil to include hourly wind speed data rather than daily, and divided all values by
16 to normalize to Kayra.  (16 is March Average for SPZO divided by my study period average)
for i=1:8760
    if i<=744; %january hours
        V(i)=20*10/36;
    elseif 744<i && i<=1416; %february hours
        V(i)=18*10/36;
    elseif 1416<i && i<=2160; %march hours
        V(i)=18*10/36;
    elseif 2160<i && i<=2880; %april hours
        V(i)=16*10/36;
    elseif 2880<i && i<=3624; %may hours
        V(i)=18*10/36;
    elseif 3624<i && i<=4344; %june hours
        V(i)=16*10/36;
    elseif 4344<i && i<=5088;%july hours
        V(i)=16*10/36;
    elseif 5088<i && i<=5832; %august hours
        V(i)=20*10/36;
    elseif 5832<i && i<=6552; %september hours
        V(i)=20*10/36;
    elseif 6552<i && i<=7296; %october hours
        V(i)=22*10/36;
    elseif 7296<i && i<=8016; %november hours
        V(i)=22*10/36;
    elseif 8016<i && i<=8760; %december hours
        V(i)=20*10/36;
    end
end
V = V/16;
```

```
%load wind data from study period (March 13, 1:00PM - March 30, 10:00AM
%2010) (only if we're using Cuzco2010):
%if strcmp(datfile,'Cuzco2010.dat')
if usevergilwind == 1;
    load('kayranew.mat')
    V(1717:2122) = kayranew.wspeed(194:end); %insert wind speed data into V vector
end
disp('wind speed imported successfully')


%Introduction and differentiation of the walls and tube
disp('initializing geometry...')
[surfacedescriptube,Ntube,wtube]=SurfaceGeometry(ELEMENT,'Tube');
[surfacedescripwall1,Nwall1,wwall1]=SurfaceGeometry(ELEMENT,'Wall1');
[surfacedescripwall2,Nwall2,wwall2]=SurfaceGeometry(ELEMENT,'Wall2');

surfacedescripcover=0;
Ncover=0;
wcover=0;


%Precalculate Total Solar Radiation incident on the elements of the digester (only need to run
this when geometry changes):
disp('calculating solar radiation. . .')
HOUR=1;
for day=1:365
    for hr=1:24
        S_Cover(day,hr) =
SolarRadiationElementData(MATERIAL,Slopes,ELEMENT,DirectNormalSolarRadiation(day,hr),DiffuseHorizo
ntalSolarRadiation(day,hr),'Cover',theta,omega,day,hr,surfacedescripcover,Ncover,wcover);
```

```
        S_Cover_H(HOUR) = S_Cover(day,hr);
        S_Wall1(day,hr) =
SolarRadiationElementData(MATERIAL,Slopes,ELEMENT,DirectNormalSolarRadiation(day,hr),DiffuseHorizo
ntalSolarRadiation(day,hr),'Wall1',theta,omega,day,hr,surfacedescripwall1,Nwall1,wwall1);
        S_Wall1_H(HOUR) = S_Wall1(day,hr);
        S_Wall2(day,hr) =
SolarRadiationElementData(MATERIAL,Slopes,ELEMENT,DirectNormalSolarRadiation(day,hr),DiffuseHorizo
ntalSolarRadiation(day,hr),'Wall2',theta,omega,day,hr,surfacedescripwall2,Nwall2,wwall2);
        S_Wall2_H(HOUR) = S_Wall2(day,hr);
        S_Tube(day,hr) =
SolarRadiationElementData(MATERIAL,Slopes,ELEMENT,DirectNormalSolarRadiation(day,hr),DiffuseHorizo
ntalSolarRadiation(day,hr),'Tube',theta,omega,day,hr,surfacedescriptube,Ntube,wtube);
        S_Tube_H(HOUR) = S_Tube(day,hr);
        hr=hr+1;
        HOUR=HOUR+1;
    end
    day=day+1;
end

% save('SolarRadGeom.mat', 'S_Cover', 'S_Wall1', 'S_Wall2', 'S_Tube');
%load('SolarRadGeom.mat');



%Precalculate view factors for each element of the digester (only need to
%run this when geometry changes).
disp('calculating viewfactors...');

%populate a struct with values for view factors which can be called later
VF.Tube_Wall1 = ViewFactor(ELEMENT,'Tube','Wall1');
```

```
VF.Tube_Cover = ViewFactor(ELEMENT,'Tube','Cover');
VF.Tube_Wall2 = ViewFactor(ELEMENT,'Tube','Wall2');
VF.Wall1_Cover = ViewFactor(ELEMENT,'Wall1','Cover');
VF.Wall1_Wall2 = ViewFactor(ELEMENT,'Wall1','Wall2');
VF.Wall1_Tube = ViewFactor(ELEMENT,'Wall1','Tube');
VF.Wall2_Cover = ViewFactor(ELEMENT,'Wall2','Cover');
VF.Wall2_Wall1 = ViewFactor(ELEMENT,'Wall2','Wall1');
VF.Wall2_Tube = ViewFactor(ELEMENT,'Wall2','Tube');
VF.Cover_Wall2 = ViewFactor(ELEMENT,'Cover','Wall2');
VF.Cover_Tube = ViewFactor(ELEMENT,'Cover','Tube');
VF.Cover_Wall1 = ViewFactor(ELEMENT,'Cover','Wall1');
VF.Tube_Slurry = ViewFactor(ELEMENT,'Tube','Cover');
VF.Slurry_Tube = ViewFactor(ELEMENT,'Slurry','Tube');
% save('VF.mat','VF')
% load('VF.mat')


%INITIALIZATION-----------------------------------------------
disp('initializing temperatures...')
T_c = NaN(51,1);
T_t = NaN(51,1); %
T_aint = NaN(51,1); % Temp air internal
T_g = NaN(51,1); % Temp biogas?
h_rad_c_sky = NaN(51,1);
h_conv_c_wind = NaN(51,1);

T_w1 = NaN(365,24);
h_rad_w1_sky = NaN(365,24);
h_conv_w1_ext = NaN(365,24);
T_w2 = NaN(365,24);
```

```
h_rad_w2_sky = NaN(365,24);
h_conv_w2_ext = NaN(365,24);
T_s = NaN(365,24);
h_cond_s_grSide = NaN(365,24);
h_cond_s_grBase = NaN(365,24);

%Initial Temperatures (K)
    %Elements with thermal mass
    T0_w1=21+273;
    T0_w2=22+273;
    T0_s=18+273;
    %Elements without thermal mass
    T0_c=20+273;
    T0_t=23+273;
    T0_aint=24+273;
    T0_g=25+273;



%Iterations over one year to initialize the temperatures
    %Elements with thermal mass
    T_w1(1,1)=T0_w1;
    T_w2(1,1)=T0_w2;
    T_s(1,1)=T0_s;
    %Elements without thermal mass
    T_c(1)=T0_c;
    T_t(1)=T0_t;
    T_aint(1)=T0_aint;
    T_g(1)=T0_g;
```

```
Exit=0;
Exit2=0;
H=0;


%initialize for speed:
T_grSide = NaN(1,365);
T_grBase = NaN(1,365);
T_amb_K = NaN(365,24);
T_sky = NaN(365,24);
HOUR = NaN(1,8760);
T_amb_K_H = NaN(1,8760);
T_sky_H = NaN(1,8760);

Tc = NaN(365,24);
Tt = NaN(365,24);
Taint = NaN(365,24);
Tg = NaN(365,24);
Sc = NaN(365,24);
St = NaN(365,24);
hrad_c_sky = NaN(365,24);
hconv_c_wind = NaN(365,24);

Tc_H = NaN(1,8760);
Tt_H = NaN(1,8760);
Taint_H = NaN(1,8760);
Tg_H = NaN(1,8760);
Sc_H = NaN(1,8760);
St_H = NaN(1,8760);
hrad_c_sky_H = NaN(1,8760);
```

```
hconv_c_wind_H = NaN(1,8760);

Losses_rad_c_sky_H = NaN(1,8760);
Losses_rad_c_sky = NaN(365,24);
Losses_c_wind_H = NaN(1,8760);
Losses_c_wind = NaN(365,24);

%store the data in a vector [hour of the year]
T_w1_H = NaN(1,8760);
T_w2_H = NaN(1,8760);
T_s_H = NaN(1,8760);
h_rad_w1_sky_H = NaN(1,8760);
h_conv_w1_ext_H = NaN(1,8760);
h_rad_w2_sky_H = NaN(1,8760);
h_conv_w2_ext_H = NaN(1,8760);
h_cond_s_grSide_H = NaN(1,8760);
h_cond_s_grBase_H = NaN(1,8760);

%Calculate the heat losses to the exterior
Losses_rad_w1_sky_H = NaN(1,8760);
Losses_rad_w1_sky = NaN(365,24);
Losses_conv_w1_ext_H = NaN(1,8760);
Losses_conv_w1_ext = NaN(365,24);
Losses_rad_w2_sky_H = NaN(1,8760);
Losses_rad_w2_sky = NaN(365,24);
Losses_conv_w2_ext_H = NaN(1,8760);
Losses_conv_w2_ext = NaN(365,24);
Losses_cond_s_grSide_H = NaN(1,8760);
Losses_cond_s_grSide = NaN(365,24);
Losses_cond_s_grBase_H = NaN(1,8760);
```

```
Losses_cond_s_grBase = NaN(365,24);

Month1 = NaN(1,8760);
DayOfMonth1 = NaN(1,8760);
disp('starting simulation. . .')
for d=1:365 % loop days of the year
    d1=d;
    tic
    [T_grSide(d),T_grBase(d)]=TempSoil(MATERIAL,ELEMENT,d,Tt_max,Tt_min,Tavg,I);
    T_amb_K(d,1)=T_amb_C(d,1)+273;
    T_sky(d,1)=0.0552*T_amb_K(d,1)^1.5;


    for h=1:23
        H=(d-1)*24+h;
        HOUR(H)=H;

        T_amb_K(d,h+1)=T_amb_C(d,h)+273;
        T_sky(d,h+1)=0.0552*T_amb_K(d,h)^1.5; %Temperature of
        T_amb_K_H(H)=T_amb_K(d,h);
        T_sky_H(H)=T_sky(d,h);

        i=2;


[T_c(i),h_rad_c_sky(i),h_conv_c_wind(i)]=TempCover(Slopes,MATERIAL,ELEMENT,DirectNormalSolarRadiat
ion,DiffuseHorizontalSolarRadiation,V(H),z,theta,omega,d,h,T_amb_K(d,h),T_aint(i-
1),T_w2(d,h),T_t(i-1),T_w1(d,h),T_c(i-1),surfacedescripcover,Ncover,wcover,S_Cover(d,h),VF);

[T_t(i)]=TempTube(MATERIAL,ELEMENT,DirectNormalSolarRadiation,DiffuseHorizontalSolarRadiation,z,th
```

```
eta,omega,d,h,T_t(i-1),T_c(i-1),T_w1(d,h),T_w2(d,h),T_s(d,h),T_aint(i-1),T_g(i-
1),surfacedescriptube,Ntube,wtube,S_Tube(d,h),VF);
        T_aint(i)=TempAirInt(MATERIAL,ELEMENT,z,theta,T_c(i-1),T_aint(i-
1),T_w1(d,h),T_w2(d,h),T_t(i-1));
        T_g(i)=TempBiogas(T_t(i-1),T_s(d,h));

        while ((abs(T_c(i)-T_c(i-1))>1)||(abs(T_t(i)-T_t(i-1))>1)||(abs(T_aint(i)-T_aint(i-
1))>1)||(abs(T_g(i)-T_g(i-1))>1))&&(Exit==0)
            i=i+1;


[T_c(i),h_rad_c_sky(i),h_conv_c_wind(i)]=TempCover(Slopes,MATERIAL,ELEMENT,DirectNormalSolarRadiat
ion,DiffuseHorizontalSolarRadiation,V(H),z,theta,omega,d,h,T_amb_K(d,h),T_aint(i-
1),T_w2(d,h),T_t(i-1),T_w1(d,h),T_c(i-1),surfacedescripcover,Ncover,wcover,S_Cover(d,h),VF);

[T_t(i)]=TempTube(MATERIAL,ELEMENT,DirectNormalSolarRadiation,DiffuseHorizontalSolarRadiation,z,th
eta,omega,d,h,T_t(i-1),T_c(i-1),T_w1(d,h),T_w2(d,h),T_s(d,h),T_aint(i-1),T_g(i-
1),surfacedescriptube,Ntube,wtube,S_Tube(d,h),VF);
            T_aint(i)=TempAirInt(MATERIAL,ELEMENT,z,theta,T_c(i-1),T_aint(i-
1),T_w1(d,h),T_w2(d,h),T_t(i-1));
            T_g(i)=TempBiogas(T_t(i-1),T_s(d,h));

            if i>50
                Exit=1;
            end
        end
        %Initialization of the variables for the iterations,
        %keeping the results obtained before
        Exit=0;
        T_c(1)=T_c(i);
```

```
        T_t(1)=T_t(i);
        T_aint(1)=T_aint(i);
        T_g(1)=T_g(i);

        %Store the data in a matrix [day,hour]
        Tc(d,h)=T_c(1);
        Tt(d,h)=T_t(1);
        Taint(d,h)=T_aint(1);
        Tg(d,h)=T_g(1);
        hrad_c_sky(d,h)=h_rad_c_sky(i);
        hconv_c_wind(d,h)=h_conv_c_wind(i);

        %Store the data in a vector [hour of the year]
        Tc_H(H)=T_c(1);
        Tt_H(H)=T_t(1);
        Taint_H(H)=T_aint(1);
        Tg_H(H)=T_g(1);
        hrad_c_sky_H(H)=h_rad_c_sky(i);
        hconv_c_wind_H(H)=h_conv_c_wind(i);

        %Calculate the heat loss to the exterior
        Losses_rad_c_sky_H(H)=hrad_c_sky_H(H)*ELEMENT(5,2)*(Tc_H(H)-T_sky_H(H));
        Losses_rad_c_sky(d,h)=Losses_rad_c_sky_H(H);
        Losses_c_wind_H(H)=hconv_c_wind_H(H)*ELEMENT(5,2)*(Tc_H(H)-T_amb_K_H(H));
        Losses_c_wind(d,h)=Losses_c_wind_H(H);

        %Calculate the temperatures of the elements with thermal mass

[T_w1(d,h+1),h_rad_w1_sky(d,h+1),h_conv_w1_ext(d,h+1)]=TempWall1(MATERIAL,ELEMENT,DirectNormalSola
```

```
rRadiation,DiffuseHorizontalSolarRadiation,V(H),z,theta,omega,d,h+1,T_t(1),T_c(1),T_amb_K(d,h+1),T
_aint(1),T_w2(d,h),T_w1(d,h),surfacedescripwall1,Nwall1,wwall1,S_Wall1(d,h),VF);

[T_w2(d,h+1),h_rad_w2_sky(d,h+1),h_conv_w2_ext(d,h+1)]=TempWall2(MATERIAL,ELEMENT,DirectNormalSola
rRadiation,DiffuseHorizontalSolarRadiation,V(H),z,theta,omega,d,h+1,T_t(1),T_c(1),T_amb_K(d,h+1),T
_aint(1),T_w1(d,h),T_w2(d,h),surfacedescripwall2,Nwall2,wwall2,S_Wall2(d,h),VF);

[T_s(d,h+1),h_cond_s_grSide(d,h+1),h_cond_s_grBase(d,h+1)]=TempSlurry(MATERIAL,ELEMENT,z,theta,h+1
,m_load,T_t(1),T_s(d,h),T_g(1),T_grSide(d),T_grBase(d),T_amb_K(d,h+1),VF);

        %store the data in a vector [hour of the year]
        T_w1_H(H)=T_w1(d,h);
        T_w2_H(H)=T_w2(d,h);
        T_s_H(H)=T_s(d,h);
        h_rad_w1_sky_H(H)=h_rad_w1_sky(d,h);
        h_conv_w1_ext_H(H)=h_conv_w1_ext(d,h);
        h_rad_w2_sky_H(H)=h_rad_w2_sky(d,h);
        h_conv_w2_ext_H(H)=h_conv_w2_ext(d,h);
        h_cond_s_grSide_H(H)=h_cond_s_grSide(d,h);
        h_cond_s_grBase_H(H)=h_cond_s_grBase(d,h);

        %Calculate the heat losses to the exterior
        Losses_rad_w1_sky_H(H)=h_rad_w1_sky_H(H)*ELEMENT(5,3)*(T_w1_H(H)-T_sky_H(H));
        Losses_rad_w1_sky(d,h)=Losses_rad_w1_sky_H(H);
        Losses_conv_w1_ext_H(H)=h_conv_w1_ext_H(H)*ELEMENT(5,3)*(T_w1_H(H)-T_amb_K_H(H));
        Losses_conv_w1_ext(d,h)=Losses_conv_w1_ext_H(H);
        Losses_rad_w2_sky_H(H)=h_rad_w2_sky_H(H)*ELEMENT(5,4)*(T_w2_H(H)-T_sky_H(H));
        Losses_rad_w2_sky(d,h)=Losses_rad_w2_sky_H(H);
        Losses_conv_w2_ext_H(H)=h_conv_w2_ext_H(H)*ELEMENT(5,4)*(T_w2_H(H)-T_amb_K_H(H));
        Losses_conv_w2_ext(d,h)=Losses_conv_w2_ext_H(H);
```

```
        Losses_cond_s_grSide_H(H)=h_cond_s_grSide_H(H)*ELEMENT(5,7)*(T_s_H(H)-T_grSide(d));
        Losses_cond_s_grSide(d,h)=Losses_cond_s_grSide_H(H);
        Losses_cond_s_grBase_H(H)=h_cond_s_grBase_H(H)*ELEMENT(5,8)*(T_s_H(H)-T_grBase(d));
        Losses_cond_s_grBase(d,h)=Losses_cond_s_grBase_H(H);

        Month1(H)=Month(d);
        DayOfMonth1(H)=DayOfMonth(d);

    end
    h=24;

    H=(d-1)*24+h;
    HOUR(H)=H;

    T_amb_K(d,h)=T_amb_C(d,h)+273;
    T_sky(d,h)=0.0552*T_amb_K(d,h)^1.5;
    T_amb_K_H(H)=T_amb_K(d,h);
    T_sky_H(H)=T_sky(d,h);

    i=2;


[T_c(i),h_rad_c_sky(i),h_conv_c_wind(i)]=TempCover(Slopes,MATERIAL,ELEMENT,DirectNormalSolarRadiat
ion,DiffuseHorizontalSolarRadiation,V(H),z,theta,omega,d,h,T_amb_K(d,h),T_aint(i-
1),T_w2(d,h),T_t(i-1),T_w1(d,h),T_c(i-1),surfacedescripcover,Ncover,wcover,S_Cover(d,h),VF);

[T_t(i)]=TempTube(MATERIAL,ELEMENT,DirectNormalSolarRadiation,DiffuseHorizontalSolarRadiation,z,th
eta,omega,d,h,T_t(i-1),T_c(i-1),T_w1(d,h),T_w2(d,h),T_s(d,h),T_aint(i-1),T_g(i-
1),surfacedescriptube,Ntube,wtube,S_Tube(d,h),VF);
```

```
    T_aint(i)=TempAirInt(MATERIAL,ELEMENT,z,theta,T_c(i-1),T_aint(i-1),T_w1(d,h),T_w2(d,h),T_t(i-
1));
    T_g(i)=TempBiogas(T_t(i-1),T_s(d,h));

    while ((abs(T_c(i)-T_c(i-1))>1)||(abs(T_t(i)-T_t(i-1))>1)||(abs(T_aint(i)-T_aint(i-
1))>1)||(abs(T_g(i)-T_g(i-1))>1))&&(Exit2==0)
        i=i+1;


[T_c(i),h_rad_c_sky(i),h_conv_c_wind(i)]=TempCover(Slopes,MATERIAL,ELEMENT,DirectNormalSolarRadiat
ion,DiffuseHorizontalSolarRadiation,V(H),z,theta,omega,d,h,T_amb_K(d,h),T_aint(i-
1),T_w2(d,h),T_t(i-1),T_w1(d,h),T_c(i-1),surfacedescripcover,Ncover,wcover,S_Cover(d,h),VF);

[T_t(i)]=TempTube(MATERIAL,ELEMENT,DirectNormalSolarRadiation,DiffuseHorizontalSolarRadiation,z,th
eta,omega,d,h,T_t(i-1),T_c(i-1),T_w1(d,h),T_w2(d,h),T_s(d,h),T_aint(i-1),T_g(i-
1),surfacedescriptube,Ntube,wtube,S_Tube(d,h),VF);
        T_aint(i)=TempAirInt(MATERIAL,ELEMENT,z,theta,T_c(i-1),T_aint(i-
1),T_w1(d,h),T_w2(d,h),T_t(i-1));
        T_g(i)=TempBiogas(T_t(i-1),T_s(d,h));

        if i>50
            Exit2=1;
        end
    end
    %Initilization of the variables for teh iterations, keeping the
    %last results obtained before
    Exit2=0;
    T_c(1)=T_c(i);
    T_t(1)=T_t(i);
    T_aint(1)=T_aint(i);
```

```
T_g(1)=T_g(i);

%Store the results in a matrix [day,hour]
Tc(d,h)=T_c(1);
Tt(d,h)=T_t(1);
Taint(d,h)=T_aint(1);
Tg(d,h)=T_g(1);
hrad_c_sky(d,h)=h_rad_c_sky(i);
hconv_c_wind(d,h)=h_conv_c_wind(i);

%Store the results in a vector [hour of the year]
Tc_H(H)=T_c(1);
Tt_H(H)=T_t(1);
Taint_H(H)=T_aint(1);
Tg_H(H)=T_g(1);
hrad_c_sky_H(H)=h_rad_c_sky(i);
hconv_c_wind_H(H)=h_conv_c_wind(i);

%Calculate the heat losses with the exterior
Losses_rad_c_sky_H(H)=hrad_c_sky_H(H)*ELEMENT(5,2)*(Tc_H(H)-T_sky_H(H));
Losses_rad_c_sky(d,h)=Losses_rad_c_sky_H(H);
Losses_c_wind_H(H)=hconv_c_wind_H(H)*ELEMENT(5,2)*(Tc_H(H)-T_amb_K_H(H));
Losses_c_wind(d,h)=Losses_c_wind_H(H);

%Store the results in a vector[hour of the year]
T_w1_H(H)=T_w1(d,h);
T_w2_H(H)=T_w2(d,h);
T_s_H(H)=T_s(d,h);
h_rad_w1_sky_H(H)=h_rad_w1_sky(d,h);
h_conv_w1_ext_H(H)=h_conv_w1_ext(d,h);
```

```
    h_rad_w2_sky_H(H)=h_rad_w2_sky(d,h);
    h_conv_w2_ext_H(H)=h_conv_w2_ext(d,h);
    h_cond_s_grSide_H(H)=h_cond_s_grSide(d,h);
    h_cond_s_grBase_H(H)=h_cond_s_grBase(d,h);

    %Calculate the losses to the exterior
    Losses_rad_w1_sky_H(H)=h_rad_w1_sky_H(H)*ELEMENT(5,3)*(T_w1_H(H)-T_sky_H(H));
    Losses_rad_w1_sky(d,h)=Losses_rad_w1_sky_H(H);
    Losses_conv_w1_ext_H(H)=h_conv_w1_ext_H(H)*ELEMENT(5,3)*(T_w1_H(H)-T_amb_K_H(H));
    Losses_conv_w1_ext(d,h)=Losses_conv_w1_ext_H(H);
    Losses_rad_w2_sky_H(H)=h_rad_w2_sky_H(H)*ELEMENT(5,4)*(T_w2_H(H)-T_sky_H(H));
    Losses_rad_w2_sky(d,h)=Losses_rad_w2_sky_H(H);
    Losses_conv_w2_ext_H(H)=h_conv_w2_ext_H(H)*ELEMENT(5,4)*(T_w2_H(H)-T_amb_K_H(H));
    Losses_conv_w2_ext(d,h)=Losses_conv_w2_ext_H(H);
    Losses_cond_s_grSide_H(H)=h_cond_s_grSide_H(H)*ELEMENT(5,7)*(T_s_H(H)-T_grSide(d));
    Losses_cond_s_grSide(d,h)=Losses_cond_s_grSide_H(H);
    Losses_cond_s_grBase_H(H)=h_cond_s_grBase_H(H)*ELEMENT(5,8)*(T_s_H(H)-T_grBase(d));
    Losses_cond_s_grBase(d,h)=Losses_cond_s_grBase_H(H);

    %Calculate the temperatures of the elements with thermal mass from the first hour of
    %the following day if we are not on the last day of the year
    if d~=365
        T_amb_K(d+1,1)=T_amb_C(d+1,1)+273;
        T_sky(d+1,1)=0.0552*T_amb_K(d+1,1)^1.5;


[T_w1(d+1,1),h_rad_w1_sky(d+1,1),h_conv_w1_ext(d+1,1)]=TempWall1(MATERIAL,ELEMENT,DirectNormalSola
rRadiation,DiffuseHorizontalSolarRadiation,V(d+1),z,theta,omega,d+1,h,T_t(1),T_c(1),T_amb_K(d+1,1)
,T_aint(1),T_w2(d,h),T_w1(d,h),surfacedescripwall1,Nwall1,wwall1,S_Wall1(d,h),VF);
```

```
[T_w2(d+1,1),h_rad_w2_sky(d+1,1),h_conv_w2_ext(d+1,1)]=TempWall2(MATERIAL,ELEMENT,DirectNormalSola
rRadiation,DiffuseHorizontalSolarRadiation,V(d+1),z,theta,omega,d+1,h,T_t(1),T_c(1),T_amb_K(d+1,1)
,T_aint(1),T_w1(d,h),T_w2(d,h),surfacedescripwall2,Nwall2,wwall2,S_Wall2(d,h),VF);

[T_s(d+1,1),h_cond_s_grSide(d+1,1),h_cond_s_grBase(d+1,1)]=TempSlurry(MATERIAL,ELEMENT,z,theta,h+1
,m_load,T_t(1),T_s(d,h),T_g(1),T_grSide(d),T_grBase(d),T_amb_K(d+1,1),VF);
    elseif d==365
        %Initialization of the temperatures of the elements with thermal mass
        %for the next calculatetions
        T_amb_K(1,1)=T_amb_C(1,1)+273;
        T_sky(1,1)=0.0552*T_amb_K(1,1)^1.5;


[T_w1(1,1),h_rad_w1_sky(1,1),h_conv_w1_ext(1,1)]=TempWall1(MATERIAL,ELEMENT,DirectNormalSolarRadia
tion,DiffuseHorizontalSolarRadiation,V(1),z,theta,omega,1,h,T_t(1),T_c(1),T_amb_K(1,1),T_aint(1),T
_w2(d,h),T_w1(d,h),surfacedescripwall1,Nwall1,wwall1,S_Wall1(d,h),VF);

[T_w2(1,1),h_rad_w2_sky(1,1),h_conv_w2_ext(1,1)]=TempWall2(MATERIAL,ELEMENT,DirectNormalSolarRadia
tion,DiffuseHorizontalSolarRadiation,V(1),z,theta,omega,1,h,T_t(1),T_c(1),T_amb_K(1,1),T_aint(1),T
_w1(d,h),T_w2(d,h),surfacedescripwall2,Nwall2,wwall2,S_Wall2(d,h),VF);

[T_s(1,1),h_cond_s_grSide(1,1),h_cond_s_grBase(1,1)]=TempSlurry(MATERIAL,ELEMENT,z,theta,h,m_load,
T_t(1),T_s(d,h),T_g(1),T_grSide(d),T_grBase(d),T_amb_K(1,1),VF);
    end
if d==182
    disp('25%')
end
    Month1(H)=Month(d);
    DayOfMonth1(H)=DayOfMonth(d);
```

```
    %toc
end

%xlswrite('SimulacionInicializacion.xls', [Month1' DayOfMonth1' HOUR' T_amb_K_H' T_sky_H' Tc_H'
Taint_H' T_w1_H' T_w2_H' Tt_H' Tg_H' T_s_H' Sc_H' Losses_rad_c_sky_H' Losses_c_wind_H'
Losses_rad_w1_sky_H' Losses_conv_w1_ext_H' Losses_rad_w2_sky_H' Losses_conv_w2_ext_H'
Losses_cond_s_grSide_H' Losses_cond_s_grBase_H']);
%time1=toc;
%No need to initialize the temperatures without thermal mass
%we'll just use the results from the last iteration

disp('50%')

Exit=0;
Exit2=0;
H=0;
%tic;
for d=1:365
    d2=d;
    [T_grSide(d),T_grBase(d)]=TempSoil(MATERIAL,ELEMENT,d,Tt_max,Tt_min,Tavg,I);
    T_amb_K(d,1)=T_amb_C(d,1)+273;
    T_sky(d,1)=0.0552*T_amb_K(d,1)^1.5;

    for h=1:23
        H=(d-1)*24+h;
        HOUR(H)=H;

        T_amb_K(d,h+1)=T_amb_C(d,h)+273;
        T_sky(d,h+1)=0.0552*T_amb_K(d,h)^1.5;
        T_amb_K_H(H)=T_amb_K(d,h);
```

```
        T_sky_H(H)=T_sky(d,h);

        i=2;


[T_c(i),h_rad_c_sky(i),h_conv_c_wind(i)]=TempCover(Slopes,MATERIAL,ELEMENT,DirectNormalSolarRadiat
ion,DiffuseHorizontalSolarRadiation,V(H),z,theta,omega,d,h,T_amb_K(d,h),T_aint(i-
1),T_w2(d,h),T_t(i-1),T_w1(d,h),T_c(i-1),surfacedescripcover,Ncover,wcover,S_Cover(d,h),VF);

[T_t(i)]=TempTube(MATERIAL,ELEMENT,DirectNormalSolarRadiation,DiffuseHorizontalSolarRadiation,z,th
eta,omega,d,h,T_t(i-1),T_c(i-1),T_w1(d,h),T_w2(d,h),T_s(d,h),T_aint(i-1),T_g(i-
1),surfacedescriptube,Ntube,wtube,S_Tube(d,h),VF);
        T_aint(i)=TempAirInt(MATERIAL,ELEMENT,z,theta,T_c(i-1),T_aint(i-
1),T_w1(d,h),T_w2(d,h),T_t(i-1));
        T_g(i)=TempBiogas(T_t(i-1),T_s(d,h));

        while ((abs(T_c(i)-T_c(i-1))>1)||(abs(T_t(i)-T_t(i-1))>1)||(abs(T_aint(i)-T_aint(i-
1))>1)||(abs(T_g(i)-T_g(i-1))>1))&&(Exit==0)
            i=i+1;


[T_c(i),h_rad_c_sky(i),h_conv_c_wind(i)]=TempCover(Slopes,MATERIAL,ELEMENT,DirectNormalSolarRadiat
ion,DiffuseHorizontalSolarRadiation,V(H),z,theta,omega,d,h,T_amb_K(d,h),T_aint(i-
1),T_w2(d,h),T_t(i-1),T_w1(d,h),T_c(i-1),surfacedescripcover,Ncover,wcover,S_Cover(d,h),VF);

[T_t(i)]=TempTube(MATERIAL,ELEMENT,DirectNormalSolarRadiation,DiffuseHorizontalSolarRadiation,z,th
eta,omega,d,h,T_t(i-1),T_c(i-1),T_w1(d,h),T_w2(d,h),T_s(d,h),T_aint(i-1),T_g(i-
1),surfacedescriptube,Ntube,wtube,S_Tube(d,h),VF);
            T_aint(i)=TempAirInt(MATERIAL,ELEMENT,z,theta,T_c(i-1),T_aint(i-
1),T_w1(d,h),T_w2(d,h),T_t(i-1));
```

```
    T_g(i)=TempBiogas(T_t(i-1),T_s(d,h));

    if i>50
        Exit=1;
    end
end
%Initialization of the variables for teh iterations, keeping                    o the
%the last results obtained before
Exit=0;
T_c(1)=T_c(i);
T_t(1)=T_t(i);
T_aint(1)=T_aint(i);
T_g(1)=T_g(i);

%Store the data in a matrix [day,hour]
Tc(d,h)=T_c(1);
Tt(d,h)=T_t(1);
Taint(d,h)=T_aint(1);
Tg(d,h)=T_g(1);
hrad_c_sky(d,h)=h_rad_c_sky(i);
hconv_c_wind(d,h)=h_conv_c_wind(i);

%%Store the data in a vector
Tc_H(H)=T_c(1);
Tt_H(H)=T_t(1);
Taint_H(H)=T_aint(1);
Tg_H(H)=T_g(1);
hrad_c_sky_H(H)=h_rad_c_sky(i);
hconv_c_wind_H(H)=h_conv_c_wind(i);
```

```
        %Calculate the losses of heat to the exterior
        Losses_rad_c_sky_H(H)=hrad_c_sky_H(H)*ELEMENT(5,2)*(Tc_H(H)-T_sky_H(H));
        Losses_rad_c_sky(d,h)=Losses_rad_c_sky_H(H);
        Losses_c_wind_H(H)=hconv_c_wind_H(H)*ELEMENT(5,2)*(Tc_H(H)-T_amb_K_H(H));
        Losses_c_wind(d,h)=Losses_c_wind_H(H);

        %Calculate the termperatures of the elements with thermal mass

[T_w1(d,h+1),h_rad_w1_sky(d,h+1),h_conv_w1_ext(d,h+1)]=TempWall1(MATERIAL,ELEMENT,DirectNormalSola
rRadiation,DiffuseHorizontalSolarRadiation,V(H),z,theta,omega,d,h+1,T_t(1),T_c(1),T_amb_K(d,h+1),T
_aint(1),T_w2(d,h),T_w1(d,h),surfacedescripwall1,Nwall1,wwall1,S_Wall1(d,h),VF);

[T_w2(d,h+1),h_rad_w2_sky(d,h+1),h_conv_w2_ext(d,h+1)]=TempWall2(MATERIAL,ELEMENT,DirectNormalSola
rRadiation,DiffuseHorizontalSolarRadiation,V(H),z,theta,omega,d,h+1,T_t(1),T_c(1),T_amb_K(d,h+1),T
_aint(1),T_w1(d,h),T_w2(d,h),surfacedescripwall2,Nwall2,wwall2,S_Wall2(d,h),VF);

[T_s(d,h+1),h_cond_s_grSide(d,h+1),h_cond_s_grBase(d,h+1)]=TempSlurry(MATERIAL,ELEMENT,z,theta,h+1
,m_load,T_t(1),T_s(d,h),T_g(1),T_grSide(d),T_grBase(d),T_amb_K(d,h+1),VF);

        %Store the data in a vector [hour of the year]
        T_w1_H(H)=T_w1(d,h);
        T_w2_H(H)=T_w2(d,h);
        T_s_H(H)=T_s(d,h);
        h_rad_w1_sky_H(H)=h_rad_w1_sky(d,h);
        h_conv_w1_ext_H(H)=h_conv_w1_ext(d,h);
        h_rad_w2_sky_H(H)=h_rad_w2_sky(d,h);
        h_conv_w2_ext_H(H)=h_conv_w2_ext(d,h);
        h_cond_s_grSide_H(H)=h_cond_s_grSide(d,h);
        h_cond_s_grBase_H(H)=h_cond_s_grBase(d,h);
```

```
        %Calculate the heat losses to the exterior
        Losses_rad_w1_sky_H(H)=h_rad_w1_sky_H(H)*ELEMENT(5,3)*(T_w1_H(H)-T_sky_H(H));
        Losses_rad_w1_sky(d,h)=Losses_rad_w1_sky_H(H);
        Losses_conv_w1_ext_H(H)=h_conv_w1_ext_H(H)*ELEMENT(5,3)*(T_w1_H(H)-T_amb_K_H(H));
        Losses_conv_w1_ext(d,h)=Losses_conv_w1_ext_H(H);
        Losses_rad_w2_sky_H(H)=h_rad_w2_sky_H(H)*ELEMENT(5,4)*(T_w2_H(H)-T_sky_H(H));
        Losses_rad_w2_sky(d,h)=Losses_rad_w2_sky_H(H);
        Losses_conv_w2_ext_H(H)=h_conv_w2_ext_H(H)*ELEMENT(5,4)*(T_w2_H(H)-T_amb_K_H(H));
        Losses_conv_w2_ext(d,h)=Losses_conv_w2_ext_H(H);
        Losses_cond_s_grSide_H(H)=h_cond_s_grSide_H(H)*ELEMENT(5,7)*(T_s_H(H)-T_grSide(d));
        Losses_cond_s_grSide(d,h)=Losses_cond_s_grSide_H(H);
        Losses_cond_s_grBase_H(H)=h_cond_s_grBase_H(H)*ELEMENT(5,8)*(T_s_H(H)-T_grBase(d));
        Losses_cond_s_grBase(d,h)=Losses_cond_s_grBase_H(H);


    end
    h=24;

    H=(d-1)*24+h;
    HOUR(H)=H;

    T_amb_K(d,h)=T_amb_C(d,h)+273;
    T_sky(d,h)=0.0552*T_amb_K(d,h)^1.5;
    T_amb_K_H(H)=T_amb_K(d,h);
    T_sky_H(H)=T_sky(d,h);

    i=2;


[T_c(i),h_rad_c_sky(i),h_conv_c_wind(i)]=TempCover(Slopes,MATERIAL,ELEMENT,DirectNormalSolarRadiat
```

```
ion,DiffuseHorizontalSolarRadiation,V(H),z,theta,omega,d,h,T_amb_K(d,h),T_aint(i-
1),T_w2(d,h),T_t(i-1),T_w1(d,h),T_c(i-1),surfacedescripcover,Ncover,wcover,S_Cover(d,h),VF);

[T_t(i)]=TempTube(MATERIAL,ELEMENT,DirectNormalSolarRadiation,DiffuseHorizontalSolarRadiation,z,th
eta,omega,d,h,T_t(i-1),T_c(i-1),T_w1(d,h),T_w2(d,h),T_s(d,h),T_aint(i-1),T_g(i-
1),surfacedescriptube,Ntube,wtube,S_Tube(d,h),VF);
    T_aint(i)=TempAirInt(MATERIAL,ELEMENT,z,theta,T_c(i-1),T_aint(i-1),T_w1(d,h),T_w2(d,h),T_t(i-
1));
    T_g(i)=TempBiogas(T_t(i-1),T_s(d,h));

    while ((abs(T_c(i)-T_c(i-1))>1)||(abs(T_t(i)-T_t(i-1))>1)||(abs(T_aint(i)-T_aint(i-
1))>1)||(abs(T_g(i)-T_g(i-1))>1))&&(Exit2==0)
        i=i+1;


[T_c(i),h_rad_c_sky(i),h_conv_c_wind(i)]=TempCover(Slopes,MATERIAL,ELEMENT,DirectNormalSolarRadiat
ion,DiffuseHorizontalSolarRadiation,V(H),z,theta,omega,d,h,T_amb_K(d,h),T_aint(i-
1),T_w2(d,h),T_t(i-1),T_w1(d,h),T_c(i-1),surfacedescripcover,Ncover,wcover,S_Cover(d,h),VF);

[T_t(i)]=TempTube(MATERIAL,ELEMENT,DirectNormalSolarRadiation,DiffuseHorizontalSolarRadiation,z,th
eta,omega,d,h,T_t(i-1),T_c(i-1),T_w1(d,h),T_w2(d,h),T_s(d,h),T_aint(i-1),T_g(i-
1),surfacedescriptube,Ntube,wtube,S_Tube(d,h),VF);
        T_aint(i)=TempAirInt(MATERIAL,ELEMENT,z,theta,T_c(i-1),T_aint(i-
1),T_w1(d,h),T_w2(d,h),T_t(i-1));
        T_g(i)=TempBiogas(T_t(i-1),T_s(d,h));

        if i>50
            Exit2=1;
        end
    end
```

```
%Initialize the variables for teh iterations, keeping the
%last results obtained before
Exit2=0;
T_c(1)=T_c(i);
T_t(1)=T_t(i);
T_aint(1)=T_aint(i);
T_g(1)=T_g(i);

%Store the data in a matrix [day,hour]
Tc(d,h)=T_c(1);
Tt(d,h)=T_t(1);
Taint(d,h)=T_aint(1);
Tg(d,h)=T_g(1);
hrad_c_sky(d,h)=h_rad_c_sky(i);
hconv_c_wind(d,h)=h_conv_c_wind(i);

%Store the data in a vector [hour of the year]
Tc_H(H)=T_c(1);
Tt_H(H)=T_t(1);
Taint_H(H)=T_aint(1);
Tg_H(H)=T_g(1);
hrad_c_sky_H(H)=h_rad_c_sky(i);
hconv_c_wind_H(H)=h_conv_c_wind(i);

%Calculate the losses of heat to the exterior
Losses_rad_c_sky_H(H)=hrad_c_sky_H(H)*ELEMENT(5,2)*(Tc_H(H)-T_sky_H(H));
Losses_rad_c_sky(d,h)=Losses_rad_c_sky_H(H);
Losses_c_wind_H(H)=hconv_c_wind_H(H)*ELEMENT(5,2)*(Tc_H(H)-T_amb_K_H(H));
Losses_c_wind(d,h)=Losses_c_wind_H(H);
```

```
%Store the data in a vector [hour of the year]
T_w1_H(H)=T_w1(d,h);
T_w2_H(H)=T_w2(d,h);
T_s_H(H)=T_s(d,h);
h_rad_w1_sky_H(H)=h_rad_w1_sky(d,h);
h_conv_w1_ext_H(H)=h_conv_w1_ext(d,h);
h_rad_w2_sky_H(H)=h_rad_w2_sky(d,h);
h_conv_w2_ext_H(H)=h_conv_w2_ext(d,h);
h_cond_s_grSide_H(H)=h_cond_s_grSide(d,h);
h_cond_s_grBase_H(H)=h_cond_s_grBase(d,h);

%Calculate the losses of heat to the exterior
Losses_rad_w1_sky_H(H)=h_rad_w1_sky_H(H)*ELEMENT(5,3)*(T_w1_H(H)-T_sky_H(H));
Losses_rad_w1_sky(d,h)=Losses_rad_w1_sky_H(H);
Losses_conv_w1_ext_H(H)=h_conv_w1_ext_H(H)*ELEMENT(5,3)*(T_w1_H(H)-T_amb_K_H(H));
Losses_conv_w1_ext(d,h)=Losses_conv_w1_ext_H(H);
Losses_rad_w2_sky_H(H)=h_rad_w2_sky_H(H)*ELEMENT(5,4)*(T_w2_H(H)-T_sky_H(H));
Losses_rad_w2_sky(d,h)=Losses_rad_w2_sky_H(H);
Losses_conv_w2_ext_H(H)=h_conv_w2_ext_H(H)*ELEMENT(5,4)*(T_w2_H(H)-T_amb_K_H(H));
Losses_conv_w2_ext(d,h)=Losses_conv_w2_ext_H(H);
Losses_cond_s_grSide_H(H)=h_cond_s_grSide_H(H)*ELEMENT(5,7)*(T_s_H(H)-T_grSide(d));
Losses_cond_s_grSide(d,h)=Losses_cond_s_grSide_H(H);
Losses_cond_s_grBase_H(H)=h_cond_s_grBase_H(H)*ELEMENT(5,8)*(T_s_H(H)-T_grBase(d));
Losses_cond_s_grBase(d,h)=Losses_cond_s_grBase_H(H);

%Calculate the temperatures of the elements for the first hour of the following day
%if we're not on the last day of the year
if d~=365
    T_amb_K(d+1,1)=T_amb_C(d+1,1)+273;
    T_sky(d+1,1)=0.0552*T_amb_K(d+1,1)^1.5;
```

```
[T_w1(d+1,1),h_rad_w1_sky(d+1,1),h_conv_w1_ext(d+1,1)]=TempWall1(MATERIAL,ELEMENT,DirectNormalSola
rRadiation,DiffuseHorizontalSolarRadiation,V(d+1),z,theta,omega,d+1,h,T_t(1),T_c(1),T_amb_K(d+1,1)
,T_aint(1),T_w2(d,h),T_w1(d,h),surfacedescripwall1,Nwall1,wwall1,S_Wall1(d,h),VF);

[T_w2(d+1,1),h_rad_w2_sky(d+1,1),h_conv_w2_ext(d+1,1)]=TempWall2(MATERIAL,ELEMENT,DirectNormalSola
rRadiation,DiffuseHorizontalSolarRadiation,V(d+1),z,theta,omega,d+1,h,T_t(1),T_c(1),T_amb_K(d+1,1)
,T_aint(1),T_w1(d,h),T_w2(d,h),surfacedescripwall2,Nwall2,wwall2,S_Wall2(d,h),VF);

[T_s(d+1,1),h_cond_s_grSide(d+1,1),h_cond_s_grBase(d+1,1)]=TempSlurry(MATERIAL,ELEMENT,z,theta,h+1
,m_load,T_t(1),T_s(d,h),T_g(1),T_grSide(d),T_grBase(d),T_amb_K(d+1,1),VF);
    end

    Month1(H)=Month(d);
    DayOfMonth1(H)=DayOfMonth(d);
if d==182
    disp('75%')
end
end
disp('100%')

format bank;
disp('Convection Cover to Wind:')
mean(Losses_c_wind_H)
disp('Conduction Slurry to Base:')
mean(Losses_cond_s_grBase_H)
disp('Conduction Slurry to Sides:')
mean(Losses_cond_s_grSide_H)
disp('Convection Wall1 to Wind:')
```

```
mean(Losses_conv_w1_ext_H)
disp('Convection Wall2 to Wind:')
mean(Losses_conv_w2_ext_H)
disp('Radiation Cover to Sky:')
mean(Losses_rad_c_sky_H)
disp('Radiation Wall 1 to Sky:')
mean(Losses_rad_w1_sky_H)
disp('Radiation Wall 2 to Sky:')
mean(Losses_rad_w2_sky_H)

disp('Solar Radiation on Cover:')
mean(S_Cover_H)
disp('Solar Radiation on Wall 1:')
mean(S_Wall1_H)
disp('Solar Radiation on Wall 2:')
mean(S_Wall2_H)
disp('Solar Radiation on Tube:')
mean(S_Tube_H)



%time2=toc;
```

B.3 Digester design CASE

B.3.1.2 Main digester Tank model

```
%_____________________________BIODIGESTER_____________________________%
%This program allows you to calculate the temperatures of every element of
%the biodigester for any day of the year, any hour of the day.
%The first phase is the initialization of the initial conditions to
%take into account the thermal inertia of certain elements of the digester.
%The second phase is the program itself.
_____________________________________________________________________%


%tic;
%Coordinates of the study site
z=3800; %Altutude of the study site
theta=-13.5125; %Latitude always between +90° and -90°
Longitude=-71.975833;
m_load=40; %total mass of the slurry addition
%Orientation and inclination of the biodigester and greenhouse roof
    omega=49; %orientation from south (West is +)
    beta=30; %inclination of the roof in degrees
%Initialization of the geometric parameters
    %Compositen of the biogas
    PerCH4=0.6; %percentage CH4 in the biogas by volume
    PerCO2=0.4; %percentage CO2 in the biogas by volume
    %Thicknesses (m)
    Th_insUpper=0.04; %thickness of upper insulation on both sides of the trench
    Th_insLower=0.06; %thickness of lower insulation on both sides of the trench
    Th_insBase=0.08; %thickness of insulation at the base of the trench
```

```
    Th_cover=0.5e-3; %thickness of the plastic cover
    Th_tube=2.5e-3; %thickness of the digester plastic
    %Widths (m)
    W_trTop=1.2; %Upper width of the trench
    W_trSide=0.23; % relative (horizontal) width of the sloping walls of the trench
    W_ww=0.3; %cross-sectional width of the adobe walls
    D_tube=1.5*2/pi; %diameter of the biodigester tube
    %Heights (m)
    H_tr=0.7; %Height of the trench
    k_straw=0.32;

    usevergilwind=0;   % Dont use Vergil wind as measured specific data to Peru project (set to 1
if required)
    datfile='Cuzco2012.Dat';
    CoverTransmissivity=0.65;
    Slopes = 1;
    if Slopes == 1
        H_w1 = 0.5;
        H_T = 1.03;
    else
            H_w1 = 0.5;
            H_T = 1.03;
    end

    %Lenths (m)
    L_ext=5.6; %Exterior length of the digester including the greenhouse
    L_int=5; %Length of the interior of the digester (length of the trench)

%Materials of each element
    MatAir='Air'; %Material of the outdoor the air
```

```
    MatCover='Agrofilm'; %Material of the cover
    MatAirInt='Air'; %Material of the interior air
    MatWall1='Adobe'; %Material of Wall1
    MatWall2='Adobe'; %Material of Wall2
    MatTube='Geomembrane'; %Material of the digester tube
    MatBiogas='Biogas'; %Material of the Biogas
    MatSlurry='Slurry'; %Material of the slurry
    MatSoil='Soil'; %Material of the soil
    MatInsul='Straw'; %Material of insulation


%Calculations of all other geometric parameters and introduction of the
%properties of the materials used
[ELEMENT,MATERIAL]=PropElement(k_straw,CoverTransmissivity,L_ext,L_int,H_w1,H_T,Slopes,W_trTop,W_w
w,H_tr,W_trSide,Th_cover,Th_tube,D_tube,Th_insBase,Th_insUpper,Th_insLower,PerCH4,PerCO2,MatAir,Ma
tCover,MatAirInt,MatWall1,MatWall2,MatTube,MatBiogas,MatSlurry,MatSoil,MatInsul);

disp('loading weather data...');
%Load ambient temperature and radiation data
[T_amb_C,SlurryTemp,TotalHorizontalSolarRadiation,DiffuseHorizontalSolarRadiation,DirectNormalSola
rRadiation,Month,DayOfMonth]=ImportData1(datfile);
[T_max,T_min,Tt_max,Tt_min,Tavg,I]=TempAmbientMaxMin(T_amb_C);

%Load wind speed data
disp('loading wind speed data...')
V = NaN(1,365);

%updated by Vergil to include hourly wind speed data rather than daily, and divided all values by
16 to normalize to Kayra.  (16 is March Average for SPZO divided by my study period average)
for i=1:8760
```

```
    if i<=744; %january hours
        V(i)=20*10/36;
    elseif 744<i && i<=1416; %february hours
        V(i)=18*10/36;
    elseif 1416<i && i<=2160; %march hours
        V(i)=18*10/36;
    elseif 2160<i && i<=2880; %april hours
        V(i)=16*10/36;
    elseif 2880<i && i<=3624; %may hours
        V(i)=18*10/36;
    elseif 3624<i && i<=4344; %june hours
        V(i)=16*10/36;
    elseif 4344<i && i<=5088;%july hours
        V(i)=16*10/36;
    elseif 5088<i && i<=5832; %august hours
        V(i)=20*10/36;
    elseif 5832<i && i<=6552; %september hours
        V(i)=20*10/36;
    elseif 6552<i && i<=7296; %october hours
        V(i)=22*10/36;
    elseif 7296<i && i<=8016; %november hours
        V(i)=22*10/36;
    elseif 8016<i && i<=8760; %december hours
        V(i)=20*10/36;
    end
end
V = V/16;
%load wind data from study period (March 13, 1:00PM - March 30, 10:00AM
%2010) (only if we're using Cuzco2010):
%if strcmp(datfile,'Cuzco2010.dat')
```

```
if usevergilwind == 1;
    load('kayranew.mat')
    V(1717:2122) = kayranew.wspeed(194:end); %insert wind speed data into V vector
end
disp('wind speed imported successfully')


%Introduction and differentiation of the walls and tube
disp('initializing geometry...')
[surfacedescriptube,Ntube,wtube]=SurfaceGeometry(ELEMENT,'Tube');
[surfacedescripwall1,Nwall1,wwall1]=SurfaceGeometry(ELEMENT,'Wall1');
[surfacedescripwall2,Nwall2,wwall2]=SurfaceGeometry(ELEMENT,'Wall2');

surfacedescripcover=0;
Ncover=0;
wcover=0;


%Precalculate Total Solar Radiation incident on the elements of the digester (only need to run
this when geometry changes):
disp('calculating solar radiation. . .')
HOUR=1;
for day=1:365
    for hr=1:24
        S_Cover(day,hr) =
SolarRadiationElementData(MATERIAL,Slopes,ELEMENT,DirectNormalSolarRadiation(day,hr),DiffuseHorizo
ntalSolarRadiation(day,hr),'Cover',theta,omega,day,hr,surfacedescripcover,Ncover,wcover);
        S_Cover_H(HOUR) = S_Cover(day,hr);
```

```
        S_Wall1(day,hr) =
SolarRadiationElementData(MATERIAL,Slopes,ELEMENT,DirectNormalSolarRadiation(day,hr),DiffuseHorizo
ntalSolarRadiation(day,hr),'Wall1',theta,omega,day,hr,surfacedescripwall1,Nwall1,wwall1);
        S_Wall1_H(HOUR) = S_Wall1(day,hr);
        S_Wall2(day,hr) =
SolarRadiationElementData(MATERIAL,Slopes,ELEMENT,DirectNormalSolarRadiation(day,hr),DiffuseHorizo
ntalSolarRadiation(day,hr),'Wall2',theta,omega,day,hr,surfacedescripwall2,Nwall2,wwall2);
        S_Wall2_H(HOUR) = S_Wall2(day,hr);
        S_Tube(day,hr) =
SolarRadiationElementData(MATERIAL,Slopes,ELEMENT,DirectNormalSolarRadiation(day,hr),DiffuseHorizo
ntalSolarRadiation(day,hr),'Tube',theta,omega,day,hr,surfacedescriptube,Ntube,wtube);
        S_Tube_H(HOUR) = S_Tube(day,hr);
        hr=hr+1;
        HOUR=HOUR+1;
    end
    day=day+1;
end

% save('SolarRadGeom.mat', 'S_Cover', 'S_Wall1', 'S_Wall2', 'S_Tube');
%load('SolarRadGeom.mat');



%Precalculate view factors for each element of the digester (only need to
%run this when geometry changes).
disp('calculating viewfactors...');

%populate a struct with values for view factors which can be called later
VF.Tube_Wall1 = ViewFactor(ELEMENT,'Tube','Wall1');
VF.Tube_Cover = ViewFactor(ELEMENT,'Tube','Cover');
```

```
VF.Tube_Wall2 = ViewFactor(ELEMENT,'Tube','Wall2');
VF.Wall1_Cover = ViewFactor(ELEMENT,'Wall1','Cover');
VF.Wall1_Wall2 = ViewFactor(ELEMENT,'Wall1','Wall2');
VF.Wall1_Tube = ViewFactor(ELEMENT,'Wall1','Tube');
VF.Wall2_Cover = ViewFactor(ELEMENT,'Wall2','Cover');
VF.Wall2_Wall1 = ViewFactor(ELEMENT,'Wall2','Wall1');
VF.Wall2_Tube = ViewFactor(ELEMENT,'Wall2','Tube');
VF.Cover_Wall2 = ViewFactor(ELEMENT,'Cover','Wall2');
VF.Cover_Tube = ViewFactor(ELEMENT,'Cover','Tube');
VF.Cover_Wall1 = ViewFactor(ELEMENT,'Cover','Wall1');
VF.Tube_Slurry = ViewFactor(ELEMENT,'Tube','Cover');
VF.Slurry_Tube = ViewFactor(ELEMENT,'Slurry','Tube');
% save('VF.mat','VF')
% load('VF.mat')


%INITIALIZATION-----------------------------------------------
disp('initializing temperatures...')
T_c = NaN(51,1);
T_t = NaN(51,1); %
T_aint = NaN(51,1); % Temp air internal
T_g = NaN(51,1); % Temp biogas?
h_rad_c_sky = NaN(51,1);
h_conv_c_wind = NaN(51,1);

T_w1 = NaN(365,24);
h_rad_w1_sky = NaN(365,24);
h_conv_w1_ext = NaN(365,24);
T_w2 = NaN(365,24);
h_rad_w2_sky = NaN(365,24);
```

```
h_conv_w2_ext = NaN(365,24);
T_s = NaN(365,24);
h_cond_s_grSide = NaN(365,24);
h_cond_s_grBase = NaN(365,24);

%Initial Temperatures (K)
    %Elements with thermal mass
    T0_w1=21+273;
    T0_w2=22+273;
    T0_s=18+273;
    %Elements without thermal mass
    T0_c=20+273;
    T0_t=23+273;
    T0_aint=24+273;
    T0_g=25+273;



%Iterations over one year to initialize the temperatures
    %Elements with thermal mass
    T_w1(1,1)=T0_w1;
    T_w2(1,1)=T0_w2;
    T_s(1,1)=T0_s;
    %Elements without thermal mass
    T_c(1)=T0_c;
    T_t(1)=T0_t;
    T_aint(1)=T0_aint;
    T_g(1)=T0_g;

Exit=0;
```

```
Exit2=0;
H=0;


%initialize for speed:
T_grSide = NaN(1,365);
T_grBase = NaN(1,365);
T_amb_K = NaN(365,24);
T_sky = NaN(365,24);
HOUR = NaN(1,8760);
T_amb_K_H = NaN(1,8760);
T_sky_H = NaN(1,8760);

Tc = NaN(365,24);
Tt = NaN(365,24);
Taint = NaN(365,24);
Tg = NaN(365,24);
Sc = NaN(365,24);
St = NaN(365,24);
hrad_c_sky = NaN(365,24);
hconv_c_wind = NaN(365,24);

Tc_H = NaN(1,8760);
Tt_H = NaN(1,8760);
Taint_H = NaN(1,8760);
Tg_H = NaN(1,8760);
Sc_H = NaN(1,8760);
St_H = NaN(1,8760);
hrad_c_sky_H = NaN(1,8760);
hconv_c_wind_H = NaN(1,8760);
```

```
T=NaN(1,8760);
Nus = [];


Losses_rad_c_sky_H = NaN(1,8760);
Losses_rad_c_sky = NaN(365,24);
Losses_c_wind_H = NaN(1,8760);
Losses_c_wind = NaN(365,24);

%store the data in a vector [hour of the year]
T_w1_H = NaN(1,8760);
T_w2_H = NaN(1,8760);
T_s_H = NaN(1,8760);
h_rad_w1_sky_H = NaN(1,8760);
h_conv_w1_ext_H = NaN(1,8760);
h_rad_w2_sky_H = NaN(1,8760);
h_conv_w2_ext_H = NaN(1,8760);
h_cond_s_grSide_H = NaN(1,8760);
h_cond_s_grBase_H = NaN(1,8760);

%Calculate the heat losses to the exterior
Losses_rad_w1_sky_H = NaN(1,8760);
Losses_rad_w1_sky = NaN(365,24);
Losses_conv_w1_ext_H = NaN(1,8760);
Losses_conv_w1_ext = NaN(365,24);
Losses_rad_w2_sky_H = NaN(1,8760);
Losses_rad_w2_sky = NaN(365,24);
Losses_conv_w2_ext_H = NaN(1,8760);
Losses_conv_w2_ext = NaN(365,24);
Losses_cond_s_grSide_H = NaN(1,8760);
```

```
Losses_cond_s_grSide = NaN(365,24);
Losses_cond_s_grBase_H = NaN(1,8760);
Losses_cond_s_grBase = NaN(365,24);

Month1 = NaN(1,8760);
DayOfMonth1 = NaN(1,8760);
disp('starting simulation. . .')
for d=1:24 % loop days of the year
    d1=d;
    tic
    [T_grSide(d),T_grBase(d)]=TempSoil(MATERIAL,ELEMENT,d,Tt_max,Tt_min,Tavg,I);
    T_amb_K(d,1)=T_amb_C(d,1)+273;
    T_sky(d,1)=0.0552*T_amb_K(d,1)^1.5;
%     disp(d);

    for h=1:23
        H=(d-1)*24+h;
        HOUR(H)=H;
        disp(H)
        T(H)=SlurryTemp(d,h);
        T_amb_K(d,h+1)=T_amb_C(d,h)+273;
        T_sky(d,h+1)=0.0552*T_amb_K(d,h)^1.5; %Temperature of
        T_amb_K_H(H)=T_amb_K(d,h);
        T_sky_H(H)=T_sky(d,h);


        count = 1;
        i=2;
```

```
[T_c(i),h_rad_c_sky(i),h_conv_c_wind(i)]=TempCover(Slopes,MATERIAL,ELEMENT,DirectNormalSolarRadiat
ion,DiffuseHorizontalSolarRadiation,V(H),z,theta,omega,d,h,T_amb_K(d,h),T_aint(i-
1),T_w2(d,h),T_t(i-1),T_w1(d,h),T_c(i-1),surfacedescripcover,Ncover,wcover,S_Cover(d,h),VF);

[T_t(i)]=TempTube(MATERIAL,ELEMENT,DirectNormalSolarRadiation,DiffuseHorizontalSolarRadiation,z,th
eta,omega,d,h,T_t(i-1),T_c(i-1),T_w1(d,h),T_w2(d,h),T_s(d,h),T_aint(i-1),T_g(i-
1),surfacedescriptube,Ntube,wtube,S_Tube(d,h),VF);
        T_aint(i)=TempAirInt(MATERIAL,ELEMENT,z,theta,T_c(i-1),T_aint(i-
1),T_w1(d,h),T_w2(d,h),T_t(i-1));
        T_g(i)=TempBiogas(T_t(i-1),T_s(d,h));

        while ((abs(T_c(i)-T_c(i-1))>1)||(abs(T_t(i)-T_t(i-1))>1)||(abs(T_aint(i)-T_aint(i-
1))>1)||(abs(T_g(i)-T_g(i-1))>1))&&(Exit==0)
            i=i+1;


[T_c(i),h_rad_c_sky(i),h_conv_c_wind(i)]=TempCover(Slopes,MATERIAL,ELEMENT,DirectNormalSolarRadiat
ion,DiffuseHorizontalSolarRadiation,V(H),z,theta,omega,d,h,T_amb_K(d,h),T_aint(i-
1),T_w2(d,h),T_t(i-1),T_w1(d,h),T_c(i-1),surfacedescripcover,Ncover,wcover,S_Cover(d,h),VF);

[T_t(i)]=TempTube(MATERIAL,ELEMENT,DirectNormalSolarRadiation,DiffuseHorizontalSolarRadiation,z,th
eta,omega,d,h,T_t(i-1),T_c(i-1),T_w1(d,h),T_w2(d,h),T_s(d,h),T_aint(i-1),T_g(i-
1),surfacedescriptube,Ntube,wtube,S_Tube(d,h),VF);
            T_aint(i)=TempAirInt(MATERIAL,ELEMENT,z,theta,T_c(i-1),T_aint(i-
1),T_w1(d,h),T_w2(d,h),T_t(i-1));
            T_g(i)=TempBiogas(T_t(i-1),T_s(d,h));

            if i>50
                Exit=1;
```

```
    end
end
%Initialization of the variables for the iterations,
%keeping the results obtained before
Exit=0;
T_c(1)=T_c(i);
T_t(1)=T_t(i);
T_aint(1)=T_aint(i);
T_g(1)=T_g(i);

%Store the data in a matrix [day,hour]
Tc(d,h)=T_c(1);
Tt(d,h)=T_t(1);
Taint(d,h)=T_aint(1);
Tg(d,h)=T_g(1);
hrad_c_sky(d,h)=h_rad_c_sky(i);
hconv_c_wind(d,h)=h_conv_c_wind(i);

%Store the data in a vector [hour of the year]
Tc_H(H)=T_c(1);
Tt_H(H)=T_t(1);
Taint_H(H)=T_aint(1);
Tg_H(H)=T_g(1);
hrad_c_sky_H(H)=h_rad_c_sky(i);
hconv_c_wind_H(H)=h_conv_c_wind(i);

%Calculate the heat loss to the exterior
Losses_rad_c_sky_H(H)=hrad_c_sky_H(H)*ELEMENT(5,2)*(Tc_H(H)-T_sky_H(H));
Losses_rad_c_sky(d,h)=Losses_rad_c_sky_H(H);
Losses_c_wind_H(H)=hconv_c_wind_H(H)*ELEMENT(5,2)*(Tc_H(H)-T_amb_K_H(H));
```

```
        Losses_c_wind(d,h)=Losses_c_wind_H(H);

        %Calculate the temperatures of the elements with thermal mass

[T_w1(d,h+1),h_rad_w1_sky(d,h+1),h_conv_w1_ext(d,h+1)]=TempWall1(MATERIAL,ELEMENT,DirectNormalSola
rRadiation,DiffuseHorizontalSolarRadiation,V(H),z,theta,omega,d,h+1,T_t(1),T_c(1),T_amb_K(d,h+1),T
_aint(1),T_w2(d,h),T_w1(d,h),surfacedescripwall1,Nwall1,wwall1,S_Wall1(d,h),VF);

[T_w2(d,h+1),h_rad_w2_sky(d,h+1),h_conv_w2_ext(d,h+1)]=TempWall2(MATERIAL,ELEMENT,DirectNormalSola
rRadiation,DiffuseHorizontalSolarRadiation,V(H),z,theta,omega,d,h+1,T_t(1),T_c(1),T_amb_K(d,h+1),T
_aint(1),T_w1(d,h),T_w2(d,h),surfacedescripwall2,Nwall2,wwall2,S_Wall2(d,h),VF);

[T_s(d,h+1),h_cond_s_grSide(d,h+1),h_cond_s_grBase(d,h+1)]=TempSlurry(MATERIAL,ELEMENT,z,theta,h+1
,m_load,T_t(1),T_s(d,h),T_g(1),T_grSide(d),T_grBase(d),T(H),VF);

        %store the data in a vector [hour of the year]
        T_w1_H(H)=T_w1(d,h);
        T_w2_H(H)=T_w2(d,h);
        T_s_H(H)=T_s(d,h);
        h_rad_w1_sky_H(H)=h_rad_w1_sky(d,h);
        h_conv_w1_ext_H(H)=h_conv_w1_ext(d,h);
        h_rad_w2_sky_H(H)=h_rad_w2_sky(d,h);
        h_conv_w2_ext_H(H)=h_conv_w2_ext(d,h);
        h_cond_s_grSide_H(H)=h_cond_s_grSide(d,h);
        h_cond_s_grBase_H(H)=h_cond_s_grBase(d,h);

        %Calculate the heat losses to the exterior
        Losses_rad_w1_sky_H(H)=h_rad_w1_sky_H(H)*ELEMENT(5,3)*(T_w1_H(H)-T_sky_H(H));
        Losses_rad_w1_sky(d,h)=Losses_rad_w1_sky_H(H);
        Losses_conv_w1_ext_H(H)=h_conv_w1_ext_H(H)*ELEMENT(5,3)*(T_w1_H(H)-T_amb_K_H(H));
```

```
        Losses_conv_w1_ext(d,h)=Losses_conv_w1_ext_H(H);
        Losses_rad_w2_sky_H(H)=h_rad_w2_sky_H(H)*ELEMENT(5,4)*(T_w2_H(H)-T_sky_H(H));
        Losses_rad_w2_sky(d,h)=Losses_rad_w2_sky_H(H);
        Losses_conv_w2_ext_H(H)=h_conv_w2_ext_H(H)*ELEMENT(5,4)*(T_w2_H(H)-T_amb_K_H(H));
        Losses_conv_w2_ext(d,h)=Losses_conv_w2_ext_H(H);
        Losses_cond_s_grSide_H(H)=h_cond_s_grSide_H(H)*ELEMENT(5,7)*(T_s_H(H)-T_grSide(d));
        Losses_cond_s_grSide(d,h)=Losses_cond_s_grSide_H(H);
        Losses_cond_s_grBase_H(H)=h_cond_s_grBase_H(H)*ELEMENT(5,8)*(T_s_H(H)-T_grBase(d));
        Losses_cond_s_grBase(d,h)=Losses_cond_s_grBase_H(H);

        Month1(H)=Month(d);
        DayOfMonth1(H)=DayOfMonth(d);

    end
    h=24;

    H=(d-1)*24+h;
    HOUR(H)=H;

    T_amb_K(d,h)=T_amb_C(d,h)+273;
    T_sky(d,h)=0.0552*T_amb_K(d,h)^1.5;
    T_amb_K_H(H)=T_amb_K(d,h);
    T_sky_H(H)=T_sky(d,h);

    i=2;


[T_c(i),h_rad_c_sky(i),h_conv_c_wind(i)]=TempCover(Slopes,MATERIAL,ELEMENT,DirectNormalSolarRadiat
ion,DiffuseHorizontalSolarRadiation,V(H),z,theta,omega,d,h,T_amb_K(d,h),T_aint(i-
1),T_w2(d,h),T_t(i-1),T_w1(d,h),T_c(i-1),surfacedescripcover,Ncover,wcover,S_Cover(d,h),VF);
```

```
[T_t(i)]=TempTube(MATERIAL,ELEMENT,DirectNormalSolarRadiation,DiffuseHorizontalSolarRadiation,z,th
eta,omega,d,h,T_t(i-1),T_c(i-1),T_w1(d,h),T_w2(d,h),T_s(d,h),T_aint(i-1),T_g(i-
1),surfacedescriptube,Ntube,wtube,S_Tube(d,h),VF);
    T_aint(i)=TempAirInt(MATERIAL,ELEMENT,z,theta,T_c(i-1),T_aint(i-1),T_w1(d,h),T_w2(d,h),T_t(i-
1));
    T_g(i)=TempBiogas(T_t(i-1),T_s(d,h));

    while ((abs(T_c(i)-T_c(i-1))>1)||(abs(T_t(i)-T_t(i-1))>1)||(abs(T_aint(i)-T_aint(i-
1))>1)||(abs(T_g(i)-T_g(i-1))>1))&&(Exit2==0)
        i=i+1;


[T_c(i),h_rad_c_sky(i),h_conv_c_wind(i)]=TempCover(Slopes,MATERIAL,ELEMENT,DirectNormalSolarRadiat
ion,DiffuseHorizontalSolarRadiation,V(H),z,theta,omega,d,h,T_amb_K(d,h),T_aint(i-
1),T_w2(d,h),T_t(i-1),T_w1(d,h),T_c(i-1),surfacedescripcover,Ncover,wcover,S_Cover(d,h),VF);

[T_t(i)]=TempTube(MATERIAL,ELEMENT,DirectNormalSolarRadiation,DiffuseHorizontalSolarRadiation,z,th
eta,omega,d,h,T_t(i-1),T_c(i-1),T_w1(d,h),T_w2(d,h),T_s(d,h),T_aint(i-1),T_g(i-
1),surfacedescriptube,Ntube,wtube,S_Tube(d,h),VF);
        T_aint(i)=TempAirInt(MATERIAL,ELEMENT,z,theta,T_c(i-1),T_aint(i-
1),T_w1(d,h),T_w2(d,h),T_t(i-1));
        T_g(i)=TempBiogas(T_t(i-1),T_s(d,h));

        if i>50
            Exit2=1;
        end
    end
    %Initilization of the variables for teh iterations, keeping the
    %last results obtained before
```

```
Exit2=0;
T_c(1)=T_c(i);
T_t(1)=T_t(i);
T_aint(1)=T_aint(i);
T_g(1)=T_g(i);

%Store the results in a matrix [day,hour]
Tc(d,h)=T_c(1);
Tt(d,h)=T_t(1);
Taint(d,h)=T_aint(1);
Tg(d,h)=T_g(1);
hrad_c_sky(d,h)=h_rad_c_sky(i);
hconv_c_wind(d,h)=h_conv_c_wind(i);

%Store the results in a vector [hour of the year]
Tc_H(H)=T_c(1);
Tt_H(H)=T_t(1);
Taint_H(H)=T_aint(1);
Tg_H(H)=T_g(1);
hrad_c_sky_H(H)=h_rad_c_sky(i);
hconv_c_wind_H(H)=h_conv_c_wind(i);

%Calculate the heat losses with the exterior
Losses_rad_c_sky_H(H)=hrad_c_sky_H(H)*ELEMENT(5,2)*(Tc_H(H)-T_sky_H(H));
Losses_rad_c_sky(d,h)=Losses_rad_c_sky_H(H);
Losses_c_wind_H(H)=hconv_c_wind_H(H)*ELEMENT(5,2)*(Tc_H(H)-T_amb_K_H(H));
Losses_c_wind(d,h)=Losses_c_wind_H(H);

%Store the results in a vector[hour of the year]
T_w1_H(H)=T_w1(d,h);
```

```
T_w2_H(H)=T_w2(d,h);
T_s_H(H)=T_s(d,h);
h_rad_w1_sky_H(H)=h_rad_w1_sky(d,h);
h_conv_w1_ext_H(H)=h_conv_w1_ext(d,h);
h_rad_w2_sky_H(H)=h_rad_w2_sky(d,h);
h_conv_w2_ext_H(H)=h_conv_w2_ext(d,h);
h_cond_s_grSide_H(H)=h_cond_s_grSide(d,h);
h_cond_s_grBase_H(H)=h_cond_s_grBase(d,h);

%Calculate the losses to the exterior
Losses_rad_w1_sky_H(H)=h_rad_w1_sky_H(H)*ELEMENT(5,3)*(T_w1_H(H)-T_sky_H(H));
Losses_rad_w1_sky(d,h)=Losses_rad_w1_sky_H(H);
Losses_conv_w1_ext_H(H)=h_conv_w1_ext_H(H)*ELEMENT(5,3)*(T_w1_H(H)-T_amb_K_H(H));
Losses_conv_w1_ext(d,h)=Losses_conv_w1_ext_H(H);
Losses_rad_w2_sky_H(H)=h_rad_w2_sky_H(H)*ELEMENT(5,4)*(T_w2_H(H)-T_sky_H(H));
Losses_rad_w2_sky(d,h)=Losses_rad_w2_sky_H(H);
Losses_conv_w2_ext_H(H)=h_conv_w2_ext_H(H)*ELEMENT(5,4)*(T_w2_H(H)-T_amb_K_H(H));
Losses_conv_w2_ext(d,h)=Losses_conv_w2_ext_H(H);
Losses_cond_s_grSide_H(H)=h_cond_s_grSide_H(H)*ELEMENT(5,7)*(T_s_H(H)-T_grSide(d));
Losses_cond_s_grSide(d,h)=Losses_cond_s_grSide_H(H);
Losses_cond_s_grBase_H(H)=h_cond_s_grBase_H(H)*ELEMENT(5,8)*(T_s_H(H)-T_grBase(d));
Losses_cond_s_grBase(d,h)=Losses_cond_s_grBase_H(H);

%Calculate the temperatures of the elements with thermal mass from the first hour of
%the following day if we are not on the last day of the year
if d~=24
    T_amb_K(d+1,1)=T_amb_C(d+1,1)+273;
    T_sky(d+1,1)=0.0552*T_amb_K(d+1,1)^1.5;
```

```
[T_w1(d+1,1),h_rad_w1_sky(d+1,1),h_conv_w1_ext(d+1,1)]=TempWall1(MATERIAL,ELEMENT,DirectNormalSola
rRadiation,DiffuseHorizontalSolarRadiation,V(d+1),z,theta,omega,d+1,h,T_t(1),T_c(1),T_amb_K(d+1,1)
,T_aint(1),T_w2(d,h),T_w1(d,h),surfacedescripwall1,Nwall1,wwall1,S_Wall1(d,h),VF);

[T_w2(d+1,1),h_rad_w2_sky(d+1,1),h_conv_w2_ext(d+1,1)]=TempWall2(MATERIAL,ELEMENT,DirectNormalSola
rRadiation,DiffuseHorizontalSolarRadiation,V(d+1),z,theta,omega,d+1,h,T_t(1),T_c(1),T_amb_K(d+1,1)
,T_aint(1),T_w1(d,h),T_w2(d,h),surfacedescripwall2,Nwall2,wwall2,S_Wall2(d,h),VF);

[T_s(d+1,1),h_cond_s_grSide(d+1,1),h_cond_s_grBase(d+1,1)]=TempSlurry(MATERIAL,ELEMENT,z,theta,h+1
,m_load,T_t(1),T_s(d,h),T_g(1),T_grSide(d),T_grBase(d),T(d+1),VF);
    elseif d==24
        %Initialization of the temperatures of the elements with thermal mass
        %for the next calculatetions
        T_amb_K(1,1)=T_amb_C(1,1)+273;
        T_sky(1,1)=0.0552*T_amb_K(1,1)^1.5;


[T_w1(1,1),h_rad_w1_sky(1,1),h_conv_w1_ext(1,1)]=TempWall1(MATERIAL,ELEMENT,DirectNormalSolarRadia
tion,DiffuseHorizontalSolarRadiation,V(1),z,theta,omega,1,h,T_t(1),T_c(1),T_amb_K(1,1),T_aint(1),T
_w2(d,h),T_w1(d,h),surfacedescripwall1,Nwall1,wwall1,S_Wall1(d,h),VF);

[T_w2(1,1),h_rad_w2_sky(1,1),h_conv_w2_ext(1,1)]=TempWall2(MATERIAL,ELEMENT,DirectNormalSolarRadia
tion,DiffuseHorizontalSolarRadiation,V(1),z,theta,omega,1,h,T_t(1),T_c(1),T_amb_K(1,1),T_aint(1),T
_w1(d,h),T_w2(d,h),surfacedescripwall2,Nwall2,wwall2,S_Wall2(d,h),VF);

[T_s(1,1),h_cond_s_grSide(1,1),h_cond_s_grBase(1,1)]=TempSlurry(MATERIAL,ELEMENT,z,theta,h,m_load,
T_t(1),T_s(d,h),T_g(1),T_grSide(d),T_grBase(d),T_amb_K(1,1),VF);
    end
if d==24
```

```
    disp('25%')
end
    Month1(H)=Month(d);
    DayOfMonth1(H)=DayOfMonth(d);
    %toc

end
```

B.4 Biochemical model

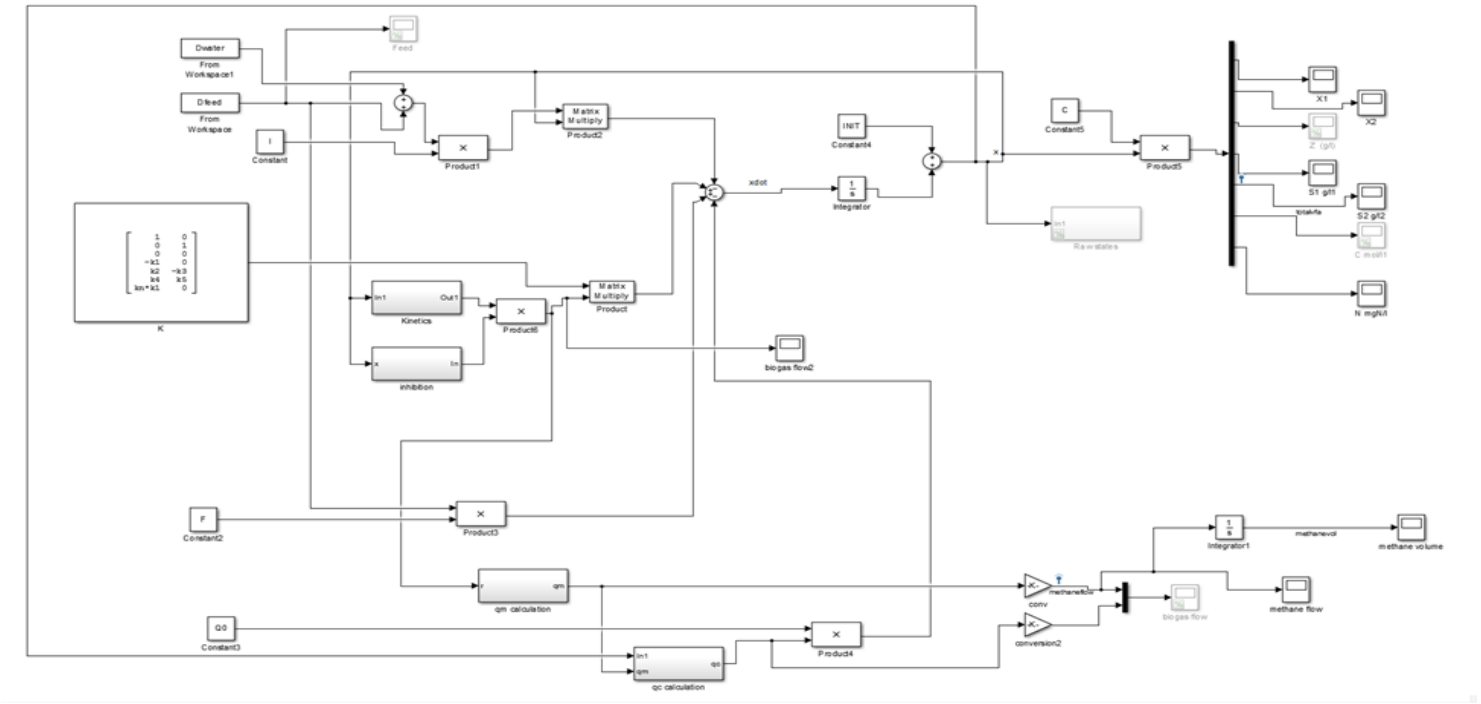

Diagram of 2R model

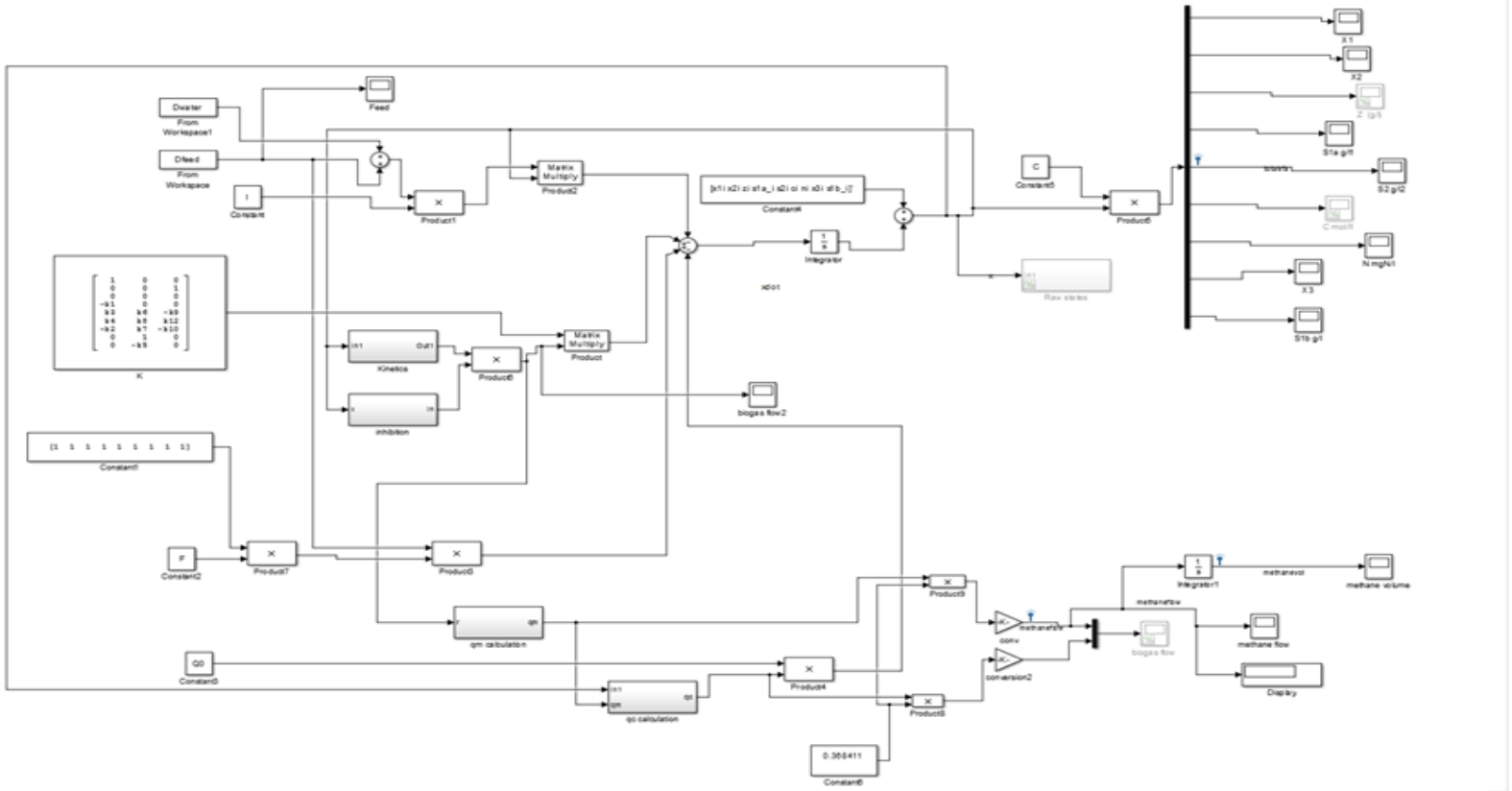

Diagram of 3R model

Diagram of the cardinal temperature model

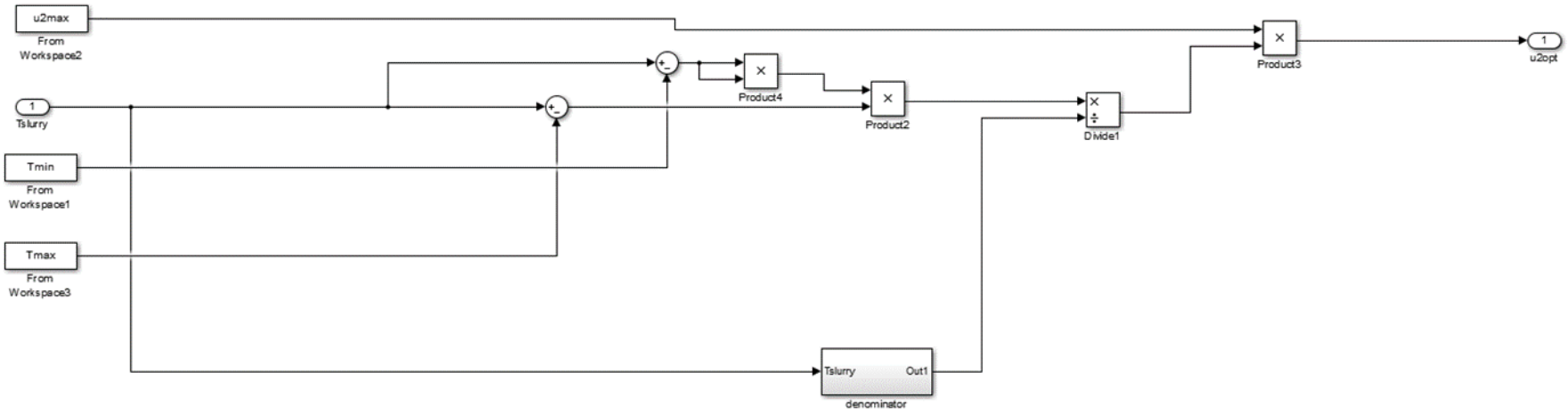

B.5 Code for Parameter estimation

```
%Expvfa=sdo.Experiment('fractionation');
Expgas=sdo.Experiment('fractionation1');
Exp=sdo.Experiment('fractionation1');

% Add signal logging for VFA, experimental data and add
to experiment
% vfa=Simulink.SimulationData.Signal;
% vfa.Name = 'totalvfa';
% vfa.BlockPath = 'fractionation/Demux';
% vfa.PortType = 'outport';
% vfa.PortIndex = 5;
% vfa.Values = timeseries(VFA,VFAtime);
% Expvfa.OutputData= vfa;

% Add signal logging for methane flow, experimental data
and add to experiment
methaneflow=Simulink.SimulationData.Signal;
methaneflow.Name = 'methaneflow';
methaneflow.BlockPath = 'fractionation1/conv';
methaneflow.PortType = 'outport';
methaneflow.PortIndex = 1;
methaneflow.Values = timeseries(gasrate,timegas);
%Expgas.OutputData= methaneflow;

% Add signal logging for methane vol, experimental data
and add to experiment
methanevol=Simulink.SimulationData.Signal;
methanevol.Name = 'methanevol';
methanevol.BlockPath = 'fractionation1/Integrator1';
methanevol.PortType = 'outport';
methanevol.PortIndex = 1;
methanevol.Values = timeseries(gasvol,timegas);
%Expgas.OutputData= methaneflow;

 %Exp.OutputData = [vfa ; methaneflow ; methanevol];
 %Exp.OutputData = [vfa ; methaneflow];
  Exp.OutputData=[methaneflow,methanevol];
%Exp = [Expvfa ;Expgas];

% Set parameters for estimation

p =
sdo.getParameterFromModel('fractionation1',{'k5','khyd'}
);

% For Contois p contains
{'k1','kx1','u1max','ks2','ki2','u2max','kin'}
```

```
for n = 1:2
    p(n).Minimum = 0;
end

% Calculate the cost function for the parameter values p
and experimetnal
% comparisons contained in Exp

estFcn = @(p) Bernard_model_Contois_cost1(p,Exp);


opt = sdo.OptimizeOptions;
opt.Method = 'lsqnonlin';
opt.MethodOptions.TolFun=1e-8;
opt.MethodOptions.TolX=1e-8;
opt.MethodOptions.MaxIter=100;
% opt.UseParallel = 'always';
% opt.OptimizedModel = 'fractionation';
%p_opt = p;
p_opt = sdo.optimize(estFcn,p,opt);

% Make a plot of the Methane flow and VFA to compare the
outputs of the
% calibrated model and the experimental data.

Exp = setEstimatedValues(Exp, p_opt);
Simulator = createSimulator(Exp);
Simulator = sim(Simulator);

SimLog =
find(Simulator.LoggedData,get_param('fractionation1','Si
gnalLoggingName'));
%vfasim=find(SimLog,'totalvfa');
methaneflowsim=find(SimLog,'methaneflow');
methanevolsim = find(SimLog,'methanevol');

figure(1);
plot(methaneflow.Values.Time,methaneflow.Values.Data,met
haneflowsim.Values.Time,methaneflowsim.Values.Data);
grid;
legend('methaneflowexp','methanflowsim');
% figure(2);
%
plot(vfa.Values.Time,vfa.Values.Data,vfasim.Values.Time,
vfasim.Values.Data);
% grid;
% legend('vfaexp','vfasim');
figure(3);
```

```
plot(methanevol.Values.Time,methanevol.Values.Data,metha
nevolsim.Values.Time,methanevolsim.Values.Data,timegas,g
asvol);
grid;
legend('methanevolexp','methanvolsim').
```

Reference

(If provided.)

1. Batley, S.L., et al., *Citizen versus consumer: challenges in the UK green power market.* Energy Policy, 2001. **29**(6): p. 479-487.
2. Fuss, S., et al., *Impact of climate policy uncertainty on the adoption of electricity generating technologies.* Energy Policy, 2009. **37**(2): p. 733-743.
3. Longo, A., A. Markandya, and M. Petrucci, *The internalization of externalities in the production of electricity: Willingness to pay for the attributes of a policy for renewable energy.* Ecological Economics, 2008. **67**(1): p. 140-152.
4. Stigka, E.K., J.A. Paravantis, and G.K. Mihalakakou, *Social acceptance of renewable energy sources: A review of contingent valuation applications.* Renewable and Sustainable Energy Reviews, 2014. **32**: p. 100-106.
5. Economou, A., *Renewable energy resources and sustainable development in Mykonos (Greece).* Renewable and Sustainable Energy Reviews, 2010. **14**(5): p. 1496-1501.
6. Li, H., et al., *Public support for reducing US reliance on fossil fuels: Investigating household willingness-to-pay for energy research and development.* Ecological Economics, 2009. **68**(3): p. 731-742.
7. Lo, K., *A critical review of China's rapidly developing renewable energy and energy efficiency policies.* Renewable and Sustainable Energy Reviews, 2014. **29**: p. 508-516.
8. Lanteigne, M., *China's Maritime Security and the "Malacca Dilemma".* Asian Security, 2008. **4**(2): p. 143-161.
9. Danchev, S., G. Maniatis, and A. Tsakanikas, *Returns on investment in electricity producing photovoltaic systems under de-escalating feed-in tariffs: The case of Greece.* Renewable and Sustainable Energy Reviews, 2010. **14**(1): p. 500-505.
10. Evans, A., V. Strezov, and T.J. Evans, *Assessment of sustainability indicators for renewable energy technologies.* Renewable and Sustainable Energy Reviews, 2009. **13**(5): p. 1082-1088.
11. Lund, H., *Renewable energy strategies for sustainable development.* Energy, 2007. **32**(6): p. 912-919.
12. Baños, R., et al., *Optimization methods applied to renewable and sustainable energy: A review.* Renewable and Sustainable Energy Reviews, 2011. **15**(4): p. 1753-1766.
13. Hepbasli, A., *A key review on exergetic analysis and assessment of renewable energy resources for a sustainable future.* Renewable and Sustainable Energy Reviews, 2008. **12**(3): p. 593-661.
14. Prakash, R. and I.K. Bhat, *Energy, economics and environmental impacts of renewable energy systems.* Renewable and Sustainable Energy Reviews, 2009. **13**(9): p. 2716-2721.
15. EIA, *Annual Energy Outlook 2012 with Projections to 203*. 2012.

16. Yuksel, I., *Southeastern Anatolia Project (GAP) for Irrigation and Hydroelectric Power in Turkey.* Energy Exploration & Exploitation, 2006. **24**(4): p. 361-370.
17. Dursun, B. and C. Gokcol, *The role of hydroelectric power and contribution of small hydropower plants for sustainable development in Turkey.* Renewable Energy, 2011. **36**(4): p. 1227-1235.
18. Yüksel, I., *Hydropower for sustainable water and energy development.* Renewable and Sustainable Energy Reviews, 2010. **14**(1): p. 462-469.
19. Mishra, S., S. Singal, and D. Khatod, *Optimal installation of small hydropower plant—A review.* Renewable and Sustainable Energy Reviews, 2011. **15**(8): p. 3862-3869.
20. Balkhair, K.S. and K.U. Rahman, *Sustainable and economical small-scale and low-head hydropower generation: A promising alternative potential solution for energy generation at local and regional scale.* Applied Energy, 2017. **188**: p. 378-391.
21. Paish, O., *Small hydro power: technology and current status.* Renewable and Sustainable Energy Reviews, 2002. **6**(6): p. 537-556.
22. Kaldellis, J.K. and D. Zafirakis, *The wind energy (r) evolution: A short review of a long history.* Renewable Energy, 2011. **36**(7): p. 1887-1901.
23. Baumeister, C. and L. Kilian, *Forty Years of Oil Price Fluctuations: Why the Price of Oil May Still Surprise Us.* Journal of Economic Perspectives, 2016. **30**(1): p. 139-60.
24. C, S., *Revisiting solar power's past.* Technology Review, 1995 p. 38–47.
25. Timilsina, G.R., L. Kurdgelashvili, and P.A. Narbel, *Solar energy: Markets, economics and policies.* Renewable and Sustainable Energy Reviews, 2012. **16**(1): p. 449-465.
26. M., H., *On the global and regional potential of renewable energy sources.* 2004, Faculteit Scheikunde,Universiteit Utrecht;.
27. T., B., *Solar revolution.The economic transformation of the global energy industry.* 2006(Cambridge, MA).
28. REN21., *Global status report.Paris: 2005 to 2011 Issues.* 2005.
29. Zhang, X., et al., *Review of R&D progress and practical application of the solar photovoltaic/thermal (PV/T) technologies.* Renewable and Sustainable Energy Reviews, 2012. **16**(1): p. 599-617.
30. Abbasi, T., S. Tauseef, and S. Abbasi, *Anaerobic digestion for global warming control and energy generation—an overview.* Renewable and Sustainable Energy Reviews, 2012. **16**(5): p. 3228-3242.
31. Marchaim, U., *Biogas processes for sustainable development*. 1992: Food & Agriculture Org.
32. Donoso-Bravo, A., et al., *Model selection, identification and validation in anaerobic digestion: A review.* Water Research, 2011. **45**(17): p. 5347-5364.
33. Pfluger, A., et al., *Anaerobic digestion and biogas beneficial use at municipal wastewater treatment facilities in Colorado: A case study examining barriers to widespread implementation.* Journal of Cleaner Production, 2019. **206**: p. 97-107.

34. Batstone, D. and P. Jensen, *4.17-Anaerobic Processes.* Treatise on Water Science, 2011: p. 615-640.
35. Ranieri, L., et al., *Energy Recovery from the Organic Fraction of Municipal Solid Waste: A Real Options-Based Facility Assessment.* 2018. **10**(2): p. 368.
36. DEFRA, *European Experience of Small-Scale and On-Farm AD* 2010: p. 1-89.
37. EBA, *Optimal use of biogas from waste streams: An assessment of the potential of biogas from*

digestion in the EU beyond 2020. 2016.
38. Wrap, *Household Food and Drink Waste in the UK* 2009.
39. Banks, C.J., Heaven, S., Zhang, Y., Baier, U. , *Food waste digestion: Anaerobic Digestion of Food Waste for a*

Circular Economy. . IEA Bioenergy Task 37, 2018.
40. WMR. *Richgro Bioenergy Plant, .* 2016 [cited Available http://wastemanagementreview.

com.au/richgro-bioenergy-plant-jandakot-westernaustralia, last accessed Oct 2018. 21/09/2018]; Available from: http://wastemanagementreview.

com.au/richgro-bioenergy-plant-jandakot-westernaustralia.
41. Bioenergy, I., *IEA Bioenergy Task 37 Denmark*

Country Report Esbjerg, . 2017.
42. Surendra, K.C., et al., *Household anaerobic digester for bioenergy production in developing countries: opportunities and challenges.* Environmental Technology, 2013. **34**(13-14): p. 1671-1689.
43. Rajendran, K., S. Aslanzadeh, and M.J. Taherzadeh, *Household Biogas Digesters—A Review.* Energies, 2012. **5**(8): p. 2911-2942.
44. Bond, T. and M.R. Templeton, *History and future of domestic biogas plants in the developing world.* Energy for Sustainable Development, 2011. **15**(4): p. 347-354.
45. Fulford, D., *Small-scale, Rural Biogas Programmes: a Handbook*. 2015.
46. Karki, *a training manual for extension, kathmandu, CM for food and agriculture organisation*. 1999.
47. Zuzhang, X., *Domestic bigas in China a changing China*. 2013.
48. Harter, J., *The Diffusion of Biogas Technology and its impact on sustainable Rural development in China, Wolfen, Germany:*. 2010, Universitat, Duisburg-Essen.
49. Chen, L., et al., *The progress and prospects of rural biogas production in China.* Energy Policy, 2012. **51**: p. 58-63.
50. Ashden. *Appropriate Rural Technology Institute: Biogas production from food waste for urban homes*. 2006 [cited 2018 7 may]; Available from: https://www.ashden.org/winners/the-appropriate-rural-technology-institute-arti.
51. Chen, Y., et al., *Household biogas use in rural China: A study of opportunities and constraints.* Renewable and Sustainable Energy Reviews, 2010. **14**(1): p. 545-549.

52. Jiang, X., S.G. Sommer, and K.V. Christensen, *A review of the biogas industry in China.* Energy Policy, 2011. **39**(10): p. 6073-6081.
53. CAREI, *China Rural Energy Industry Development Report 2012*. 2012, China Association of Rural Energy Industry (CAREI), Beijing.
54. Khanal, S.K., *Anaerobic Biotechnology for Bioenergy Production: Principles and Applications*. 2011: Wiley.
55. Abbasi, T., S.M. Tauseef, and S.A. Abbasi, *A Brief History of Anaerobic Digestion and "Biogas"*, in *Biogas Energy*, T. Abbasi, S.M. Tauseef, and S.A. Abbasi, Editors. 2012, Springer New York: New York, NY. p. 11-23.
56. Lawbuary, J. *Biogas Technology in India: More than Gandhi's Dream*. 2000 [cited 2019 12 January]; Available from: http://www.ganesha.co.uk/Articles/Biogas%20Technology%20in%20India.htm.
57. Engineers, N.B.o.C., *Handbook on Biogas and Its Applications (from Waste & Renewable Resources with Engineering & Design Concepts)(2nd Revised Edition)*. 2004, NIIR PROJECT CONSULTANCY SERVICES. p. 384.
58. Ramana, V., *Biogas programme in India*. 1991: TIDE. 1-18.
59. Chauhan, D.S.a.S., S.K., *Non-Conventional Energy Resources (As per GBTU/MTU Syllabus)*. 3rd ed. 2012: New Age International. 268.
60. Ashden. *Biotech: Management of domestic and Municipal waste at source prioduces biogas for cooking and electricity generation*. 2007 [cited 2018 21 May]; Available from: https://www.ashden.org/winners/biotech.
61. Ashden. *Shaanxi Mothers, China; Domestic biogas for cooking and lighting*. 2006 [cited 2018 7 May]; Available from: https://www.ashden.org/winners/shaanxi-mothers.
62. Ashden. *SKG Sangha, India; Biogas for cooking plus fertiliser from slurry*. 2007 [cited 2018 7 MAY]; Available from: https://www.ashden.org/winners/skg-sangha.
63. SNV., *Building viable domestic biogas programmes: success factors in sector development*. 2009.
64. Ngumah, C.C., et al., *BIOGAS POTENTIAL OF ORGANIC WASTE IN NIGERIA.* Journal of Urban and Environmental Engineering, 2013. **7**(1): p. 110-116.
65. Roopnarain, A. and R. Adeleke, *Current status, hurdles and future prospects of biogas digestion technology in Africa.* Renewable and Sustainable Energy Reviews, 2017. **67**: p. 1162-1179.
66. Salami, H.A., et al., *A Review on the Current Status of Municipal Solid Waste Management in Nigeria: Problems and Solutions.* 2018.
67. H. A. Salami1*, J.O.A., T. T. Bademosi1, S. O. Lawal1, O. O. Olutayo1an, *Current Status of Municipal Solid Waste Management in Nigeria: Problems and Solutions.* Journal of Engineering Research and Reports, 2018. **3(4): 1-16, 2018; Article no.JERR.46618**.
68. OYEBODE , O.J., *Solid Waste Management for Sustainable Development and Public health: A Case Study of Lagos State in Nigeria.* Universal Journal of Public Health, 2013. **1.3**: p. 33 - 39.

69. C.Owhor, H.O.S.a.A., *Assessment of Solid Waste Management Practice in*

Port Harcourt Metropolis, Rivers State, Nigeria. Journal of Geography, Environment and Earth Science

16(2): 1-10, 2018(SSN: 2454-7352).

70. Ogunjuyigbe, A.S.O., T.R. Ayodele, and M.A. Alao, *Electricity generation from municipal solid waste in some selected cities of Nigeria: An assessment of feasibility, potential and technologies.* Renewable and Sustainable Energy Reviews, 2017. **80**: p. 149-162.
71. Ferrer, I., et al., *Biogas production in low-cost household digesters at the Peruvian Andes.* Biomass and Bioenergy, 2011. **35**(5): p. 1668-1674.
72. Lansing, S., et al., *Methane production in low-cost, unheated, plug-flow digesters treating swine manure and used cooking grease.* Bioresource Technology, 2010. **101**(12): p. 4362-4370.
73. Perrigault, T., et al., *Towards thermal design optimization of tubular digesters in cold climates: A heat transfer model.* Bioresource Technology, 2012. **124**: p. 259-268.
74. Axaopoulos, P., et al., *Simulation and experimental performance of a solar-heated anaerobic digester.* Solar Energy, 2001. **70**(2): p. 155-164.
75. El-Mashad, H.M., W.K.P. van Loon, and G. Zeeman, *A Model of Solar Energy Utilisation in the Anaerobic Digestion of Cattle Manure.* Biosystems Engineering, 2003. **84**(2): p. 231-238.
76. El-Mashad, H.M., et al., *Design of A Solar Thermophilic Anaerobic Reactor for Small Farms.* Biosystems Engineering, 2004. **87**(3): p. 345-353.
77. Yiannopoulos, A.C., I.D. Manariotis, and C.V. Chrysikopoulos, *Design and analysis of a solar reactor for anaerobic wastewater treatment.* Bioresource Technology, 2008. **99**(16): p. 7742-7749.
78. Garfí, M., et al., *Psychrophilic anaerobic digestion of guinea pig manure in low-cost tubular digesters at high altitude.* Bioresource Technology, 2011. **102**(10): p. 6356-6359.
79. Martí-Herrero, J., et al., *Cow, sheep and llama manure at psychrophilic anaerobic co-digestion with low cost tubular digesters in cold climate and high altitude.* Bioresource Technology, 2015. **181**: p. 238-246.
80. Martí-Herrero, J., et al., *How to report biogas production when monitoring small-scale digesters in field.* Biomass and Bioenergy, 2016. **84**: p. 31-36.
81. Poggio, D.A., *Modificationand experimental calibration of ADM1 for modelling the anaerobic digestion of solid wastesin demand driven applications*, in *School of Chemical and Process Engineering*. 2015, University of Leeds. p. 257.
82. Dwivedi, V., *Thermal modelling and control of Domestic Hot water Tank*, in *Department of Mechanical Engineering*. 2009, University of Strathclyde. p. 94.

83. Batstone, D.J., et al., *The IWA Anaerobic Digestion Model No 1(ADM 1).* Water Science & Technology, 2002. **45**(10): p. 65-73.
84. Bernard, O., et al., *Dynamical model development and parameter identification for an anaerobic wastewater treatment process.* Biotechnology and Bioengineering, 2001. **75**(4): p. 424-438.
85. Mairet, F., et al., *Three-reaction model for the anaerobic digestion of microalgae.* Biotechnology and Bioengineering, 2012. **109**(2): p. 415-425.
86. BP, *BP Statistical Review of World Energy*. 2014.
87. IEO, *EIA Energy Outlook: Assessment of long-term world energy markets.* . 2017, Energy Information Administration. p. 76.
88. BP, *BP EnergyOutlook, 2035*. 2014.
89. Chiaramonti, D., A. Oasmaa, and Y. Solantausta, *Power generation using fast pyrolysis liquids from biomass.* Renewable and Sustainable Energy Reviews, 2007. **11**(6): p. 1056-1086.
90. Collard, F.-X. and J. Blin, *A review on pyrolysis of biomass constituents: Mechanisms and composition of the products obtained from the conversion of cellulose, hemicelluloses and lignin.* Renewable and Sustainable Energy Reviews, 2014. **38**: p. 594-608.
91. Pavlostathis, S. and E. Giraldo-Gomez, *Kinetics of anaerobic treatment.* Water Science & Technology, 1991. **24**(8): p. 35-59.
92. Carballa, M., L. Regueiro, and J.M. Lema, *Microbial management of anaerobic digestion: exploiting the microbiome-functionality nexus.* Current opinion in biotechnology, 2015. **33**: p. 103-111.
93. McMahon, K.D., et al., *Microbial population dynamics during start-up and overload conditions of anaerobic digesters treating municipal solid waste and sewage sludge.* Biotechnology and Bioengineering, 2004. **87**(7): p. 823-834.
94. Angelidaki, I., et al., *Biomethanation and its potential.* Methods Enzymol, 2011. **494**(16): p. 327-351.
95. Tong, X., P.L. McCarty, and R. Isaacson, *Microbial hydrolysis of lignocellulosic materials.* Methane from community wastes., 1991: p. 61-100.
96. Ekama, G.A., S.W. Sötemann, and M.C. Wentzel, *Biodegradability of activated sludge organics under anaerobic conditions.* Water Research, 2007. **41**(1): p. 244-252.
97. Ward, A.J., et al., *Optimisation of the anaerobic digestion of agricultural resources.* Bioresource Technology, 2008. **99**(17): p. 7928-7940.
98. Vavilin, V., et al., *Hydrolysis kinetics in anaerobic degradation of particulate organic material: an overview.* Waste Management, 2008. **28**(6): p. 939-951.
99. Hills, D.J. and K. Nakano, *Effects of particle size on anaerobic digestion of tomato solid wastes.* Agricultural wastes, 1984. **10**(4): p. 285-295.
100. Sharma, S.K., et al., *Effect of particle size on biogas generation from biomass residues.* Biomass, 1988. **17**(4): p. 251-263.

101. Vavilin, V., S. Rytov, and L.Y. Lokshina, *A description of hydrolysis kinetics in anaerobic degradation of particulate organic matter.* Bioresource Technology, 1996. **56**(2): p. 229-237.
102. Sanders, W.T.M., *Anaerobic hydrolysis during digestion of complex substrates*. 2001: sn].
103. Costello, D.J., P.F. Greenfield, and P.L. Lee, *Dynamic modelling of a single-stage high-rate anaerobic reactor—I. Model derivation.* Water Research, 1991. **25**(7): p. 847-858.
104. Drapcho, C.M., N.P. Nhuan, and T.H. Walker, *Biofuels engineering process technology*. 2008: McGraw-Hill New York, NY, USA:.
105. Bruce, N., R. Perez-Padilla, and R. Albalak, *Indoor air pollution in developing countries: A major environmental and public health challenge.* World Health Organization. Bulletin of the World Health Organization, 2000. **78**(9): p. 1078-92.
106. Katuwal, H. and A.K. Bohara, *Biogas: A promising renewable technology and its impact on rural households in Nepal.* Renewable and Sustainable Energy Reviews, 2009. **13**(9): p. 2668-2674.
107. Roubík, H. and J. Mazancová, *Small-scale biogas plants in central Vietnam and biogas appliances with a focus on a flue gas analysis of biogas cook stoves.* Renewable Energy, 2019. **131**: p. 1138-1145.
108. GTZ/ISAT, *Biogas Digest: Biogas-application and product development.* 1999. **II**.
109. Santerre, M.T. and K.R. Smith, *Measures of appropriateness: the resource requirements of anaerobic digestion (biogas) systems.* World Development, 1982. **10**(3): p. 239-261.
110. Klavon, K.H., et al., *Economic analysis of small-scale agricultural digesters in the United States.* Biomass and Bioenergy, 2013. **54**: p. 36-45.
111. Bonten, L.T.C., et al., *Bio-slurry as fertilizer : is bio-slurry from household digesters a better fertilizer than manure? : a literature review*. 2014, Alterra, Wageningen-UR: Wageningen.
112. Heegde, D.G.E.D.K.S.F.t., *Report on the feasibility study of a national programme for domestic biogas in Ethiopia. .* 2006, SNV – Ethiopia.
113. Heegde, E.N.w.L.C.S.F.E.W.t., *Programme Implementation Document Tanzania Domestic Biogas Programme*. 2009.
114. Mengistu, M., et al., *A review on biogas technology and its contributions to sustainable rural livelihood in Ethiopia.* Renewable and Sustainable Energy Reviews, 2015. **48**: p. 306-316.
115. Cuéllar, A.D. and M.E. Webber, *Cow power: the energy and emissions benefits of converting manure to biogas.* Environmental Research Letters, 2008. **3**(3): p. 034002.
116. Tiwary, A., et al., *Emerging perspectives on environmental burden minimisation initiatives from anaerobic digestion technologies for community scale biomass valorisation.* Renewable and Sustainable Energy Reviews, 2015. **42**: p. 883-901.
117. Ciotola, R.J., S. Lansing, and J.F. Martin, *Emergy analysis of biogas production and electricity generation from small-scale agricultural digesters.* Ecological Engineering, 2011. **37**(11): p. 1681-1691.

118. Wu, X., et al., *Emergy-based sustainability assessment of an integrated production system of cattle, biogas, and greenhouse vegetables: Insight into the comprehensive utilization of wastes on a large-scale farm in Northwest China.* Ecological Engineering, 2013. **61**: p. 335-344.
119. Wu, X., et al., *Emergy and greenhouse gas assessment of a sustainable, integrated agricultural model (SIAM) for plant, animal and biogas production: Analysis of the ecological recycle of wastes.* Resources, Conservation and Recycling, 2015. **96**: p. 40-50.
120. Martí-Herrero, J., et al., *Improvement through low cost biofilm carrier in anaerobic tubular digestion in cold climate regions.* Bioresource Technology, 2014. **167**: p. 87-93.
121. Walekhwa, P.N., D. Lars, and J. Mugisha, *Economic viability of biogas energy production from family-sized digesters in Uganda.* Biomass and Bioenergy, 2014. **70**: p. 26-39.
122. Amigun, B. and H. von Blottnitz, *Capacity-cost and location-cost analyses for biogas plants in Africa.* Resources, Conservation and Recycling, 2010. **55**(1): p. 63-73.
123. Abert, J.G. and R.M. Vancil, *A graphical approach to determine the economics of recovering resources from municipal solid waste.* Conservation & Recycling, 1977. **1**(3–4): p. 299-314.
124. Ferrer, I., et al., *Pilot project of biogas production from pig manure and urine mixture at ambient temperature in Ventanilla (Lima, Peru).* Waste Management, 2009. **29**(1): p. 168-173.
125. Gosling, D., *Biogas for Thailand's rural development: transferring the technology.* Biomass, 1982. **2**(4): p. 309-316.
126. Singh, K.J. and S.S. Sooch, *Comparative study of economics of different models of family size biogas plants for state of Punjab, India.* Energy Conversion and Management, 2004. **45**(9–10): p. 1329-1341.
127. Axaopoulos, P. and P. Panagakis, *Energy and economic analysis of biogas heated livestock buildings.* Biomass and Bioenergy, 2003. **24**(3): p. 239-248.
128. Adeoti, O., et al., *Engineering design and economic evaluation of a family-sized biogas project in Nigeria.* Technovation, 2000. **20**(2): p. 103-108.
129. Rajendran, K., et al., *Experimental and economical evaluation of a novel biogas digester.* Energy Conversion and Management, 2013. **74**(0): p. 183-191.
130. White, A.J., D.W. Kirk, and J.W. Graydon, *Analysis of small-scale biogas utilization systems on Ontario cattle farms.* Renewable Energy, 2011. **36**(3): p. 1019-1025.
131. Amigun, B. and H.v. Blottnitz, *Investigation of scale economies for African biogas installations.* Energy Conversion and Management, 2007. **48**(12): p. 3090-3094.
132. Anderson, R.C., D. Hilborn, and A. Weersink, *An economic and functional tool for assessing the financial feasibility of farm-based anaerobic digesters.* Renewable Energy, 2013. **51**: p. 85-92.
133. Ghimire, P.C., *SNV supported domestic biogas programmes in Asia and Africa.* Renewable Energy, 2013. **49**: p. 90-94.

134. BPO, *Support Project to the Biogas Programme for the Animal Husbandry Sector in some Provinces of Vietnam*. 2006. p. 52.
135. G Dekelver, A.N., S Ruzigana, *Implementation plan: national programme on domestic biogas in Rwanda*. 2006. p. 59.
136. Heegde, F.t., *Institutional arrangments for the Uganda Domestic Biogas Programme*. 2009.
137. Bajgain, S., *Implementation Plan National Domestic Biogas and Manure Programmein Bangladesh*. 2006, SNV (Netherland Development Organisation). p. 79.
138. Ngigi, A., *Kenya National Domestic Biogas Programme: An initiative under the Africa Biogas partnership programme*. 2009. p. 88.
139. Boers, W., *National Biogas Programme Ethiopia Programme Implementation Document* 2008: P.O. Box 8063 Addis Ababa Ethiopia. p. 118.
140. van Nes, W., Lam,J., ter Heegde, F. and Marre, F, *Building viable domestic biogas programmes: success factor in sector development*. 2009.
141. Tomar, S.S., *Status of biogas plant in India.* Renewable Energy, 1994. **5**(5-8): p. 829-831.
142. Khandelwal, K.C., *Country Report on financing of domestic plants in India*. 2008.
143. Adam, J., *Biogas energy for rural development: opportunities, challenges and lacuna of implementation.* SESAM/ARTES South Asian Regional Workshop, Nepal, 2008.
144. De Alwis, A., *Biogas–a review of Sri Lanka's performance with a renewable energy technology.* Energy for Sustainable Development, 2002. **6**(1): p. 30-37.
145. Ashden. *Kigali Insitute of science, Technology and Management*. 2005 [cited 2018 12 April]; Available from: https://www.ashden.org/winners/kist.
146. Bajgan S, S.I., *A successful model of public private partnership for ruralhousehold energy supply.* . 2005: Kigali, Rwanda:.
147. Ghimire, P.C., *Technical study of biogas plants installed in Bangladesh*. 2005: Dhaka. p. 1-91.
148. Hyman, J. and R. Bailis, *Assessment of the Cambodian National Biodigester Program.* Energy for Sustainable Development, 2018. **46**: p. 11-22.
149. Ortiz, W., J. Terrapon-Pfaff, and C. Dienst, *Understanding the diffusion of domestic biogas technologies. Systematic conceptualisation of existing evidence from developing and emerging countries.* Renewable and Sustainable Energy Reviews, 2017. **74**: p. 1287-1299.
150. Landi, M., B.K. Sovacool, and J. Eidsness, *Cooking with gas: policy lessons from Rwanda's National Domestic Biogas Program (NDBP).* Energy for Sustainable Development, 2013. **17**(4): p. 347-356.
151. Hivos. *Carbon finance*. 2018 [cited 2018 13 June 2018]; Available from: https://hivoscarboncredits.org/domestic-biogas/.

152. Kangmin, L.a.H., M-W. *'Biogas China', Institute of science in society, London.* 2006 [cited 2018 12 June]; Available from: http://www.i-sis.org.uk/BiogasChina.php.
153. BPO, *BP I Final Report : Support project to the Biogas programme for the Animal Husbandry sector in some provinces of Vietnam*. 2006, Hanoi.
154. Fulford, D., *Running a Biogas Programme: A Handbook*. 1988: Intermediate Technology Publications.
155. Clemens, H., et al., *Africa Biogas Partnership Program: A review of clean cooking implementation through market development in East Africa.* Energy for Sustainable Development, 2018. **46**: p. 23-31.
156. Guy Dekelver, A.N., Silas Ruzigana, , *Implementation Plan National Programme on Domestic Biogas in Rwanda*. 2006: Kigali, Rwanda. p. 59.
157. Nepal, D.G., *POLICIES FOR PROMOTINGINVESTMENT IN ENERGY SUSTAINABILITYA CASE OF BIOGAS SECTOR OF NEPAL*, in *OECD Global Forum on International Investmen*. 2008: OECD Conference Centre, Paris, France. p. 20.
158. BSP-Nepal, *Biogas support programme Phase IV (2003-2010): profile and stories*. 2009, Biogas Support programme: Kathmandu.
159. SNV, *Renewable (rural) energy olicies, gender equality and social Inclusion analysis*. 2012: Kathmandu, Nepal.
160. BSP-Nepal, *District and fiscal year wise production of biogas plants (Unpublished)*, A. Subedi, Editor. 2015: Katmandu, Nepal.
161. Subedi, S.K.A., *Domestic biogas production and use in Nepal : a simple, reliable, clean and cost-effective solution to provide energy security to the rural households : a thesis presented in partial fulfilment of the requirements for the degree of Doctor of Philosophy (PhD) in Energy Management at Massey University, Palmerston North, New Zealand*. 2015, Massey University.
162. BSP-Nepal, *BSP, Year Book 2009*. 2009: Katmandu, Nepal.
163. BSP-Nepal, *BSP 2011/12*. 2012: Katmandu, Nepal.
164. ABP, *Mid-Term Review of the Asia Biogas Programme*. 2008.
165. Tuygen, K.D., *Overview of biogas technology in Vietnam*. 2009, Department of Livestock production.
166. Ashden. *MARD/SNV: Biogas for smallholders in Vietnam*. 2010 [cited 208 12 JULY]; Available from: https://www.ashden.org/winners/mard-snv#continue.
167. Roubík, H., et al., *Addressing problems at small-scale biogas plants: a case study from central Vietnam.* Journal of Cleaner Production, 2016. **112**: p. 2784-2792.
168. Guy Dekelver, S.R., Jan Lam, *Report on the feasibility study for a Biogas Support Programme in the Republic of Rwanda*. 2005, SNV.
169. McIntosh, B., *Review and Recommendations for Household Biodigesters in Cambodia.* The Cambodia Research Centre for Development, Phnom Penh (2004), 2004.
170. Buysman, E. and A.P.J. Mol, *Market-based biogas sector development in least developed countries —The case of Cambodia.* Energy Policy, 2013. **63**: p. 44-51.

171. SNV, *Biodigester support programme Cambodia feasibility study.* . 2004: Phnom Penh.
172. NBP, *PROGRAMME ARRANGEMENT and IMPLEMENTATION DOCUMENT NATIONAL BIODIGESTER PROGRAMME in CAMBODIA*. 2006: Phnom Penh, Cambodia.
173. UK, E., *Feasibility Study (Kenya)*. 2007, ETC Gropu for shell Foundation: kenya.
174. Kossmann, W.P., U. Habermehl, S., Hoerz, T., Kramer, P and Klingler, B., *Biogas Digest Volume IV: Country Reports, Germany:.* ISAT and GTZ, 1997.
175. Gitonga, *Biogas promotion in kenya, practical Action.* Publishing, Rudby, Uk, 1997.
176. Bensah, E., *Biogas technology dissemination in Ghana: history, current status, future prospects, and policy significance*. Vol. 1. 2010.
177. Alenyorege, R.B.S.B., *Physical Feasibility of Domestic Biogas in the Upper East Region of Ghana*. 2008, SNV Ghana, Northern Portfolio.
178. KITE, *Feasibility study report on domestic biogas in Ghana.* . 2008, Kumasi Institute of Technology, Energy and Environment (KITE).
179. IDCOL, *FINAL REPORT Biogas Audit Bangladesh 2011 -2013*. 2013.
180. Khan, E.U. and A.R. Martin, *Review of biogas digester technology in rural Bangladesh.* Renewable and Sustainable Energy Reviews, 2016. **62**: p. 247-259.
181. ABPP. *Uganda Biogas programme*. 2009 [cited 2018 12 July]; Available from: https://www.africabiogas.org/countries/uganda/.
182. Limited, A.l. *Biogas digester*. 2018 [cited 2018 12]; Available from: https://avenamlinks.com/product-category/biogas-plant/.
183. Gautam, R., S. Baral, and S. Herat, *Biogas as a sustainable energy source in Nepal: Present status and future challenges.* Renewable and Sustainable Energy Reviews, 2009. **13**(1): p. 248-252.
184. Daxiong, Q., et al., *Diffusion and innovation in the Chinese biogas program.* World Development, 1990. **18**(4): p. 555-563.
185. Akinbami, J.F., et al., *Biogas energy use in Nigeria: current status, future prospects and policy implications.* Renewable and Sustainable Energy Reviews, 2001. **5**(1): p. 97-112.
186. Bartlett, Z., et al., *Economic and Environmental Analysis of Farm-Scale Biodigesters to Produce Energy for Kitchen Stove Use*, in *2014 Montreal, Quebec Canada July 13 – July 16, 2014*. 2014, ASABE: St. Joseph, MI. p. 1.
187. Werner, U., U. Stöhr, and N. Hees, *Biogas plants in animal husbandry.* Deutsches Zentrum für Entwicklungstechnologien-GATE, 1989.
188. Singh, N. and R. Gupta, *Community biogas plants in India.* Biological Wastes, 1990. **32**(2): p. 149-153.
189. Devkota, G.P., *Biogas Technology in Nepal: A sustainable soruces of energy for rural people*. 2001: Kathmandu.
190. Cheng, S., et al., *Development and application of prefabricated biogas digesters in developing countries.* Renewable and Sustainable Energy Reviews, 2014. **34**(0): p. 387-400.

191. digestr, a. *Waste and By-product Utilization 2*. 2018 [cited 2018 12]; Available from: http://ecoursesonline.iasri.res.in/mod/page/view.php?id=1430.
192. Fulford, D., *Small-Scale Rural Biogas Programmes: A Handbook*. 2015: Practical Action Publishing.
193. Luer, M., *Installation manual for low-cost polyethylene tube digesters.* GTZ/EnDev, Germany, 2010.
194. Martí-Herrero, J. and J. Cipriano, *Design methodology for low cost tubular digesters.* Bioresource Technology, 2012. **108**(0): p. 21-27.
195. Appels, L., et al., *Principles and potential of the anaerobic digestion of waste-activated sludge.* Progress in Energy and Combustion Science, 2008. **34**(6): p. 755-781.
196. Masse, D.I., L. Masse, and F. Croteau, *The effect of temperature fluctuations on psychrophilic anaerobic sequencing batch reactors treating swine manure.* Bioresource Technology, 2003. **89**(1): p. 57-62.
197. Alvarez, R., S. Villca, and G. Liden, *Biogas production from llama and cow manure at high altitude.* Biomass and Bioenergy, 2006. **30**(1): p. 66-75.
198. Alvarez, R. and G. Lidén, *The effect of temperature variation on biomethanation at high altitude.* Bioresource Technology, 2008. **99**(15): p. 7278-7284.
199. Alvarez, R., S. Villca, and G. Lidén, *Biogas production from llama and cow manure at high altitude.* Biomass and Bioenergy, 2006. **30**(1): p. 66-75.
200. Kalia, A.K. and S.S. Kanwar, *Temperature profiles of biogas plants operating under hilly conditions.* Biological Wastes, 1989. **30**(3): p. 217-224.
201. Kalia, A.K. and S.S. Kanwar, *Long-term evaluation of a fixed dome Janata biogas plant in hilly conditions.* Bioresource Technology, 1998. **65**(1–2): p. 61-63.
202. Kanwar, S.S. and R.L. Guleri, *Performance evaluation of a family-size, rubber-balloon biogas plant under hilly conditions.* Bioresource Technology, 1994. **50**(2): p. 119-121.
203. Kalia, A.K., *Development and evaluation of a fixed dome plug flow anaerobic digester.* Biomass, 1988. **16**(4): p. 225-235.
204. Kanwar, S., et al., *Performance evaluation of a 1 m< sup> 3</sup> modified, fixed-dome Deenbandhu biogas plant under hilly conditions.* Bioresource Technology, 1994. **50**(3): p. 239-241.
205. Pham, C.H., et al., *Factors Affecting Process Temperature and Biogas Production in Small-scale Rural Biogas Digesters in Winter in Northern Vietnam.* Asian-Australasian Journal of Animal Sciences, 2014. **27**(7): p. 1050-1056.
206. Guo, J., et al., *Thermal modelling of the completely stirred anaerobic reactor treating pig manure at low range of mesophilic conditions.* Journal of Environmental Management, 2013. **127**: p. 18-22.
207. Gebremedhin, K., et al., *Heat transfer model for plug-flow anaerobic digesters.* Transactions of the ASAE, 2005. **48**(2): p. 777-785.

208. Terradas-Ill, G., et al., *Thermic Model to Predict Biogas Production in Unheated Fixed-Dome Digesters Buried in the Ground.* Environmental science & technology, 2014. **48**(6): p. 3253-3262.
209. Castano, J.M., J.F. Martin, and R. Ciotola, *Performance of a Small-Scale, Variable Temperature Fixed Dome Digester in a Temperate Climate.* Energies, 2014. **7**(9): p. 5701-5716.
210. Weatherford, V.C. and Z.J. Zhai, *Affordable solar-assisted biogas digesters for cold climates: Experiment, model, verification and analysis.* Applied Energy, 2015. **146**: p. 209-216.
211. Kishore, V.V.N., *A heat-transfer analysis of fixed-dome biogas plants.* Biological Wastes, 1989. **30**(3): p. 199-215.
212. Hassanein, A.A.M., et al., *Simulation and validation of a model for heating underground biogas digesters by solar energy.* Ecological Engineering, 2015. **82**: p. 336-344.
213. Hassanein, A.A.M., D. Zhang, and L. Qiu, *Solar water heating model with sun tracking system for increasing biogas production.* Transactions of the Chinese Society of Agricultural Engineering, 2011. **27**(6): p. 256-261.
214. Dong, F. and J. Lu, *Using solar energy to enhance biogas production from livestock residue – A case study of the Tongren biogas engineering pig farm in South China.* Energy, 2013. **57**(0): p. 759-765.
215. Alkhamis, T.M., et al., *Heating of a biogas reactor using a solar energy system with temperature control unit.* Solar Energy, 2000. **69**(3): p. 239-247.
216. Feng, R., et al., *Performance of a novel household solar heating thermostatic biogas system.* Applied Thermal Engineering, 2016. **96**: p. 519-526.
217. Lu, Y., et al., *Study of solar heated biogas fermentation system with a phase change thermal storage device.* Applied Thermal Engineering, 2015. **88**: p. 418-424.
218. Lu, H., et al., *Experimental Study of a Thermal Storage Technique with Phase Change Material Closure for Solar-Biogas Hybrid Fermentation System.* Ferment Technol, 2016. **5**(126): p. 2.
219. Youzhou, J., et al., *Design and preliminary experimental research on a new biogas fermentation system by solar heat pipe heating.* International Journal of Agricultural and Biological Engineering, 2016. **9**(2): p. 153.
220. Rennuit, C. and S. Sommer, *Decision Support for the Construction of Farm-Scale Biogas Digesters in Developing Countries with Cold Seasons.* Energies, 2013. **6**(10): p. 5314-5332.
221. Appels, L., et al., *Anaerobic digestion in global bio-energy production: Potential and research challenges.* Renewable and Sustainable Energy Reviews, 2011. **15**(9): p. 4295-4301.
222. Rosso, L., J.R. Lobry, and J.P. Flandrois, *An Unexpected Correlation between Cardinal Temperatures of Microbial Growth Highlighted by a New Model.* Journal of Theoretical Biology, 1993. **162**(4): p. 447-463.
223. Donoso-Bravo, A., et al., *Influence of temperature on the hydrolysis, acidogenesis and methanogenesis in mesophilic anaerobic digestion:*

parameter identification and modeling application. Water Science and Technology, 2009. **60**(1): p. 9.
224. Donoso-Bravo, A., et al., *Explicit temperature-based model for anaerobic digestion: Application in domestic wastewater treatment in a UASB reactor.* Bioresource Technology, 2013. **133**: p. 437-442.
225. Bernard, O. and B. Rémond, *Validation of a simple model accounting for light and temperature effect on microalgal growth.* Bioresource Technology, 2012. **123**: p. 520-527.
226. Graef, S.P., *Mathematical modeling and control of anaerobic digestion.* Water Research, 1974. **8**.
227. Donoso-Bravo, A., S. Pérez-Elvira, and F. Fdz-Polanco, *Simplified mechanistic model for the two-stage anaerobic degradation of sewage sludge.* Environmental Technology, 2014(ahead-of-print): p. 1-13.
228. Donoso-Bravo, A. and F. Fdz-Polanco. *Modeling of the anaerobic digestion of sewage sludge: evaluation of several reactor configurations*. in *Computer Applications in Biotechnology*. 2010.
229. Weatherford, V.C. and Z. Zhai, *Affordable solar-assisted biogas digesters for cold climates: Experiment, model, verification and analysis.* Applied Energy, 2015. **146**: p. 209-216.
230. Wang, Y. and F. Witarsa, *Application of Contois, Tessier, and first-order kinetics for modeling and simulation of a composting decomposition process.* Bioresource Technology, 2016. **220**: p. 384-393.
231. Beyenal, H., S.N. Chen, and Z. Lewandowski, *The double substrate growth kinetics of Pseudomonas aeruginosa.* Enzyme and Microbial Technology, 2003. **32**(1): p. 92-98.
232. Weatherford, V., *Verification of a thermal model for affordable solar-assisted biogas digesters in cold climates.*, in *Department of Civil Engineering*. 2010, University of Colorado. USA.
233. Incropera, F.P., et al., *Fundamentals of Heat and Mass Transfer*. 2011.
234. Hillel, D., *Introduction to soil physics*. Vol. 364. 1982: Academic press New York.
235. Datta, A.K., *Biological and bioenvironmental heat and mass transfer*. 2002: CRC Press.
236. Duffie, J.A. and W.A. Beckman, *Solar Engineering of Thermal Processes*. 1980.
237. Swinbank, W.C., *Long-wave radiation from clear skies.* Quarterly Journal of the Royal Meteorological Society, 1963. **89**(381): p. 339-348.
238. Sukhatme, S.P. and J.K. Nayak, *Solar Energy*. 2017: McGraw-Hill Education.
239. Klein, S.A., *Calculation of flat-plate collector loss coefficients.* Solar Energy, 1975. **17**(1): p. 79-80.
240. Harcourt, n.w.d.f.P. *weather datae*. 2015 [cited 2013 12/05]; Available from: www.nrel.gov.
241. Donoso-Bravo, A., et al., *Identification in an anaerobic batch system: global sensitivity analysis, multi-start strategy and optimization*

criterion selection. Bioprocess and biosystems engineering, 2013. **36**(1): p. 35-43.
242. Owhondah, R.O., et al., *Assessment and parameter identification of simplified models to describe the kinetics of semi-continuous biomethane production from anaerobic digestion of green and food waste.* Bioprocess and Biosystems Engineering, 2016. **39**(6): p. 977-992.
243. Poggio, D., et al., *Modelling the anaerobic digestion of solid organic waste–Substrate characterisation method for ADM1 using a combined biochemical and kinetic parameter estimation approach.* Waste Management, 2016. **53**: p. 40-54.
244. Strömberg, S., M. Nistor, and J. Liu, *Towards eliminating systematic errors caused by the experimental conditions in Biochemical Methane Potential (BMP) tests.* Waste Management, 2014. **34**(11): p. 1939-1948.
245. Noykova, N. and M. Gyllenberg, *Sensitivity analysis and parameter estimation in a model of anaerobic waste water treatment processes with substrate inhibition.* Bioprocess Engineering, 2000. **23**(4): p. 343-349.
246. Batstone, D., S. Tait, and D. Starrenburg, *Estimation of hydrolysis parameters in full-scale anerobic digesters.* Biotechnology and Bioengineering, 2009. **102**(5): p. 1513-1520.
247. Siegrist, H., et al., *Mathematical model for meso-and thermophilic anaerobic sewage sludge digestion.* Environmental science & technology, 2002. **36**(5): p. 1113-1123.
248. Mottet, A., et al., *New fractionation for a better bioaccessibility description of particulate organic matter in a modified ADM1 model.* Chemical Engineering Journal, 2013. **228**(0): p. 871-881.
249. Chen, Y. and A. Hashimoto, *Substrate utilization kinetic model for biological treatment process.* Biotechnology and Bioengineering, 1980. **22**(10): p. 2081-2095.
250. Münch, E.v., et al., *Mathematical modelling of prefermenters—I. Model development and verification.* Water Research, 1999. **33**(12): p. 2757-2768.
251. Tomei, M., C. Braguglia, and G. Mininni, *Anaerobic degradation kinetics of particulate organic matter in untreated and sonicated sewage sludge: role of the inoculum.* Bioresource Technology, 2008. **99**(14): p. 6119-6126.
252. Lee, M.-Y., et al., *Variation of ADM1 by using temperature-phased anaerobic digestion (TPAD) operation.* Bioresource Technology, 2009. **100**(11): p. 2816-2822.
253. Gandy, A.F. and E.T. Gandy, *Microbiology for environmental scientists and engineers*. 1980: McGraw-Hill.
254. Ouhammou, B., et al., *Design and Analysis of Integrating the Solar Thermal energy in Anaerobic Digester using TRNSYS: Application kenitra-Morocco.* Energy Procedia, 2017. **141**: p. 13-17.
255. Khoiyangbam, R., et al., *Methane emission from fixed dome biogas plants in hilly and plain regions of northern India.* Bioresource Technology, 2004. **95**(1): p. 35-39.

256. Tinarwo, V.N.a.D., *Investigation of Heat Transfer Associated with Deenbandhu Brick BuiltAnaerobic Digester Covered with Single-layer Soil Type.* NatureEnvironmentand Pollution Technology, 2017. **Vol. 17**(No. 1): p. pp. 169-173.
257. Uko, E. and I. Tamunobereton-ari, *Variability of Climatic Parameters in Port Harcourt, Nigeria*. Vol. 4. 2013. 727-730.
258. Martí-Herrero, J., R. Alvarez, and T. Flores, *Evaluation of the low technology tubular digesters in the production of biogas from slaughterhouse wastewater treatment.* Journal of Cleaner Production, 2018. **199**: p. 633-642.
259. Li, Y., et al., *Comparison of methane production potential, biodegradability, and kinetics of different organic substrates.* Bioresource Technology, 2013. **149**: p. 565-569.
260. Grosser, A., *The influence of decreased hydraulic retention time on the performance and stability of co-digestion of sewage sludge with grease trap sludge and organic fraction of municipal waste.* Journal of Environmental Management, 2017. **203**: p. 1143-1157.
261. Siddique, M.N.I. and Z.A. Wahid, *Achievements and perspectives of anaerobic co-digestion: A review.* Journal of Cleaner Production, 2018. **194**: p. 359-371.
262. Di Maria, F., et al., *Amount of energy recoverable from an existing sludge digester with the co-digestion with fruit and vegetable waste at reduced retention time.* Applied Energy, 2015. **150**: p. 9-14.
263. Dareioti, M.A. and M. Kornaros, *Anaerobic mesophilic co-digestion of ensiled sorghum, cheese whey and liquid cow manure in a two-stage CSTR system: Effect of hydraulic retention time.* Bioresource Technology, 2015. **175**: p. 553-562.
264. Mata-Alvarez, J., et al., *A critical review on anaerobic co-digestion achievements between 2010 and 2013.* Renewable and Sustainable Energy Reviews, 2014. **36**: p. 412-427.
265. Dennehy, C., et al., *Anaerobic co-digestion of pig manure and food waste; effects on digestate biosafety, dewaterability, and microbial community dynamics.* Waste Management, 2018. **71**: p. 532-541.
266. Xie, S., et al., *Anaerobic co-digestion: a critical review of mathematical modelling for performance optimization.* Bioresource Technology, 2016. **222**: p. 498-512.
267. Silvestre, G., et al., *Thermophilic anaerobic co-digestion of sewage sludge with grease waste: effect of long chain fatty acids in the methane yield and its dewatering properties.* Applied Energy, 2014. **117**: p. 87-94.
268. Fjørtoft, K., et al., *Methane production and energy evaluation of a farm scaled biogas plant in cold climate area.* Bioresource Technology, 2014. **169**: p. 72-79.
269. SW Sötemann, N.R., MC Wentzel, GA Ekama, *A steady state model for anaerobic digestion of sewage sludges.* AFRICAN JOURNALS ONLINE (AJOL), 2005. **Water SA Vol. 31(4) 2005**(511-528).
270. Sötemann, S.W., et al., *Integrated chemical, physical and biological processes modelling of anaerobic digestion of sewage sludge.* Water Science and Technology, 2006. **54**(5): p. 109-117.

271. Tomei, M.C., C.M. Braguglia, and G. Mininni, *Anaerobic degradation kinetics of particulate organic matter in untreated and sonicated sewage sludge: Role of the inoculum.* Bioresource Technology, 2008. **99**(14): p. 6119-6126.
272. El-Mashad, H.M., et al., *Effect of temperature and temperature fluctuation on thermophilic anaerobic digestion of cattle manure.* Bioresource Technology, 2004. **95**(2): p. 191-201.
273. Liu, Y., et al., *Experimental research on the thermal performance of PEX helical coil pipes for heating the biogas digester.* Applied Thermal Engineering, 2019. **147**: p. 167-176.
274. Martí-Herrero, J., et al., *Biogas from a full scale digester operated in psychrophilic conditions and fed only with fruit and vegetable waste.* Renewable Energy, 2019. **133**: p. 676-684.
275. Hreiz, R., et al., *Modeling and simulation of heat transfer phenomena in a semi-buried anaerobic digester.* Chemical Engineering Research and Design, 2017. **119**: p. 101-116.
276. Alvarez, R. and G. Lidén, *Low temperature anaerobic digestion of mixtures of llama, cow and sheep manure for improved methane production.* Biomass and Bioenergy, 2009. **33**(3): p. 527-533.